

*Republic of Iraq
Ministry of Higher Education
and Scientific Research
University of Kerbala
College of Engineering*



***An Experimental and Numerical Investigation
of Air Conditioning Cooling Enhancement
Using Nano Materials***

A Thesis

*Submitted to the Department of Mechanical Engineering in the College
of Engineering at the University of Kerbala in partial fulfillment for the
requirements of the Master of Sciences degree in Mechanical
Engineering / Thermo-Fluids Mechanics*

By

Hadeel Salah Hadi

B.Sc. 2015

Supervised By

Assist. Prof. Dr. Abbas Sahi Shareef

Dr. Haider Nadhom Azziz

Supervisors Certification

We certify that this thesis entitled (**Experimental and Numerical Investigation of Air Conditioning Cooling Enhancement Using Nano Material**) has been carried out under our supervision at the University of Kerbala / College of Engineering – Mechanical Engineering Department in partial fulfillment of the requirements for the degree of Master of Sciences in Mechanical Engineering /Thermo-Fluids Mechanics.

Signature

Signature

Assist. Prof. Dr. Abbas Sahi Shareef

Dr. Haider Nadhom Azziz

Date: / / 2019

Date: / / 2019

Linguistic Certification

I certify that this thesis entitled "***Experimental and Numerical Investigation of Air Conditioning Cooling Enhancement Using Nano Material***" that wrote by (**Hadeel Salah Hadi**) was prepared under my linguistic supervision. Its language was amended to meet the English style.

Signature:

Name: Assist. Prof. Dr. Ahmed A. A. Al-Moadhen

Title: Linguistic Advisor

Date: / / 2019

Examination Committee Certification

We certify that we have read this thesis entitled " *Experimental and Numerical Investigation of Air Conditioning Cooling Enhancement Using Nano Material*" and as an examination committee, we examined the student (**Hadeel Salah Hadi**) in its contents and that, in our opinion, it meets the standard of a thesis and is adequate for the award of the Degree of Master of Sciences in Mechanical Engineering / *Thermo-Fluids Mechanics*.

Signature:
Assist. Prof. Dr. Abbas Sahi Shareef
(Supervisor)
Date: / / 2019

Signature:
Dr. Haider Nadhom Azziz
(Supervisor)
Date: / / 2019

Signature:
Name:
(Member)
Date: / / 2019

Signature:
Name:
(Member)
Date: / / 2019

Signature:
Name:
(Chairman)
Date: / / 2019

Approval of Deanery of the College of
Engineering
University of Kerbala

Approval of Mechanical
Engineering
Department

Signature:
Assist.

Signature:

ACKNOWLEDGMENTS

I would like to gratefully and sincerely thank my supervisors Assist. Prof. Dr. Abbas Sahi Shareef and Dr. Haider Nadhom Azziz for their invaluable help, advice, guidance, understanding, and encouragement during this work. I am proud of working with them.

I would like to thank the head and staff of the Mechanical Engineering Department at Kerbala University for their support and encouragement to prepare and complete this thesis.

I would like to thank the nanotechnology group at Babylon University for their help to accomplish the experimental work.

I would like to thank the nanotechnology group at the University of Technology for their help to accomplish the experimental part of this work.

I thank my father and mother for their support which made me as ambitious as I wanted. I hope they always be well and able to get their satisfaction. I appreciate my brothers and sisters support.

Finally, and most importantly, I would like to thank Dr. Mohammed Hasan, Dr. Mohammed Wahab, my brothers and my sister Fatima. As well as my friends Hawraa Ahmed, Shaheed Mahdi, Said Maithem, and miss. Ibtihal, for their continuous help, support, and encouragement that enabled me to complete this thesis.

Abstract

The objective of this research is to study the effect of utilizing (Al_2O_3 -R22 and Ag-R22) nanofluids as heat transfer agent in the performance of the air conditioning system.

The investigation in this study has been conducted experimentally by utilizing a test rig and numerically through designing 3D models by using the Computational Fluid Dynamics (CFD) software.

The experimental tests consisted of an air conditioner, lubricant oil, working fluid system (R22), heat resistant and measuring devices such as pressure gauge, temperature recorder meter, and thermocouples. Temperature and pressure were measured in different positions.

In the numerical analysis, the static behavior of a fluid in the evaporator part of the air conditioning was determined. The suitable boundary conditions and governing equations were performed and solving by utilizing 3D Computational Fluid Dynamics (CFD) and ANSYS workbench (version 16.1). The inlet and outlet temperature and pressure were obtained from ANSYS FLUENT after input the data base from experimental work then they compared with the experimental results.

Both numerical and experimental results were proved that the pressure of the working fluid at inlet and outlet evaporator was decreased when utilizing appropriate nanofluids. While the temperatures increased with nanofluid.

The experimental results showed that the maximum difference in the temperatures was obtained at (0.15 wt. %) nanofluid for Ag-R22.

From the results, the maximum enhancement in the COP was when adding the (Ag) nanoparticles to the refrigerant R22 by (0.15% wt.) and the enhancement increased by (144.71) %.

List of Contents

Contents	Page	
Abstract	I	
List of Contents	III	
List of Figures	VI	
Chapter One		
Introduction		
1.1	Background	1
1.2	Air Conditioning	2
1.3	Nanofluid	4
1.3.1	Advantages of Nano fluids	5
1.3.2	Application of Nanofluids	5
1.3.3	Physical Properties of Nanofluids	6
1.4	Aim of the Project	7
1.5	The Structure of Thesis	7
Chapter Two		
Literature Review		
2.1	View Researches	9
2.2	The scope of this study	14
Chapter Three		
Mathematical and Modelling		
3.1	Introduction	22
3.2	Cycle Air Conditioning System	22
3.3	Assumptions for experimental system	23
3.4	Equation of the components of Unity air conditioning	23
3.4.1	Work input in compressor	23

3.4.2	Heat transfer acquired from evaporator	24
3.4.3	Coefficient of Performance	24
3.4.4	Pressure Ratio	24
3.5	Properties of Nano Fluid	24
3.6	Analysis study for the evaporator	26
3.6.1	Introduction	26
3.6.2	Design the Geometry	26
3.6.3	Mesh the Geometry	27
3.6.4	Analysis the Project	29

Chapter Four

Experimental Work

4.1	Introduction	30
4.2	Design the Testing Rig	30
4.3	The Measurement Instrument	38
4.4	Preparation of Nano fluid	39
4.4.1	Selected the Type of Nano Material and its Amount	39
4.4.2	Mixing the Nano with Lubricant oil	39
4.4.3	Mixing the Nano Lubricant oil with the refrigerant R22	40
4.4.4	Calculation the properties of Nano fluid	41
4.5	Experimental Testing	41
4.5.1	Charging the Nano Lubricant	41
4.5.2	Testing the Leakage by Charging the Air	42
4.5.3	The Vacuum of the Closed System	42
4.5.4	Charging the Refrigerant R22	42
4.5.5	Reading the Experimental Data	43
4.4.6	Calculation the Result	44

Chapter Five

The Results and Discussions

5	Introduction	46
5.1	Experimental Results of Test Rig	46
5.1.1	Temperature	46
5.1.2	Pressure	51
5.2	Calculated results	55
5.2.1	Enthalpy	55
5.2.2	Consumption Work	58

5.2.3	Effect refrigeration	59
5.2.4	Coefficient of performance	61
5.3	Simulation Results	62
5.3.1	Pure Refrigerant	62
5.3.2	Al ₂ O ₃ Nano Refrigerant Analysis	65
5.3.3	Ag Nano Refrigerant Analysis	85
5.3.4	Abstract of the Analysis Results	104
5.4	Comparison of the Experimental and Theoretical Results	107

Chapter Six

Conclusions and Recommendation

6.1	Conclusion	109
6.2	Recommendation	110
	References	-1-

Appendix –A

The Calibration of Instruments used in Thesis

A.1	The Calibration of Instruments used in Thesis	A-1
A.1.1	The temperature recorder meter and thermocouple	A-1
A.1.2	The Gage pressure	A-4
A.2	The Tests of the Nanoparticles and Properties	A-4
A.2.1	Al ₂ O ₃ Nanoparticles Tests and Properties	A-4
A.2.2	Ag Nanoparticles Tests and Properties	A-6

List of Figures

Figure	Title	Page
1.1	Schematic diagram for main parts of refrigeration system	2
3.1	Schematic Diagram	22

3.2	The Main Processes in the Air Conditioning	23
3.3	The windows of the ANSYS workbench SpaceClaim	27
3.4	The designed project	27
3.5	a) The meshing process for all projects,	28
	b) The meshing process for the mesh of air,	28
	c) The meshing process for the mesh of tube	28
3.6	Fluent table	29
3.7	Iteration and run calculation	29
4.1	The process of making the test table (a-m)	31- 34
4.2	a) Compressor,	35
	b) The valves at inlet and outlet compressor	35
4.3	The condenser	36
4.4	The three Capillary tube	36
4.5	Evaporator	37
4.6	a) Compressor of air,	37
	b) Vacuum of air	37
4.7	Electronic weight	39
4.8	Devices of mixture	40
4.9	Process the charging of the oil lubricant	41
4.10	Electronic balance for charging the refrigerant	43
4.11	Schematic diagram of the system explained the location of gages pressure and thermocouples	44
4.12	Experimental rig with their parts	45
5.1	The temperature of inlet compressor with the concentration	47
5.2	The temperature of outlet compressor with concentration	47
5.3	The temperature of inlet evaporator with concentration	48

5.4	The temperature of outlet evaporator with concentration	48
5.5	Different temperature of the evaporator with concentration	49
5.6	Enhancement the evaporator in different temperature with concentration	49
5.7	The temperature at the outlet air with the concentration	50
5.8	The different temperature of the air with the concentration	50
5.9	Enhancement in different temperature of the air with concentration	51
5.10	The pressure at inlet compressor with the concentration	51
5.11	The pressure at outlet compressor with the concentration	52
5.12	The pressure at inlet evaporator with the concentration	52
5.13	The pressure at inlet evaporator with the concentration	53
5.14	The pressure at different position with Al ₂ O ₃ Nano concentration	53
5.15	The pressure at different position with Ag nano concentration	54
5.16	The pressure ratio with the concentration	54
5.17	The enhancement in the pressure ratio with the concentration	55
5.18	Enthalpy with concentration at inlet compressor	56
5.19	Enthalpy with concentration at outlet compressor	56
5.20	Enthalpy with concentration at inlet evaporator	57
5.21	Enthalpy with concentration at outlet evaporator	57
5.22	The compressor work with the concentration	58
5.23	Enhancement The compressor work with the concentration	59

5.24	The refrigeration effect with the concentration	60
5.25	Enhancement The refrigeration effect with the concentration	60
5.26	Coefficient of performance with the concentration	61
5.27	Enhancement in a coefficient of performance with the concentration	61
5.28	a) Temperature contour of R22 for plane in mid pipes,	62
	b) Temperature contour of R22 for cross section of pipes,	63
	c) Contour temperature of R22 for the inlet and outlet	63
5.29	a) Pressure contour of R22 for the mid plane of the pipes,	64
	b) Pressure contour of R22 for the cross section of the pipes,	64
	c) Pressure contour of R22 for the inlet and outlet of the pipe	65
5.30	a) Temperature contour of 0.01% Al ₂ O ₃ for mid plane in the pipe,	65
	b) Temperature contour of 0.01% Al ₂ O ₃ for the plane in cross section of the pipe,	66
	c) Temperature contour of 0.01% Al ₂ O ₃ for inlet and outlet of the pipe,	66
	d) Temperature contour of 0.01% Al ₂ O ₃ for the pipe	67
5.31	a) Pressure contour of 0.01% Al ₂ O ₃ for mid plane in the pipe,	67
	b) Pressure contour of 0.01% Al ₂ O ₃ for the plane in cross section of the pipe,	68
	c) Pressure contour of 0.01% Al ₂ O ₃ for inlet and outlet of the pipe,	68

	d) Pressure contour of 0.01% Al ₂ O ₃ for the pipe	69
5.32	a) Temperature contour of 0.05% Al ₂ O ₃ for plane in mid pipes	69
	b) Temperature contour of 0.05% Al ₂ O ₃ for the plane in cross section of the pipe,	70
	c) Temperature contour 0.05% Al ₂ O ₃ for inlet and outlet of the pipe,	70
	d) Temperature contour 0.05% Al ₂ O ₃ for the pipe	71
5.33	a) Pressure contour 0.05% Al ₂ O ₃ for mid plane in the pipe,	71
	b) Pressure contour 0.05% Al ₂ O ₃ for the plane in cross section of the pipe,	72
	c) Pressure contour 0.05% Al ₂ O ₃ for inlet and outlet of the pipe,	72
	d) Pressure contour 0.05% Al ₂ O ₃ for the pipe	73
5.34	a) Temperature contour of 0.1% Al ₂ O ₃ for mid plane in the pipe,	73
	b) Temperature contour of 0.1% Al ₂ O ₃ for the plane in cross section of the pipe,	74
	c) Temperature contour of 0.1% Al ₂ O ₃ for inlet and outlet of the pipe,	74
	d) Temperature contour of 0.1% Al ₂ O ₃ for the pipe	75
5.35	a) Pressure contour of 0.1% Al ₂ O ₃ for mid plane in the pipe,	75
	b) Pressure contour of 0.1% Al ₂ O ₃ for the plane in cross section of the pipe,	76
	c) Pressure contour of 0.1% Al ₂ O ₃ for inlet and outlet of the pipe,	76
	d) Pressure contour of 0.1% Al ₂ O ₃ for the pipe	77

5.36	a) Temperature contour of 0.15% Al ₂ O ₃ for mid plane in the pipe,	77
	b) Temperature contour of 0.15% Al ₂ O ₃ for the plane in cross section of the pipe,	78
	c) Temperature contour of 0.15% Al ₂ O ₃ for inlet and outlet of the pipe,	78
	d) Temperature contour of 0.15% Al ₂ O ₃ for the pipe	79
5.37	a) Pressure contour of 0.15% Al ₂ O ₃ for mid plane in the pipe,	79
	b) Pressure contour of 0.15% Al ₂ O ₃ for the plane in cross section of the pipe,	80
	c) Pressure contour of 0.15% Al ₂ O ₃ for inlet and outlet of the pipe	80
	d) Pressure contour of 0.15% Al ₂ O ₃ for the pipe	81
5.38	a) Temperature contour 0.2% Al ₂ O ₃ for mid plane in the pipe	81
	b) Temperature contour for the plane in cross section of the pipe	82
	c) Temperature contour 0.2% Al ₂ O ₃ for inlet and outlet of the pipe,	82
	d) Temperature contour 0.2% Al ₂ O ₃ for the pipe	83
5.39	a) Pressure contour 0.2% Al ₂ O ₃ for mid plane in the pipe	83
	b) Pressure contour 0.2% Al ₂ O ₃ for mid plane in the pipe	84
	c) Pressure contour 0.2% Al ₂ O ₃ for inlet and outlet of the pipe,	84
	d) Pressure contour 0.2% Al ₂ O ₃ for the pipe	85
5.40	a) Temperature contour of 0.01% Ag for mid plane in the pipe,	85
	b) Temperature contour of 0.01% Ag for the plane in	86

	cross section of the pipe,	
	c) Temperature contour of 0.01%Ag for inlet and outlet of the pipe	86
5.41	a) Pressure contour of 0.01%Ag for mid plane in the pipe,	87
	b) Pressure contour of 0.01%Ag for the plane in cross section of the pipe,	87
	c) Pressure contour of 0.01%Ag for inlet and outlet of the pipe,	88
	d) Pressure contour of 0.01%Ag for the pipe	88
5.42	a) Temperature contour of 0.05%Ag for mid plane in the pipe,	89
	b) Temperature contour of 0.05%Ag for the plane in cross section of the pipe,	89
	c) Temperature contour of 0.05%Ag for inlet and outlet of the pipe,	90
	d) Temperature contour of 0.05%Ag for the pipe	90
5.43	a) Pressure contour of 0.05%Ag for mid plane in the pipe,	91
	b) Pressure contour of 0.05%Ag for the plane in cross section of the pipe,	91
	c) Pressure contour of 0.05%Ag for inlet and outlet of the pipe,	92
	d) Pressure contour of 0.05%Ag for the pipe	92
5.44	a) Temperature contour of 0.1%Ag for mid plane in the pipe,	93
	b) Temperature contour of 0.1%Ag for the plane in cross section of the pipe,	93
	c) Temperature contour of 0.1%Ag for inlet and outlet of	94

	the pipe,	
	d) Temperature contour of 0.1%Ag for the pipe	94
5.45	a) Pressure contour of 0.1%Ag for mid plane in the pipe,	95
	b) Pressure contour of 0.1%Ag for the plane in cross section of the pipe,	95
	c) Pressure contour of 0.1%Ag for inlet and outlet of the pipe,	96
	d) Pressure contour of 0.1%Ag for the pipe	96
5.46	a) Temperature contour of 0.15%Ag for mid plane in the pipe,	97
	b) Temperature contour of 0.15%Ag for the plane in cross section of the pipe,	97
	c) Temperature contour of 0.15%Ag for inlet and outlet of the pipe	98
5.47	a) Pressure contour of 0.15%Ag for mid plane in the pipe,	98
	b) Pressure contour of 0.15%Ag for the plane in cross section of the pipe,	99
	c) Pressure contour of 0.15%Ag for inlet and outlet of the pipe,	99
	d) Pressure contour of 0.15%Ag for the pipe	100
5.48	a) Temperature contour of 0.2%Ag for mid plane in the pipe,	100
	b) Temperature contour of 0.2%Ag for the plane in cross section of the pipe,	101
	c) Temperature contour of 0.2%Ag for inlet and outlet of the pipe	101
	d) Temperature contour of 0.2%Ag for the pipe	102
5.49	a) Pressure contour of 0.2%Ag for mid plane in the pipe,	102

	b) Pressure contour of 0.2%Ag for the plane in cross section of the pipe,	103
	c) Pressure contour of 0.2%Ag for inlet and outlet of the pipe,	103
	d) Pressure contour of 0.2%Ag for the pipe	104
5.50	The temperature of R22-Al ₂ O ₃ with along evaporator	105
5.51	The temperature of R22-Ag with along evaporator	105
5.52	The temperature for R22, R22-Al ₂ O ₃ and R22-Ag with along evaporator	106
5.53	The different temperature of evaporator with a concentration	106
5.54	The experimental and theoretical temperature at the outlet evaporator for the pure R22	107
5.55	The experimental and theoretical temperature at the outlet evaporator for the R22-Al ₂ O ₃	108
5.56	The experimental and theoretical temperature at the outlet evaporator for the pure R22	108
A.1	The calibration of temperature meter and thermocouples	A-3
A.2	The calibration of gage pressure	A-4
A.3	X-Ray of Al ₂ O ₃ -gamma Nanoparticles	A-6
A.4	The SEM of Al ₂ O ₃ Nanoparticles	A-6
A.5	The properties Al ₂ O ₃ nanoparticles	A-7
A.6	X-Ray of Ag-Metal Basis Nanoparticles	A-8
A.7	The SEM of Ag Nanoparticles	A-8
A.8	The properties Ag nanoparticles	A-9

Chapter One

Introduction

1.1 Background

This thesis focuses on the investigation of enhancing the coefficient of performance and reducing the energy consumption of the air conditioning process.

The use of nanotechnology has expanded in recent years and has entered the fields of heat transfer. The most important fields are cooling and the air conditioning system. The addition of nanoparticles (1-100) nm improved the properties of the operating fluid and thus improved the efficiency of the cooling system. There are a lot of researches have been made to improve the thermal properties of the Nanofluid and the performance of the air conditioning system. Nanoparticles are either directly added to the operating fluid or added to the compressor oil.

There are many applications of cooling systems, which include refrigerators, air conditioning, and wall air conditioning. All of these systems operate on a single principle and each of which consists of the following parts. The first part is the compressor that raises the gas pressure and condensate and discharges the heat out and cools the gas fluid. The part is the expansion of the high pipe that works to reduce gas pressure and finally the evaporator. The heat is drawn from the place to be cooled and gained by the gas as shown in figure (1.1).

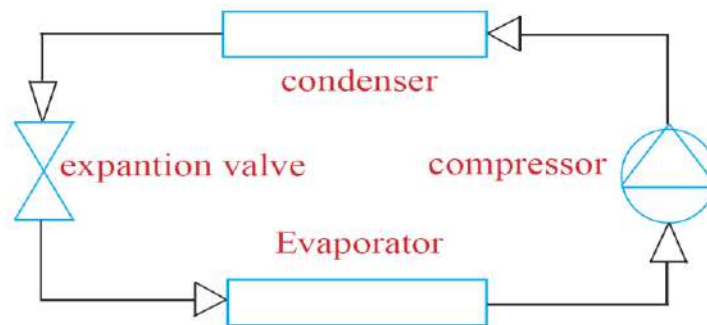


Figure (1.1): The schematic diagram for the main parts of the refrigeration system.

1.2 The Air Conditioning System

An air conditioner is a machine that performs many utilities at the same time such as conditioning the air, distributing it, and presenting it to the conditioned space.

There are many types of air conditioning such as Window Mounted, Wall Mounted, Free Standing Portable, Split Unit; Mini Split Unit and Air Cooled Chiller. In this study, the Window Type Air Conditioning Unit was selected as it considered cheap, easy to form. This unit consisted of the following main:

a. **The Compressor:** is the main component in the air conditioning system which converts from low pressure to high pressure. There are many types of refrigeration compressors such as the reciprocating, rotary, scroll and screw compressors. These compress the vapor refrigerant to a pressure slightly higher than the discharge pressure. So, the vapor refrigerant will be compressed to be in a pressure slightly higher than the pressure in the discharge. Today, the rotary compressor is great used as a testing rig in the small refrigeration systems. A rolling piston is mounted on an eccentric shaft and fixed vane sliding in a slot to remain in contact with the roller, where with rotating the piston, the vane

will move in a reciprocating motion. So, it is allowed the vapor refrigerant to input to the compression chamber to be compressed.

The Internal leakage usually concerned with the mating parts clearance, the speed and finishing of the surface, and the viscosity of the oil. Usually, HCFC-22 is used as a refrigerant in the refrigerant with rotary compressors. HFC-407C and HFC-410A with ozone depletion potential equal to zero will become the alternative refrigerants to replace HCFC-22 in the future.

b. In order to make the fluid film for disconnecting the moving surfaces, the oil lubrication has to be used. These disconnections protect the surfaces from corrosion and wear. Another advantage of using the oil was to carry the refrigerant heat away and cool it. In refrigeration systems, the mineral and synthetic oils are used for lubrication. HCFC-22 is partly oil-miscible so that the refrigerant-oil mixture can return to the compressor. HFCs and HFC blends are not miscible with mineral oil. But, it should be considered that the oil was free of solids like wax, stable chemically, and has a compatible viscosity.

c. The Evaporator is one of the major components; it works as a heat exchanger that transfers heat from the materiality being cooled to a boiling temperature. The main reason for refrigeration is to slough heat from air or other matter. It is here that the liquid refrigerant is expanded and evaporated. When the liquid refrigerant attains to the evaporator, its pressure has been reduced. So, it is much cooler than the fan air flowing around it. The refrigerant then vaporized in order to absorb the maximum amount of heat. This heat is then moved by the refrigerant from the evaporator as a low-pressure gas through a hose or line to the low side of the compressor, where the whole refrigeration cycle is regenerate.

d. The Condenser, in a cooling cycle of the refrigeration system, heat is absorbed by the vapor refrigerant in the evaporator followed by the compression of the refrigerant by the compressor. The high pressure and high temperature state of the vapor refrigerant are then converted to a liquid at the condenser. It is designed to condense successfully the compressed refrigerant vapor. Mainly, there are three kinds of the condensing unit depending on heat removal method by the condensing medium usually they are water, air or a combination of both.

e. The Expansion valves which are devices used to control the refrigerant flow in a refrigeration system. They help to facilitate the change of high pressure of the liquid refrigerant in the condensing unit to low pressure gas refrigerant in the evaporator.

f. The Capillary Tube is a tube with a small internal diameter and could be coiled for part of its length. It is installed in the suction line. A filter-drier is sometimes fitted before the tube to remove dirt or moisture from the refrigerant. This device is simple and does not have any moving part and lasts longer. In order to use this device, the amount of refrigerant in the system must be properly calibrated at the factory level.

Many types of refrigerators are used in the cooling system such as R22, R134a, R141b, R502, R11, and R600a. The refrigerator R22 is used in the experimental study which is common in fact live and mineral oil is used.

1.3 Nanofluid

Nanofluid is a new category of working fluid that is used instead of base fluid to enhance the efficiency of a system through improving the thermal and friction properties. Adding material with nanosize particles (1-

100) nm to base fluid, the surface area to heat transfer was increased so the coefficient of heat transfer increased.

The nanomaterials may be:

1. Pure metal (e.g. copper, silver, gold, and aluminum).
2. Metal oxides, carbides and metal nitrides (e.g. SiO_2 , TiO_2 , SiC , SiN , AlN).
3. Oxide ceramics (e.g. Al_2O_3 , CuO) and,
4. Different forms of carbon (e.g. carbon nanotubes, graphite, and diamond).

The basic fluids that commonly used in the air conditioning system involve water, refrigerants, bio-fluids, polymeric solutions oils, and lubricants, etc.

1.3.1 Advantages of nanofluids

It is possible to summarize the main advantages of nanofluids as follows:

1. They have a high specific surface area and therefore more heat transfer surface between particles and fluids.
2. They have high dispersion stability with predominant Brownian motion of particles.
3. They are reducing the pumping power as compared to pure liquid to achieve equivalent heat transfer intensification.
4. They are reducing the particle clogging as compared to conventional slurries, thus promoting system miniaturization.
5. They have adjustable properties, including thermal conductivity

and surface wettability, by varying particle concentrations to suit different applications.

1.3.2 Applications of nanofluids

The nanofluids can be applied in the following applications:

1. Transportation (Engine cooling/vehicle thermal management).
2. Electronics cooling (Smart Fluids).
3. Nuclear systems cooling.
4. Heat exchanger.
5. Biomedicine.
6. Other applications (heat pipes, fuel cell, Solar water heating, chillers, domestic refrigerator, Diesel combustion, Drilling, Lubrications, Thermal storage).

1.3.3 Physical Properties of nanofluids

1. Thermal Conductivity: Thermal conductivity is the most complicated and the most important one for many applications. The thermal conductivity of nanofluids depends on several factors. The volume fraction increase in thermal conductivity of nanofluid was proportional to the increase in volume fraction. The thermal conductivity of a nanofluid is increased by decreasing particle size because the smaller particle size has the ability to move easily and cause a higher level of stochastic motion. The increase in the temperature leads the thermal conductivity ratio to decrease because the increase in temperature improves the collision between the nanoparticles and guides to fashioning the nanoparticle aggregation. Also, the thermal conductivity of nanoparticles and the thermal conductivity of a nanofluid with used metal are higher than metal

oxide for the same condition.

2. Viscosity: some factors such as particle size, temperature, particle size distribution, and volume concentrations have an effect on the viscosity of nanofluid. When the temperature increases the viscosity of the nanofluid will decrease because of the intermolecular interactions between nanoparticles and fluid. Moreover, the molecules of fluid become weak when increasing the temperature. Regarding the volume fraction, where all researchers indicated, the viscosity increases nonlinearly by increasing the volume fractions because the interactions between nanoparticles and hydrodynamic forces acting on the surface of the solid particles and increase the number of particles.

3. Density: The density of nanofluids increase by increasing the volume fraction because the bulk density of nanoparticle is less than of the base fluid.

4. Specific Heat: The specific heat of nanofluids decreases by increasing the volume fraction because the specific heat of nanoparticle is less than of the base fluid and due to the increase in the thermal diffusivity too.

1.4 Aims of Project

The purpose of the experimental and numerical study involves the following:

1. Enhancement of the coefficient of the performance of the air conditioning system.
2. Comparing the experimental study with numerical analysis.

1.5 The Structure of Thesis

This thesis contains six chapters as explained below:

1. Chapter 1 includes the introduction where explain the problem, aims of the study and the whole structure.
2. Chapter 2 explores the literature review related to improving the performance of the air conditioning system and the effect of adding the nanoparticles to the refrigerant.
3. Chapter 3 describes modeling the system by using the Computational Fluid Dynamics (CFD) for the slug hydrodynamic.
4. Chapter 4 describes the experimental apparatus and the properties of fluids used and the technique for measurements. This chapter also includes a brief description of important facility components and instrumentation.
5. Chapter 5 presents the experimental and theoretical results obtained in the experiments and the performed CFD modeling. A comparison between the experimental and CFD modeling is performed in order to validate the modeling results.
6. Chapter 6 brings together all the key conclusions from this work and provides suggestions for future works.

Chapter Two

Literature Review

The increasing needs for cooling systems in various applications have led many researchers to focus on improving the efficiency of these systems as well as reducing energy consumption. In recent years, technology has been one of the ways to increase the efficiency of refrigeration systems by improving heat transferability.

2.1 View Researches

Sheng-shan Bi, et al. 2008, [1] conducted the performance of refrigerator was investigated through using TiO_2 and Al_2O_3 nanoparticles with concentration (0.06 and 0.1) % mass fraction were mixed with Mineral oil / R134a. The result showed that the energy consumption for 0.1% mass fraction was 0.26 % less than POE oil /R134a.

Peng et al. 2009, [2] investigated the pressure drop when adding CuO nanoparticles to R113 for a horizontal tube. The results showed that the maximum increased value of pressure drop was 20.8% for nanofluid.

Peng et al. 2010, [3] studied the effect of CNT in R113/oil mixture on nucleate pool boiling heat transfer characteristics. They found that the R113/oil/CNTs Nano refrigerant increase the nucleate pool boiling heat transfer coefficient by 61%.

Kedzierski 2011, [4] studied Al_2O_3 nanoparticles with R134/PAG oil at different mass fractions (0.5%, 1%, and 2%).

Shengshan Bi, et al. 2011, [5], The experimental study on a domestic refrigerator, the TiO_2 nanoparticles were used with (0.1, 0.5)g/l

concentration as nanorefrigerant to reduce the power consumption by 9.6% than pure refrigerant R600a and improve the performance.

Subramani and Prakash 2011, [6], conducted an experimental and theoretical study on VCRS, they added 0.06 % mass fraction of Al₂O₃ nanoparticles to 3GS mineral oil / R134a to improve the COP by 33% and power consumption reduce by 25% experimentally, Theoretical investigation of heat transfer coefficient increases by 53% for nanorefrigerant.

Abdel-Hadi et al. 2011, [7] studied the influence of adding CuO nanoparticles to R134a pure refrigerant on heat transfer in a vapor-compression system where the maximum enhancement value was 0.55%.

Sendil Kumar and R. Elansezhian, 2012, [8] an experimental study on the using 0.2%V of Al₂O₃ nanoparticles to HFC134a refrigerant. The result was showed that the usage energy was less 10.32% and the performance was better than the pure refrigerant.

An experimental study by **Kedzierski** 2012, [9] was presented for the density and kinematic viscosity of oil with CuO nanoparticles with the temperature range 288 K - 318 K and atmospheric pressure. The results show the increase in the density and viscosity of nano oil by increasing the mass fraction of nanoparticle.

An experimental study by **Kedzierski** 2013, [10] was conducted for the kinematic viscosity and density of the oil with Al₂O₃ nanoparticles at atmospheric pressure in the temperature 288- 318 K. The results showed that the decreasing and increasing in the viscosity of oil-Al₂O₃ related to the mass fraction and temperature while the density was decreased with temperature and increased concentration of Al₂O₃ nanoparticles.

The thermal conductivity and viscosity of (0.1 - 2%V) Al₂O₃ with R141b nanorefrigerant were investigated by **Mahbubul et al.** 2013, [11]. The results showed an increase in the viscosity by increasing the volume of concentrations of the nanoparticles for the temperature 5 to 20 °C and decrease by raising the temperature.

Sajumon.K.T et al. 2013, [12], improved the power consumption of the refrigeration system by incrementing the kinematic viscosity and reduction the friction factor by adding nanoparticles to lubricant oil of compressor. The TiO₂ nanoparticles had been used with an average size of 21 nm which enhanced the thermal properties; this led to improving the performance of the system.

The CNT (0.01wt% - 0.1wt%) was mixed with POE lubricant oil and R134a refrigerant by **Muhammad Abbas et al.** 2013 [13], to enhance the COP of the system and reduced the power consumption The result showed that the 0.1wt% was higher COP where enhanced by 4.2%.

Sun and Yang 2013, [14] investigated the effect of different nanoparticles (Cu, Al, CuO, and Al₂O₃) on flow boiling heat transfer. They found that the Cu-R141b nanorefrigerant gives the maximum heat transfer coefficient while the minimum heat transfer coefficient was for R141b/CuO.

A simulation of smooth horizontal tube with Al₂O₃/R141 was study by **I.M. Mahbubul et al.** 2013 [15]. They investigated the heat transfer coefficient and pressure drop for (0-5)% volume fraction and constant heat flux 100 kW/m², The result indicated that the pressure drop increase with increment volume fraction and the heat transfer coefficient, then the performance improved. In addition, they had other research 2014 [16] that investigated the thermophysical properties of the nanorefrigerant Al₂O₃-

R134a in a horizontal tube. So, the thermal conductivity and viscosity increased by the concentration and the pressure increased too. The significant increment was in them when increasing the concentration of nanoparticles.

Analysis of the performance of the refrigeration system was investigated by **Coumaressin, T et al.** 2014 [17]. The heat transfer coefficient was improved by using CuO nanoparticles with R134a. The results were obtained by FLUENT software for the double horizontal tube as an evaporator heat exchanger with heat flux as a load on the evaporator.

The mathematical modeling of the evaporator tube when using nanorefrigerant R134a with CuO Nanoparticles studied by **Fadhilah, SA et al.** 2014, [18]. They noted that the thermophysical properties enhanced and led to increasing the heat transfer rate in the evaporator.

Haider Ali Hussien 2014 [19], studied and investigated the COP for Air-Conditioner system by adding TiO₂ nanoparticles to mineral oil as a base fluid while the refrigerant R22 was used as a working fluid. The results showed a decrease in power consumption and increase in COP with 13.3% and 11.99% respectively.

A theoretical study for five types of refrigerant mixed with Al₂O₃ as nanoparticles by **Aktas, Melih et al.** 2015 [20]. The results showed that the COP was enhanced by adding nanoparticles and R600a / Al₂O₃ had optimum performance.

Omer A. Alawi et al. 2015 [21] made an analytic study on viscosity model of nanorefrigerant TiO₂/R123 in a refrigeration system and investigated the pressure drop with viscosity. The result showed an increment in the pressure drop when increasing the viscosity which

increased with volume concentration.

Bandgar et al. 2016 [22] carried out an experimental study of VCRS- R134a. They investigated the performance by using SiO_2 nanoparticles that mixed with POE oil/mineral oil as a lubricant with (0.5%, 1.5% and 2% mass fraction). The optimum concentration was 0.5% mass fraction where the performance was 12.16% more than pure POE oil and the power consumption was 13.89% less than pure POE oil.

N. Kamaraj and A. Manoj babu 2016 [23], investigated the performance of the refrigerator through adding (0.1 and 0.2 gram/liter) carbon black nanoparticles to POE oil/mineral oil as a lubricant with R134a. The results were indicated an optimum performance at the concentration of 0.2 gram/liter of black carbon mixed with mineral oil.

Hernández, Diana C et al. 2016 [24], made an analytic study for the horizontal tube by three types of refrigerant (R113, R123, and R134a) were mixed with (1% and 5%) volume fraction of Al_2O_3 . The results - which obtained by ANSYS FLUENT 15.0 - showed an increment in the thermophysical properties and pressure drop when increasing the concentration, where the higher efficiency was at 1% v of Al_2O_3 / R134a.

Zhelezny, VP et al. 2017 [25], studied and made an experimental investigation about the viscosity, density and solubility for R600a-mineral oil with nanoparticles Al_2O_3 and TiO_2 . The results indicated that the additive of nanoparticles to lubricant led to increasing the solubility, viscosity and density, also reduce the surface tension.

M.Z. Sharif et al. 2017 [26], developed the automotive air conditioning system performance by using SiO_2 /PAG nanolubricant through evaluated compressor work, heat absorbing, and coefficient of the

performance (COP). The maximum increment enhancement in COP was 24% at 0.05% volume concentration.

M. Anish et al. 2018 [27], investigated the performance of the domestic refrigerator by using 0.05% volume fraction for CuO in the base fluid R22 refrigerant. The results were indicated that the heat transfer rate and power consumption were better for CuO-R22 nanorefrigerant.

2.2 The scope of this study

1. The LG window air conditioning type is selected for testing, where R22 gas as a working fluid and POE/MO4E as a lubricant oil.
2. Two types of nanoparticles (Al_2O_3 , Ag) are used to improve the thermal properties of oil then refrigerant.
3. Five mass fractions (0.01-0.2) are selected to specify the optimum one of them.
4. The experimental and theoretical results are found.
5. The comparing between the experimental study and numerical analysis is done.

Table 2.1 review about this study

Authors	Refrigerant base fluid	Nano particles size	The work and results
Sheng-shan Bi, et al. (2008), [1]	Mineral oil / R134a	TiO ₂ and Al ₂ O ₃ (0.06 and 0.1) % mass fraction	Investigated the COP and results showed the energy consumption for 0.1% mass fraction was 0.26 % less than POE oil
Peng et al. 2009, [2]	R113	CuO	Investigated the pressure drop for a horizontal tube. The results showed that the maximum increased value of pressure drop was 20.8% for nanofluid.
Peng et al. 2010, [3]	R113/oil	CNT	Studied the effect of CNT on nucleate pool boiling heat transfer characteristics. It is found that the R113/oil/CNTs nanorefrigerant increase the nucleate pool boiling heat transfer coefficient by 61%.
Kedzierski 2011, [4]	R134/ PAG oil	Al ₂ O ₃ (0.5%, 1%, and 2%) mass	It is studied Al ₂ O ₃ nanoparticles with R134/ PAG oil, the results indicated that the heat transfer was enhanced for mixture

		fractions	of nanorefrigerant compared with pure R134a/ PAG oil.
Shengshan Bi, et al. 2011, [5]	R600a	TiO ₂ Nanoparticles was used with (0.1, 0.5)g/l	The experimental study led to reduce the power consumption by 9.6% and improve the performance.
Subramani and Prakash 2011, [6]	3GS mineral oil / R134a	0.06 % mass fraction of Al ₂ O ₃	Experimental and theoretical study on VCRC to improve the COP by 33% and power consumption reduced by 25% experimentally, Theoretical investigation of heat transfer coefficient increased by 53% for nanorefrigerant.
Abdel-Hadi et al. 2011, [7]	R134a	CuO	Studied the influence of adding CuO nanoparticles to R134a pure refrigerant on heat transfer in vapor-compression system where the maximum enhancement value was 0.55%.
Sendil Kumar and R. Elansezhian, 2012, [8]	HFC134a refrigerant	0.2%V of Al ₂ O ₃	The experimental study led to the usage energy was less 10.32% and the performance was better than pure refrigerant

Kedzierski 2012, [9]	oil	CuO	An experimental study was presented for the density and kinematic viscosity at a temperature range 288 K - 318 K and atmospheric pressure. The results showed the increase in the density and viscosity of nano oil with increasing of the mass fraction of nanoparticle.
Kedzierski 2013, [10]	oil	Al ₂ O ₃	The experimental study about the kinematic viscosity and density at atmospheric pressure in the temperature 288- 318 K. The results showed that the decreasing and increasing in the viscosity of oil-Al ₂ O ₃ related with the mass fraction and temperature while the density was decreased with temperature and increased the concentration of Al ₂ O ₃ nanoparticles.
Mahbubul et al. 2013, [11]	R141b	(0.1 - 2%v) Al ₂ O ₃	The thermal conductivity and viscosity were investigated. The results showed the increase in the viscosity with increasing the volume concentrations of the nanoparticles for the temperature 5 to 20 °C and decreases with raising the temperature

Sajumon.K.T et al. 2013, [12]	lubricant oil of compressor	TiO ₂ with average size 21nm	The improved in the power consumption of refrigeration system was investigated by incrementing the kinematic viscosity and reduction the friction factor. This led to improving the performance of system
Muhammad Abbas et al. 2013, [13]	POE and R134a	CNT (0,01wt% - 0.1wt%)	Enhance the COP of the system and reduction in power consumption. The result showed that the 0.1wt% was higher COP where enhanced by 4.2%.
Sun and Yang 2013, [14]	R141b	Cu, Al, CuO and Al ₂ O ₃	Investigating the effect of different nanoparticles (Cu, Al, CuO and Al ₂ O ₃) on flow boiling heat transfer. They found that the Cu-R141b nanorefrigerant gave the maximum heat transfer coefficient while the minimum heat transfer coefficient was for R141b/CuO.
I.M. Mahbubul et al. 2013, [15],	R141	(0-5)% Al ₂ O ₃ volume fraction	Investigating the heat transfer coefficient and pressure drop in simulation of smooth horizontal tube. The result indicated that the pressure drop increase by incrementing the volume fraction and also the heat transfer coefficient, then the performance

			improved.
I.M. Mahbubul, et al. 2013, [16]	R134a	Al ₂ O ₃	Investigated the thermophysical properties of nanorefrigerant in a horizontal tube, the thermal conductivity and viscosity increased with concentration as well as the pressure drop.
Coumaressin, T et al. 2014, [17]	R134a	CuO	Analysis of performance refrigeration system was investigated by FLUENT software in double horizontal tube with heat flux as a load. It found that the heat transfer coefficient was improved
Fadhilah, SA et al. 2014, [18]	R134a	CuO	The thermophysical properties enhanced that led to increase the heat transfer rate in evaporator.
Haider ali hussen 2014, [19]	mineral oil	TiO ₂	Investigating the COP for Air-Conditioner system. The results showed that decreasing in power consumption and increasing in COP with 13.3% and 11.99% respectively.
Aktas, Melih et al. 2015, [20]	five types of refrigerant	Al ₂ O ₃	The results showed that COP enhanced by adding nanoparticles and R600a / Al ₂ O ₃ had optimum performance.

Omer A. Alawi et al. 2015, [21]	R123	TiO ₂	Analysis study for viscosity model in refrigeration system, the pressure drop with viscosity investigated. The result showed the increment in the pressure drop as increase the viscosity which increase with volume concentration
Bandgar et al. 2016, [22]	POE oil / Mineral oil	(0.5%, 1.5% and 2% mass fraction) SiO ₂	The optimum concentration was 0.5% where the performance was 12.16% more than the pure POE oil and the power consumption was 13.89% less than the pure POE oil.
N. Kamaraj and A. Manoj babu 2016, [23]	POE oil / Mineral oil	(0.1 and 0.2 gram/liter) carbon black	Investigating the performance of refrigerator. The results were indicated the optimum performance at the concentration 0.2 gram / liter of carbon black mixed with mineral oil.
Hernández, Diana C et al. 2016, [24]	R113, R123 and R134a	(1% and 5% volume fraction) of Al ₂ O ₃	Analysis study for horizontal tube by ANSYS FLUENT 15.0. The results showed that an increment in the thermophysical properties and pressure drop by increasing the concentration. The higher efficiency was at 1% v of Al ₂ O ₃ / R134a.
Zhelezny, VP et al. 2017, [25]	R600a- mineral oil	Al ₂ O ₃ and TiO ₂	Conducted an experimental investigation about the viscosity, density and solubility, The results indicated the increase in the

			solubility, viscosity and density. Also reduce the surface tension.
M.Z. Sharif et al. 2017, [26]	PAG	SiO ₂	Developed the automotive air conditioning system performance. The maximum increment enhancement in COP was 24% at 0.05%.
M. Anish et al. 2018, [27]	R22	0.05% CuO volume fraction	Investigated the performance of domestic refrigerator. The results were indicated that the heat transfer rate and power consumption were better for CuO-R22 nanorefrigerant

Chapter Three

Mathematical Modelling of the System

3.1 Introduction

This chapter studies the mathematical formulation for the usage device and it contains three sections. The first section is dedicated to the work and heat transfer equations for the components of unity air conditioning. The second section is related to the thermophysical properties formula for the base working fluid and nanofluid.

3.2 Cycle of Air Conditioning System

Generally, the system of unity air conditioning consists of a compressor, a condenser, capillary tube as an expansion valve, and an evaporator as shown in Figure (3.1). There are four processes of thermodynamic for working fluid occurred in these main parts as indicated in Figure (3.2). They are isentropic compression in the compressor, isobaric heat in the condenser that absorbs heat, isenthalpic expansion in the capillary tube and isobaric heat in the evaporator that rejects heat.

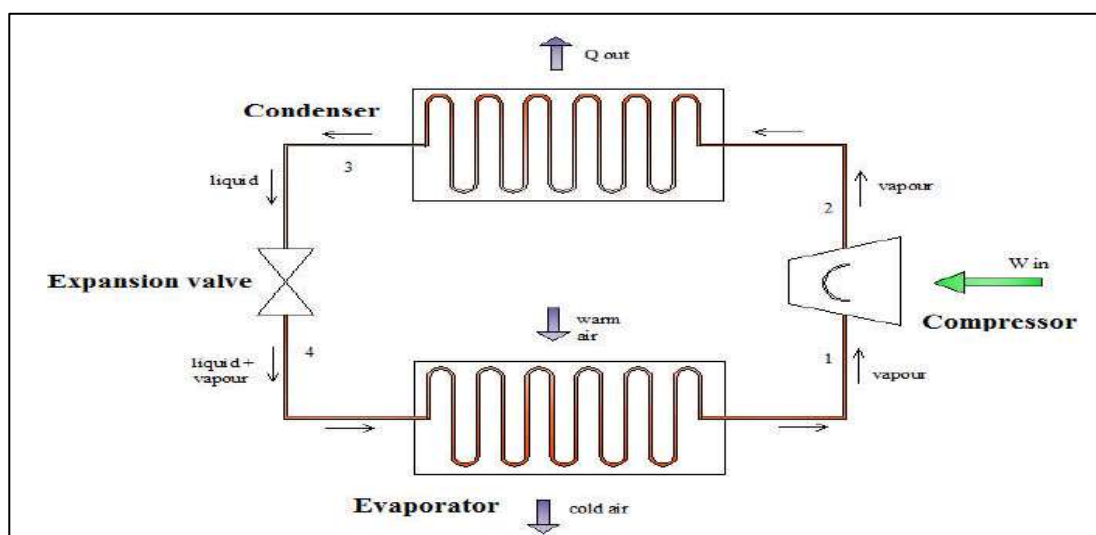


Figure (3.1): Schematic Diagram of the Unity Air Conditioning System.

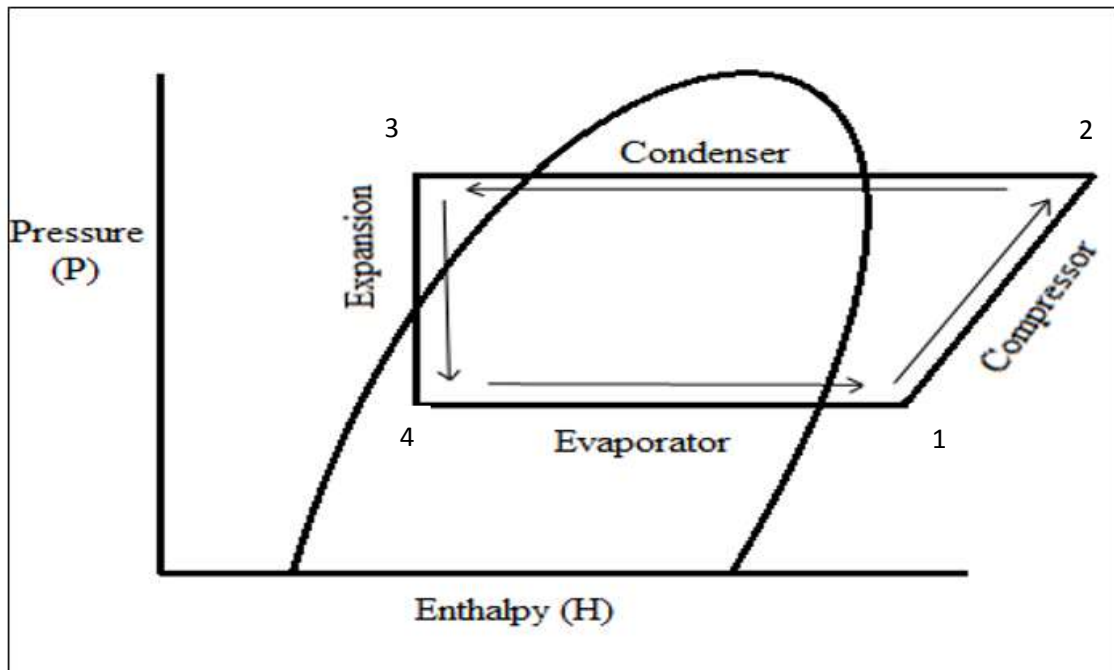


Figure (3.2): The Main Processes in the Air Conditioning.

3.3 Assumptions for the Experimental System

In this study, there are many assumptions related to the experimental system as mentioned below:

1. Steady state.
2. Newtonian flow.
3. One dimension.
4. No heat generation.
5. Constant heat flux.
6. Frictionless.

3.4 Equations of the components of unity air conditioning

3.4.1 Work input into the compressor

By increasing the temperature and pressure of the operating fluid, the energy has consumed in the compressor which, so the work input is given as [28]:

$$W_{in} = h_2 - h_1 \quad \dots (3.1)$$

Where

h_1 : The enthalpy inlet compressor.

h_2 : The enthalpy outlet compressor.

3.4.2 Heat transfer acquired from the evaporator

The heat is absorbed from conditioned space by evaporator. In this process, the working fluid is evaporating by acquired heat. So, the equation formula is given as [28]:

$$Q_{evap} = (h_1 - h_4) \quad \dots (3.2)$$

Where

h_4 : The enthalpy outlet evaporator

3.4.3 Coefficient of the Performance

The efficiency of air conditioning is represented as a Coefficient of Performance COP, which equals to the heat acquired from the evaporator (q_L) divided by the energy consumption in the compressor (w_{in}), where the energy consumption inversely effected on the COP, which can be calculated from the following equations [28]:

$$COP = \frac{Q_{evap}}{W_{in}} \quad \dots (3.3)$$

3.4.4 Pressure Ratio

Compressor pressure ratio is represented the air conditioning vapor pressure at the compressor discharge to vapor pressure at the compressor suction and is given as:

$$p_r = \frac{P_{dis}}{P_{suc}} \quad \dots (3.4)$$

3.5 Properties of the NonaffFluid

The nanoparticles firstly added to the lubricant oil then the mixture is mixed with the refrigerant, therefore, there are two steps for calculating the thermophysical properties of the final fluid Nano-Oil-Refrigerant. In the first step, the properties of nonalLubricant oil calculated according to the volume fraction of nanoparticle in the base fluid–lubricant-oil, so the mass fraction concentration should be converted to volume fraction concentration as in this equation:

$$\phi_n = \frac{\omega_n \rho_o}{\omega_n \rho_o + (1-\omega_n)\rho_n} \quad \dots (3.6)$$

And the mass fraction ω_n of the Nanoparticle/oil suspension concentration is [6]:

$$\omega_n = \frac{m_n}{m_n+m_o} \quad \dots (3.7)$$

The density of nonalubricant oil ($\rho_{n,o}$) can be determined from equation (3.7) [29]. In this study, the volume fraction in the original equation is modified by fraction mass:

$$\rho_{n,o} = (1 - \phi_n) \rho_o + \phi_n \rho_n \quad \dots (3.7)$$

Viscosity of the nanolubricant oil can be calculated from this equation [29]:

$$\mu_{n,o} = \mu_o \left[\frac{1}{(1 - \phi_n)^{2.5}} \right] \quad \dots (3.8)$$

Thermal conductivity can be found as in equation (3. 9) for nanolubricant oil, while the thermal conductivity of nano-oil-refrigerant determine from equation (3.10) as shown below:

$$K_{n,o} = K_o \frac{K_n + 2K_o - 2\phi_n(K_o - K_n)}{K_n + 2K_o + \phi_n(K_o - K_n)} \quad \dots (3.9)$$

Specific heat of the Nano lubricant oil and Nano-oil refrigerant are calculated from the equations below [30]:

$$C_{p,n,o} = (1 - \phi_n) C_{p,o} + \phi_n C_{p,n} \quad \dots (3.10)$$

3.6 Analysis of the Evaporator

3.6.1 Introduction

This section is concerned with analyzing the model of the evaporator by using the Computational Fluid Dynamics (CFD) simulation software in order to be compared with the experimental work. ANSYS 16.1 Workbench-Fluent is used in the present analysis. Three steps are done for simulation. Firstly, the geometry is designed in SpaceClaim after taking the necessary parameters from the test rig. Then, the meshing process is carried out in the workbench as a second step. Lastly, the definition of properties and boundaries are set in Fluent, so the iteration for solving the problem is run to record the analysis results.

3.6.2 Design the Geometry

The evaporator is an important part of the air conditioning system through which the heat transfer occurs with the air of condition space, so it is selected to portray the air conditioning system. The project is designed by using the ANSYS workbench SpaceClaim as shown in figure (3.3). The inner diameter of the pipe is (1) cm while the width of the evaporator is (41) cm for each (20) parallel rows as shown in figure (3.4). The thickness of the tube was neglected because of the high conductivity and easy analysis and the conditioned air is placed around this tube as shown in figures (3.4a) to (3.4c) respectively.

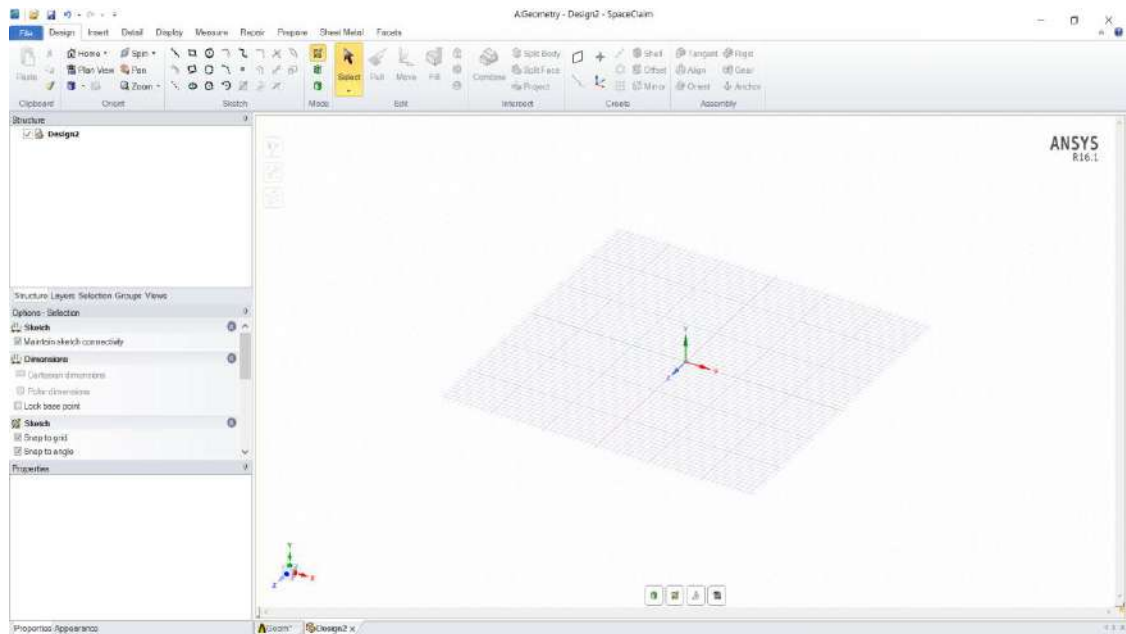


Figure (3.3): The windows of the ANSYS workbench SpaceClaim.

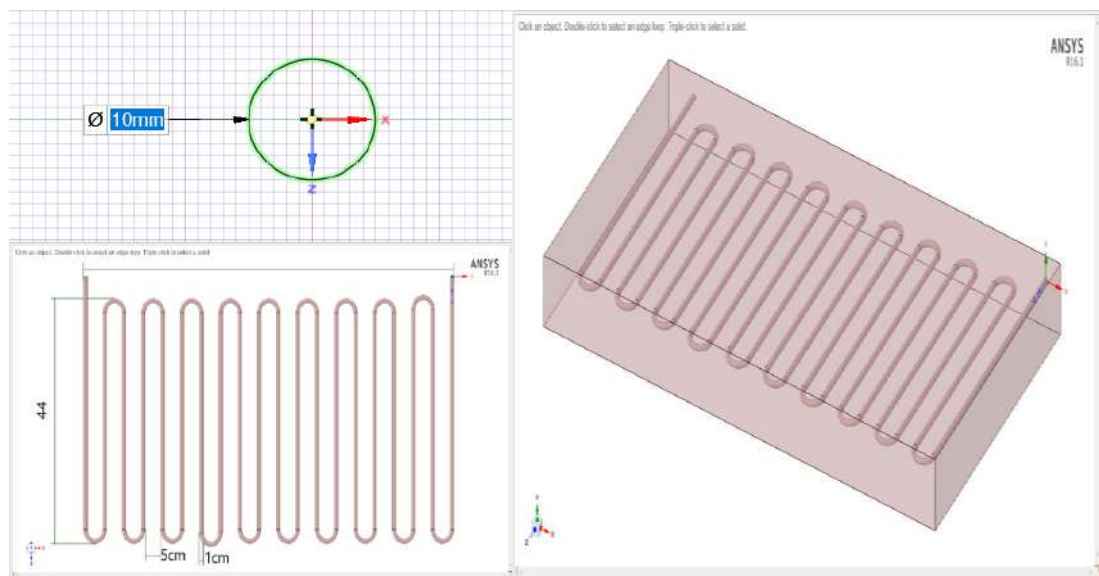


Figure (3.4): The designed project.

3.6.3 Mesh the Geometry

In the simulation, for any case, the mesh process is necessary for more accurate analysis. The project tube and its air surrounded are meshed in ANSYS workbench Fluent-meshing as shown in figure (3.5). The finite volume method is used in this problem where it is used for conservation of quantities. The number of the nodes and elements are

(7094106) and (32487636) respectively, while for the only tube are (1744158) nodes and (1596186) elements.

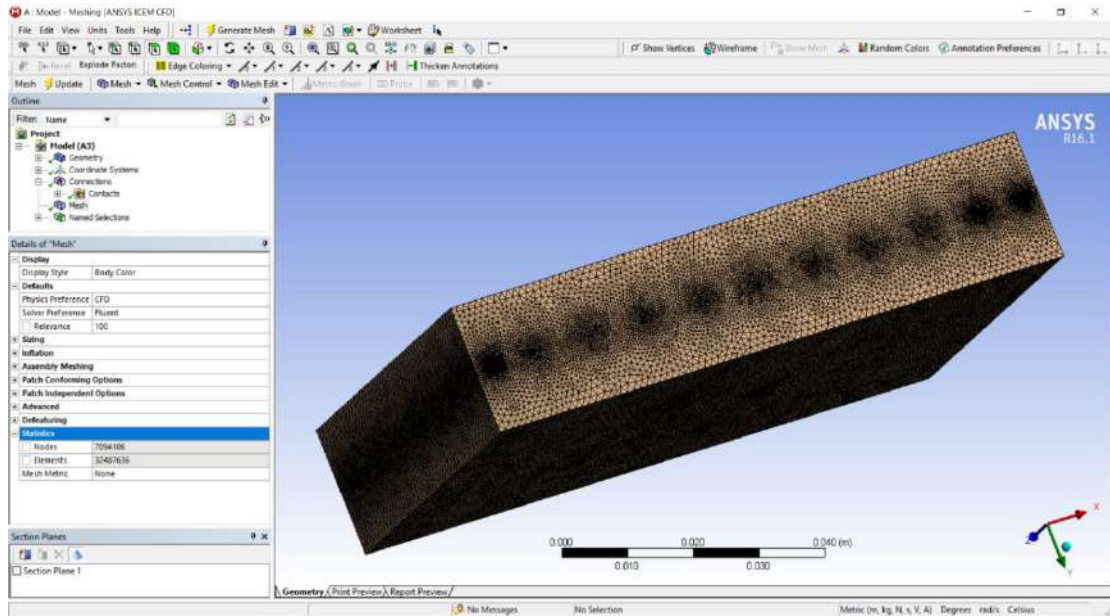


Figure (3.5a): The meshing process for all projects.



Figure (3.5b): The meshing process for the mesh of air.

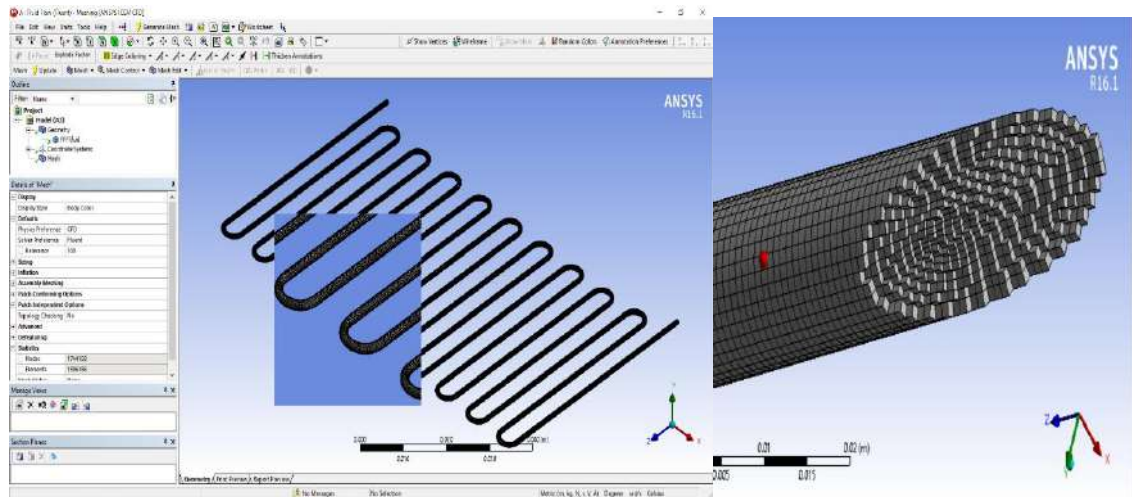


Figure (3.5c): The meshing process for the mesh of tube.

3.6.4 Analysis of the Project

After the designing and meshing steps of the project, the simulation process is started with Workbench-Fluent as shown in Figure (3.6).

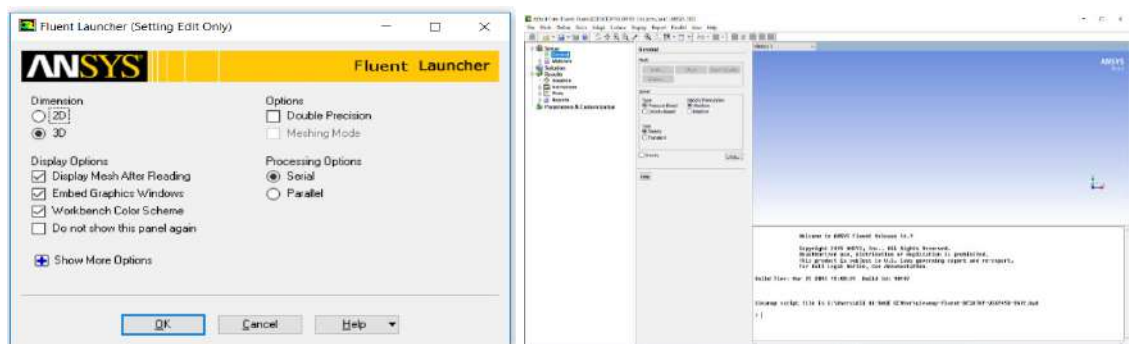


Figure (3.6): Fluent table.

The setup process is done according to the environment parameters of the experimental test such as the study time, the energy on the K-e model. Then, new material was input to the working fluid and selected the air as the materials and the working fluid gave the property of refrigerant R-22. The cells zone conditions of the refrigerant were selected for analysis without air to be easy. After that, the boundary conditions were set up such as the inlet velocity equal to (15) m/s with measuring temperature while the inlet air was equal to (6) m/s with 30°C environment

temperature. Finally, the iteration specified to run calculation is shown in figure (3.7).

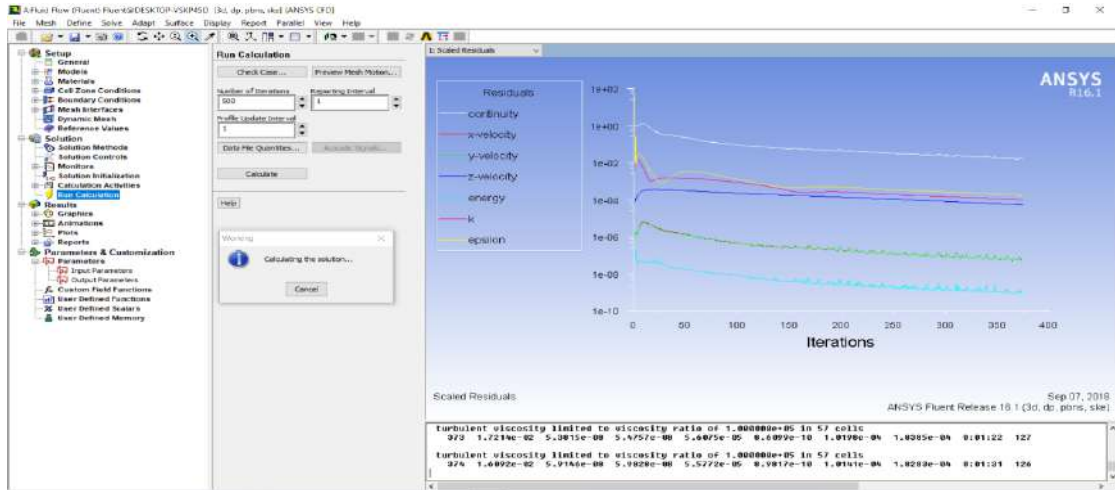


Figure (3.7): Iteration and run calculati

Chapter Four

Experimental Work

4.1 Introduction

This chapter deals with describing the steps of designing the experimental rig. The Coefficient of Performance (COP) is investigated in an air conditioning type window unit LG model (LWN224RH-4). Two types of nanoparticles are used for testing, i.e., metal oxide nanoparticles types (Al_2O_3) and basic metal nanoparticles types (Ag) with different mass concentrations (0.01, 0.05, 0.1, 0.15, 0.2) wt.% for each type of nanoparticles. The experimental rig was built to study the effect of adding the two types of nanorefrigerant in different concentrations on the efficiency of the air conditioning and the consumption energy and the refrigeration effect with the constant mass of refrigerant R22. This work was done in the fluid laboratory in the college of engineering at the University of Kerbela. This chapter includes four sections. The first section deals with the assembly of parts of the experimental rig, while the measurement instruments are explained in the second section. The third section explains the preparation of the nanofluid and the last section details the experimental testing.

4.2 The Testing Rig Design

Window type air conditioning is partially on a table with dimensions (180×80×75) cm. In addition, other minor parts which used in this system as shown in figure (4.12). These components are mentioned below:

1. Making the Frame

The test table is designed to place the testing parts on them. To facilitate the experiment, the dimensions of the table were selected as (180×80×75) cm. Figure (4.1) shows the manufacturing stages of the testing table.



a



b



c



d



e



f



g

h



i



j



k



1



m

Figure (4.1): The process of making the testing table.

2. Compressor: Two tons' rotary compressor as shown in the figure (4.2a) (MOD. QP376PBA A31DHF, SERIAL NO. 4ND02231-A-50M02-C00161) has been used in this work with the refrigerant R22

as a working fluid. The polyester oil (POE) is an ordinary lubricant in this compressor while the mineral oil 4E (MO4E) is a substitute for ordinary oil where the mineral oil is better than polyester oil [20]. To easy discharging and charging lubricant oil; two valves placed at inlet and outlet compressor in which the compressor is separated from the system by opening these valves as shown in figure (4-2b).



(a)

(b)

Figure (4.2): a. Compressor. b. The valves at inlet and outlet compressor.

3. **Condenser:** A circular copper tubes heat exchanger with dimensions (50×40×6) cm has been used as a condenser. The inner and outer of the pipe diameter was (9) mm and (10) mm respectively and the total length was (8) m. The refrigerant with high temperature and high pressure to flow in this pipe and the ambient air forced flow around the circular tube to acquire the heat from refrigerant R22 while the refrigerant rejected the heat to the ambient. A plate fins with (0.1) mm are surrounded these circular tubes that increase the processes of heat transfer. Figure (4.3) showed the condenser.
4. **Capillary tube:** The objective from the capillary tube is to get expansion in the pressure so it is represented as an expansion valve.

The inner and outer diameters are (1) mm and (3) mm respectively and the length is (150) cm. There are three pipes of the capillary tube in this system. They connected between the one pipe of the condenser and three pipes of the evaporator as shown in the figure (4.4).

5. Evaporator: A circular tubes heat exchanger with the dimensions (50×40×6) cm is used. There are three pipes in this heat exchanger, in addition, the fines with (0.1) mm thickness have surrounded these pipes. Each pipe with the inner and outer diameter (10) mm and (12) mm respectively. The evaporator placed after capillary tube and before the compressor and it absorbed the heat from the forced air of the conditioning place. Figure (4.5) shows the evaporator and its pipes.



Figure (4.3): The condenser.



Figure (4.4): The three Capillary tube.



Figure (4.5): Evaporator.

These parts mentioned above are formed the closed cycle for air conditioning system. While the minor parts in the present system will recall below:

6. Fan, blower and its motor: a fan placed before the condenser while the blower behind the evaporator to force the velocity of air that passes through the radiator of condenser and evaporator. So, it increased the heat transfer process between the refrigerant R22 and the air.

7. The Compressor of air: The testing of leakages in the present cycle has been through charging the system by the air compressor (AE 1345YU NO. 40581283) that shown in figure (4.6)



Figure (4.6): a- Compressor of air.

b- Vacuum of air.

8. The vacuum of air: the discharging of air from the closed cycle has been done by a vacuum motor which is shown in figure (4.6b) before each charging of refrigerant.
9. The two ducts: at the inlet air for the evaporator, a duct with dimension cross section (42×40) cm and the depth (50) cm put to overcome the air.
10. Heater resistance: the heater is placed at the beginning of the duct to make the input air to the evaporator at a constant temperature.

4.3 The Measurement Instrument

The experimental data have been recorded by using the following apparatuses:

- a. Thermocouples and Thermometer: Eight thermocouples type K are used to measure the temperature which converted to reading data by using thermometer device (12 channels, BTM- 4208SD, SD storage), Six

thermocouples are located on the surface of the refrigerant pipes at the inlet and outlet of each compressor, condenser, and evaporator. The two others were placed at the air input and output over the evaporator.

- b. Pressure Gauge: Three electronic gauges pressure are placed at the inlet and outlet compressor and outlet condenser, in addition, three digital pressure gauges located at the inlet and outlet evaporator and inlet condenser.
- c. Hot Wire: the conditioned air that flows through the evaporator has been measured by using a hot wire
- d. Voltmeter and Ammeter: the voltmeter is connected in parallel with the compressor and the ammeter put in series with this circle.
- e. Electronic Weight: The mass of the refrigerant has been weighted by using electronic refrigerant programmable charging scale balance (RCS-N9030).

4.4 Preparation of Nano Fluid

4.4.1 Selection of the Type of Nano Material and its Amount

Two types of Nano powder have been selected in this study. They are (Al₂O₃) and (Ag) with a size of (20) nm. It was bought from US Nano Inc. as shown in the appendix (A-1). The masses are weighted with respect to mass fraction concentration as shown in figure (4.7).



Figure (4.7): Electronic weight.

4.4.2 Mixing the Nano with Lubricant oil

The Nano powder is mixed with the base fluid in several ways. In the present work, three steps for mixing were used. Firstly, the weighted amount was added to a part of the total (150) ml oil and stirred by using a magnetic stirrer device at 50 °C for (15) min. In the second step, the mixture was suspended by ultrasonic vibration mixer at 40 °C for (10) min. In the last step, the sample added to the total pure oil (550) ml then it mixed in the mechanical mixture for (45) min at 70°C. Figure (4.8) shows the devices of mixing.



a



b



c

Figure (4.8): Devices of mixture.

4.4.3 Mixing the Nano Lubricant oil with the refrigerant R22

Preparation the nanorefrigerant is difficult in any environment so the pooling point was $(-40)^\circ\text{C}$ for atmospheric pressure. Therefore, the Nano powder, firstly, mixed with the lubricant oil then mixed with the refrigerant fluid. When the nano lubricant oil charged in the compressor unit, then some oil will recirculate in the refrigeration cycle and this led to mixing the nano lubricant.

4.5 Experimental Testing

The present experimental testing has been done in several steps as explained below:

4.5.1 Charging the Nano Lubricant

In a rotary compressor, there are two pipes; one of them was used as the inlet for the working fluid and the other was the outlet of that fluid. The charging valves were located in both of these pipes to easy used in evacuation and adding the lubricant oil as well as charging the refrigerant by them. The evacuation process of the lubricant oil has been done through separating the compressor from the system by opening the valves and then the compressor was overturned. After the lubricant oil is discharged, the prepared lubricant oil sample will be charged in compressor through the outlet pipe as shown in figure (4.9). At last, the compressor was returned to the system and connected with the closed cycle. These steps repeated at each concentration mass for both types of Nano powder.



Figure (4.9): Process of charging the lubricant oil.

4.5.2 Testing the Leakage by Charging the Air

The closed refrigeration cycle was examined for leakages after connecting the compressor. This testing has been done through charging the cycle by air at a pressure higher than the required pressure for

refrigerant R22. The compressor device (AE 1345YU NO. 40581283) was used for this process. The air remained in the refrigeration cycle for (40) min and the pressure was noted as well as the sensor of the leak was used to ensure if there was any leak and found the place in the cycle.

4.5.3 The Vacuum of the Closed System

The cycle was emptied from the air and made in a vacuum pressure at (0.8) bar gauge under the atmospheric pressure. The vacuum air device has been used.

4.5.4 Charging the Refrigerant R22

The refrigerant R22 was the working fluid in this study. After complete the above steps, the cycle was ready to charge the refrigerant R22. The amount mass of refrigerant R22 was specified as (2) kg in each concentration mass of nano powder, therefore the electronic balance device (RCS-N9030) was used for weighting the refrigerant R22 mass that charged in the refrigeration cycle. The weighed balance was zero before using it then the refrigerant R22 bottle put on the electronic balance and read the value of this mass as a reference reading. The tube was connected between the refrigerant bottle and inlet pipe of the compressor where the valve located. The valve opened to flow the refrigerant and it closed when there was a reduction in the mass by (2) kg which showed in the read data of the electronic balance. Figure (4.10) indicated this balance.



Figure (4.10): electronic balance for charging the refrigerant.

4.5.5 Reading the Experimental Data

After the working fluid was stabilized in the refrigerant cycle, the system was operated for more than half an hour so that the readings reach a stable state. The readings of pressure, temperature, voltages and current were taken. Figure (4.11) showed the location of the thermocouples and pressure gauges in the system. The pressure gauges located at a different places that are at inlet and outlet compressor, inlet and outlet evaporator and outlet evaporator. In addition, one pressure gauge which measured the total pressure where the pitot tube put at the outlet compressor in line with the direct flow of the refrigerant R22 to enable the mass flow rate in the inner cycle. The thermocouples also located in different places of the system and they are at the same places as the set of the pressure gages as the inlet condenser and at the inlet and outlet of the air of conditioning place which across through the evaporator.

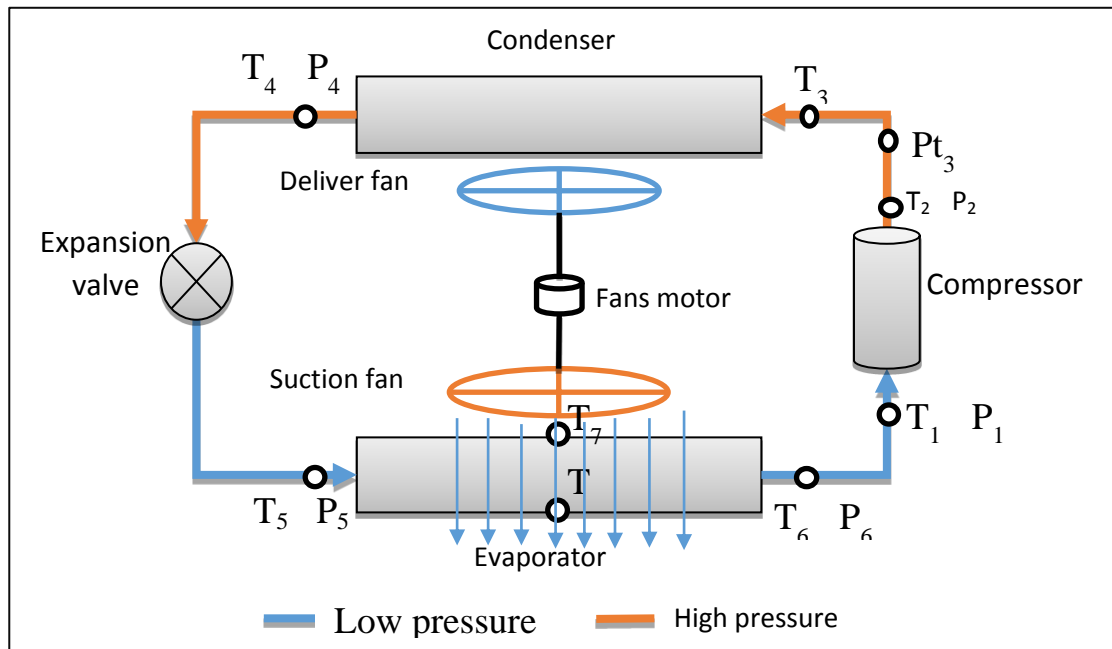


Figure (4.11): Schematic diagram of the system that explains the location of the pressure gauges and thermocouples.

4.5.6 Calculating the Result

From the read experimental data and the R22 refrigeration chart (Licensed for single user. © 2009 ASHRAE, Inc.), the thermodynamic properties can be calculated like density, enthalpy, entropy, then applying the refrigeration equation to calculate the power input, refrigeration effect and the coefficient of performance.



Figure (4.12): The experimental rig with their parts.

Chapter Five

The Results and Discussion

5. Introduction

After performing the experimental and theoretical study, it has become important to know the effect of using the two types of nanofluid (R22-Al₂O₃) and (R22-Ag) on the heat transfer enhancement. The experimental findings were extracted from measuring the temperature and pressure at specified locations described previously in chapter four. On the other hand, the numerical results were performed by using ANSYS/Fluent to simulate the pressure and temperature through the evaporator of the refrigeration system.

5.1 The Experimental Results of the Test Rig

As soon as the test rig reached the stable state, all the readings of the temperatures and static pressures can be taken at different positions. The test was work with different kinds of working fluid which are: pure refrigerant (R22), and two types of nanofluid (R22-Al₂O₃, R22-Ag) in order to decide which one can give the better performance of the air condition system.

5.1.1 Temperature

Figure (5.1) shows the relationships between the inlet temperature of the compressor and the nano concentration for the two kinds of the nanoparticles. It is appearing that the temperature increase with concentration and the maximum value was (22.7) at 0.2% of Ag nanoparticles. In figure (5.2), the outlet temperature of the compressor was indicated with mass fraction concentration. Increasing this concentration led to a decrease in the temperature until it reached the critical point where

this temperature was increased and it found 0.15% for both Ag and Al₂O₃ nanoparticles. In each concentration, the Ag was better than Al₂O₃ and the minimum temperature was (77.5) at 0.15 of Ag nanoparticles.

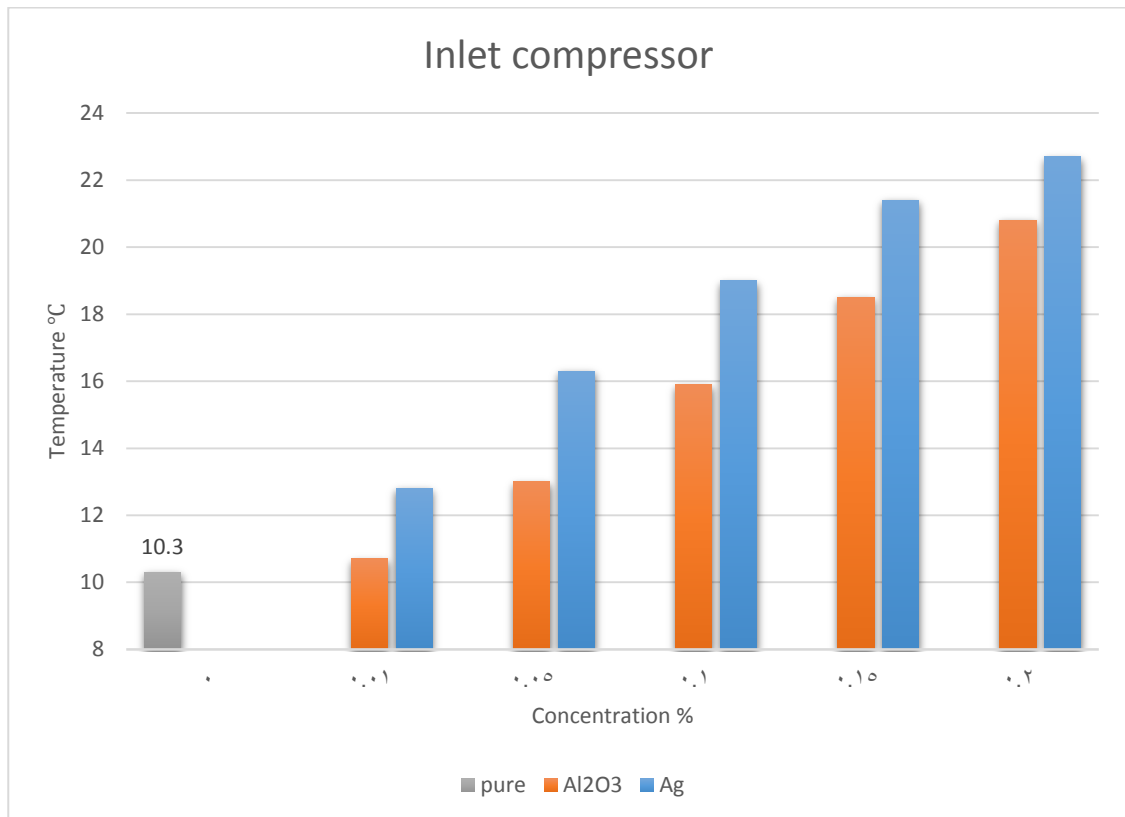


Figure (5.1): The temperature of the compressor inlet with the concentration.

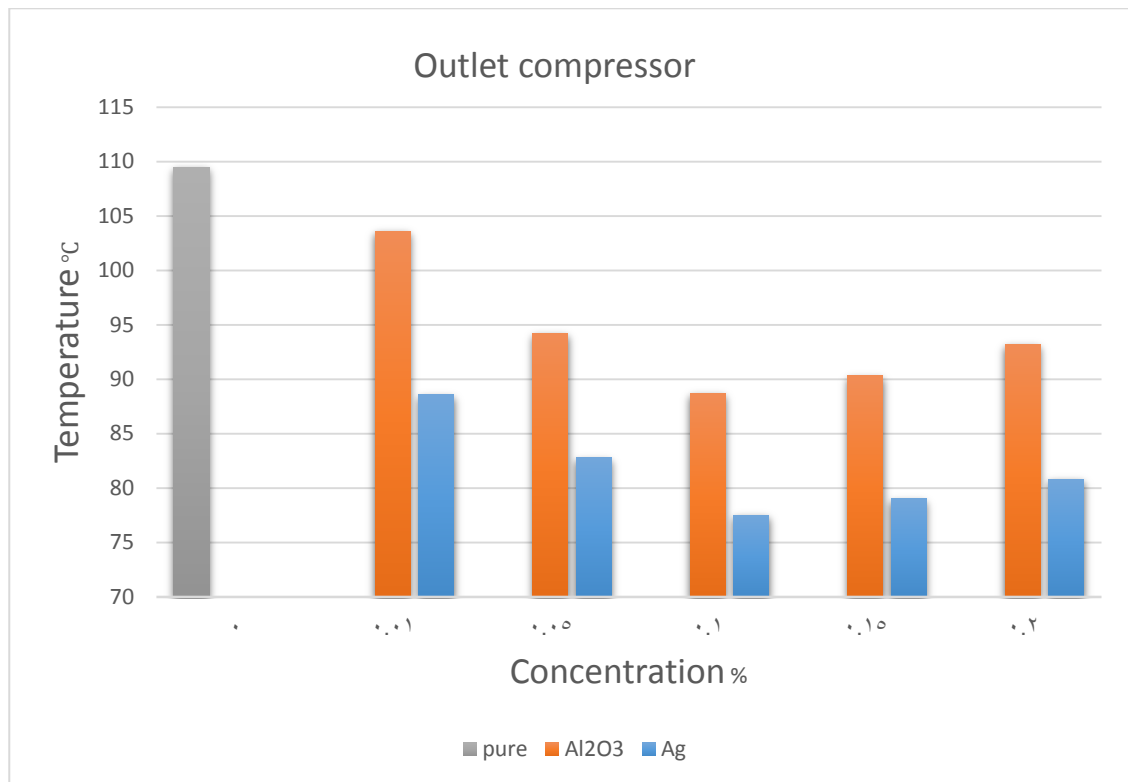


Figure (5.2): The temperature of the compressor outlet with the concentration.

The temperature decrease with the concentration at the evaporator inlet while increase at the outlet for both Al₂O₃ and Ag nanoparticles as shown in figures (5.3) and (5.4) respectively and it found that the Ag-R22 was better.

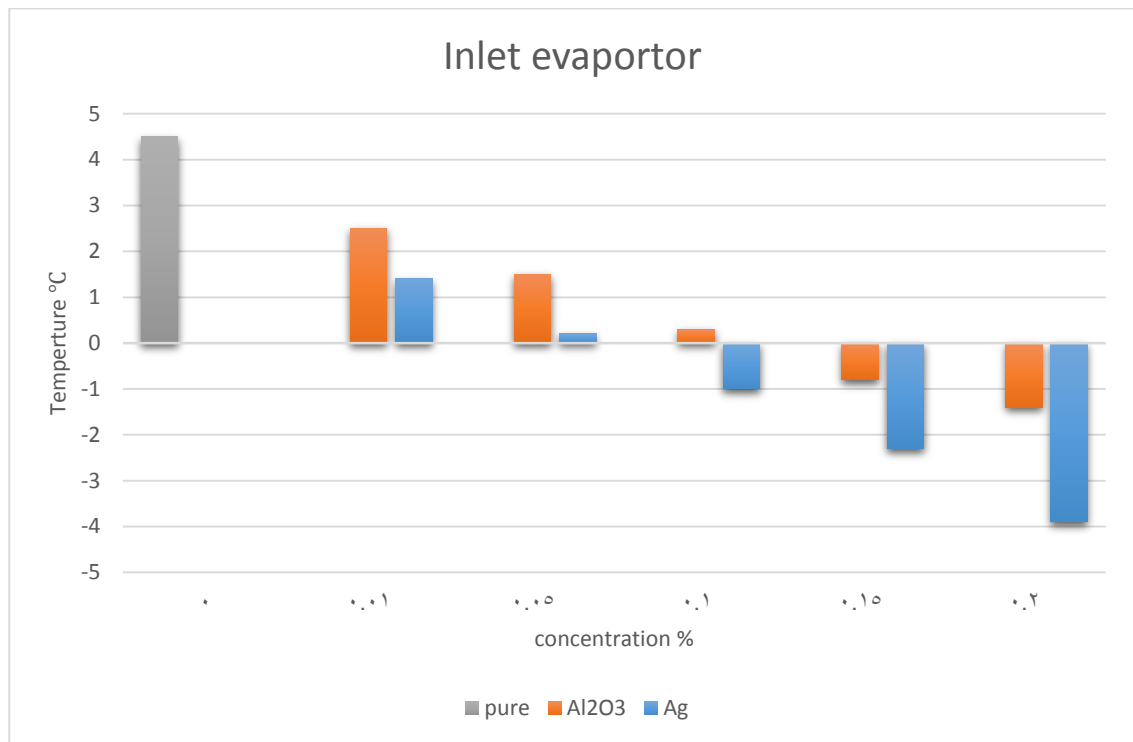


Figure (5.3): The temperature of the evaporator inlet with concentration.

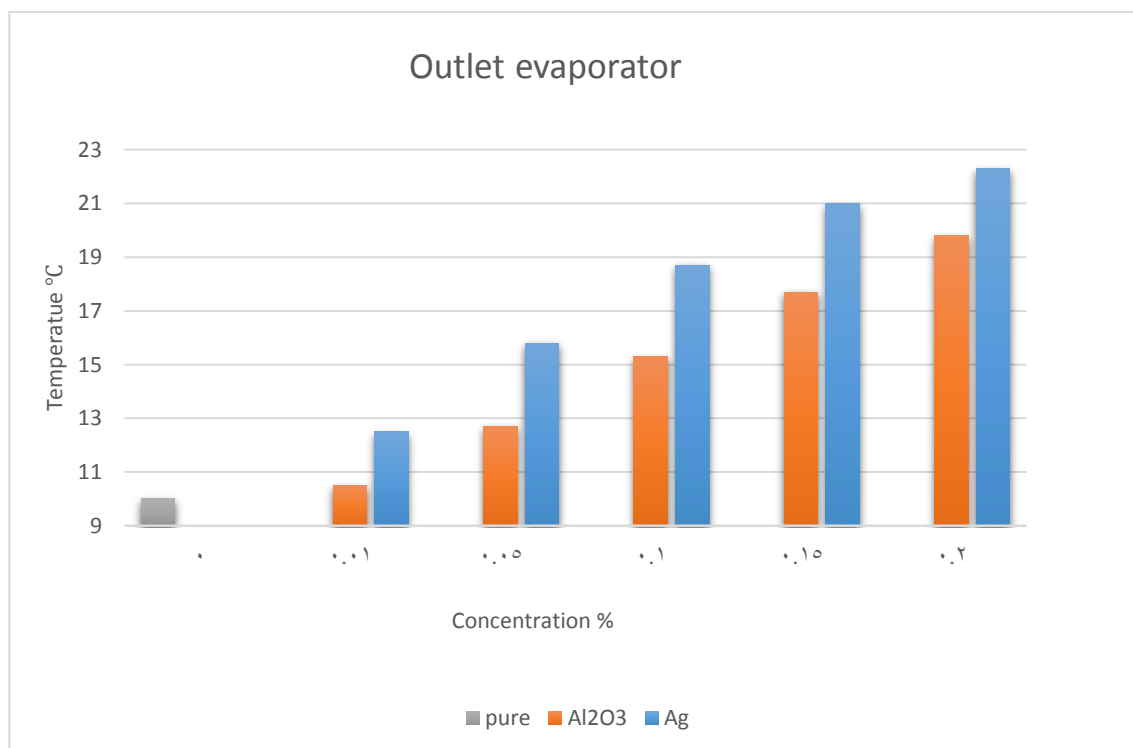


Figure (5.4): The temperature of the evaporator outlet with the concentration.

The different temperature between the evaporator inlet and outlet was indicated in the figure (4.5) for the pure refrigerant R22 and two types of nanorefrigerant R22-Al₂O₃ and R22-Ag, at each concentration and the

enhancement in ΔT is shown in figure (4.6). So, it increased with the concentration and the R22-Ag was better than R22-Al₂O₃ which the maximum enhancement was 274.28 at 0.2% Ag concentration.

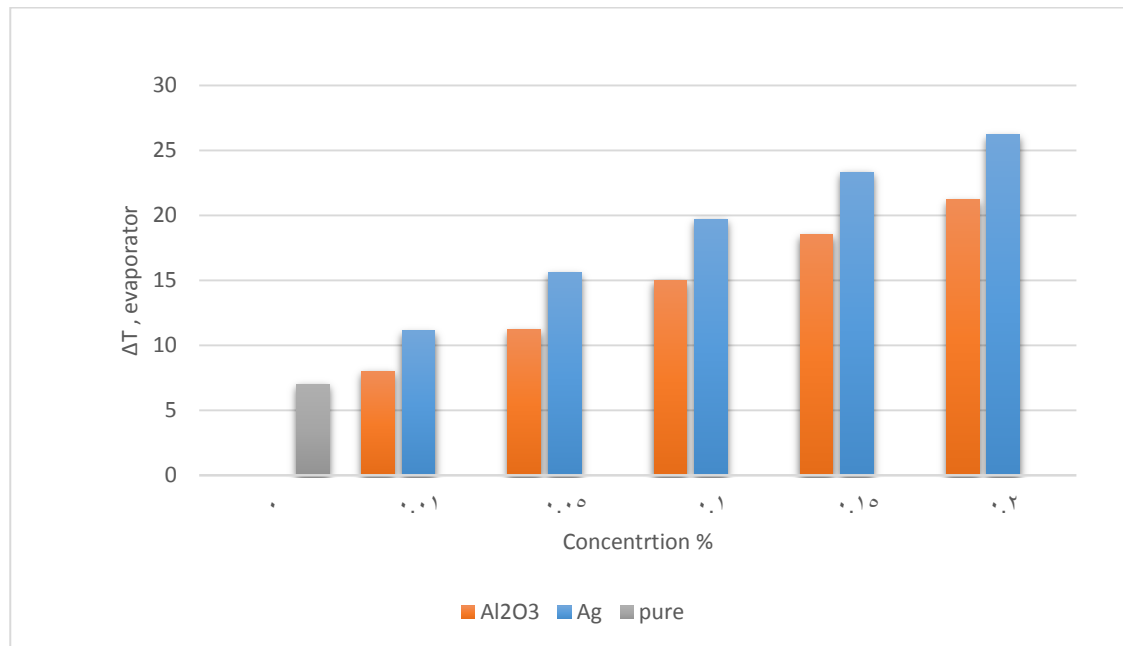


Figure (5.5): Different temperature of the evaporator with concentration.

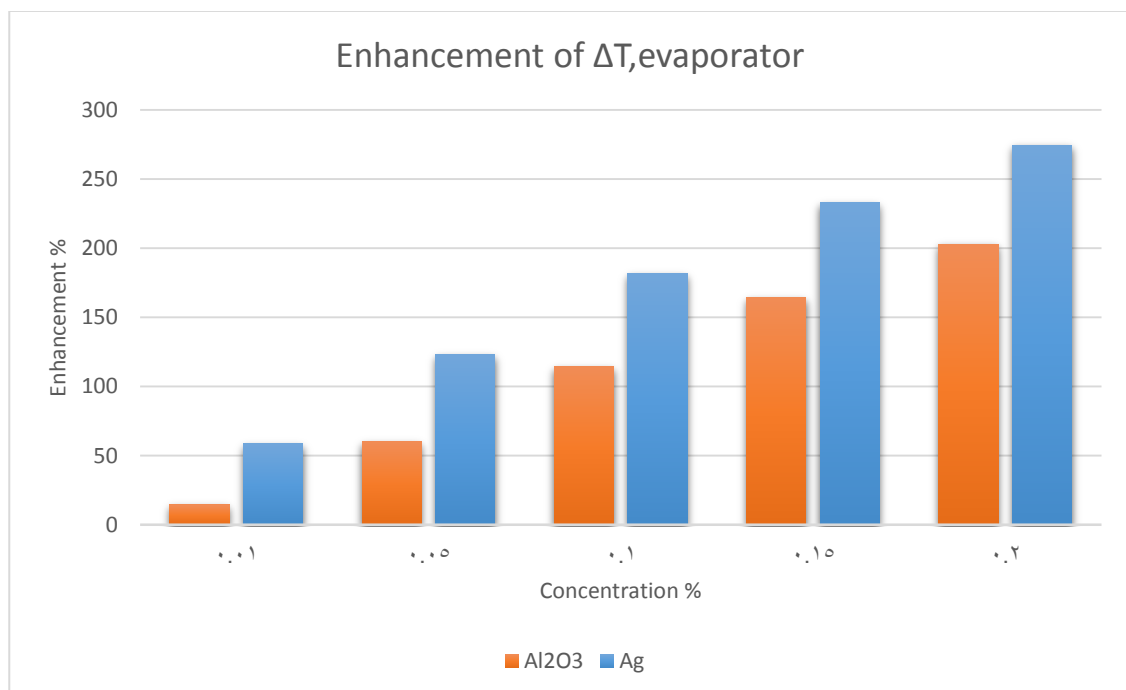


Figure (5.6): Enhancement the evaporator in different temperature with concentration.

Figure (5.7) shows the air temperature of conditioning space which decreases with concentration. Figures (5.8) and (5.9) indicate the

different temperature and the enhancement of the air conditioning space with a concentration of the nanoparticles. In each concentration, adding the Ag nanoparticles was better than Al₂O₃ nanoparticles and the maximum improvement was (263.33) at 0.2% Ag.

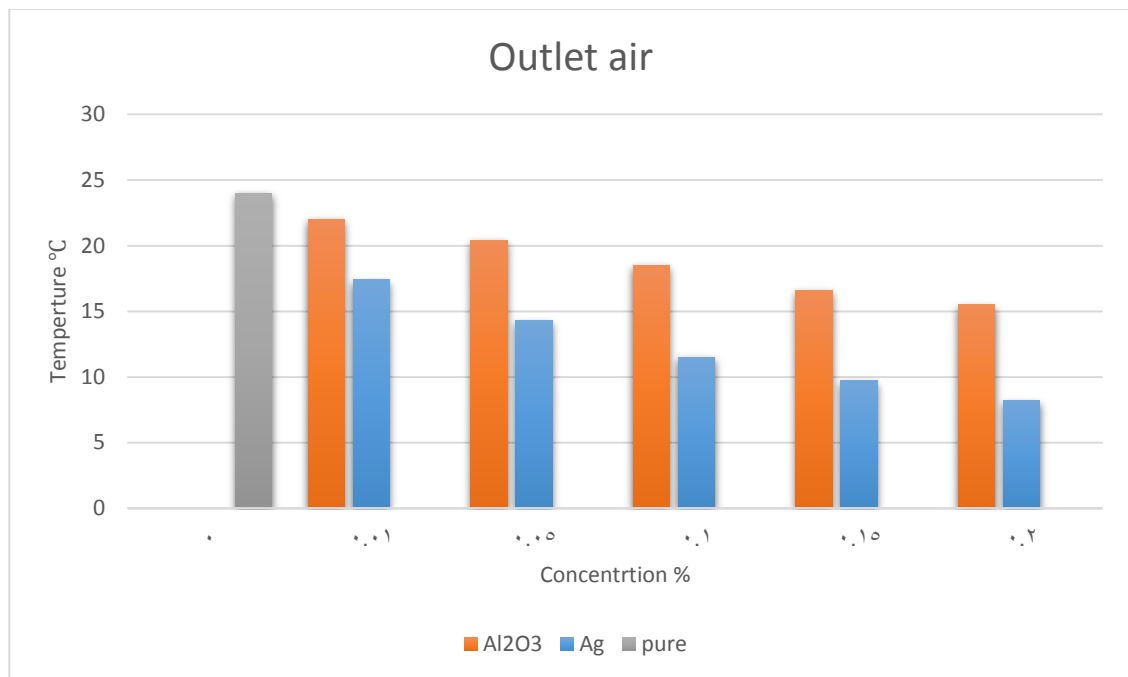


Figure (5.7): The temperature at the outlet air with the concentration.

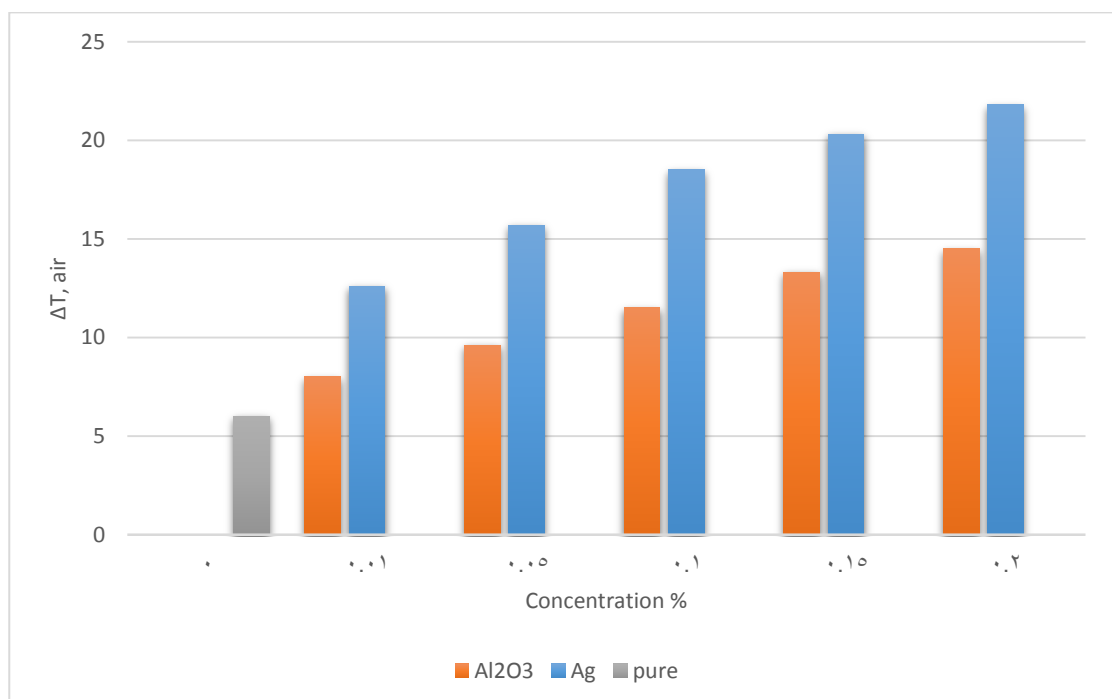


Figure (5.8): The different temperature of the air with the concentration.

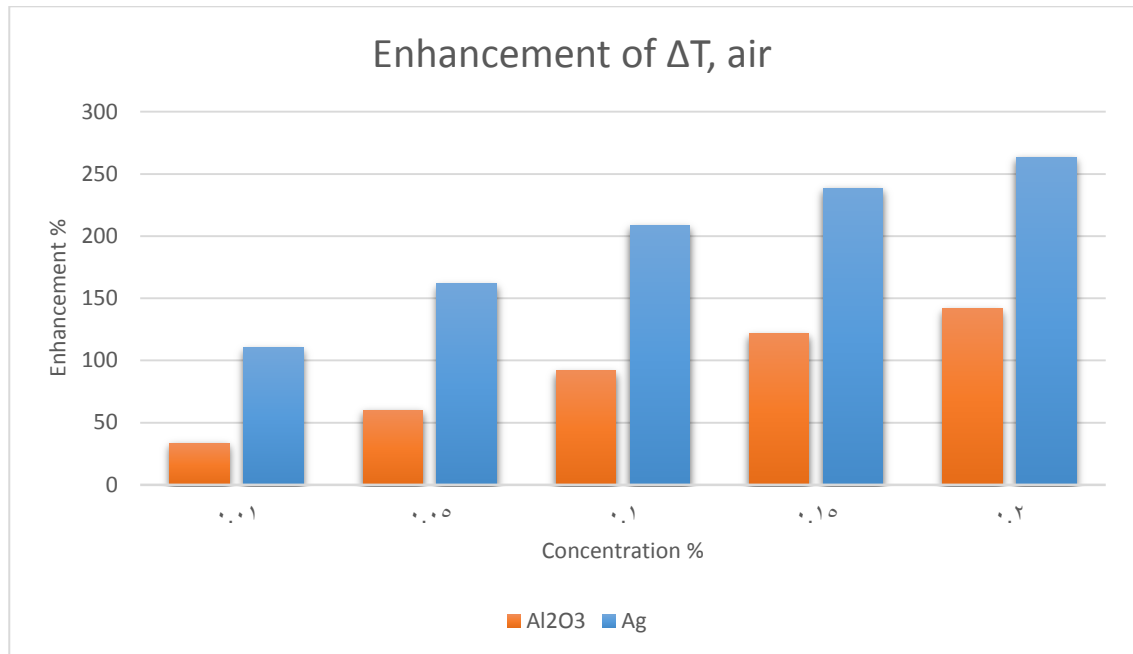


Figure (5.9): Enhancement in different temperature of the air with concentration.

5.1.2 Pressure

Figures (5.10), (5.11), (5.12) and (5.13) show the decreasing of the pressure with increasing the concentration of nanoparticles at inlet and outlet of the compressor and, inlet and outlet of the evaporator respectively for pure R22 and the two types R-Al₂O₃ and Ag-R22 of nanorefrigerant. Figures (5.14) and (5.15) show the pressure at all previous locations for R22-Al₂O₃ and R22-Ag respectively.

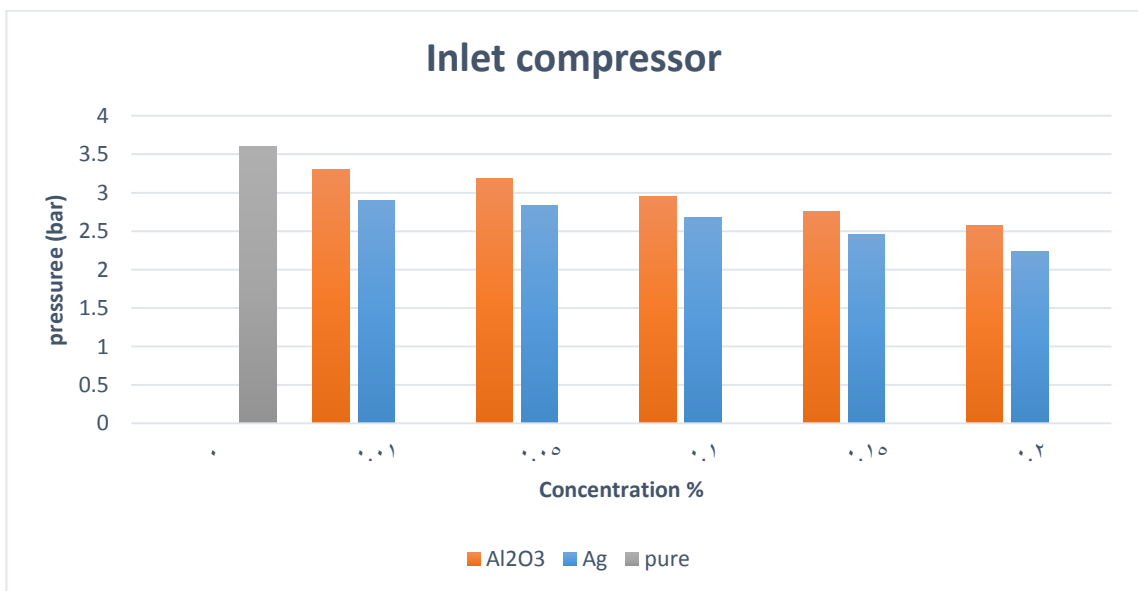


Figure (5.10): The pressure at the compressor inlet with the concentration.

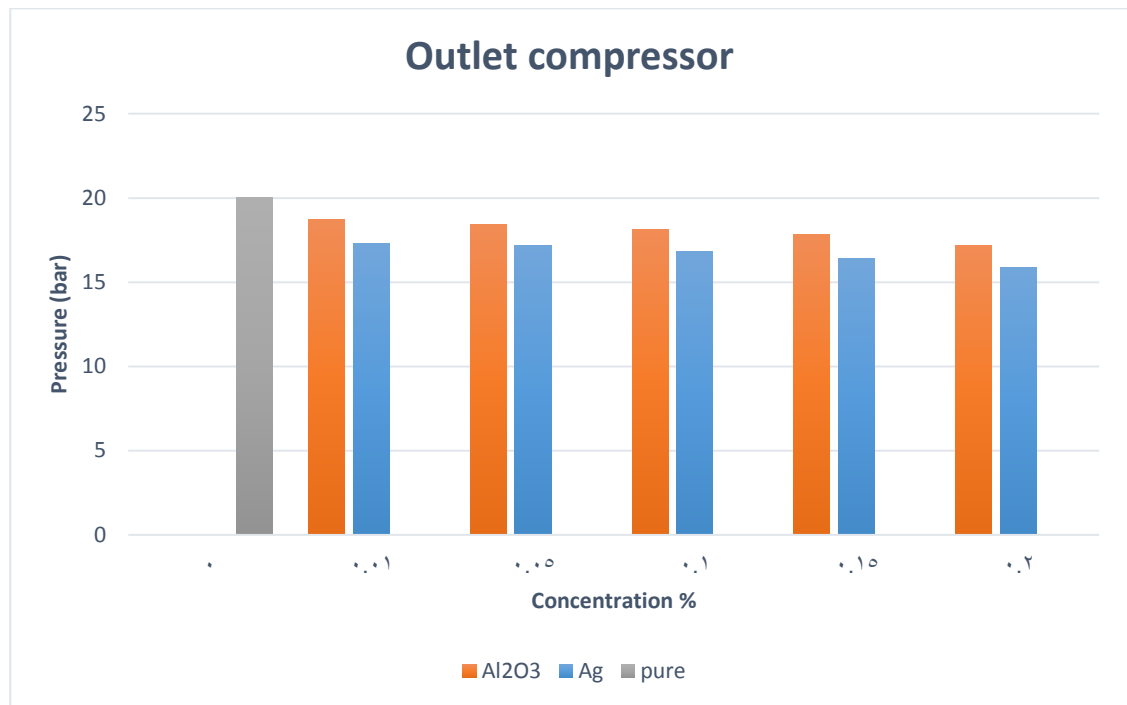


Figure (5.11): The pressure at the compressor outlet with the concentration.

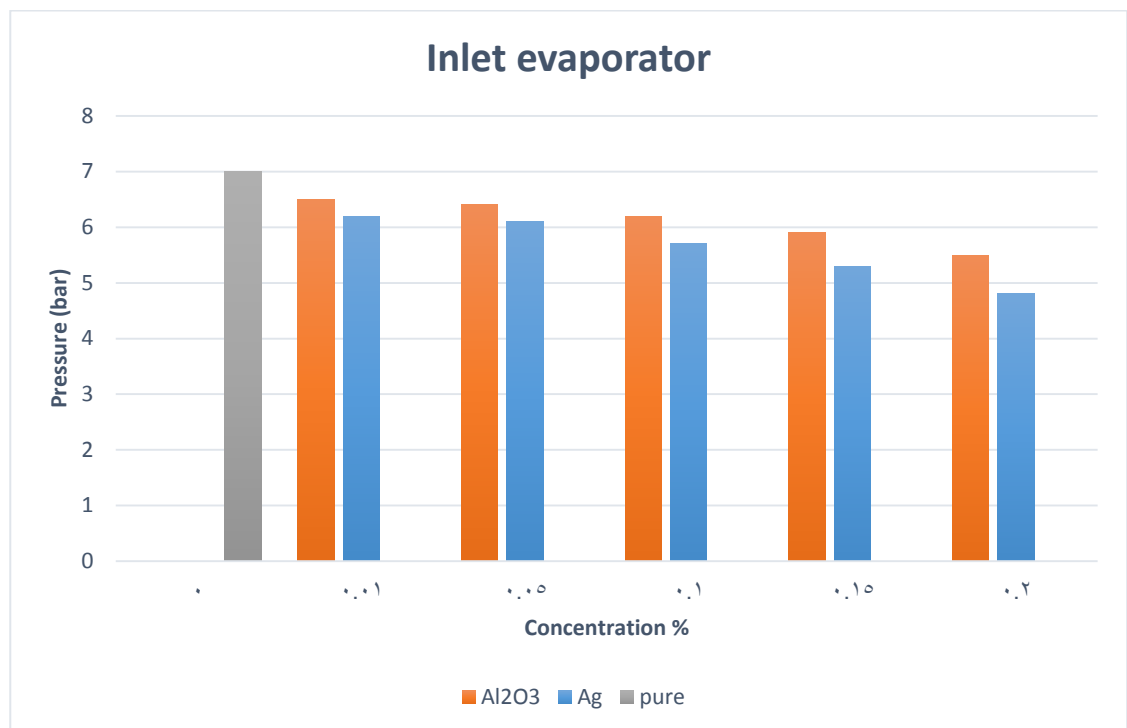


Figure (5.12): The pressure at the evaporator inlet with the concentration.

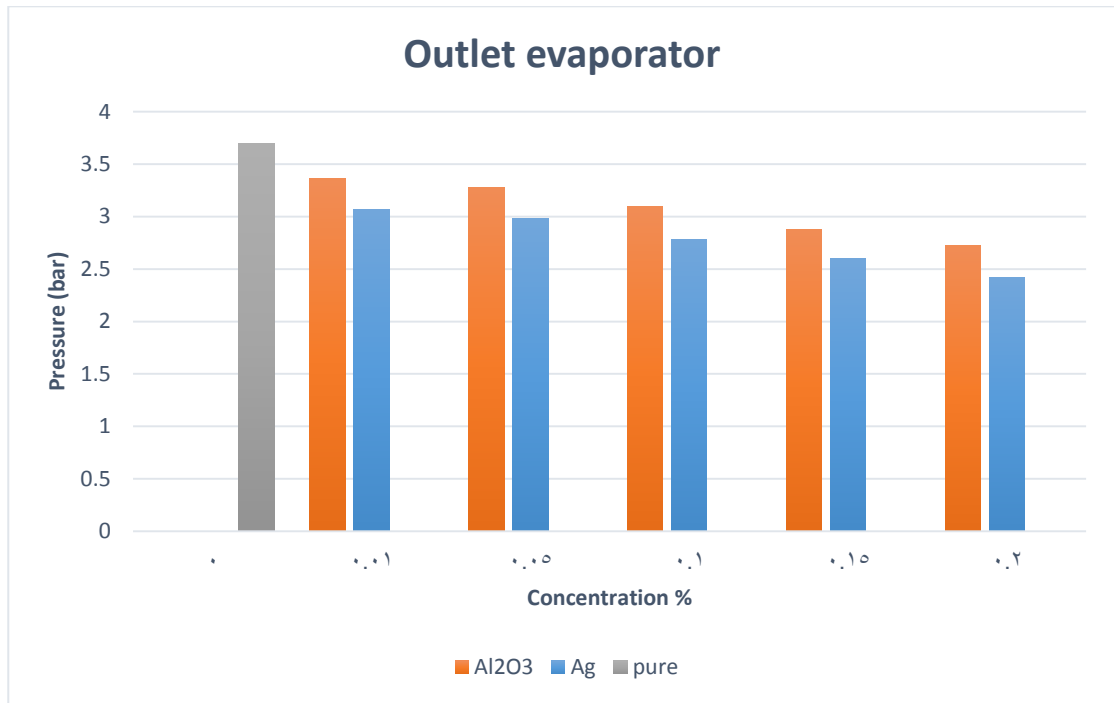


Figure (5.13): The pressure at the evaporator inlet with the concentration.

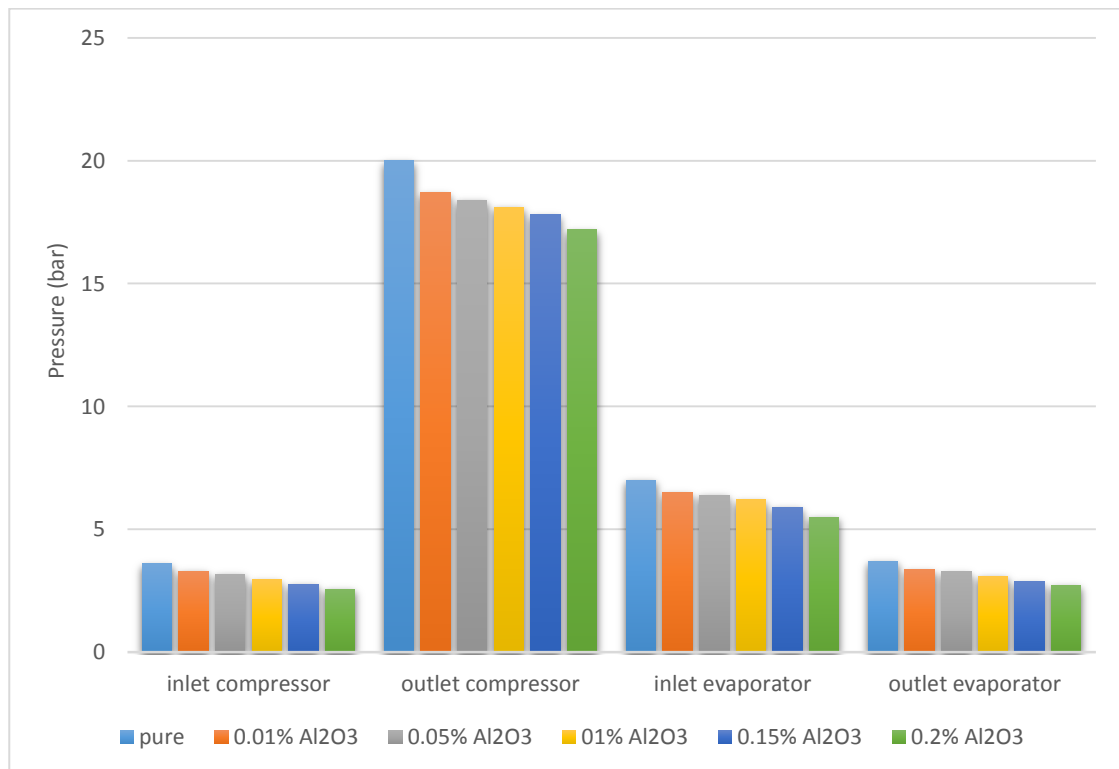


Figure (5.14): The pressure at different positions with Al₂O₃ Nano concentration.

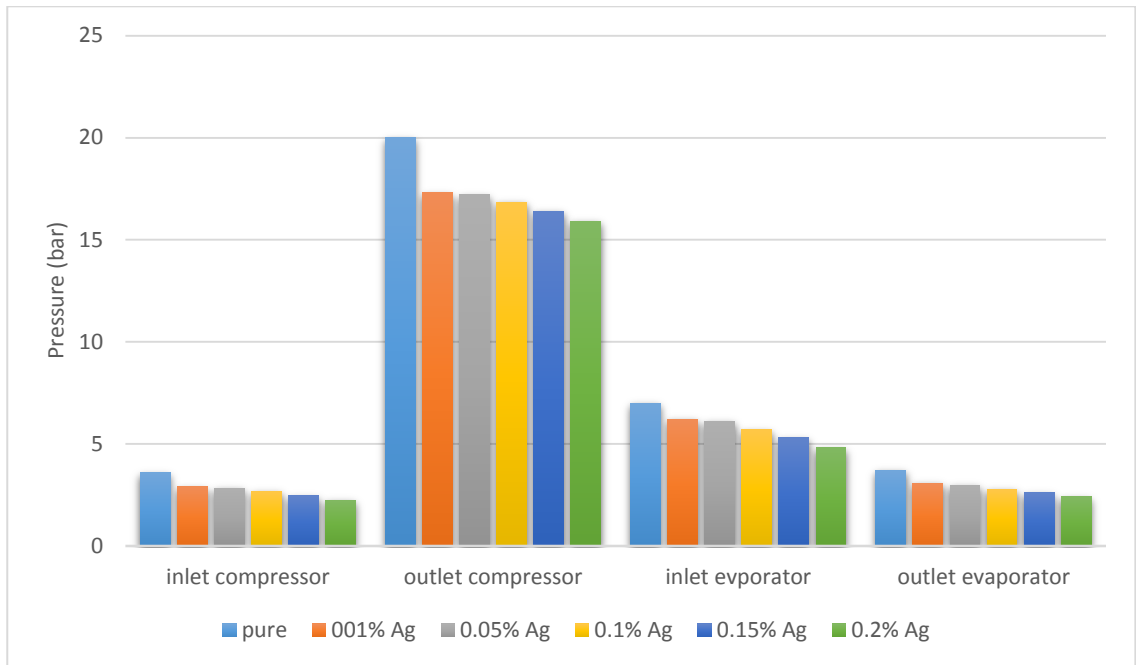


Figure (5.15): The pressure at different positions with Ag Nano concentration.

Figure (5.16) shows the pressure ratio for each pure and two types of nanorefrigerant Al₂O₃-R22 and Ag-R22. It was found that the pressure ratio increase with increasing nanoparticles concentration, in addition, the Ag-R22 was better than Al₂O₃. The improvement in the pressure ratio indicates in figure (5.17) were explaining the increase in enhancement with increase the nano concentration and the Ag-R22 nanorefrigerant was better than Al₂O₃-R22.

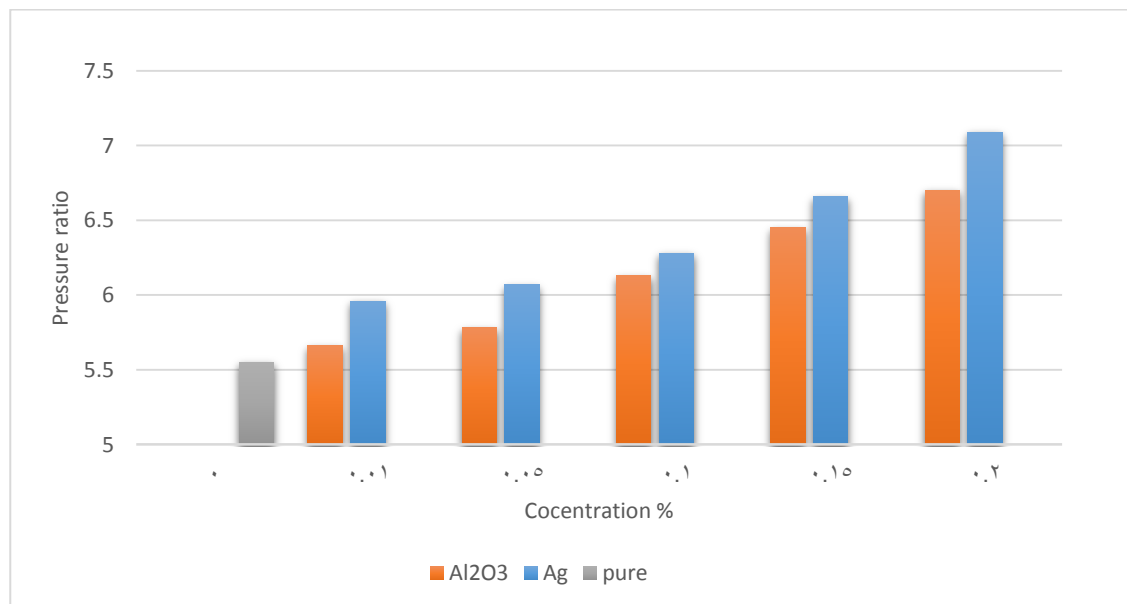


Figure (5.16): The pressure ratio with the concentration.

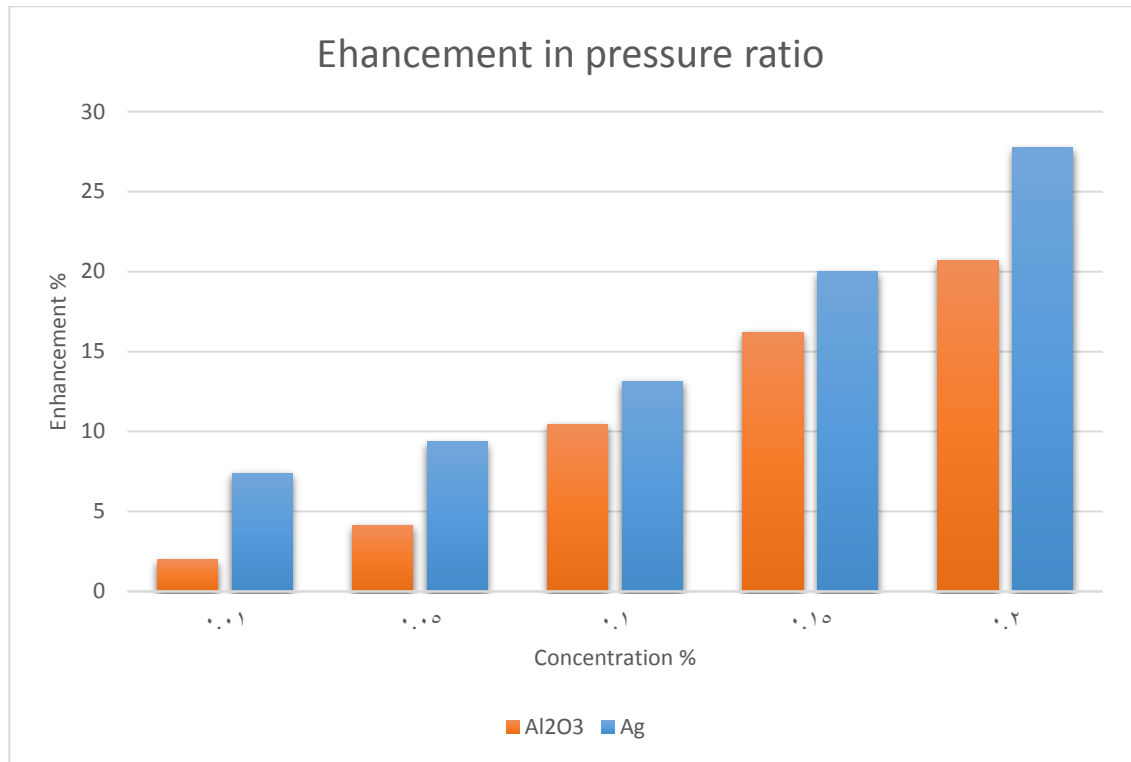


Figure (5.17): The enhancement in the pressure ratio with the concentration.

5.2 Calculated The Results

5.2.1 Enthalpy

Figures (5.18), (5.19), (5.20) and (5.21) show the enthalpy per mass with the concentration of nanoparticles for pure refrigerant R22 and two kinds of nanorefrigerant Al₂O₃-R22 and Ag-R22. The enthalpy in each case was calculated from the measured temperature and the pressure by using data table R22. Figures (5.18) and (5.21) show the enthalpy at the compressor inlet and the evaporator outlet respectively where the enthalpy increase with increasing the nano concentration and the Ag-R22 nanorefrigerant was more than Al₂O₃-R22. While decreasing the enthalpy with nano concentration at the compressor outlet and the evaporator inlet as shown in figures (5.19) and (5.20) respectively.

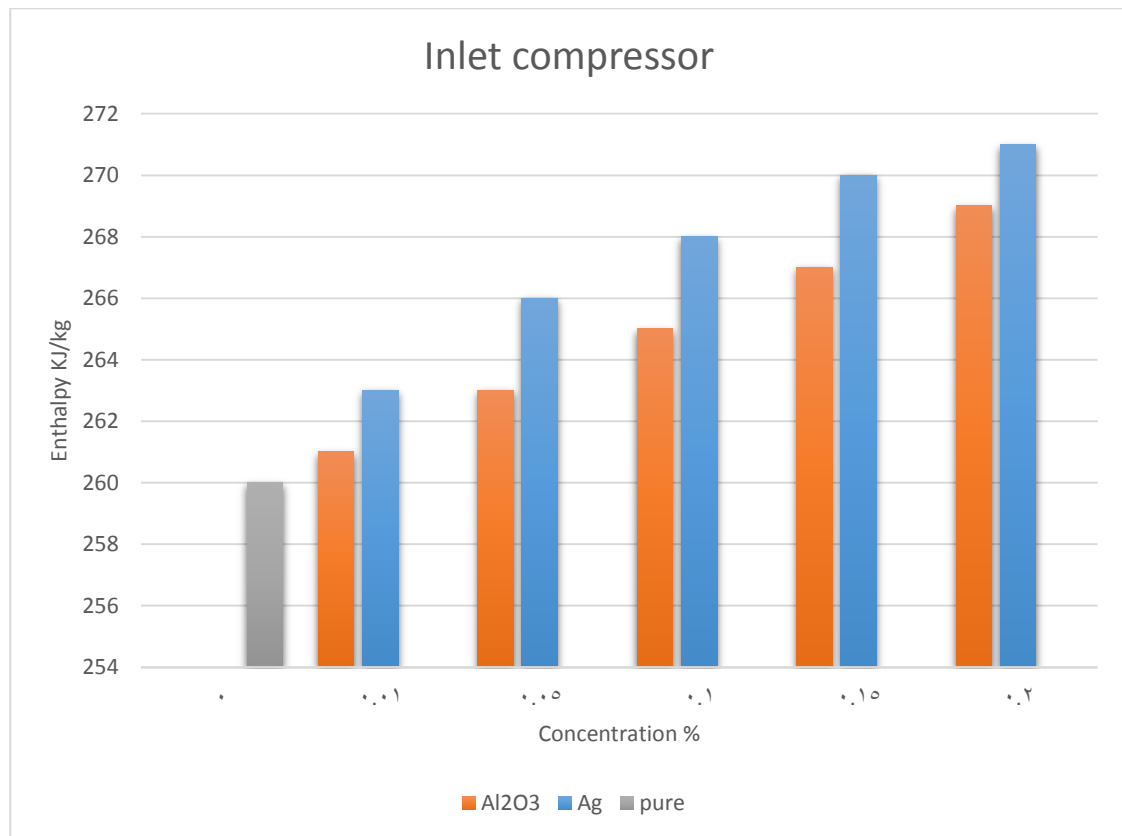


Figure (5.18): Enthalpy with concentration at the compressor inlet.

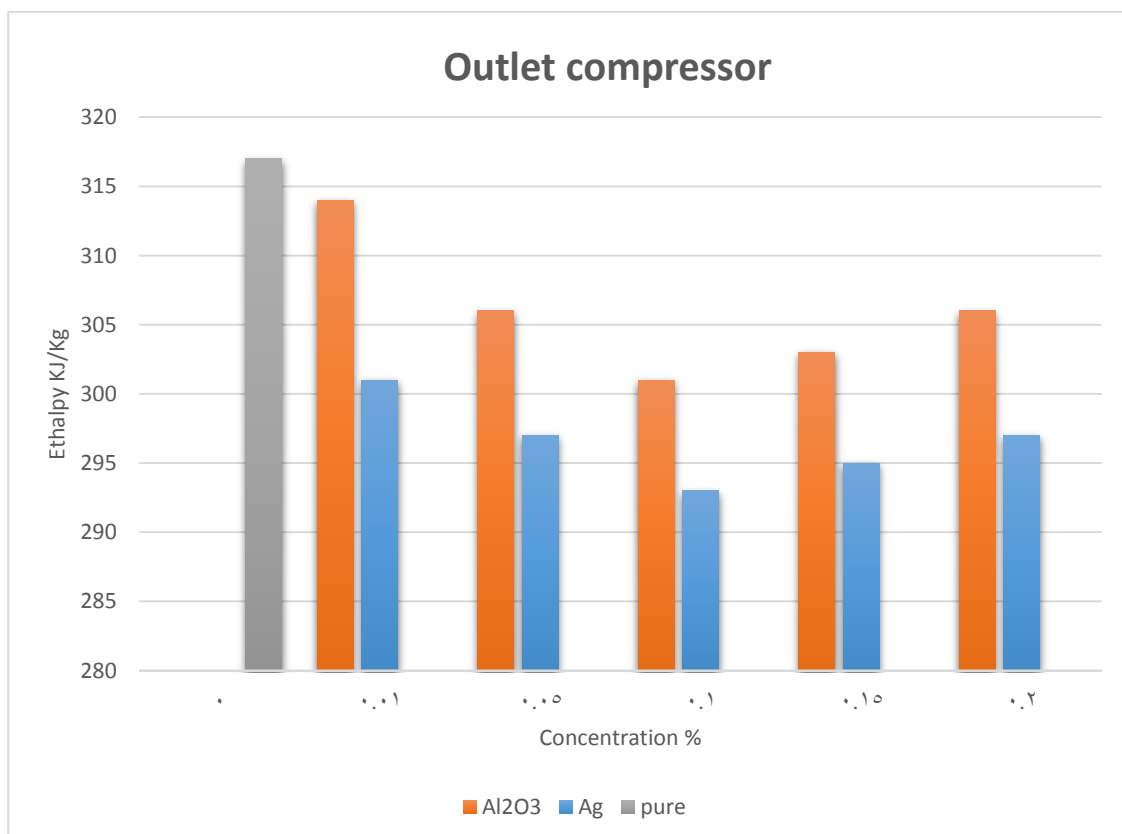


Figure (5.19): Enthalpy with concentration at the compressor outlet.

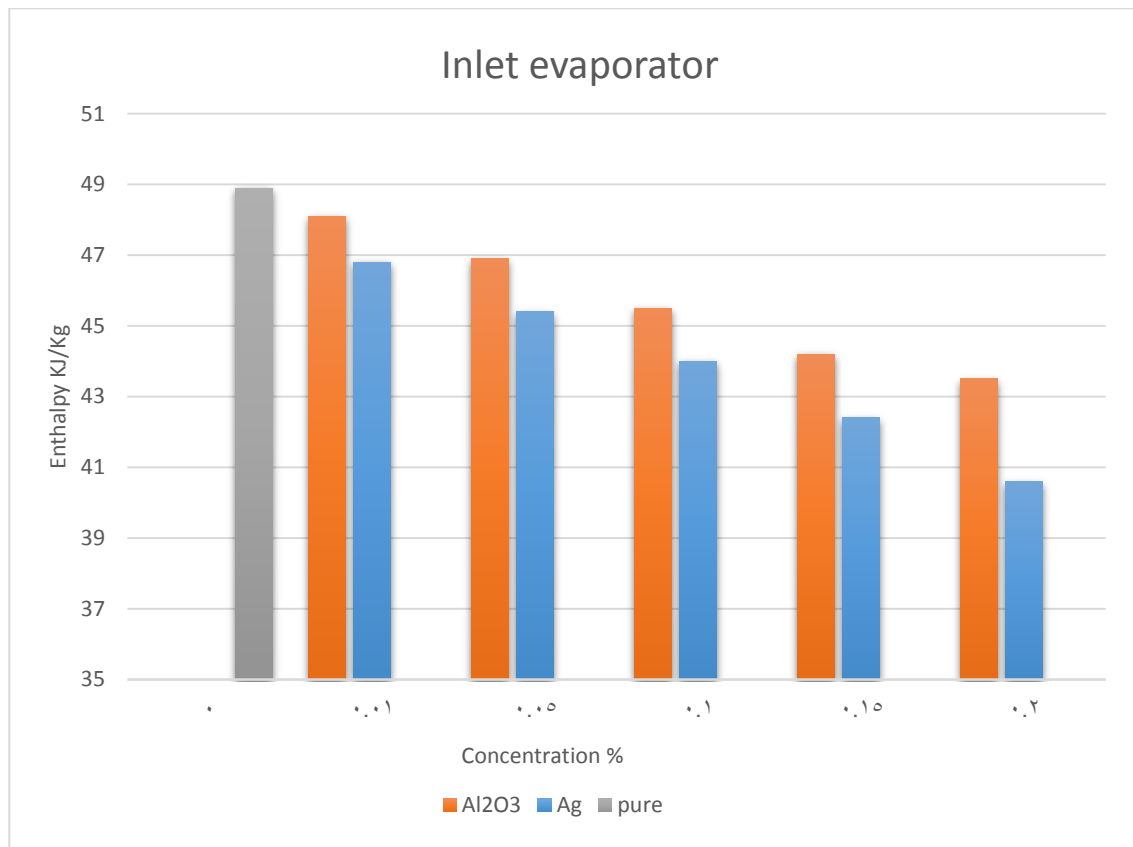


Figure (5.20): Enthalpy with concentration at the evaporator inlet.

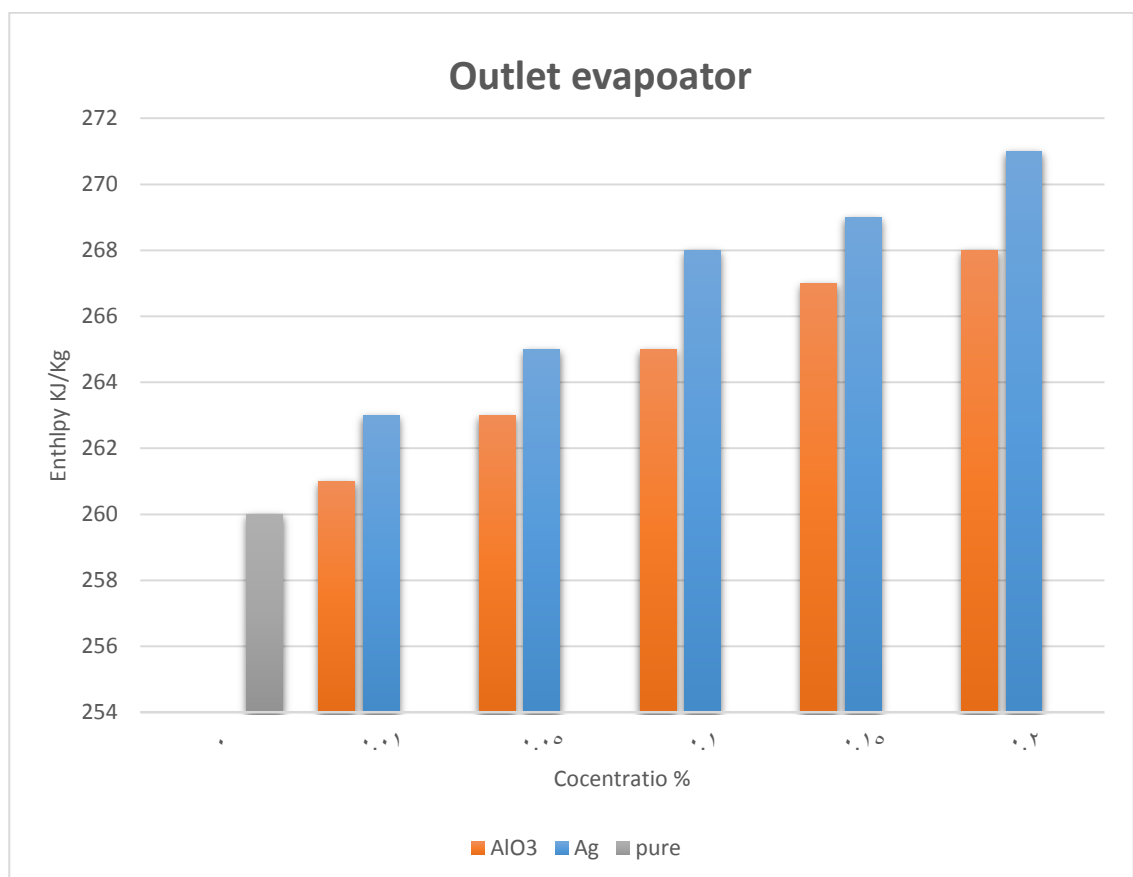


Figure (5.21): Enthalpy with concentration at the evaporator outlet.

5.2.2 Consumption Work

Figure (5.22) shows the work consumption per unit mass in the compressor with nano concentration for both Al₂O₃ and Ag. It was found that the work consumption decrease when adding the nanoparticles to the lubricant oil, where improve the properties of the lubricant coefficient of friction and the viscosity decrease as well as enhance the thermo-physical properties of the working fluid. Therefore, the enhancement in work consumption increased with increasing the nano concentration but to a specific concentration then back to decrease when incrementing the nanoparticles. So, the better was in Ag case where the maximum value was (56.14) in two concentration 0.1% and 0.15% Ag as shown in figure (5.23).

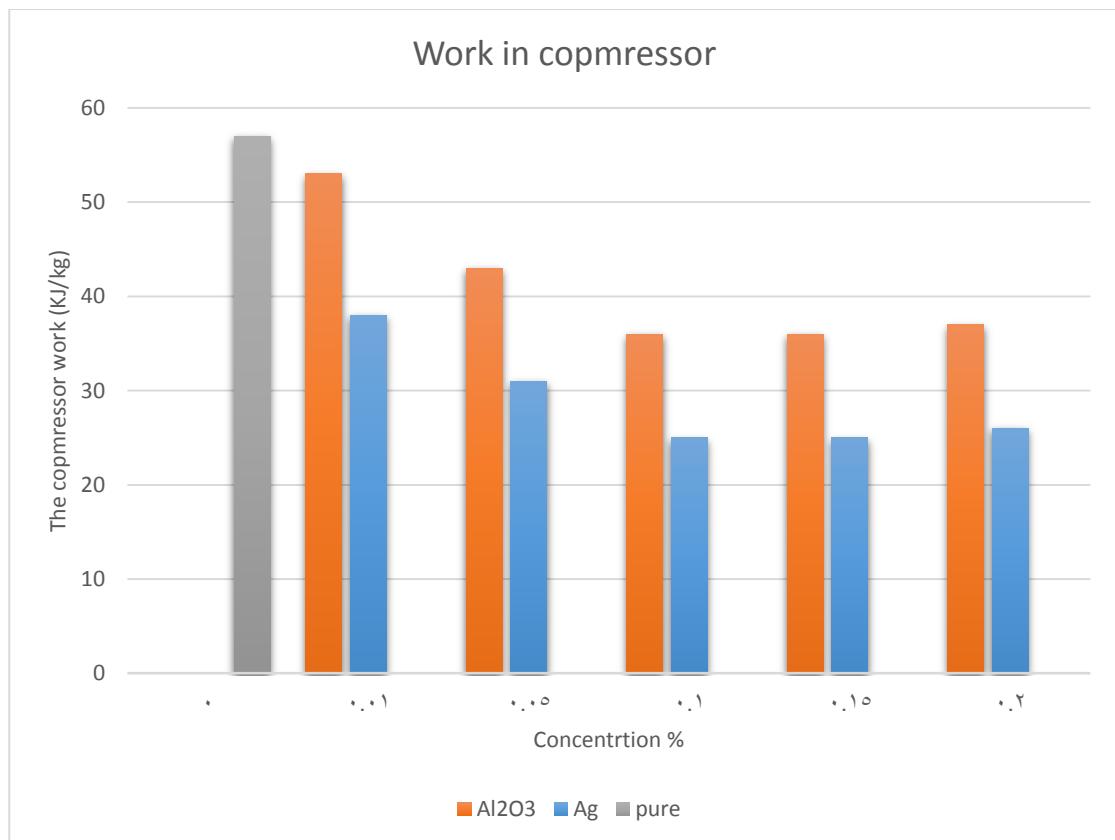


Figure (5.22): The compressor work with the concentration.

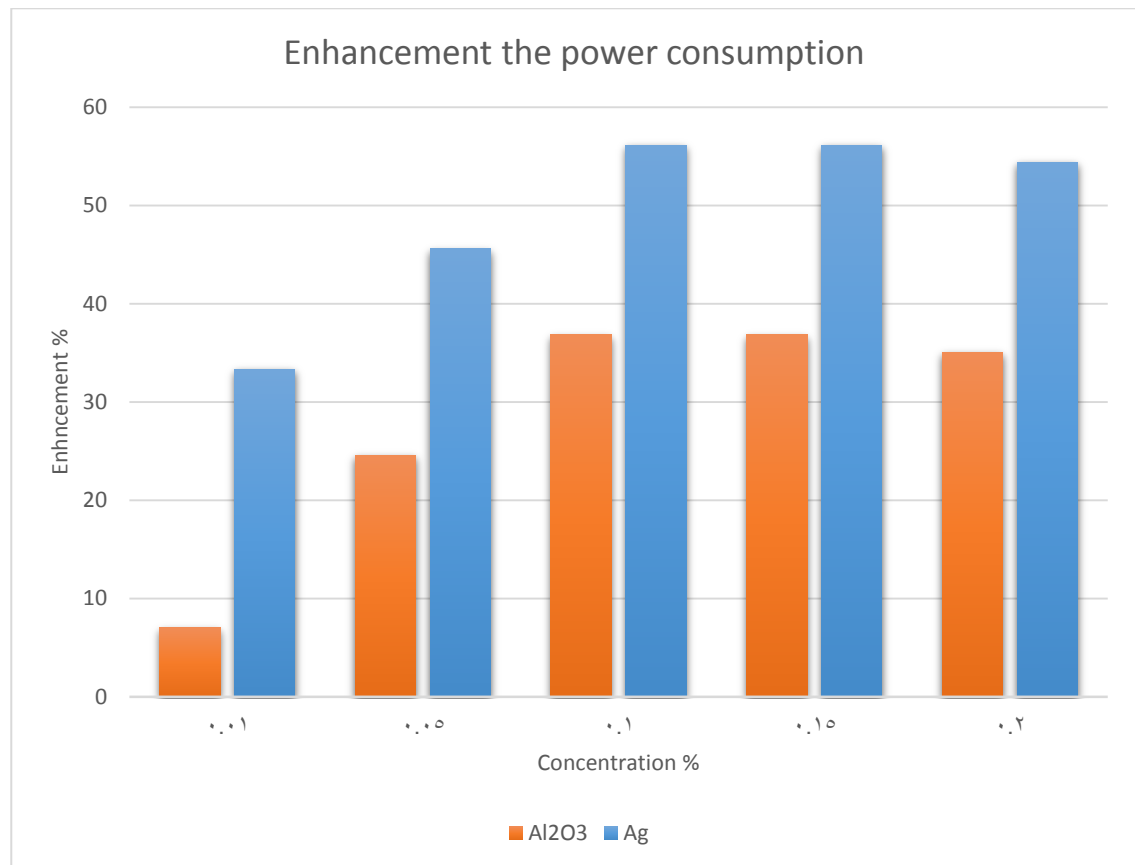


Figure (5.23): Enhancement of the compressor work with the concentration.

5.2.3 Effect of Refrigeration

Figure (5.24) shows the refrigeration effect per unit mass with nano concentration. It was found that the heat transfer per unit mass through the radiator of the air conditioning system increases with increasing the nano concentration where the thermos-physical properties of the working fluid improved when adding nanoparticles. The thermal conductivity of nanoparticles was higher than the base fluid. The enhancement of the effect of refrigeration is shown in figure (5.25). It was found that the enhancement increasing with increase nano concentration and the Ag-R22 nano-refrigerant was better than Al₂O₃ where the thermal conductivity of the nanofluid for metallic highest than nanofluid for oxide metallic, so the process of heat transfer in case of nanometallic was more. The maximum value was (230.4%) for 0.2% Ag.

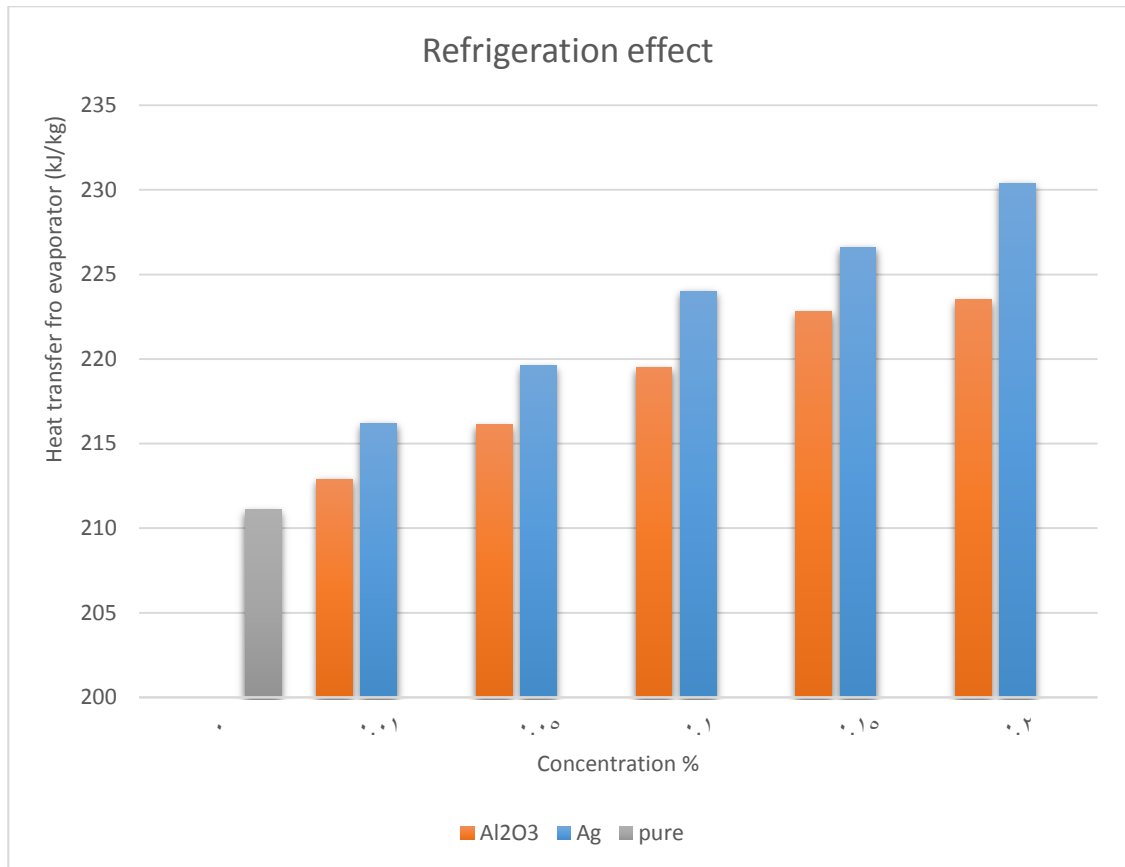


Figure (5.24): The refrigeration effect with the concentration.

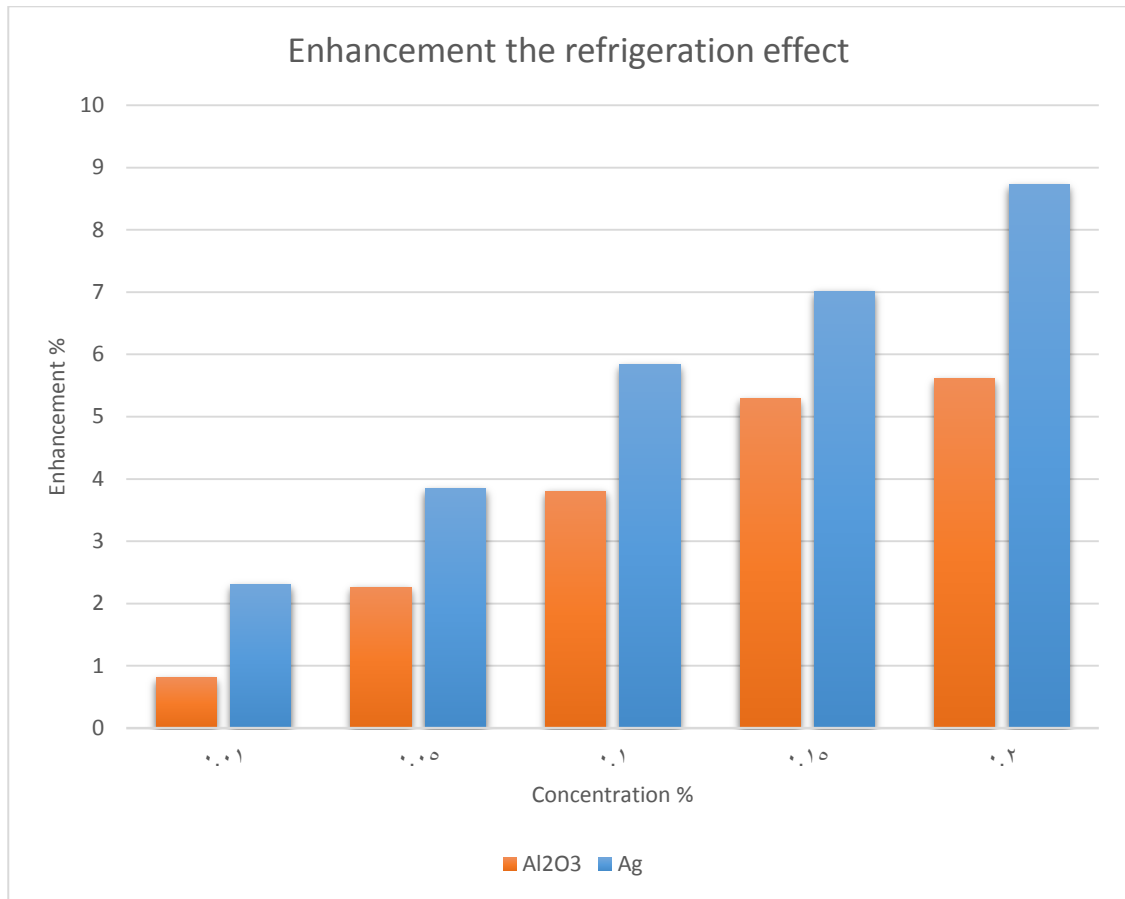


Figure (5.25): Enhancement of the refrigeration effect with the concentration.

5.2.4 The Coefficient of Performance

Figure (5.26) shows the performance of the air condition system with nano concentration for pure refrigerant R22 and two kinds of nanofluid Al₂O₃-R22 and Ag-R22. The R22-Ag was better than the using of R22-Al₂O₃, where the coefficient of performance was found equal to (9.064). However, it was found that the using of Nanofluid with low concentration gave better performance enhancement and the increasing of this concentration led to increasing the COP enhancement until it reached the critical point. This enhancement was decreased and it found to be (144.71%) in 0.15% R22-Ag.

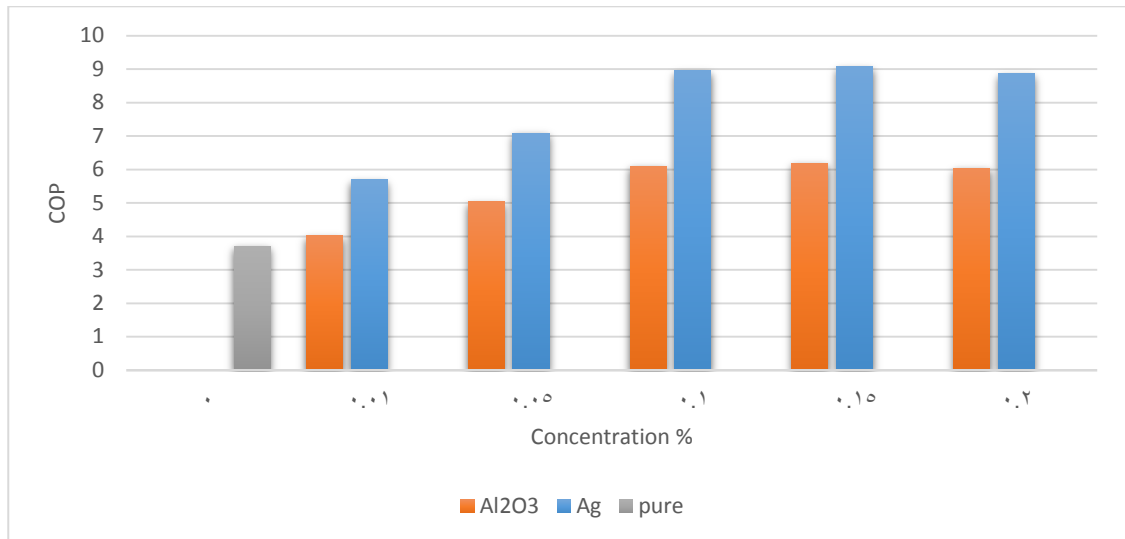


Figure (5.26): Coefficient of performance with the concentration.

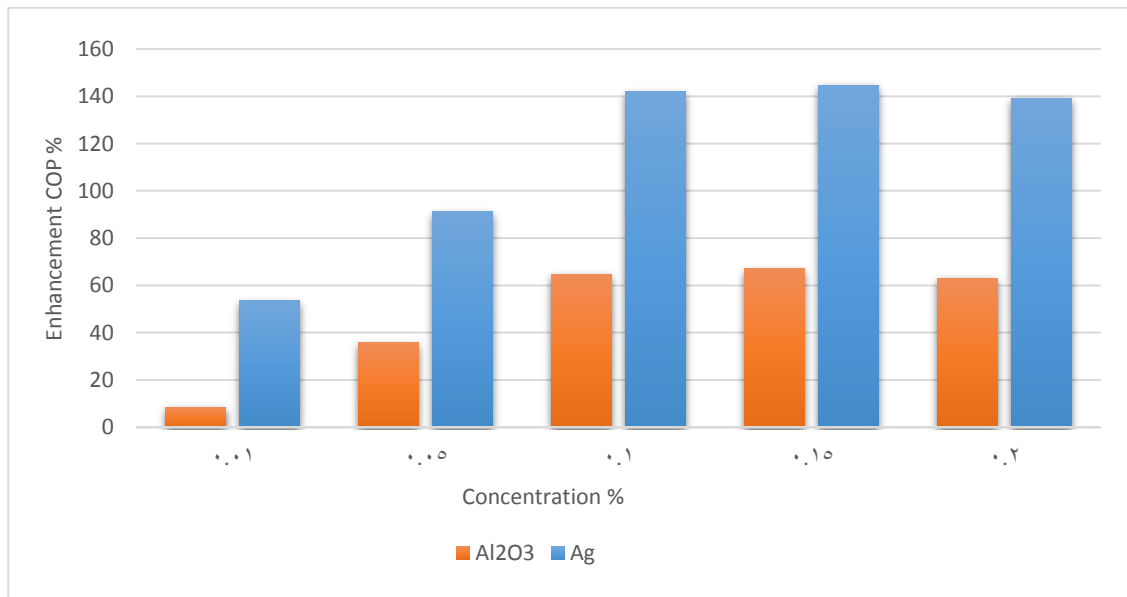


Figure (5.27): Enhancement in a coefficient of performance with the concentration.

5.3 Simulation Results

This section deals with the results analysis for the pipe of the evaporator. Then a comparison between the experimental and numerical analysis of the results for pure refrigerant is made.

5.3.1 Pure Refrigerant

The refrigerant R22 input as a new fluid material in Fluent so the properties are required. The contour of the temperature and pressure are indicated in figures (5.28) and (5.29).

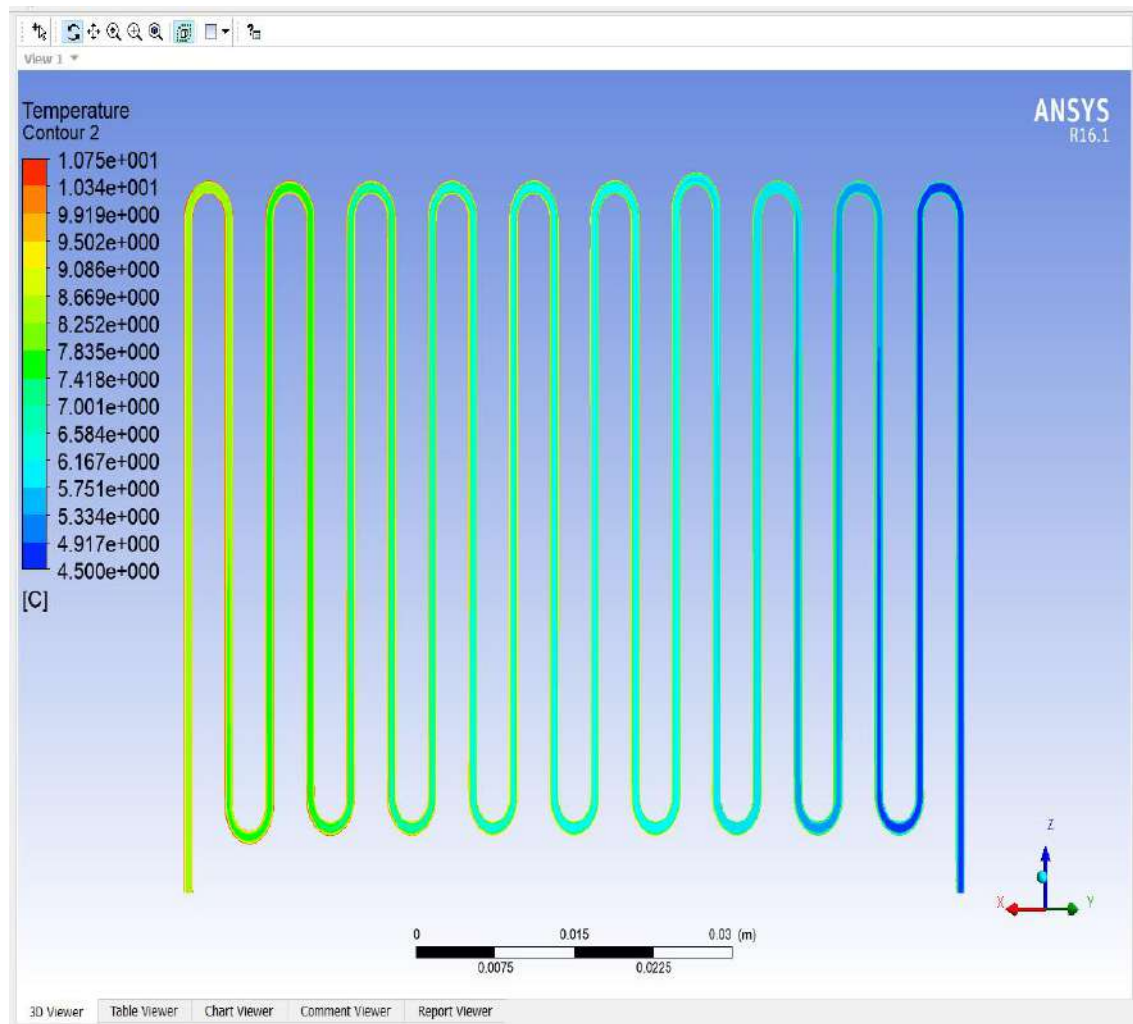


Figure (5.28a): Temperature contour of R22 for plane in mid pipes.

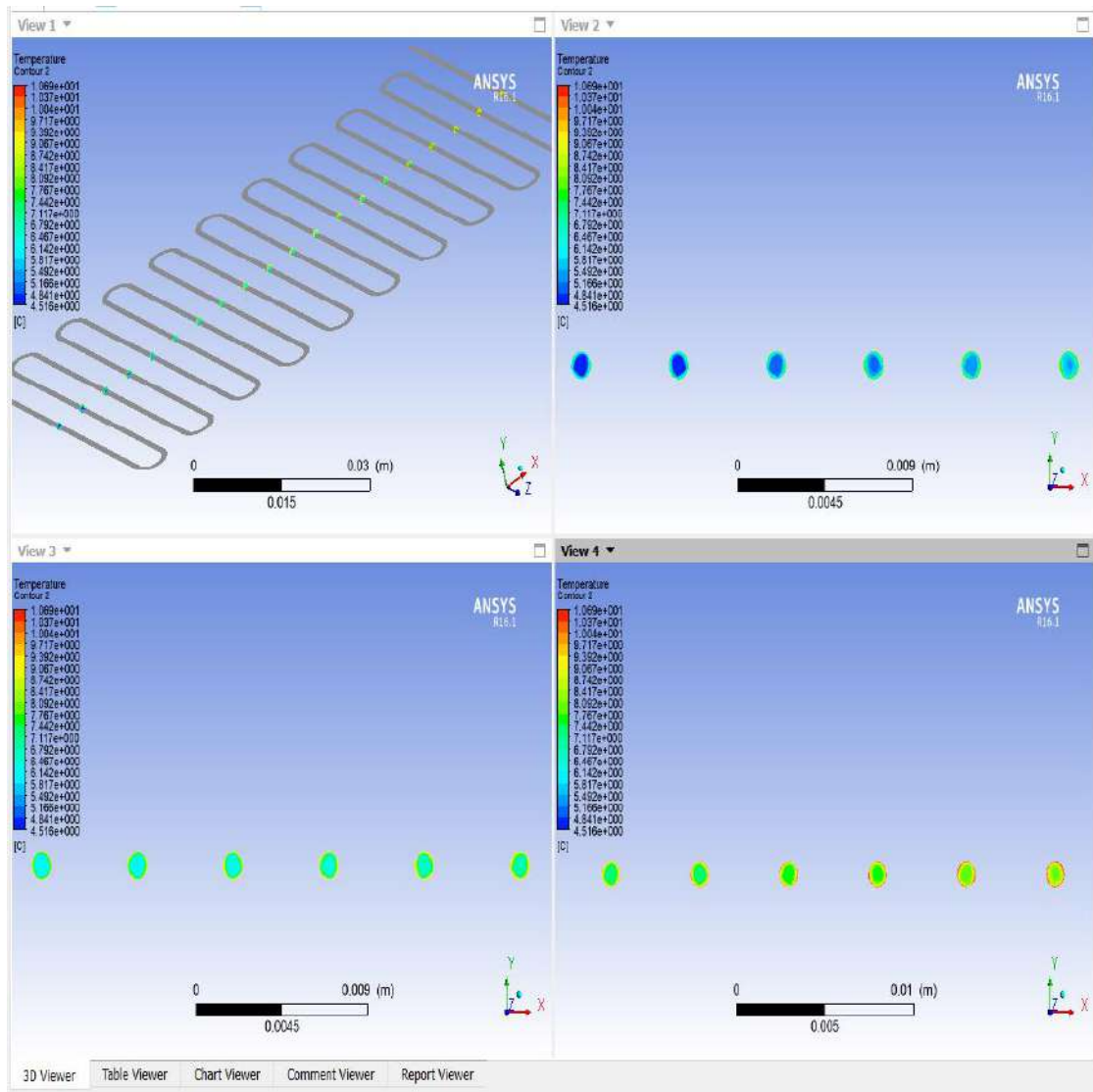


Figure (5.28b): Temperature contour of R22 for cross section of pipes.

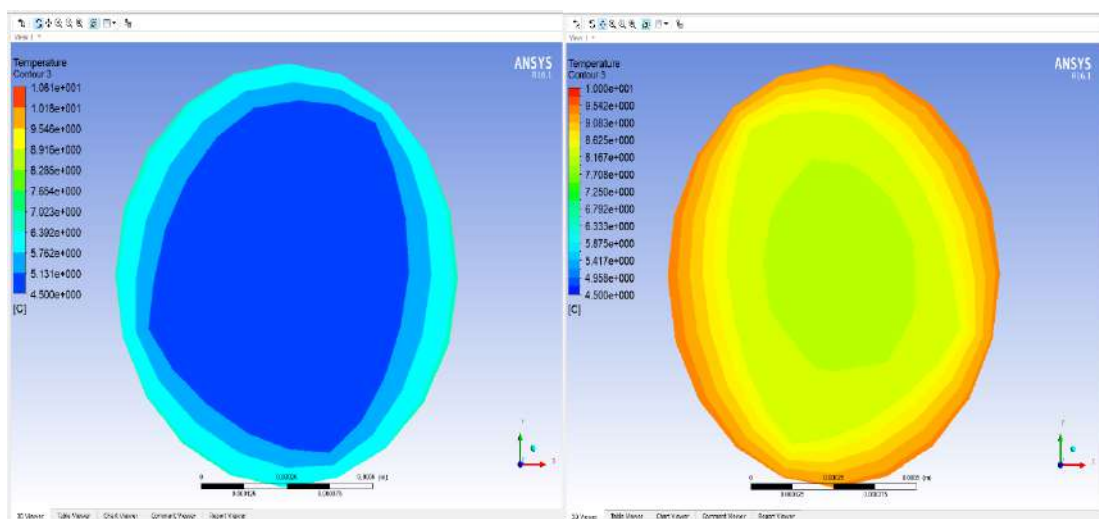


Figure (5.28c): Contour temperature of R22 for the inlet and outlet.

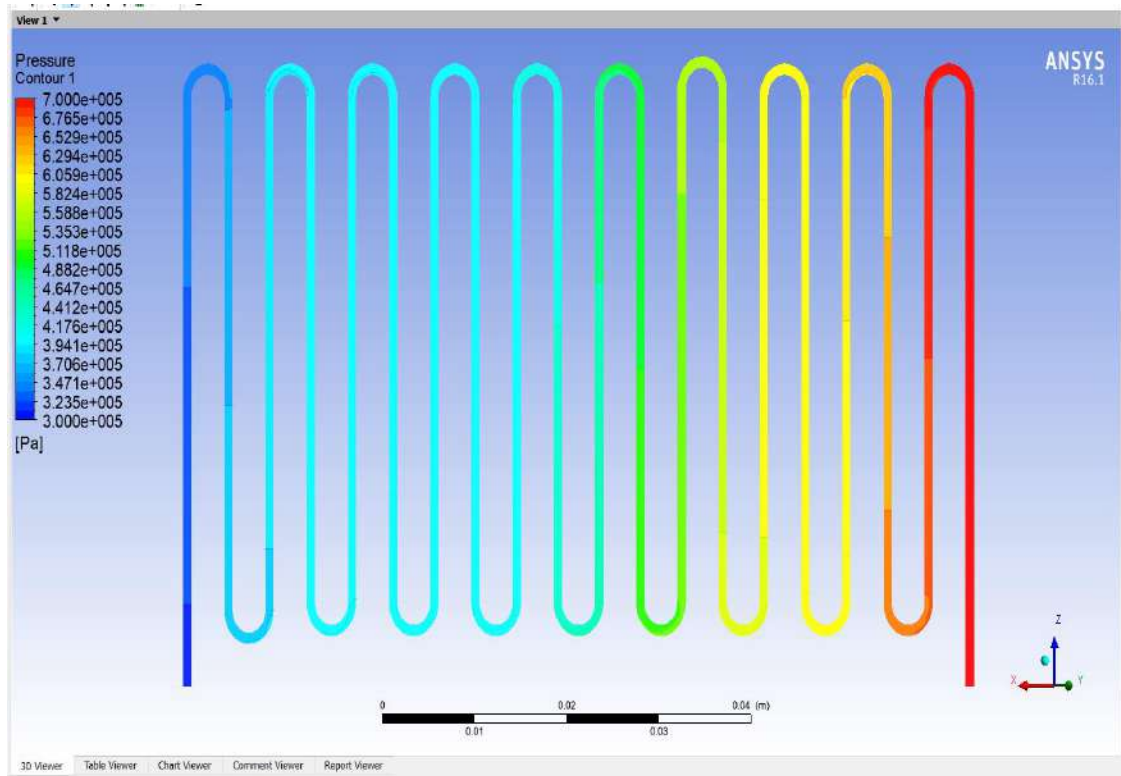


Figure (5.29a): Pressure contour of R22 for the mid plane of the pipes.

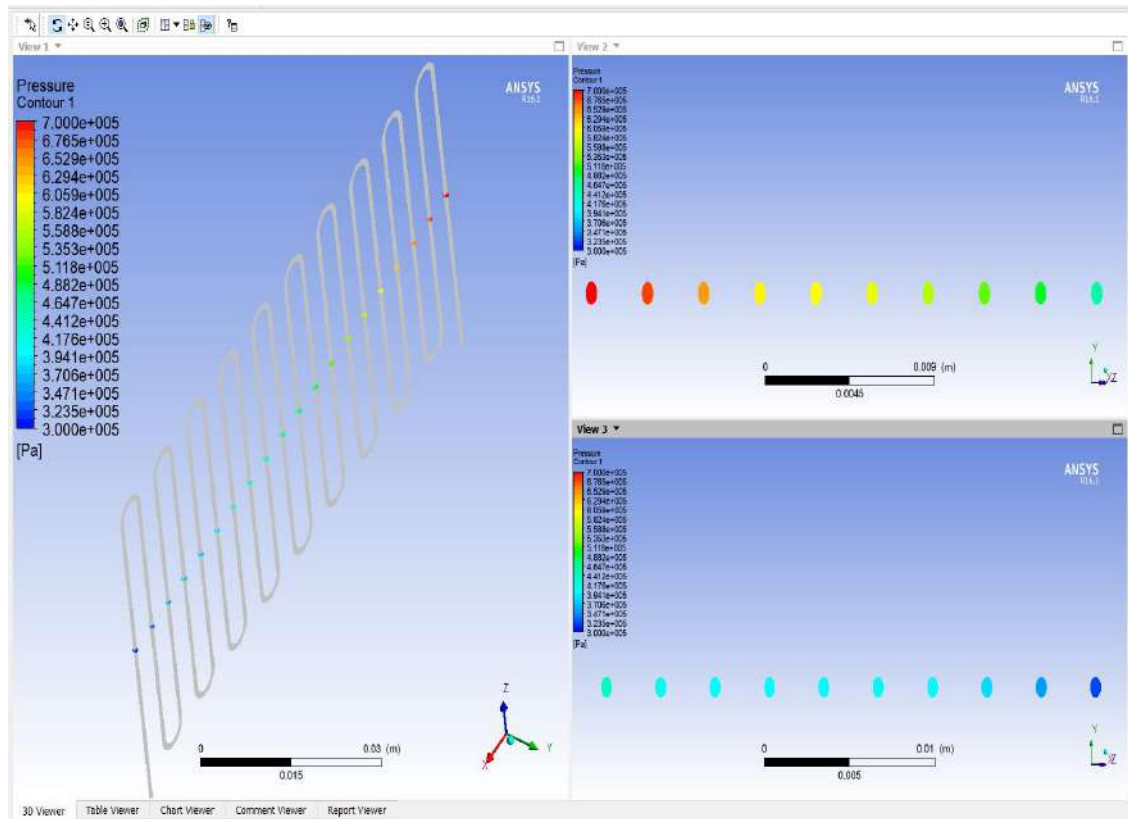


Figure (5.29b): Pressure contour of R22 for the cross section of the pipes.

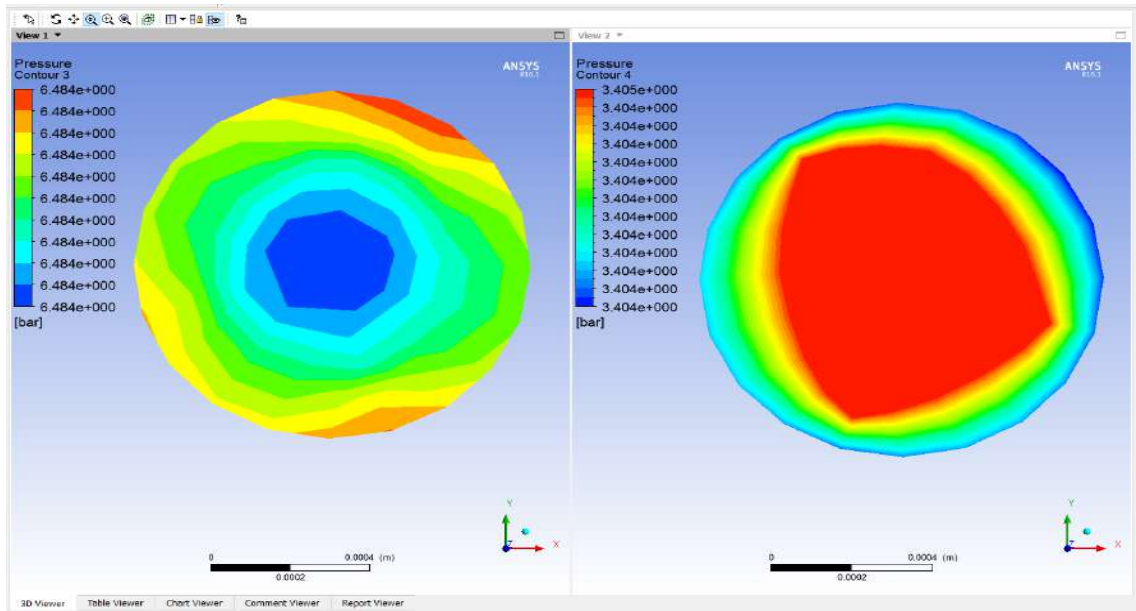


Figure (5.29c): Pressure contour of R22 for the inlet and outlet of the pipe.

5.3.2 Al₂O₃ Nano Refrigerant Analysis

This section deals with the simulation of Al₂O₃ nanorefrigerant. Figure (5.30) indicates the contour of 0.01% Al₂O₃ of the temperature for the mid plane in the pipe and the plane in the cross section of each pipe as well as the inlet and outlet sections. The enhancement in temperature is investigated when using nanofluid and this result was nearly the same as the experimental work.

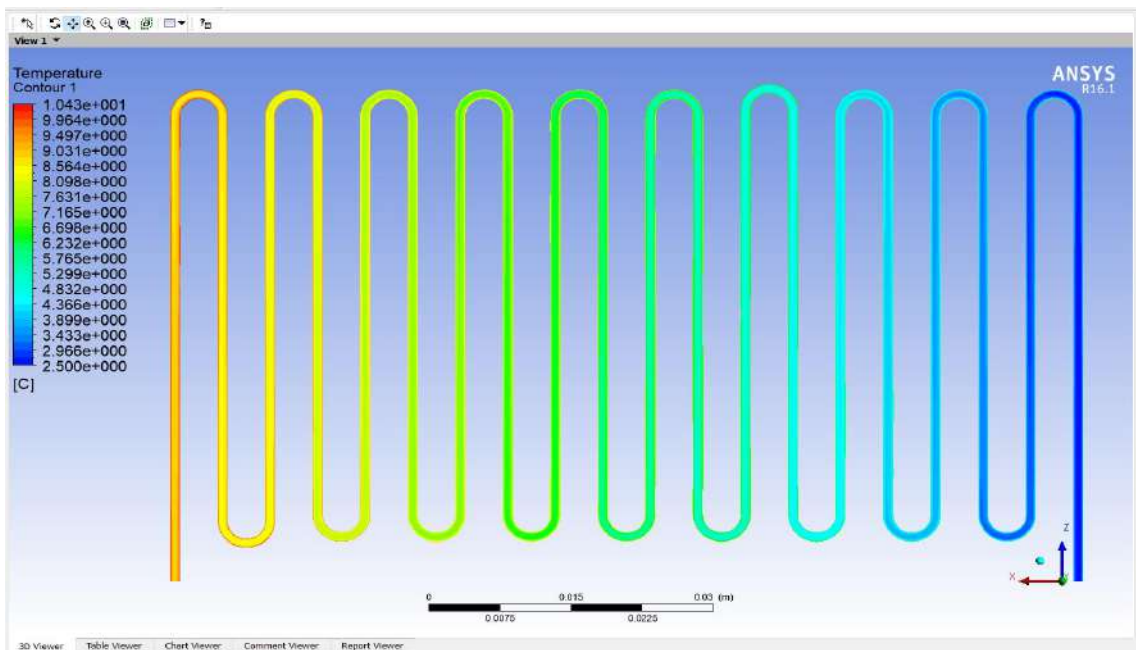


Figure (5.30a): Temperature contour of 0.01% Al₂O₃ for mid plane in the pipe.

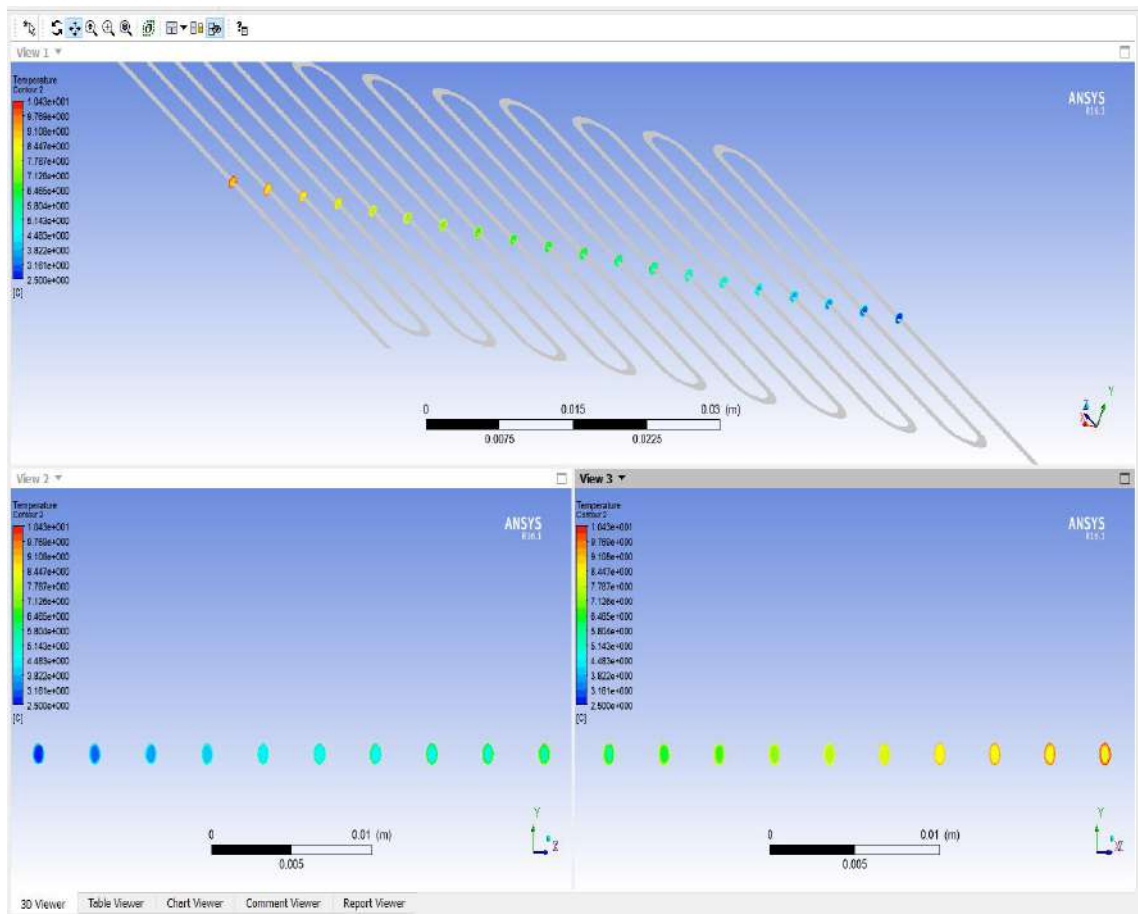


Figure (5.30b): Temperature contour of of 0.01% Al_2O_3 for the plane in cross section of the pipe.

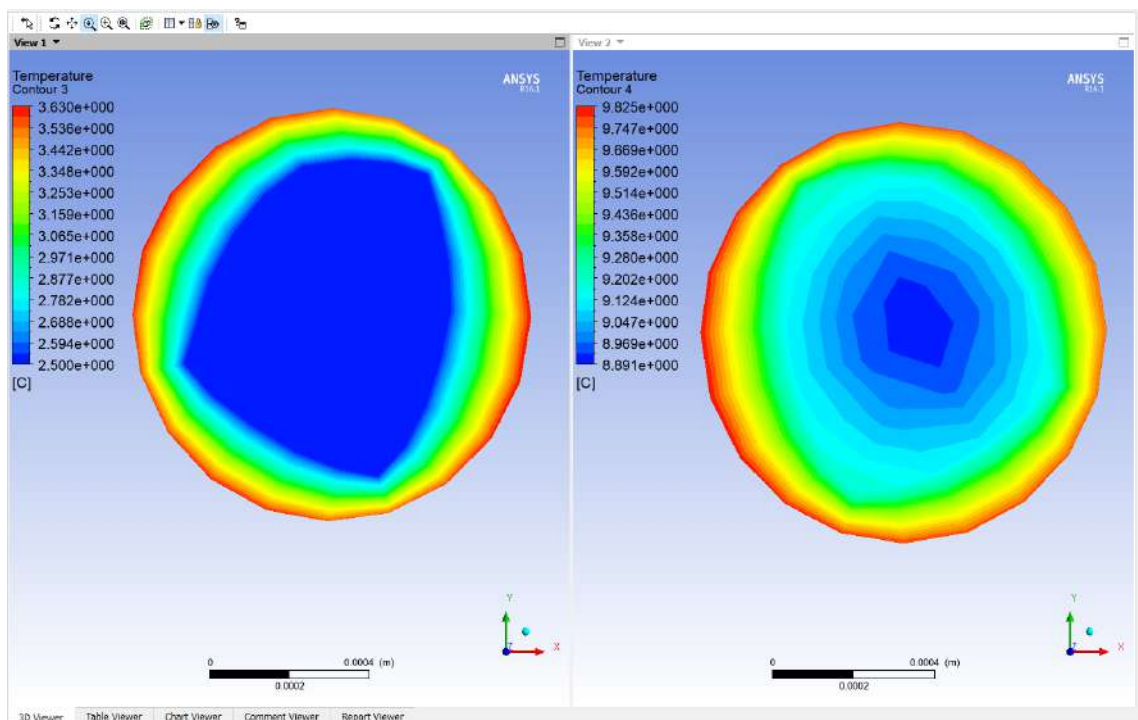


Figure (5.30c): Temperature contour of 0.01% Al_2O_3 for inlet and outlet of the pipe.

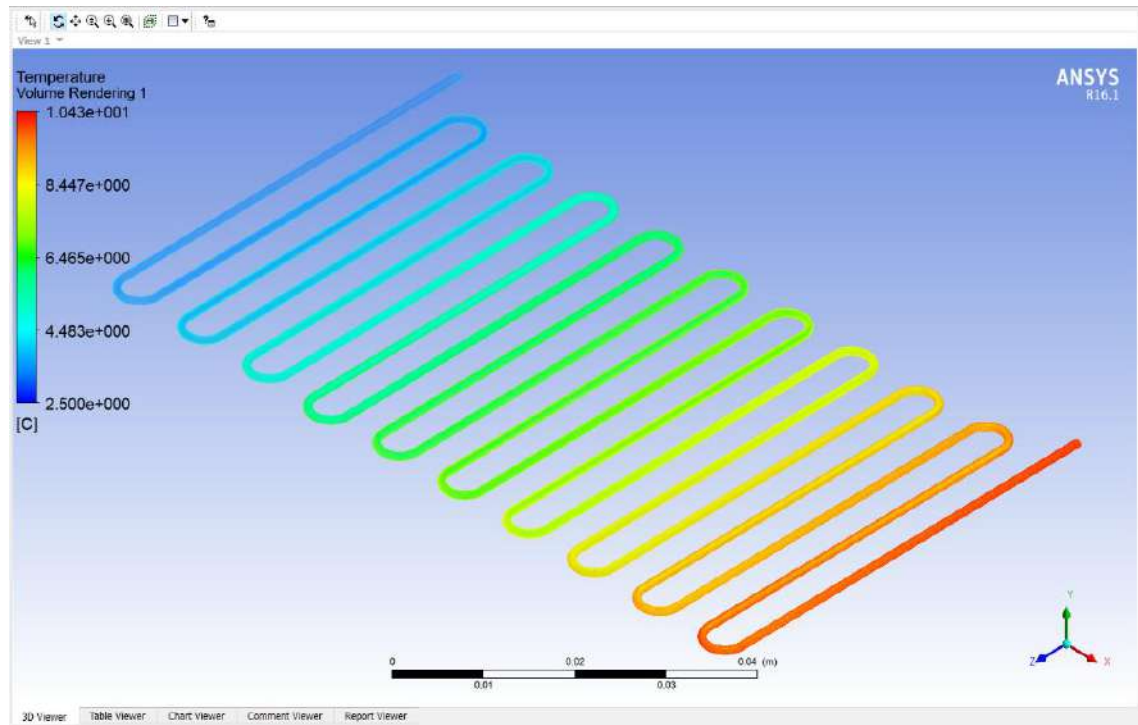


Figure (5.30d): Temperature contour of 0.01% Al_2O_3 for the pipe.

Figure (5.31) shows the contour of 0.01% Al_2O_3 of pressure for the mid plane in the pipe and the plane in cross section of each pipe as well as the inlet and outlet sections. The pressure decreases as a little with the length of the evaporator pipe.

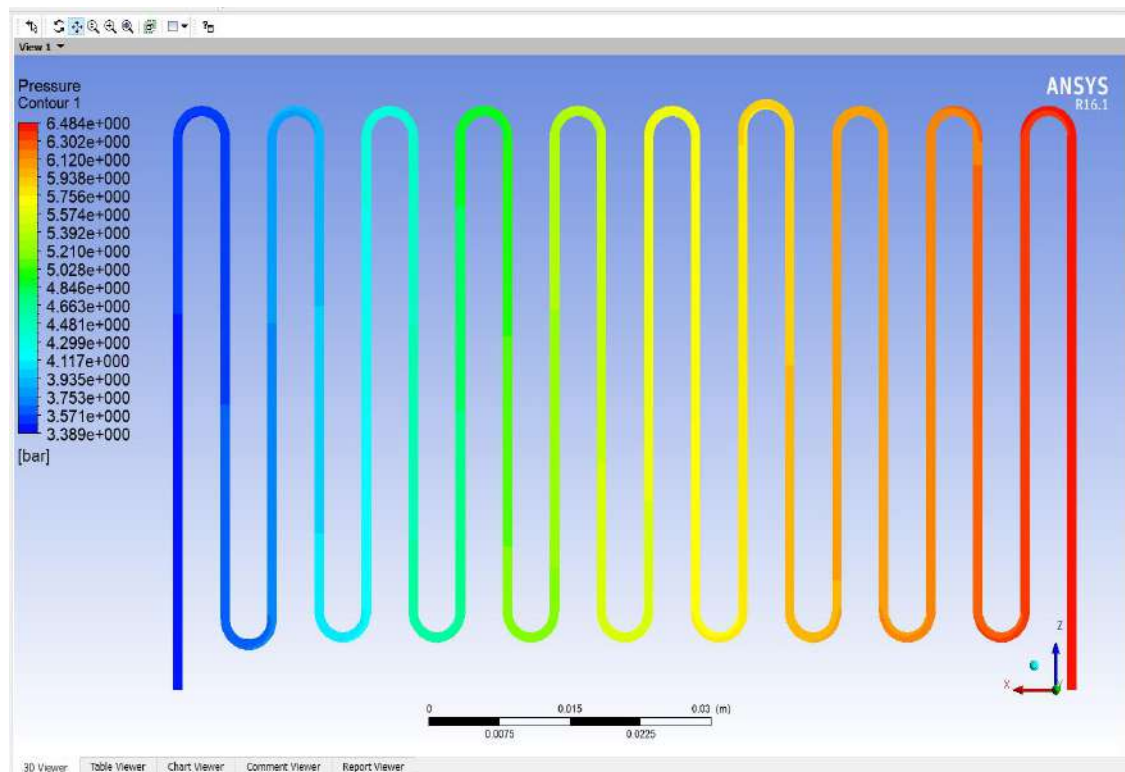


Figure (5.31a): Pressure contour of 0.01% Al_2O_3 for mid plane in the pipe.

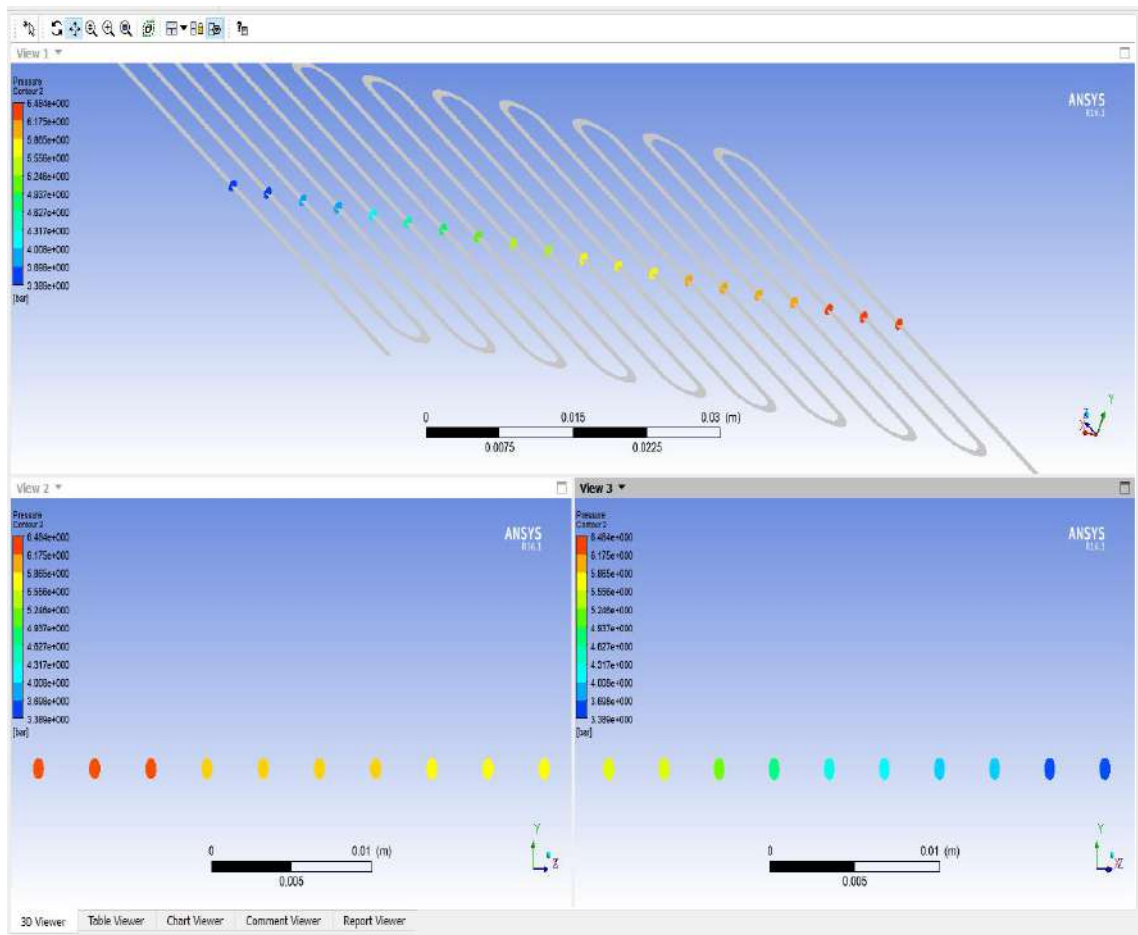


Figure (5.31b): Pressure contour of 0.01% Al_2O_3 for the plane in cross section of the pipe.

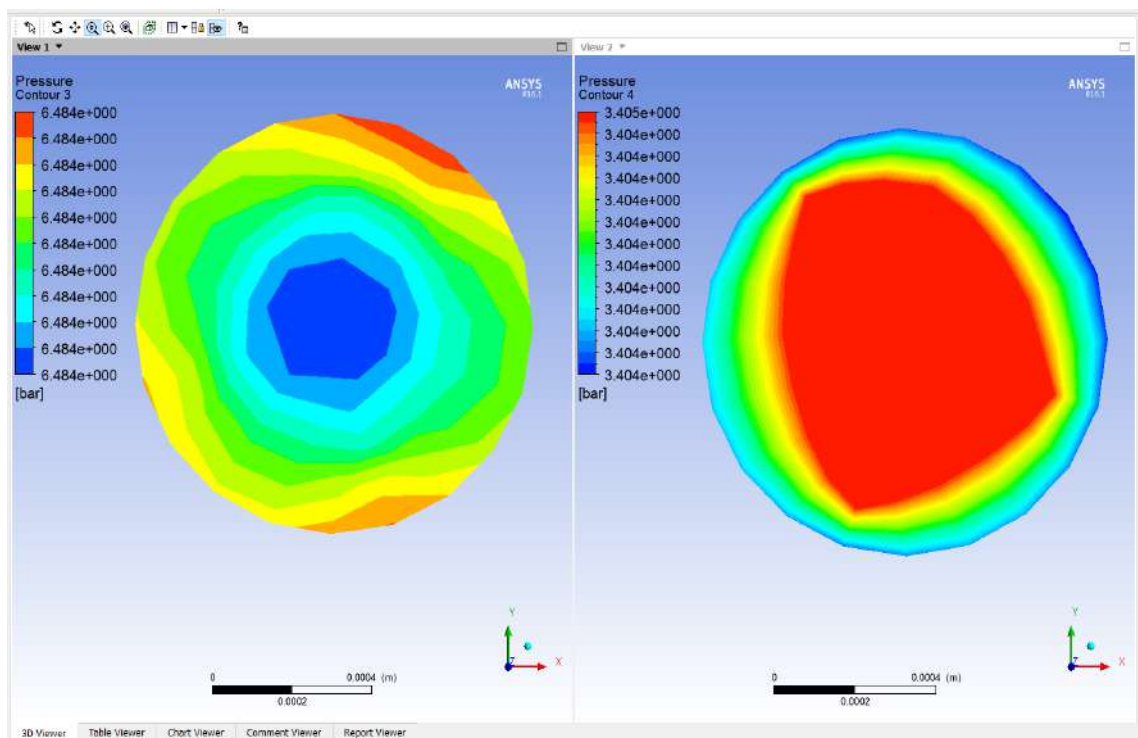


Figure (5.31c): Pressure contour of 0.01% Al_2O_3 for inlet and outlet of the pipe.

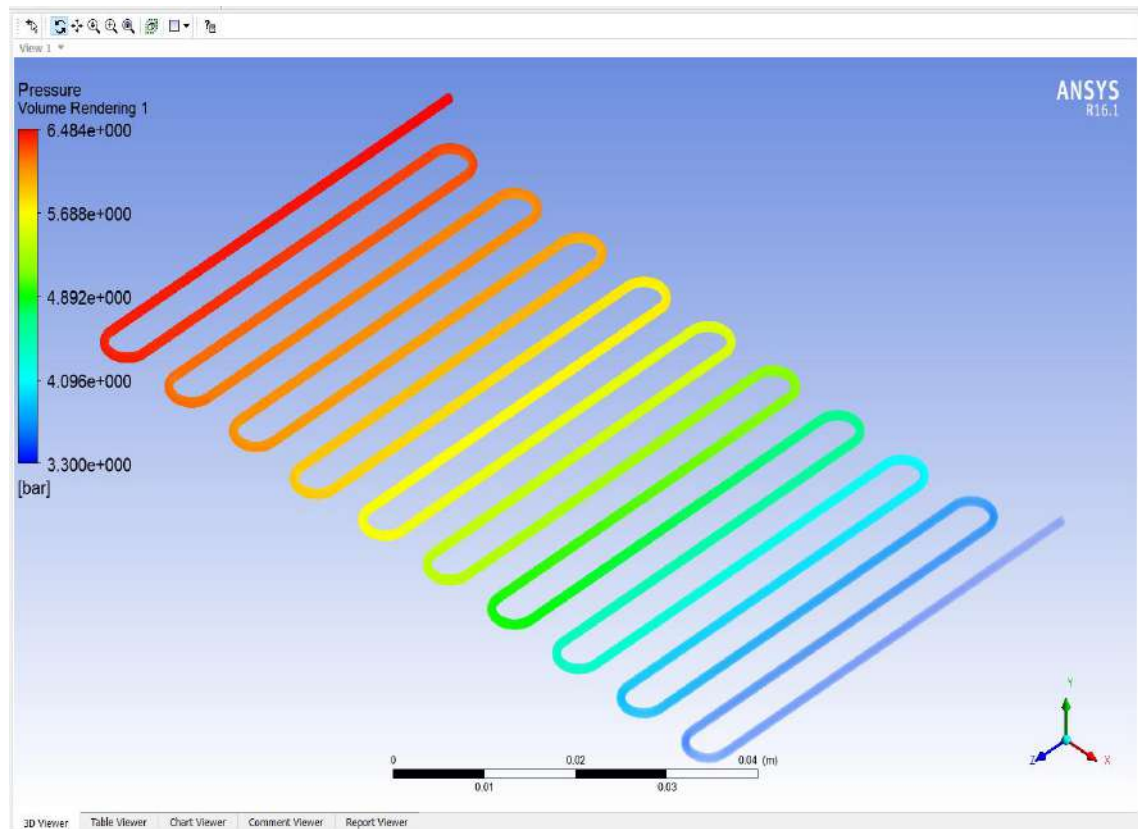


Figure (5.31d): Pressure contour of 0.01% Al_2O_3 for the pipe.

Figure (5.32) indicates the contour of 0.05% Al_2O_3 of the temperature for the mid plane in the pipe and the plane in cross section of each pipe as well as the inlet and outlet sections. The enhancement in temperature was investigated when using nanofluid and this result was nearly the same as the experimental work.

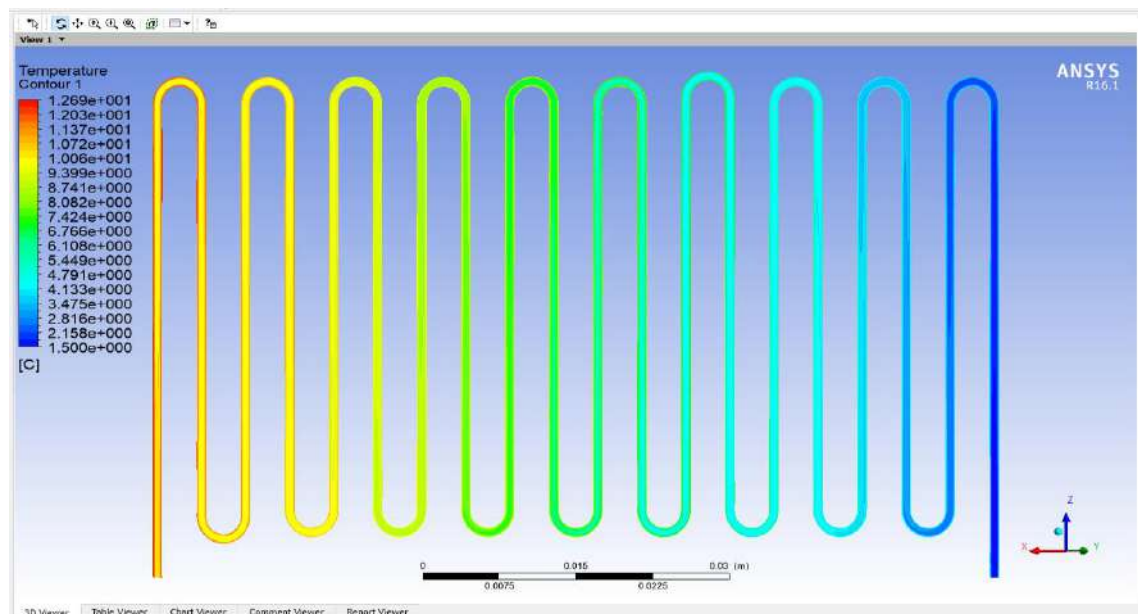


Figure (5.32a): Temperature contour of 0.05% Al_2O_3 for plane in mid pipes.

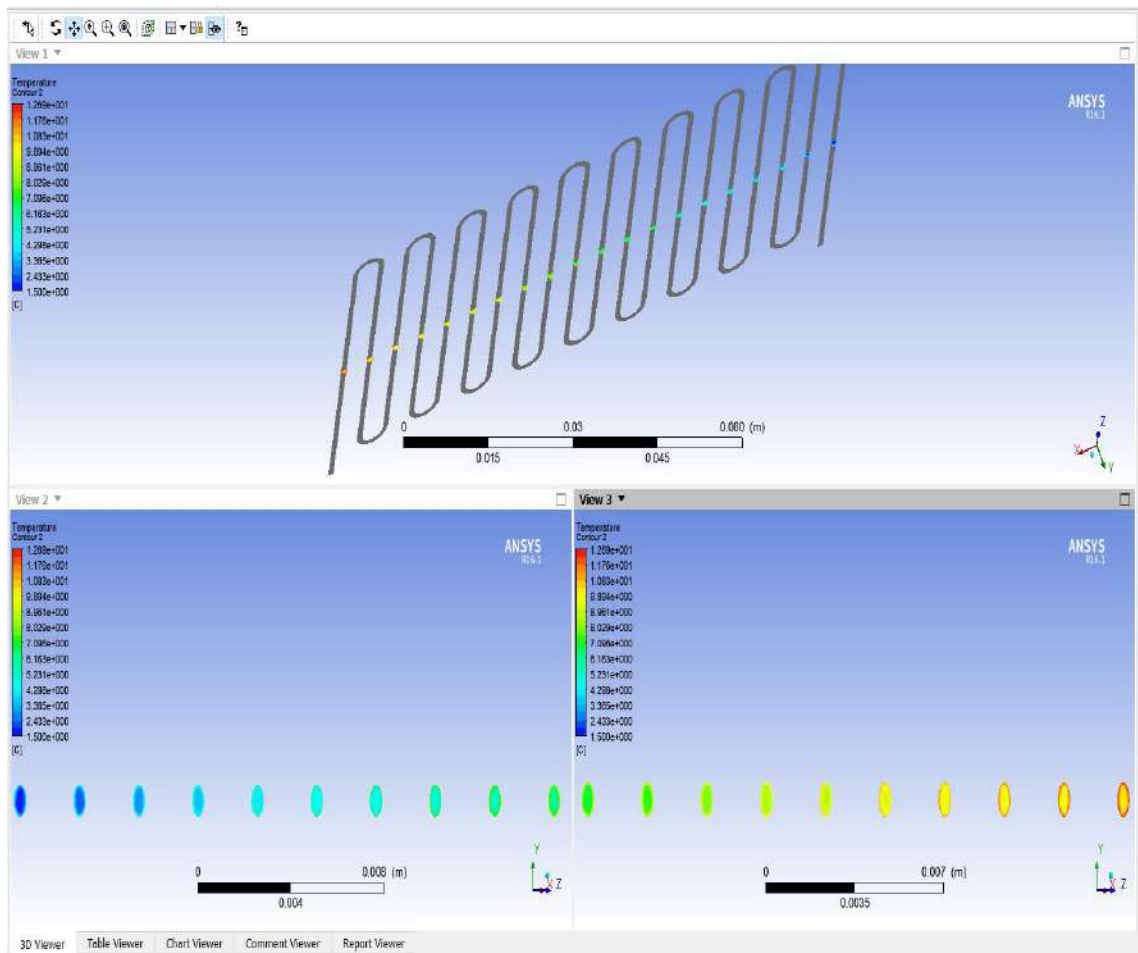


Figure (5.32b): Temperature contour of 0.05% Al_2O_3 for the plane in cross section of the pipe.

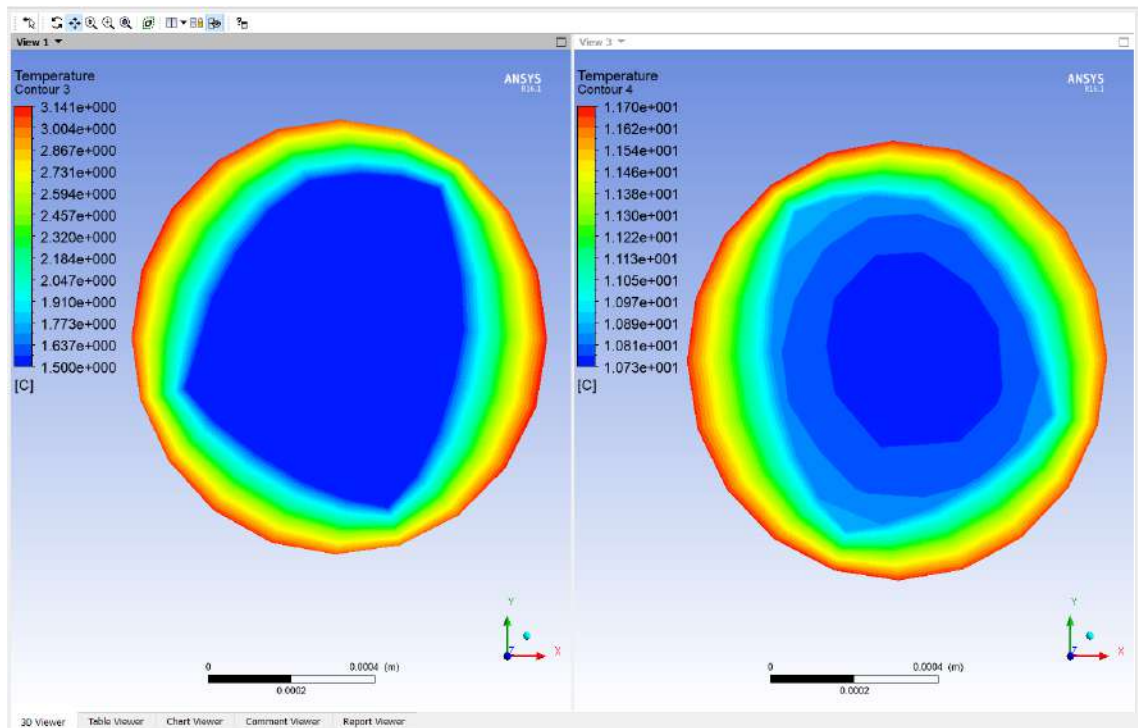


Figure (5.32c): Temperature contour of 0.05% Al_2O_3 for inlet and outlet of the pipe.

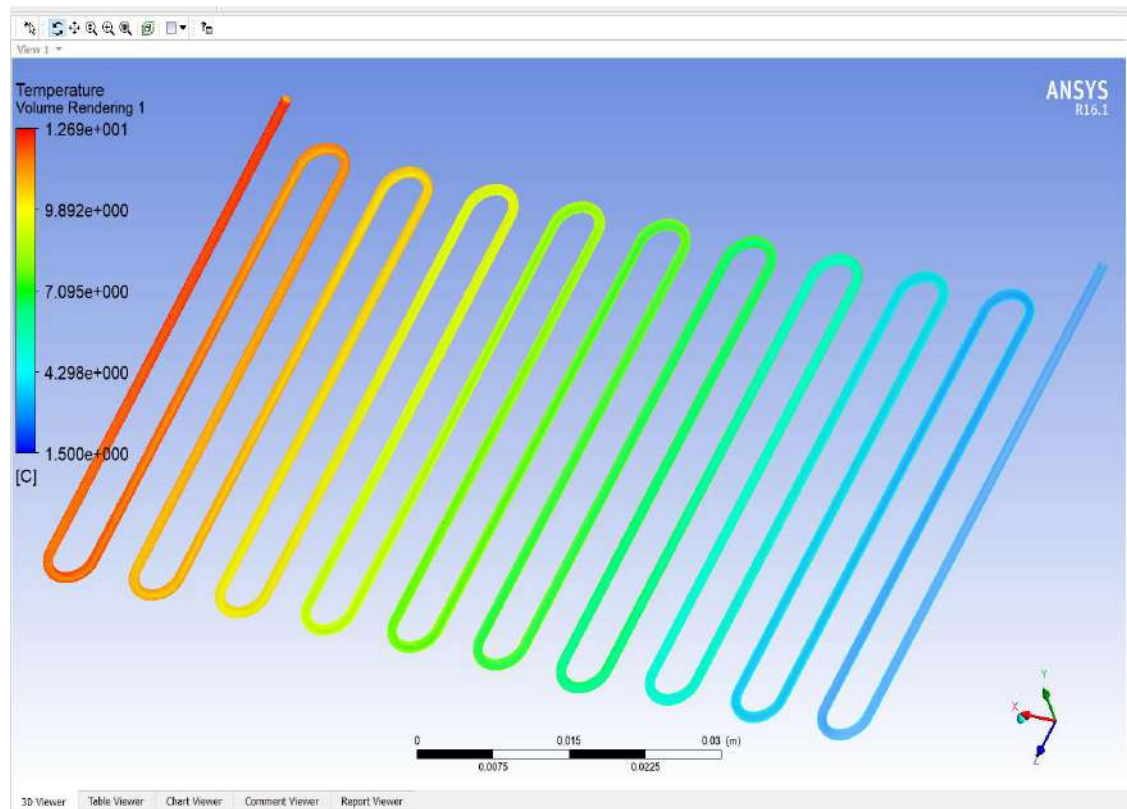


Figure (5.32d): Temperature contour of 0.05% Al_2O_3 for the pipe.

Figure (5.33) shows the contour of 0.05% Al_2O_3 pressure for the mid plane in the pipe and the plane in cross section of each pipe as well as the inlet and outlet sections. The pressure decreased as a little with the length of the evaporator pipe.

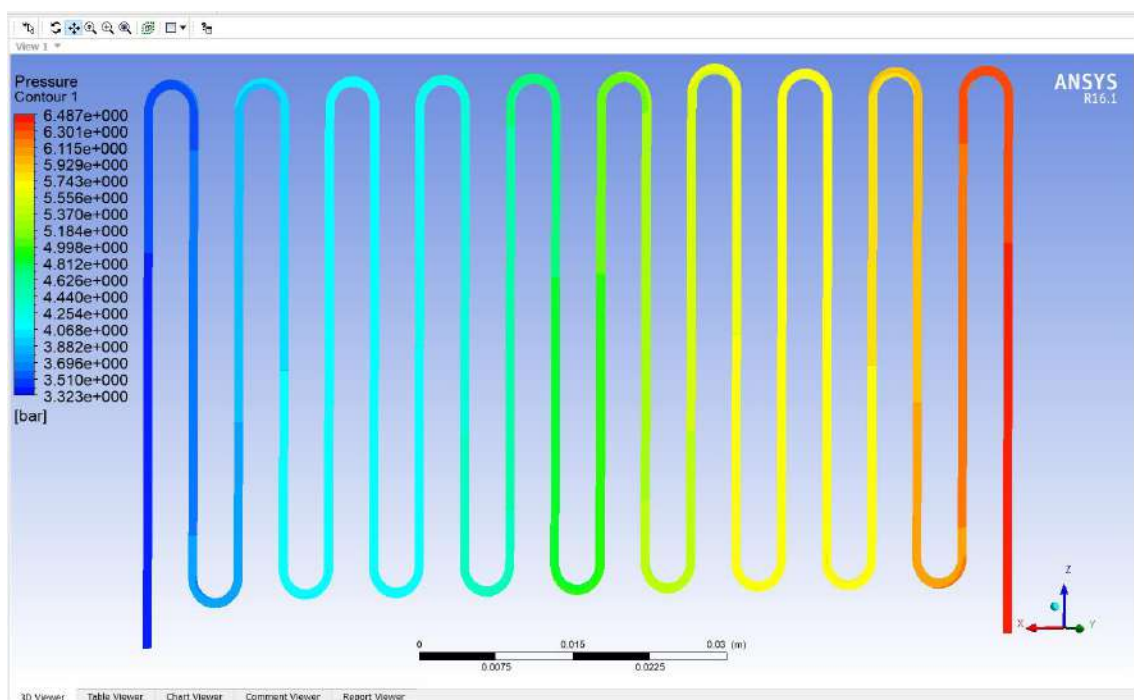


Figure (5.33a): Pressure contour of 0.05% Al_2O_3 for mid plane in the pipe.

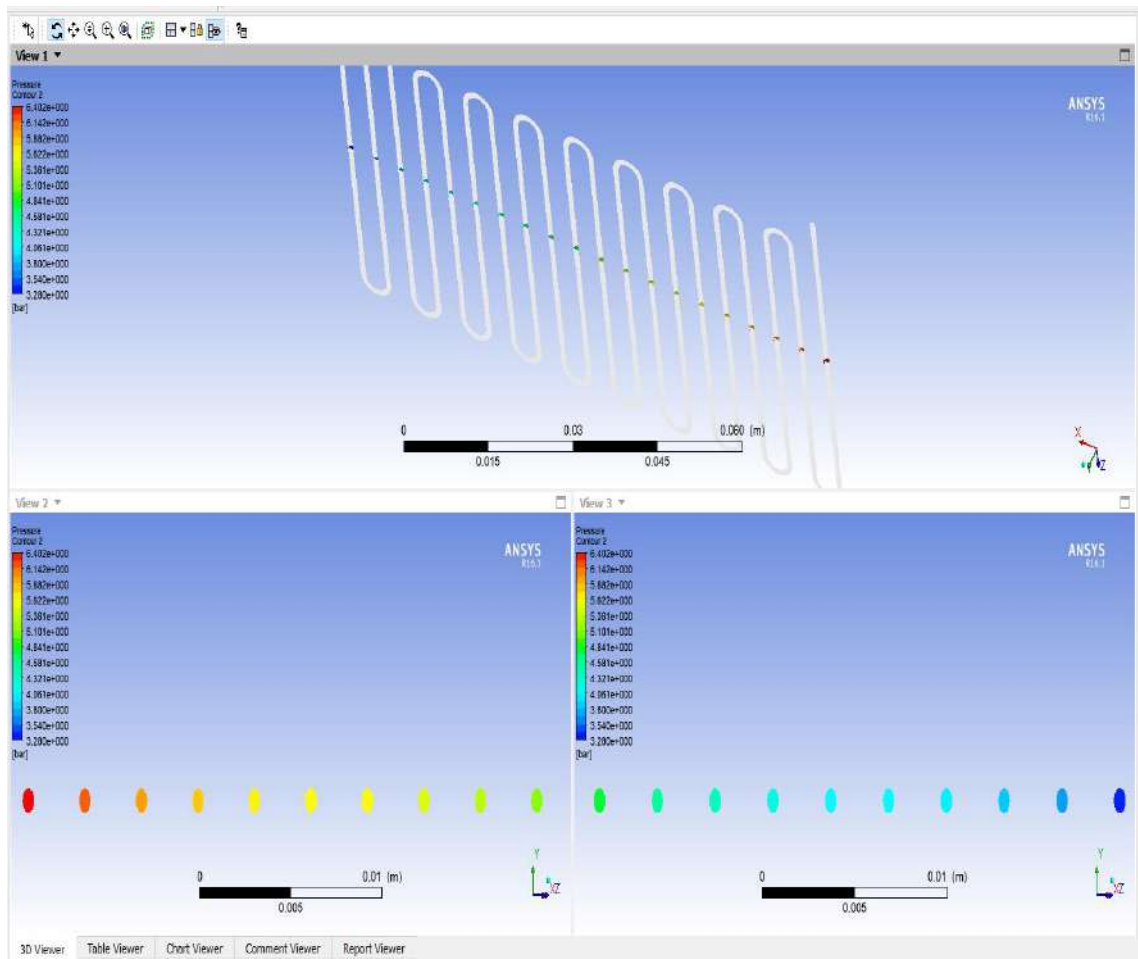


Figure (5.33b): Pressure contour of 0.05% Al_2O_3 for the plane in cross section of the pipe.

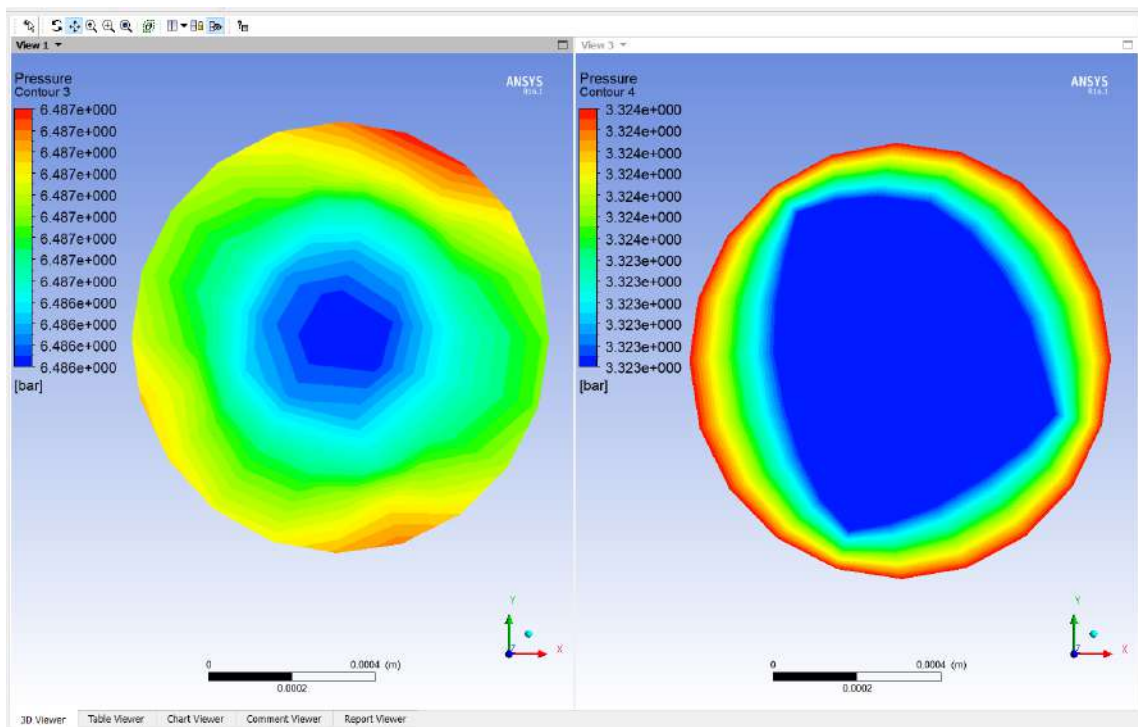


Figure (5.33c): Pressure contour of 0.05% Al_2O_3 for inlet and outlet of the pipe.

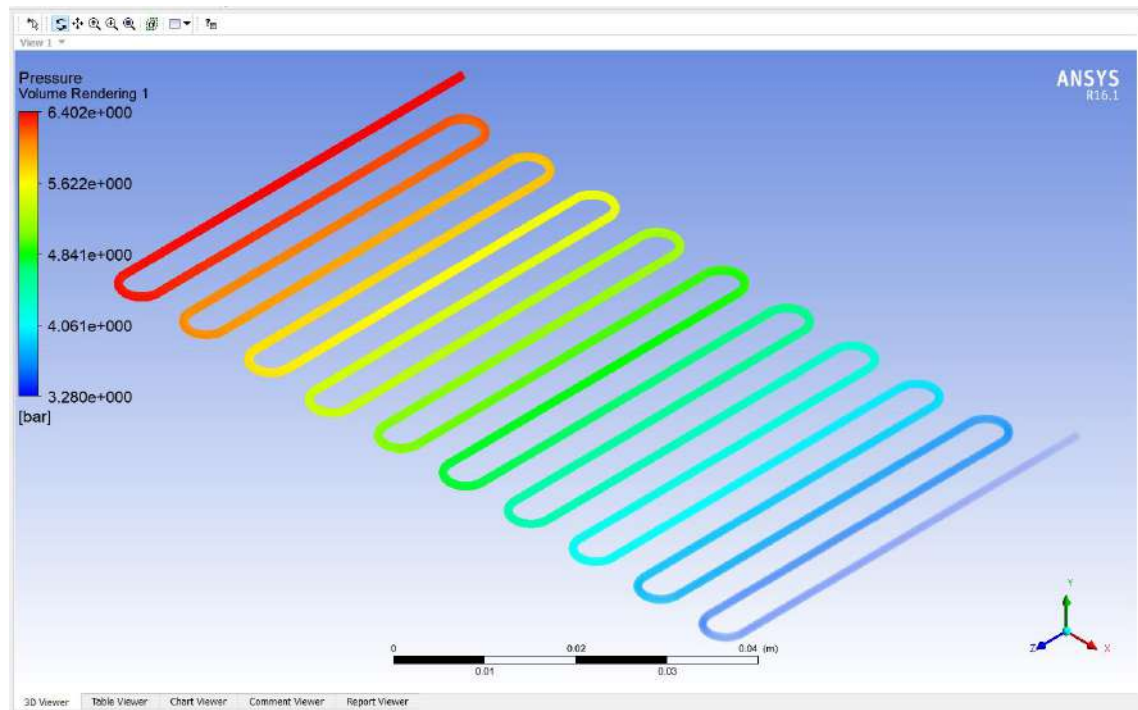


Figure (5.33d): Pressure contour of 0.05% Al_2O_3 for the pipe.

Figure (5.34) indicates the contour of 0.1% Al_2O_3 of the temperature for the mid plane in pipe and the plane in cross section of each pipe as well as the inlet and outlet sections. The enhancement in temperature was investigated when using nanofluid and this result was nearly same as the experimental work.

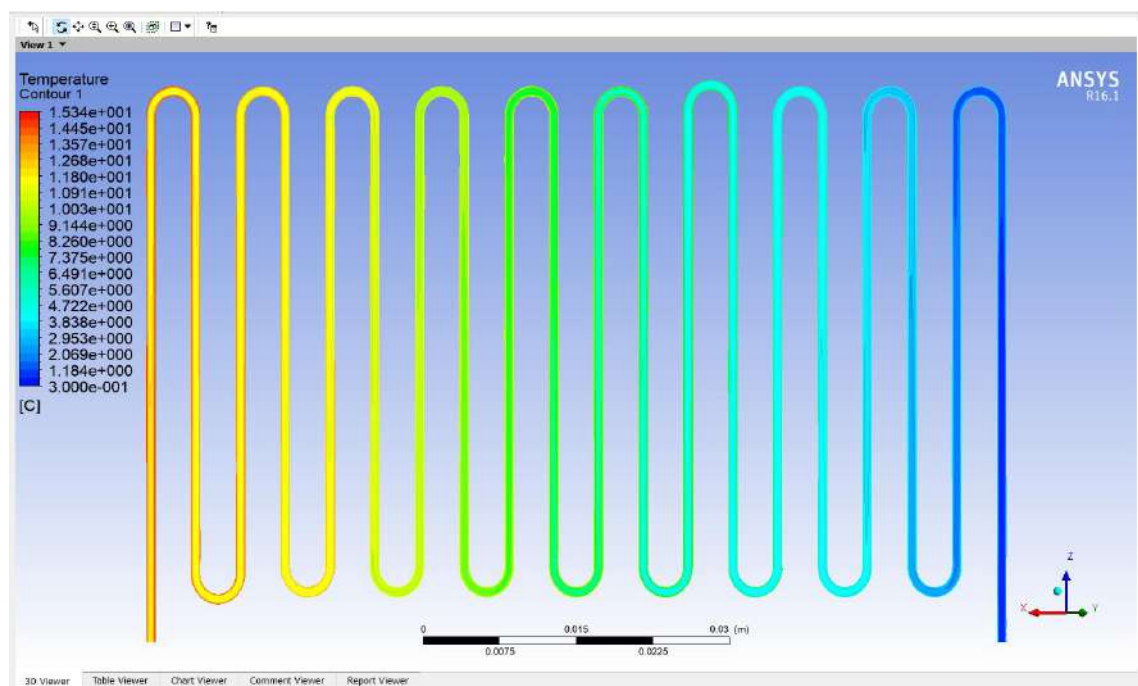


Figure (5.34a): Temperature contour of 0.1% Al_2O_3 for mid plane in the pipe.

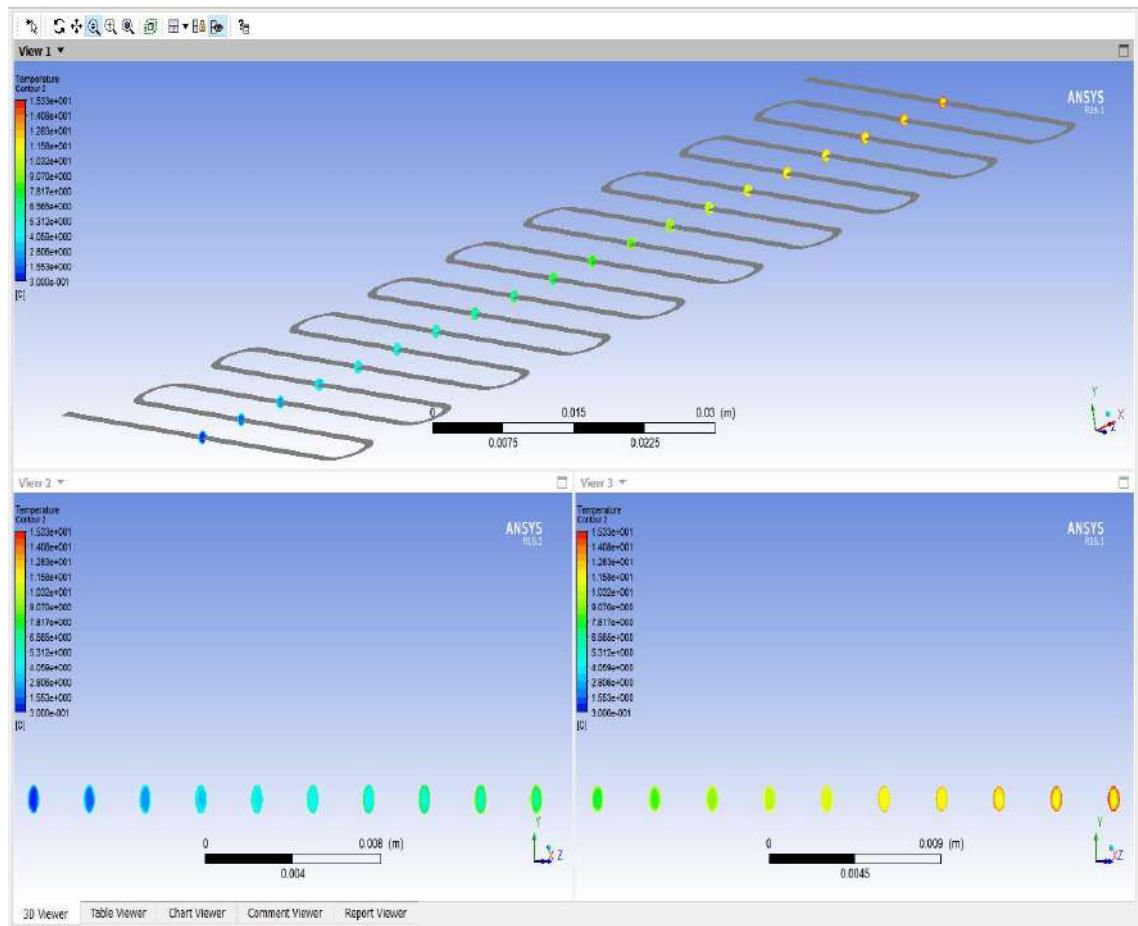


Figure (5.34b): Temperature contour of 0.1% Al₂O₃ for the plane in cross section of the pipe.

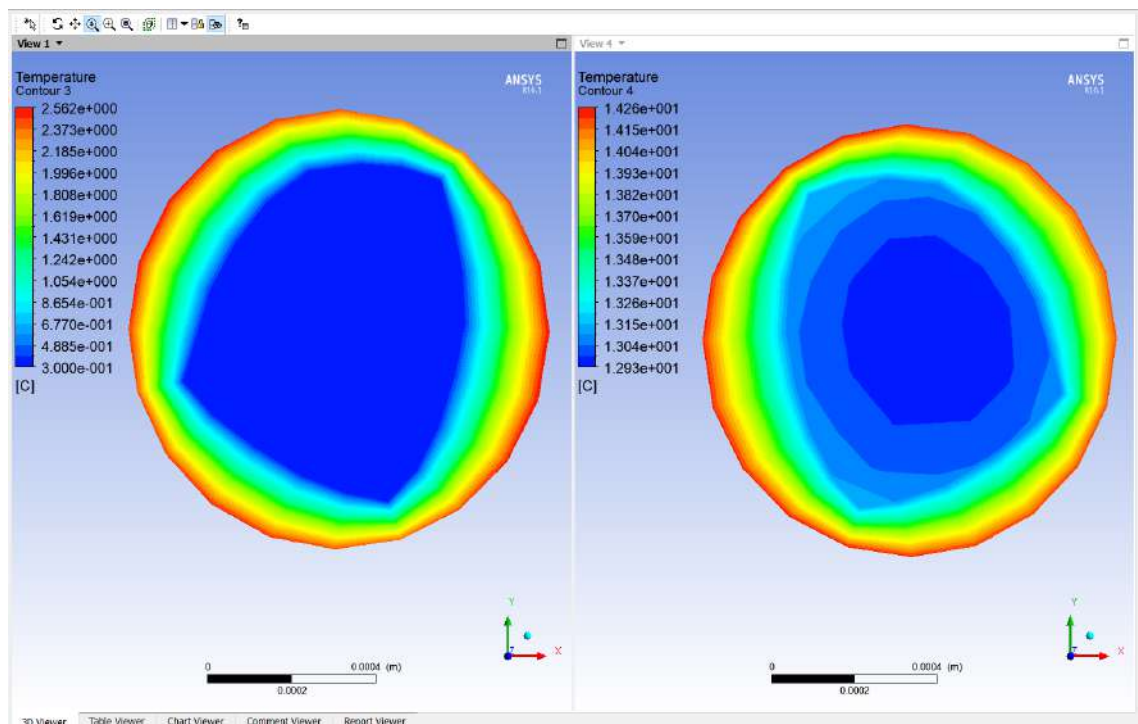


Figure (5.34c): Temperature contour of 0.1% Al₂O₃ for inlet and outlet of the pipe.

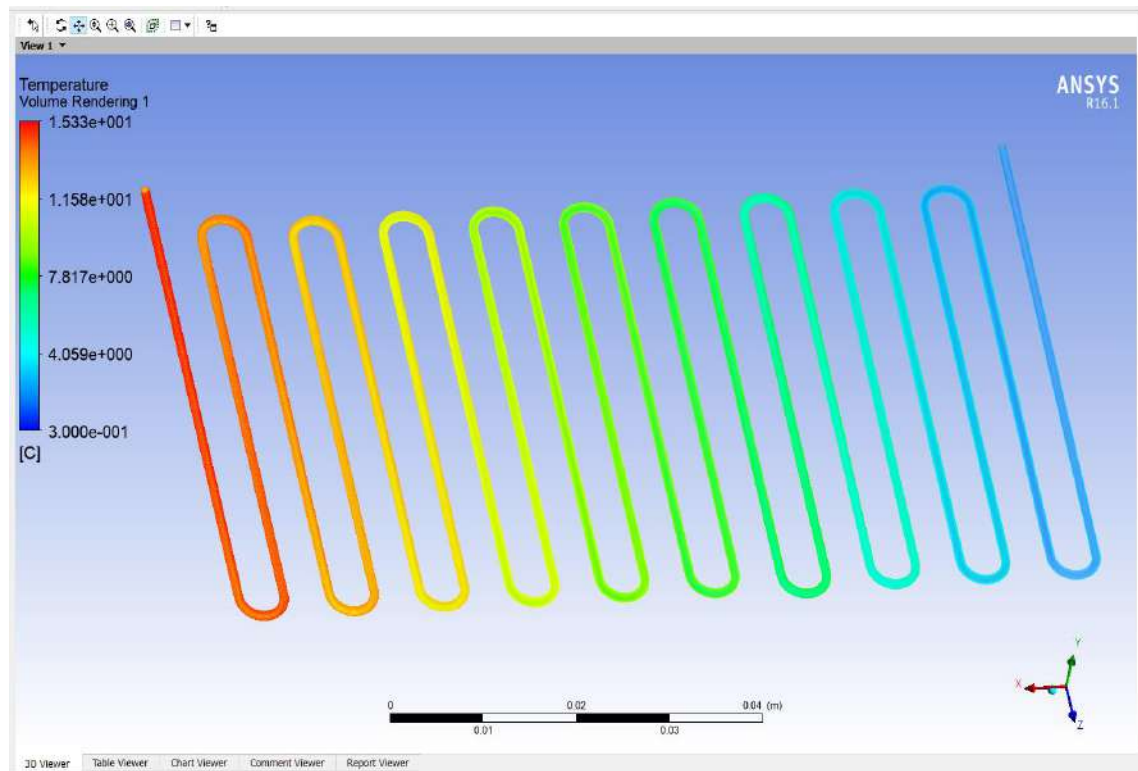


Figure (5.34d): Temperature contour of 0.1% Al_2O_3 for the pipe.

Figure (5.35) shows the contour of 0.1% Al_2O_3 of pressure for the mid plane in pipe and the plane in cross section of each pipe as well as the inlet and outlet sections. The pressure decreased as a little with the length of the evaporator pipe.

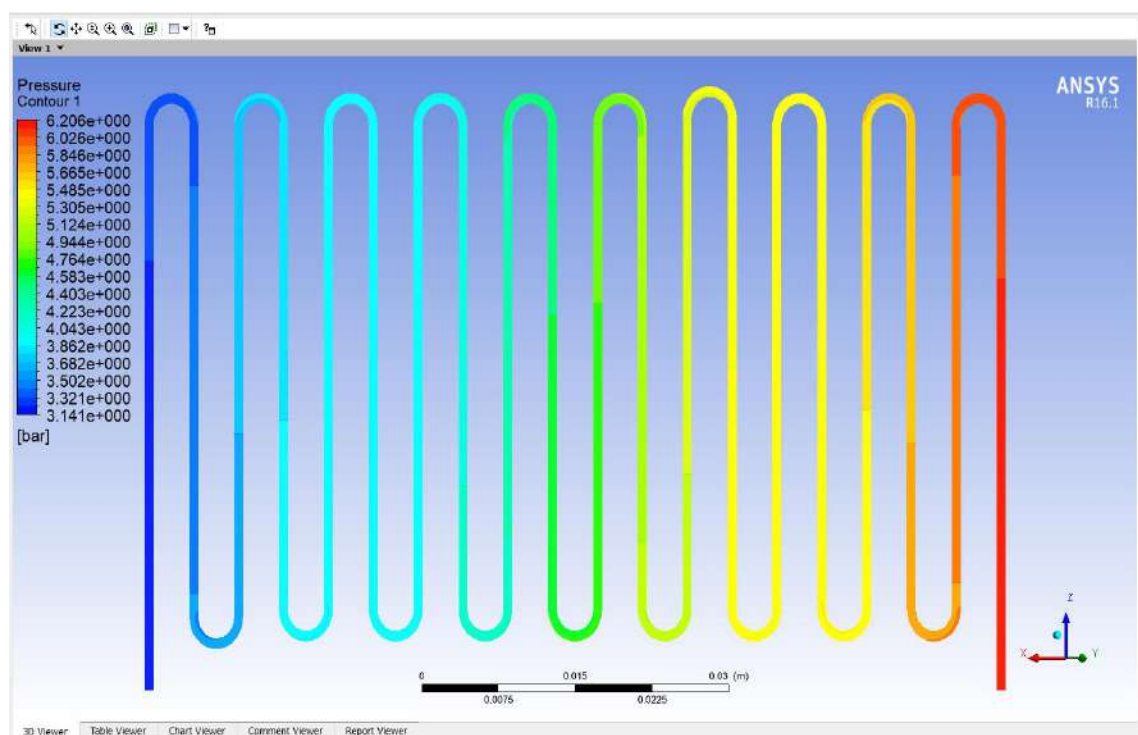


Figure (5.35a): Pressure contour of 0.1% Al_2O_3 for mid plane in the pipe.

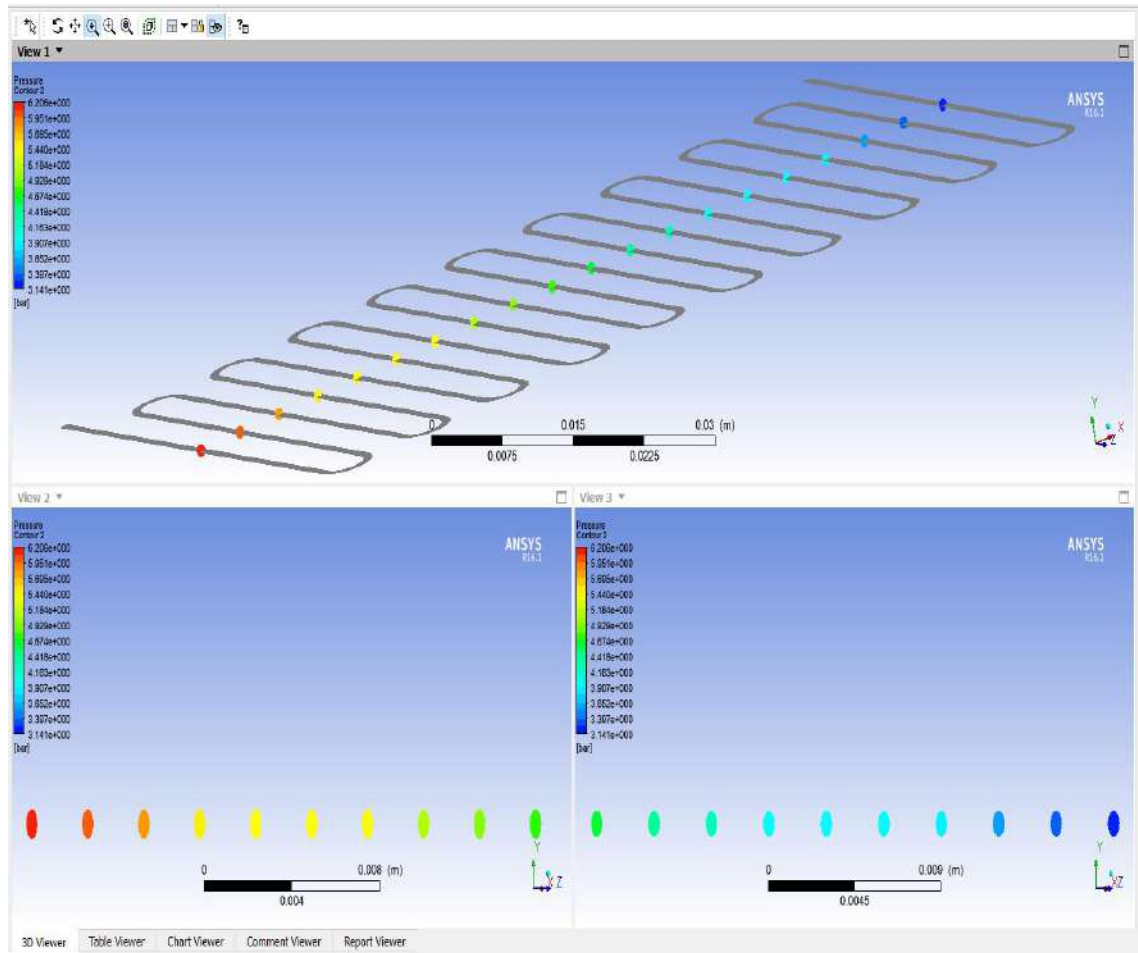


Figure (5.35b): Pressure contour of 0.1% Al₂O₃ for the plane in cross section of the pipe.

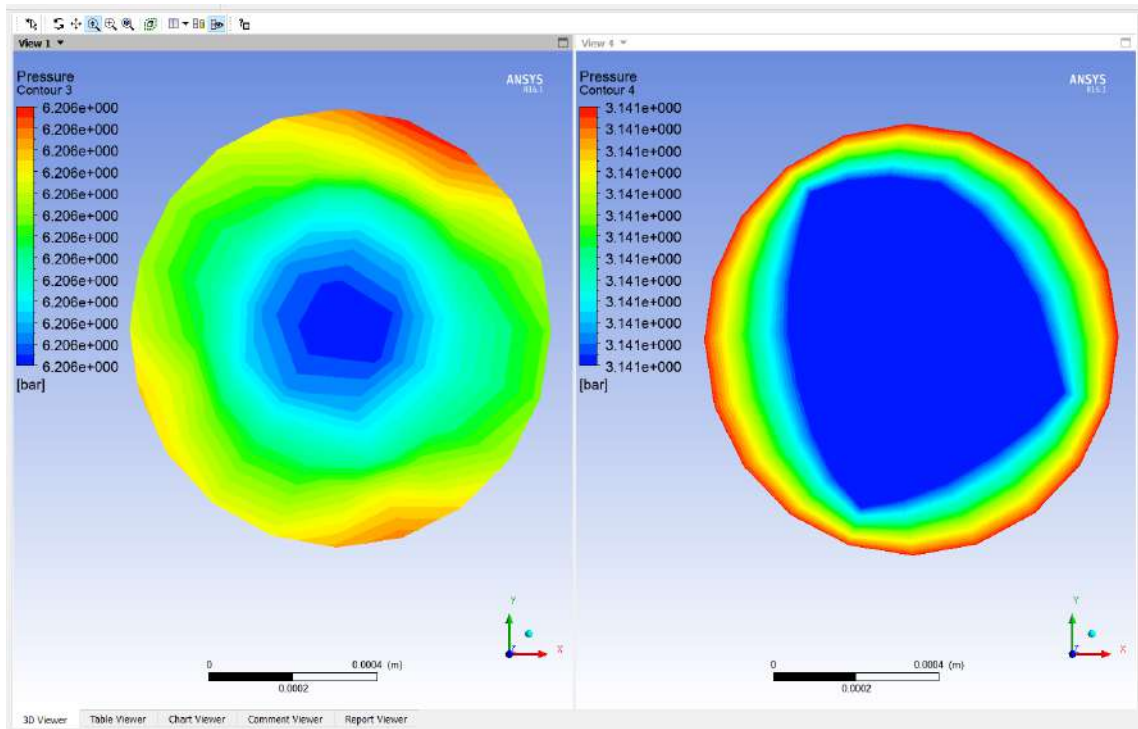


Figure (5.35c): Pressure contour of 0.1% Al₂O₃ for inlet and outlet of the pipe.

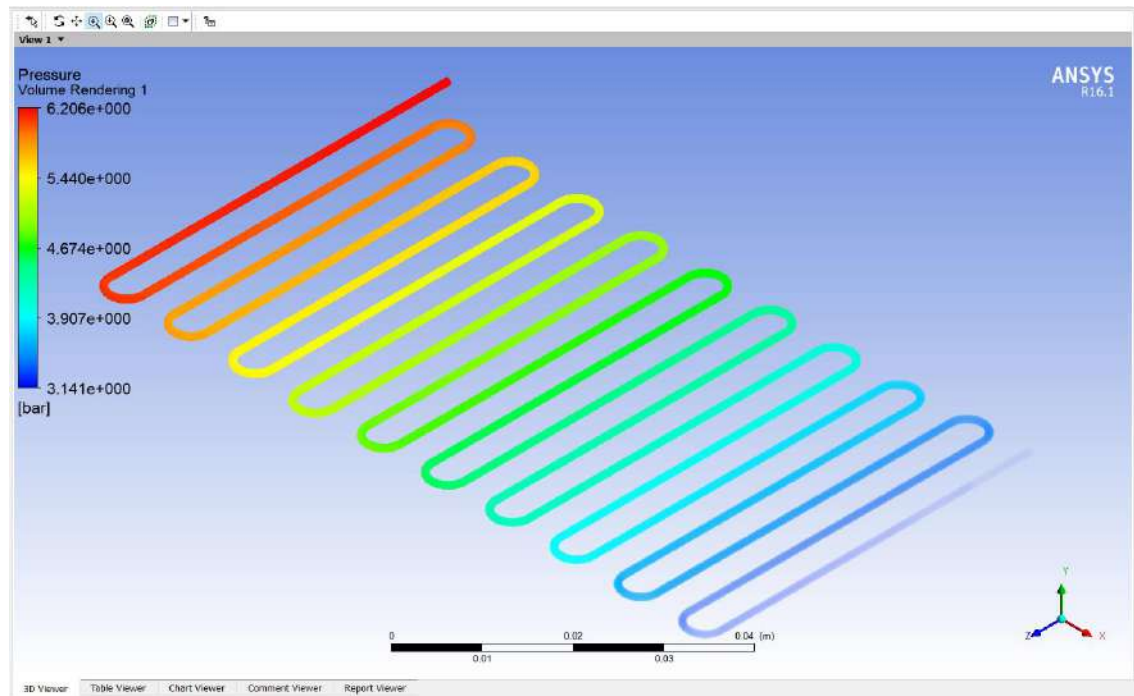


Figure (5.35d): of 0.1% Al_2O_3 Pressure contour for the pipe.

Figure (5.36) indicates the contour of 0.15% Al_2O_3 of the temperature for the mid plane in the pipe and the plane in cross section of each pipe as well as the inlet and outlet sections. The enhancement in temperature was investigated when using nanofluid and this result was nearly the same the experimental work.

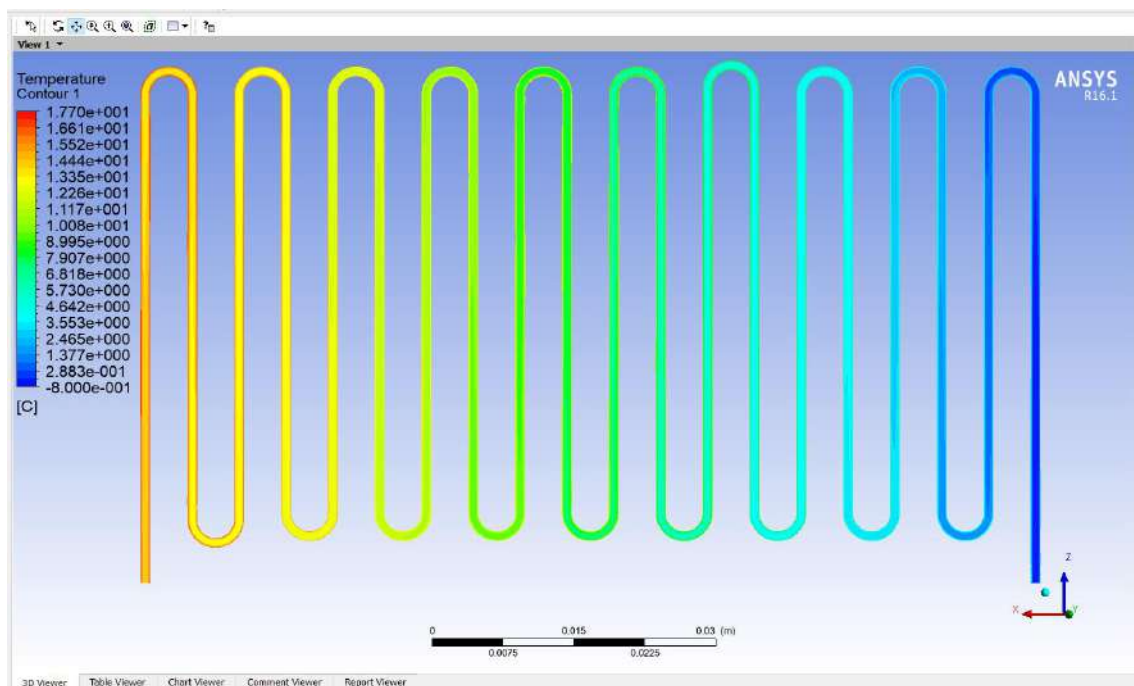


Figure (5.36a): Temperature contour of 0.15% Al_2O_3 for mid plane in the pipe.

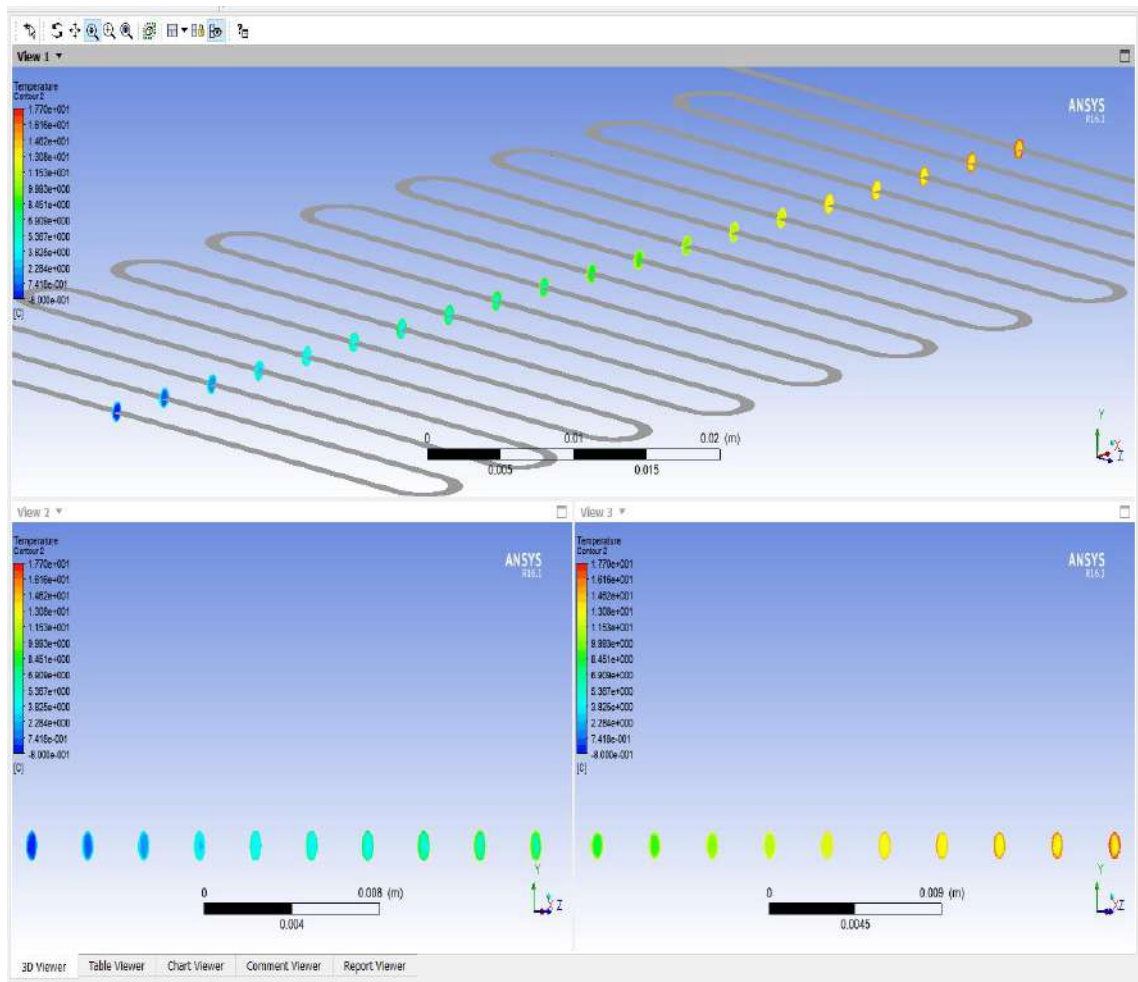


Figure (5.36b): Temperature contour of 0.15% Al₂O₃ for the plane in cross section of the pipe.

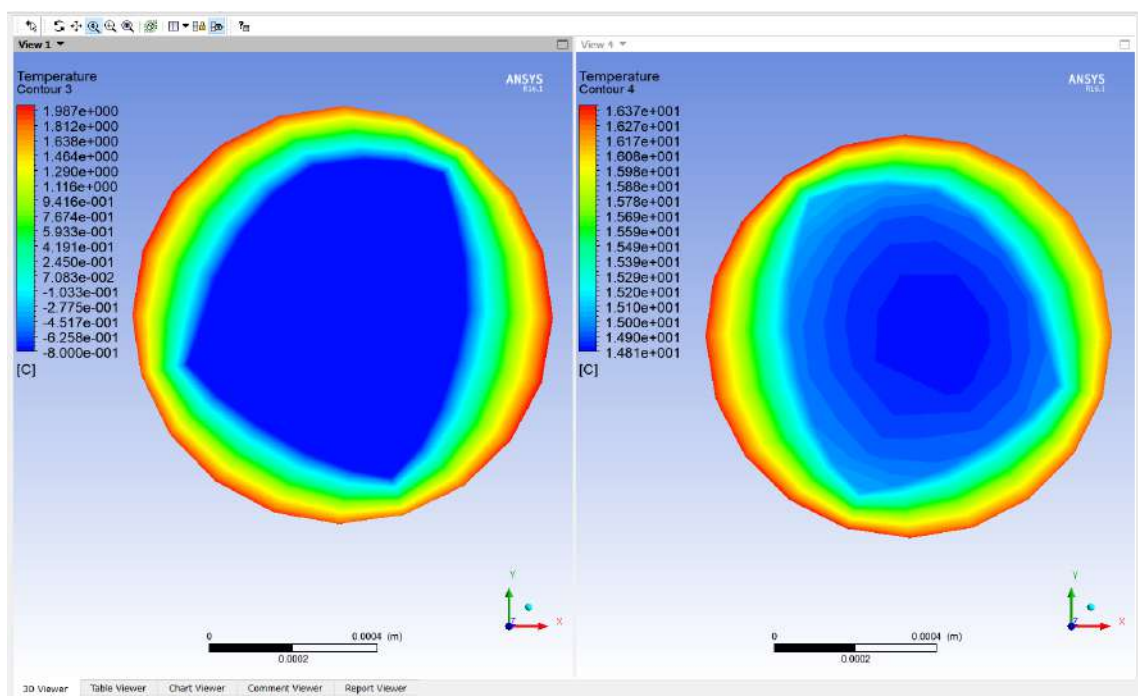


Figure (5.36c): Temperature contour of 0.15% Al₂O₃ for inlet and outlet of the pipe.

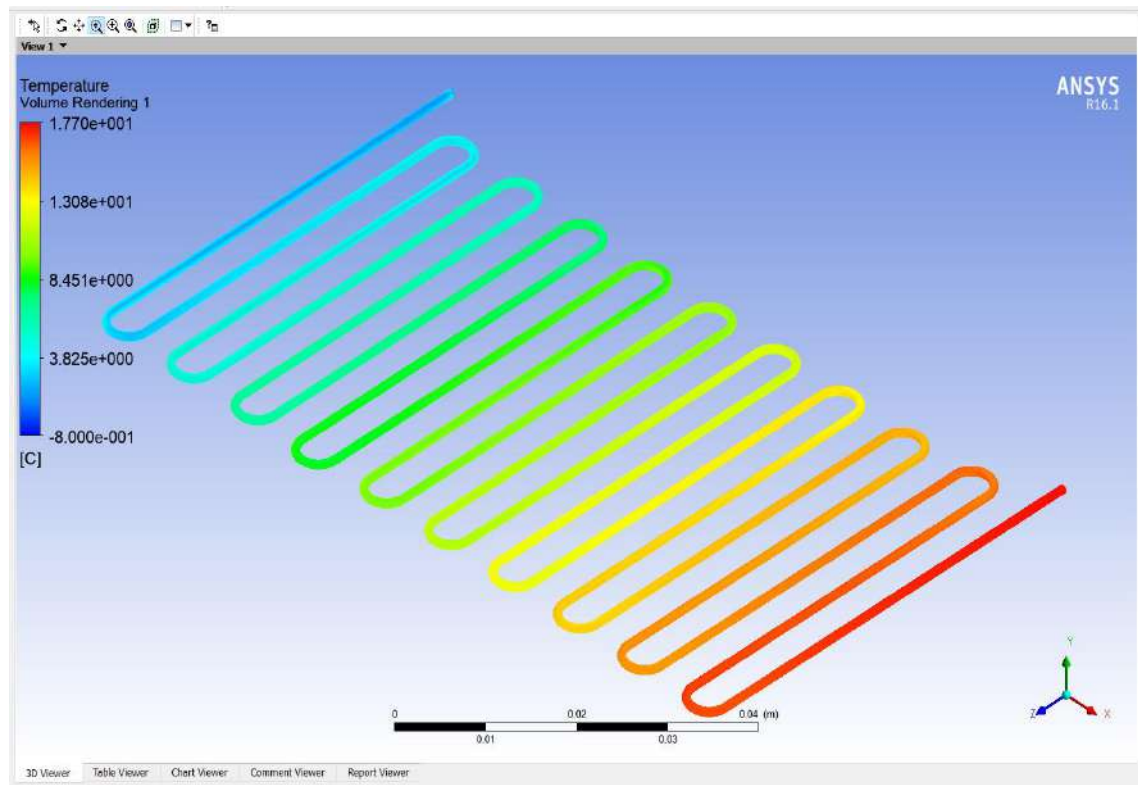


Figure (5.36d): Temperature contour of 0.15% Al₂O₃ for the pipe.

Figure (5.37) shows the contour of 0.15% Al₂O₃ of pressure for the mid plane in pipe and the plane in cross section of each pipe as well as the inlet and outlet sections. The pressure decreased as a little with the length of the evaporator pipe.

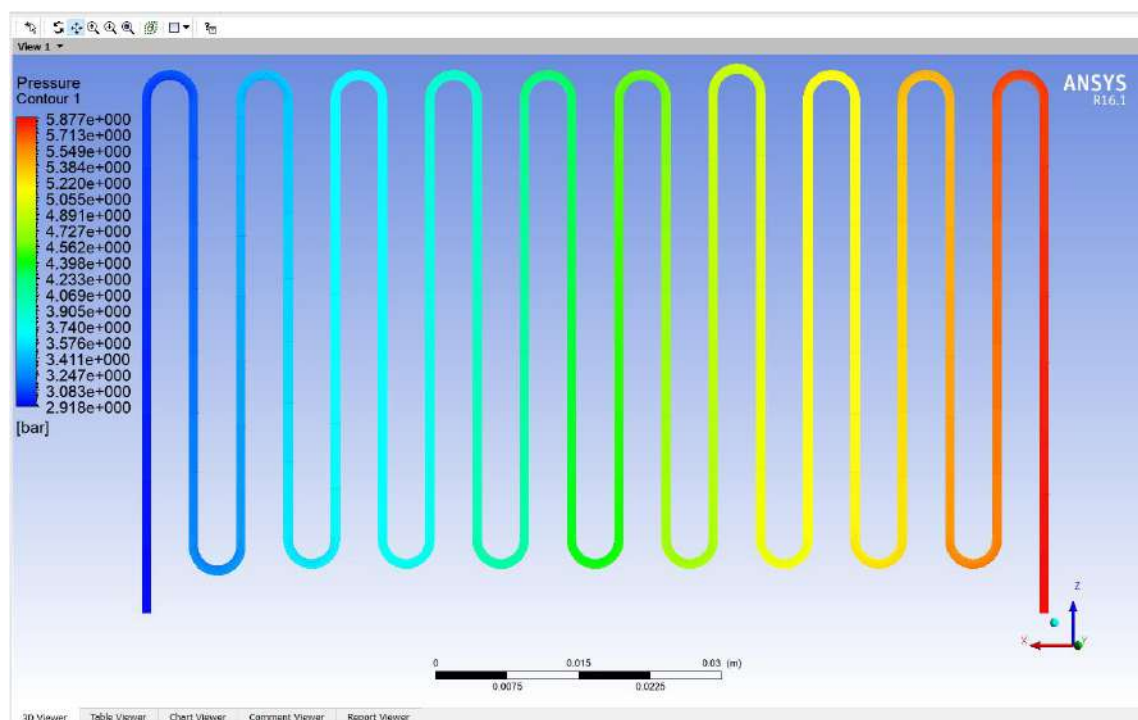


Figure (5.37a): Pressure contour of 0.15% Al₂O₃ for mid plane in the pipe.

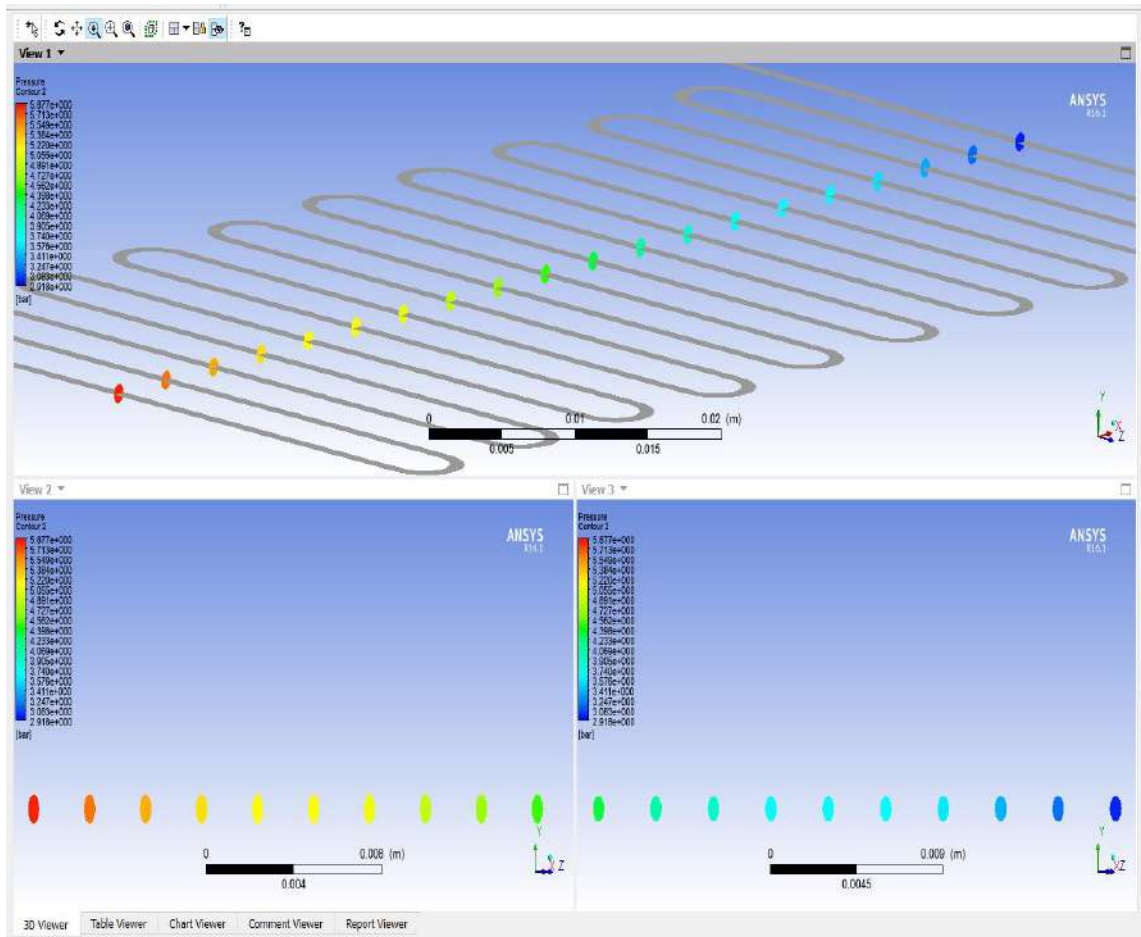


Figure (5.37b): Pressure contour of 0.15% Al₂O₃ for the plane in cross section of the pipe.

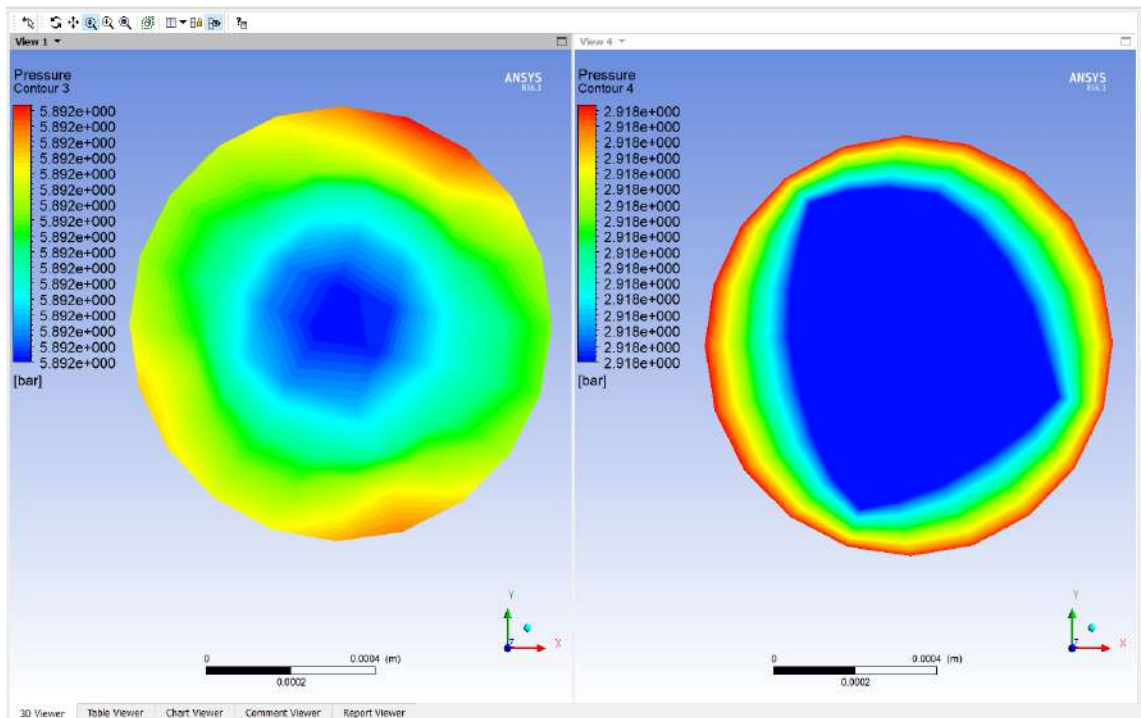


Figure (5.37c): Pressure contour of 0.15% Al₂O₃ for inlet and outlet of the pipe.

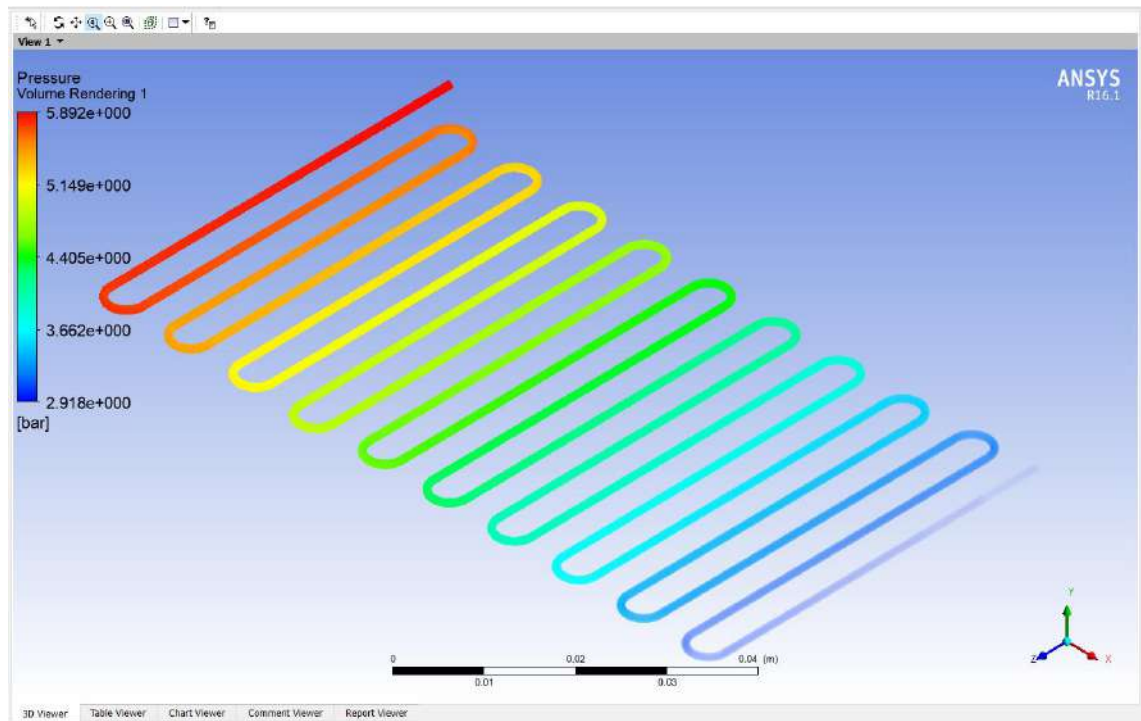


Figure (5.37d): Pressure contour of 0.15% Al_2O_3 for the pipe.

Figure (5.38) indicates the contour of 0.2% Al_2O_3 of the temperature for the mid plane in the pipe and the plane in cross section of each pipe as well as the inlet and outlet sections. The enhancement in temperature is investigated when using nanofluid and this result was nearly the same as the experimental work.

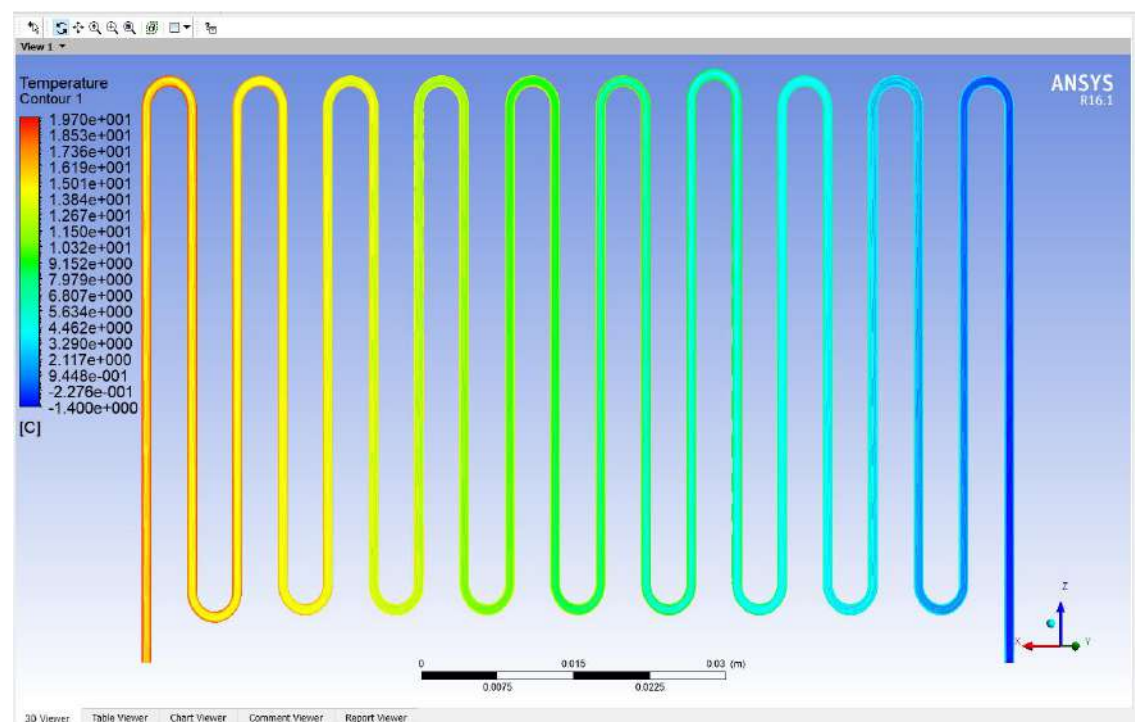


Figure (5.38a): Temperature contour 0.2% Al_2O_3 for mid plane in the pipe.

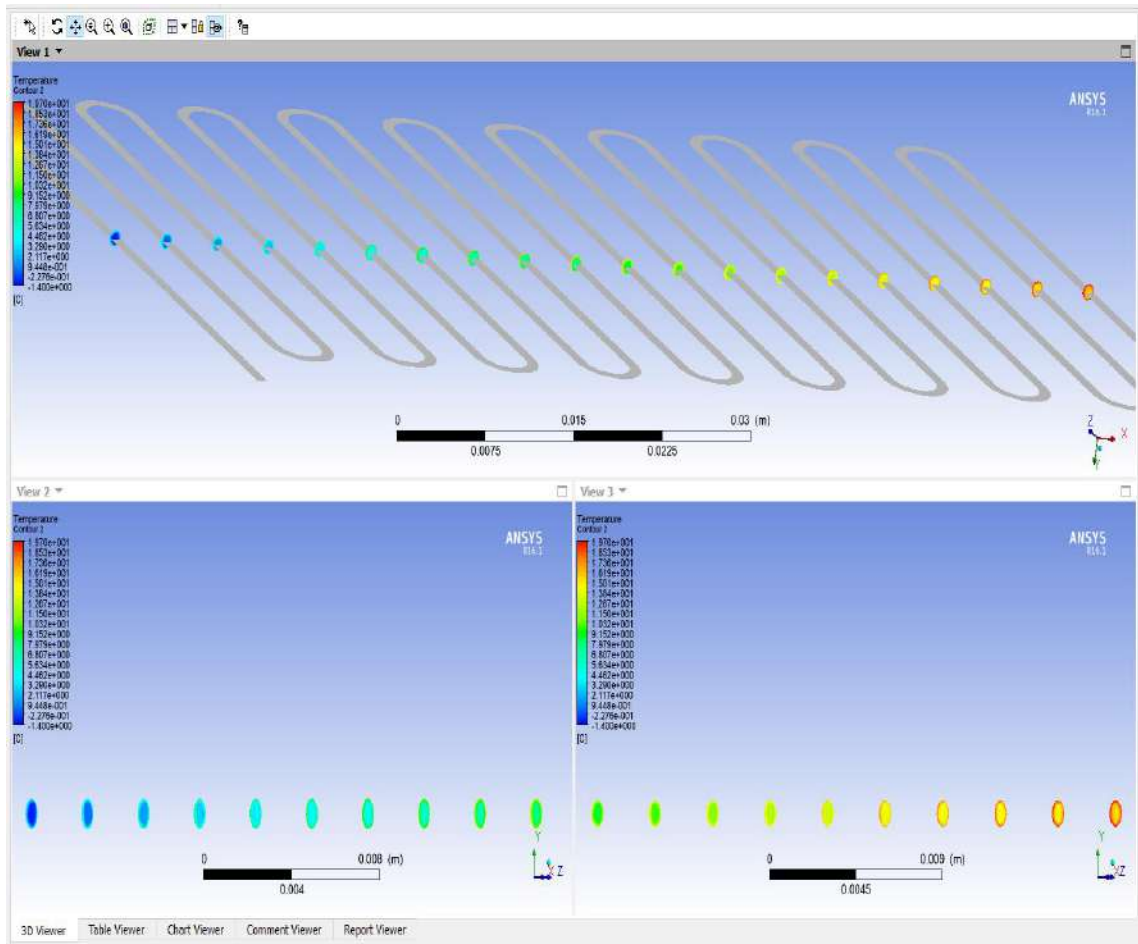


Figure (5.38b): Temperature contour 0.2% Al₂O₃ for the plane in cross section of the pipe.

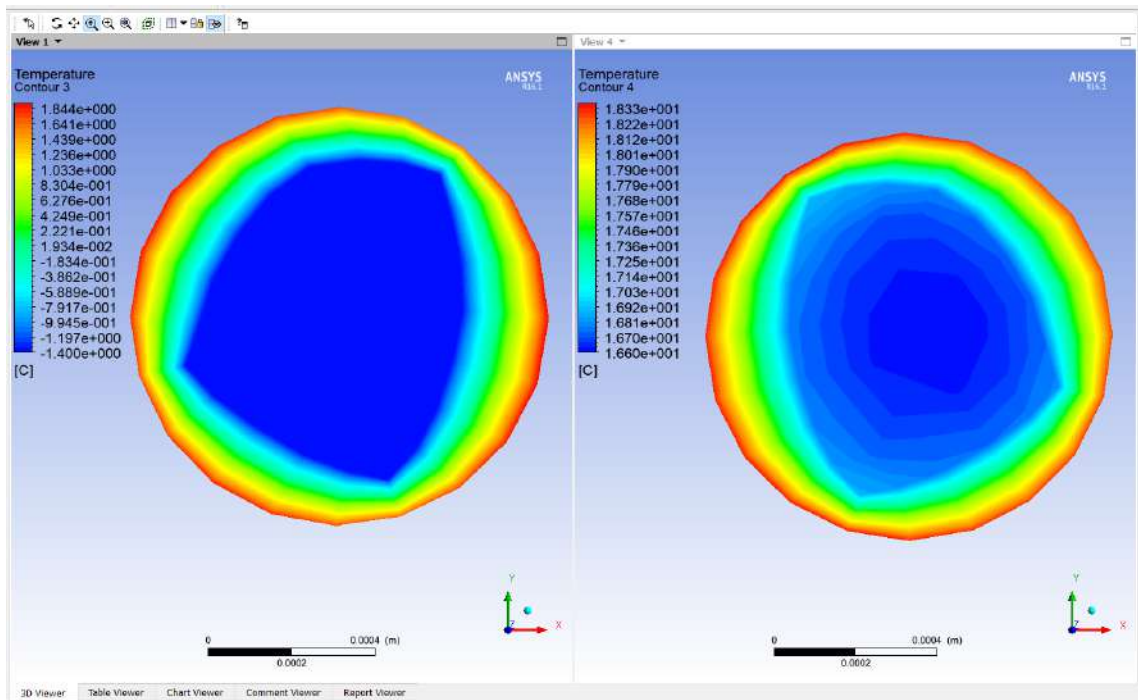


Figure (5.38c): Temperature contour 0.2% Al₂O₃ for inlet and outlet of the pipe.

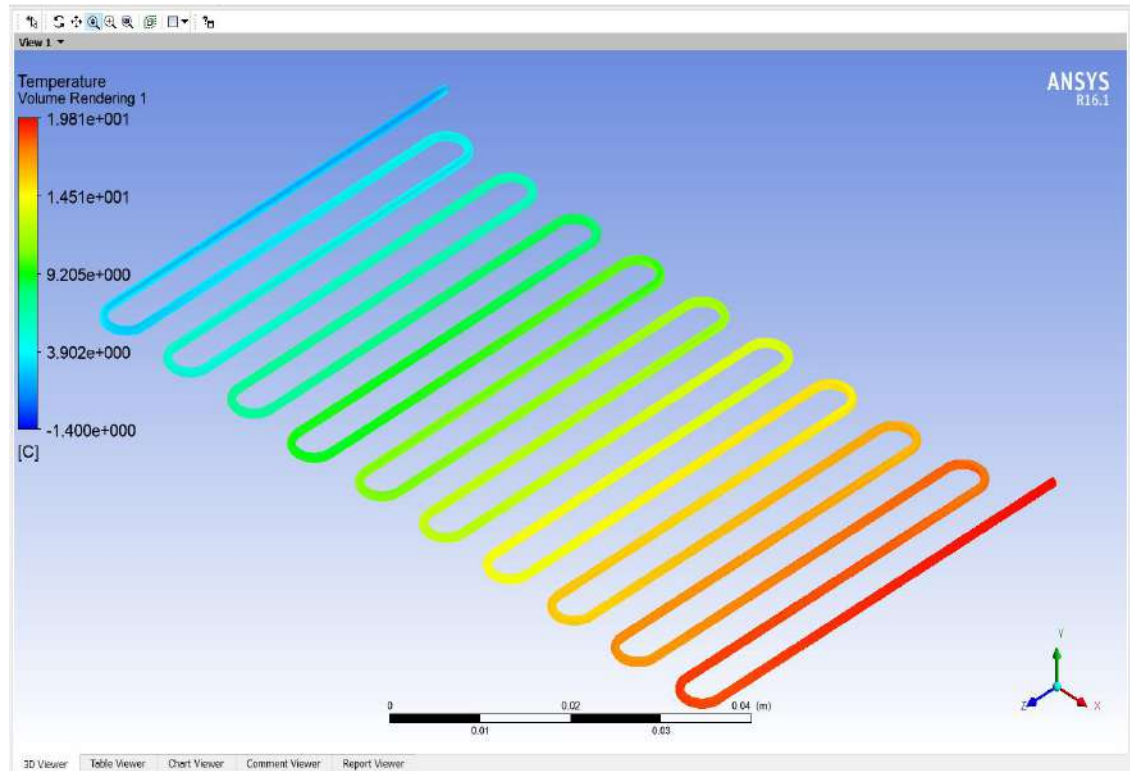


Figure (5.38d): Temperature contour 0.2% Al_2O_3 for the pipe.

Figure (5.39) shows the contour of 0.2% Al_2O_3 of pressure for the mid plane in pipe and the plane in cross section of each pipe as well as the inlet and outlet sections. The pressure decreased as a little with length of the evaporator pipe.

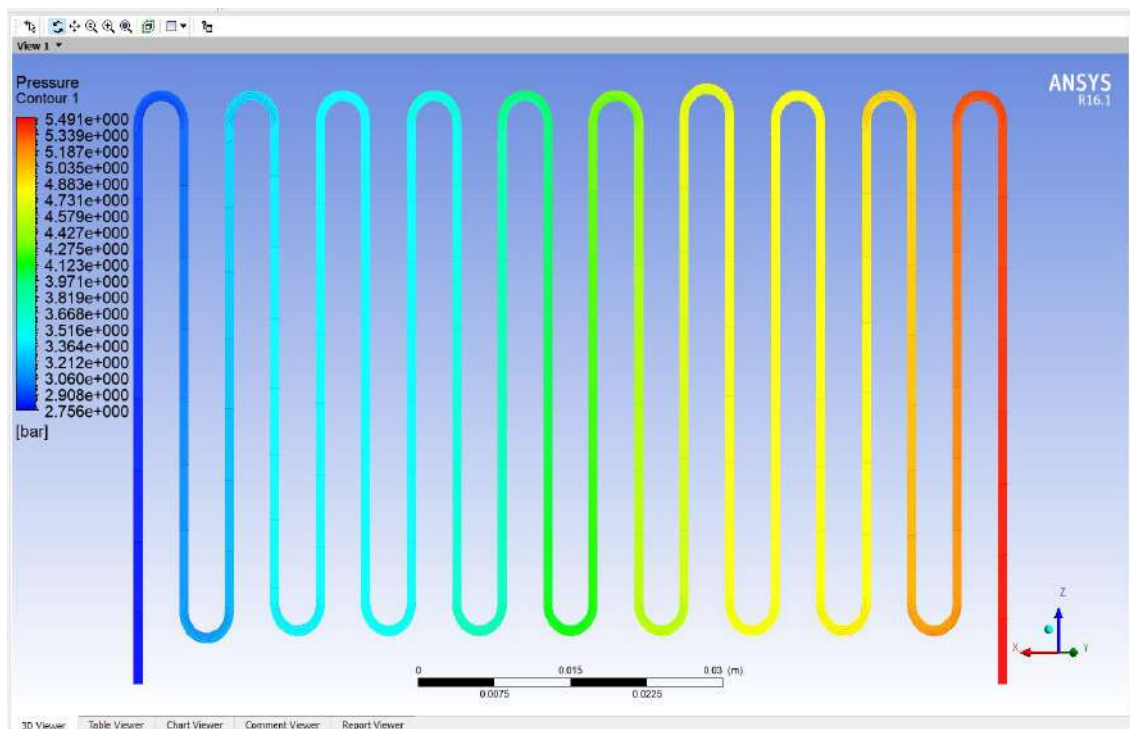


Figure (5.39a): Pressure contour 0.2% Al_2O_3 for mid plane in the pipe.

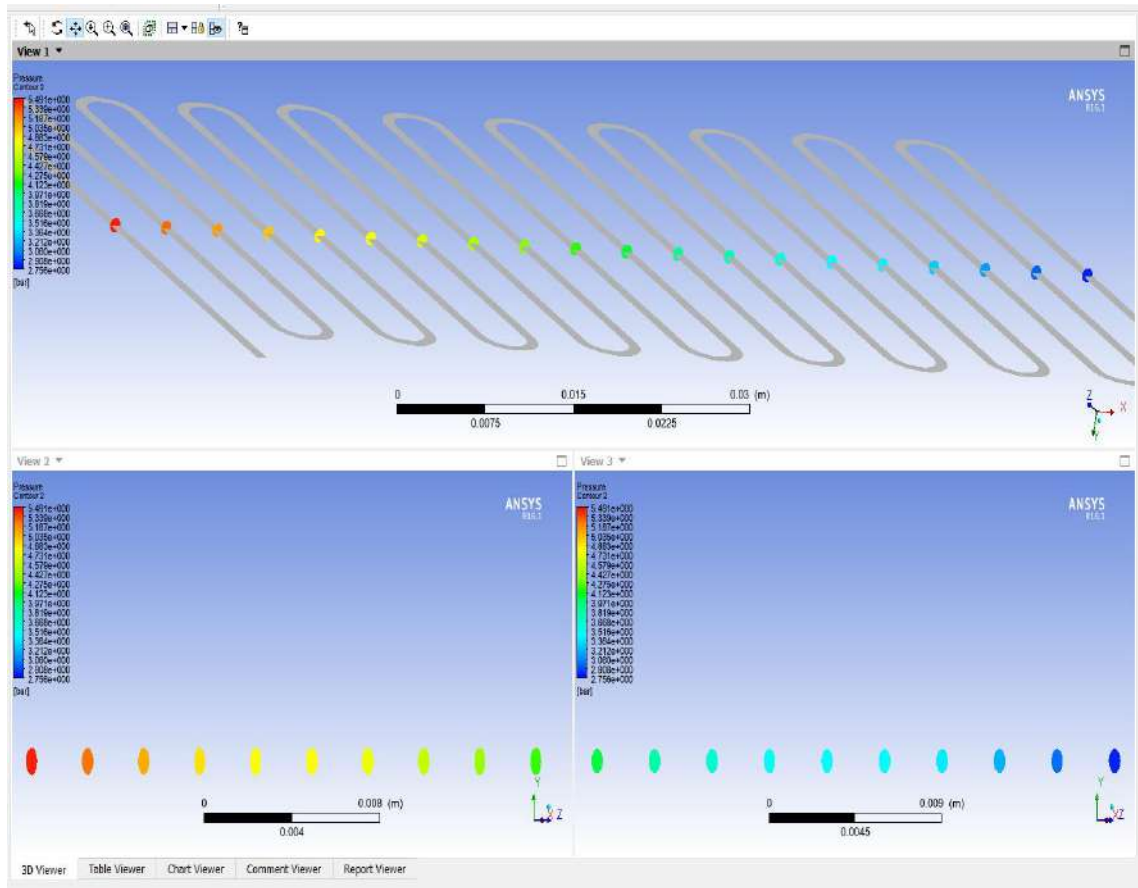


Figure (5.39b): Pressure contour 0.2% Al_2O_3 for the plane in cross section of the pipe.

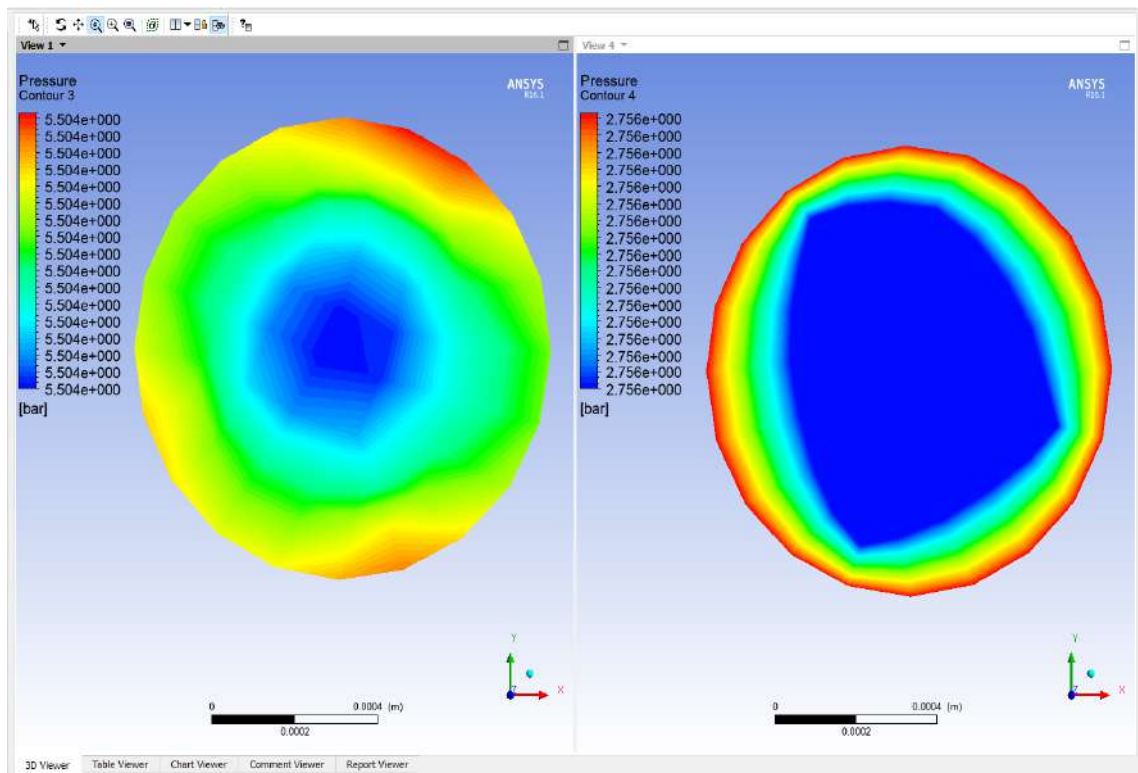


Figure (5.39c): Pressure contour 0.2% Al_2O_3 for inlet and outlet of the pipe.

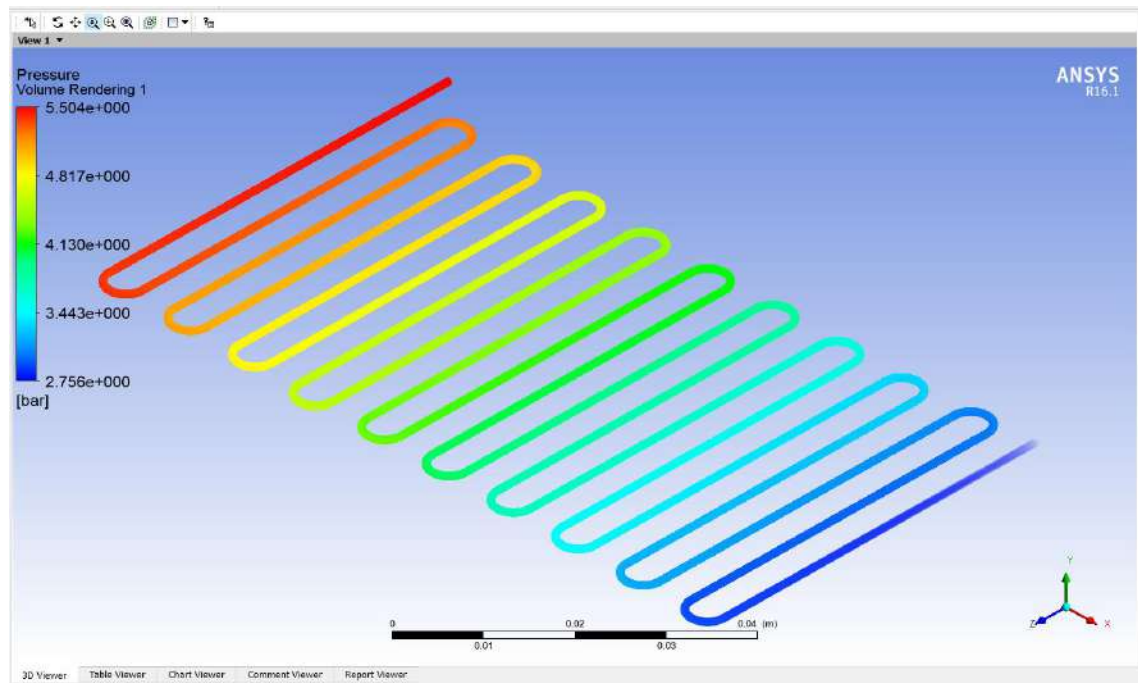


Figure (5.39d): Pressure contour 0.2% Al_2O_3 for the pipe.

5.3.3 Ag Nano Refrigerant Analysis

This section deals with the simulation of Ag nanorefrigerant. Figure (5.40) indicates the contour of 0.01% Ag of the temperature for the mid plane in pipe and the plane in cross section of each pipe as well as the inlet and outlet sections. The enhancement in temperature was investigated when using nano fluid and this result was nearly the same as the experimental work.

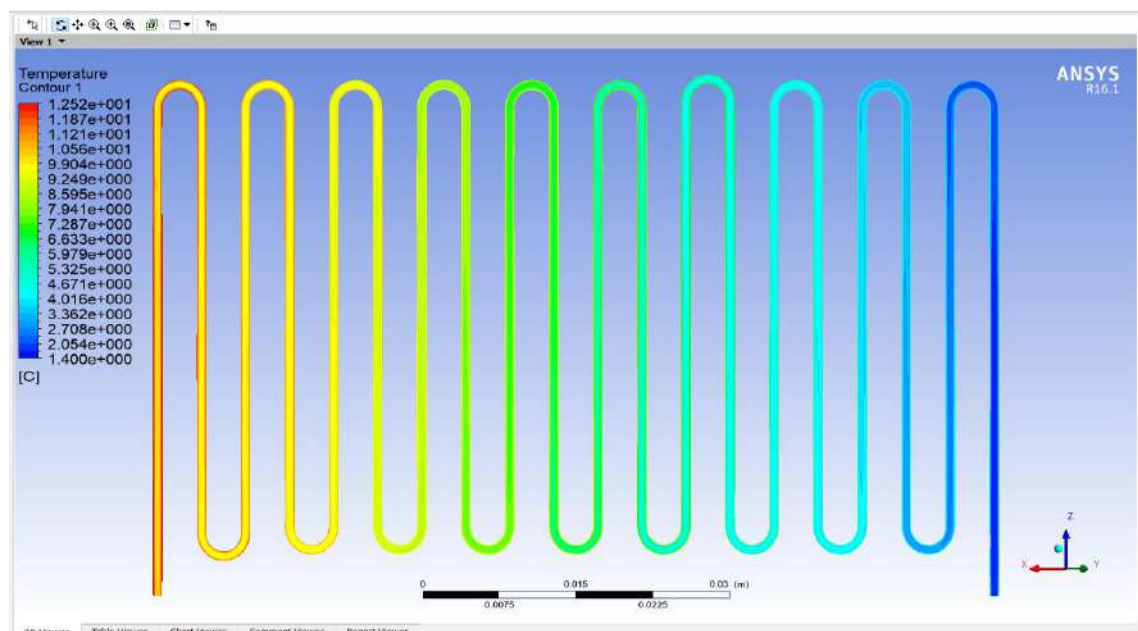


Figure (5.40a): Temperature contour of 0.01% Ag for mid plane in the pipe.

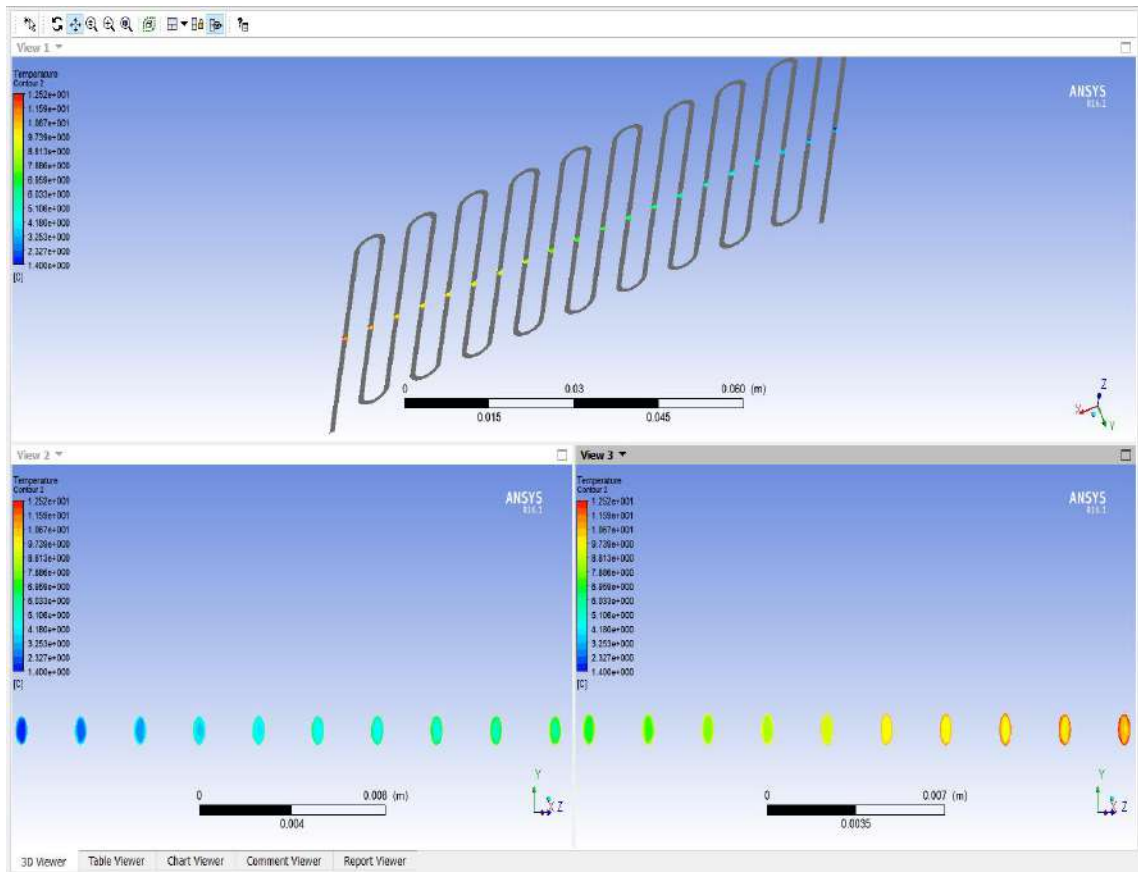


Figure (5.40b): Temperature contour of 0.01%Ag for the plane in cross section of the pipe.

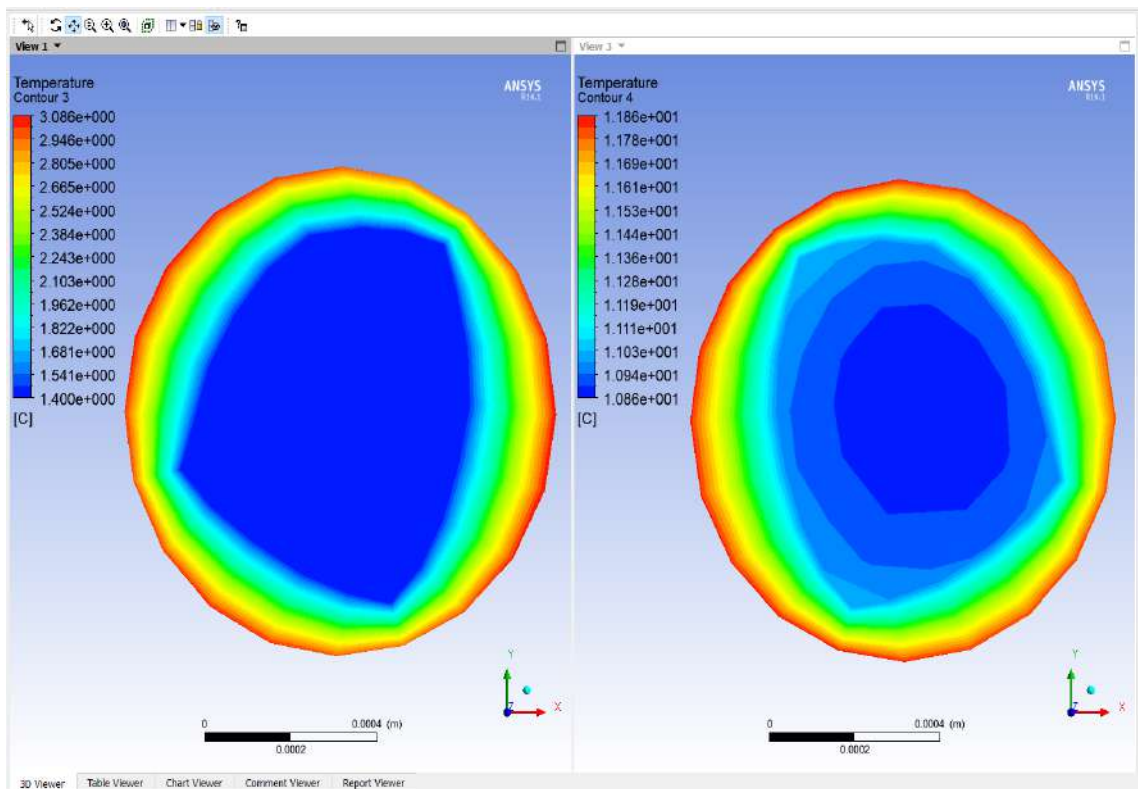


Figure (5.40c): Temperature contour of 0.01%Ag for inlet and outlet of the pipe.

Figure (5.41) shows the contour of 0.01%Ag of pressure for the mid plane in pipe and the plane in cross section of each pipe as well as the inlet and outlet sections. The pressure decreased as a little with the length of the evaporator pipe.

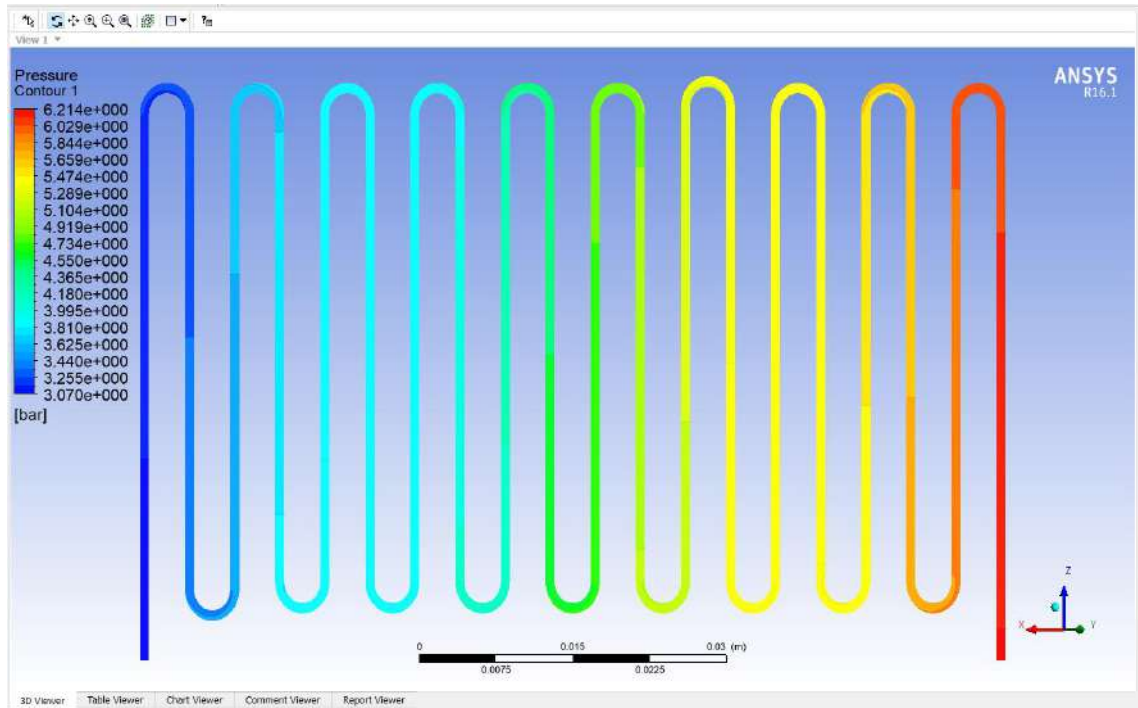


Figure (5.41a): Pressure contour of 0.01%Ag for mid plane in the pipe.

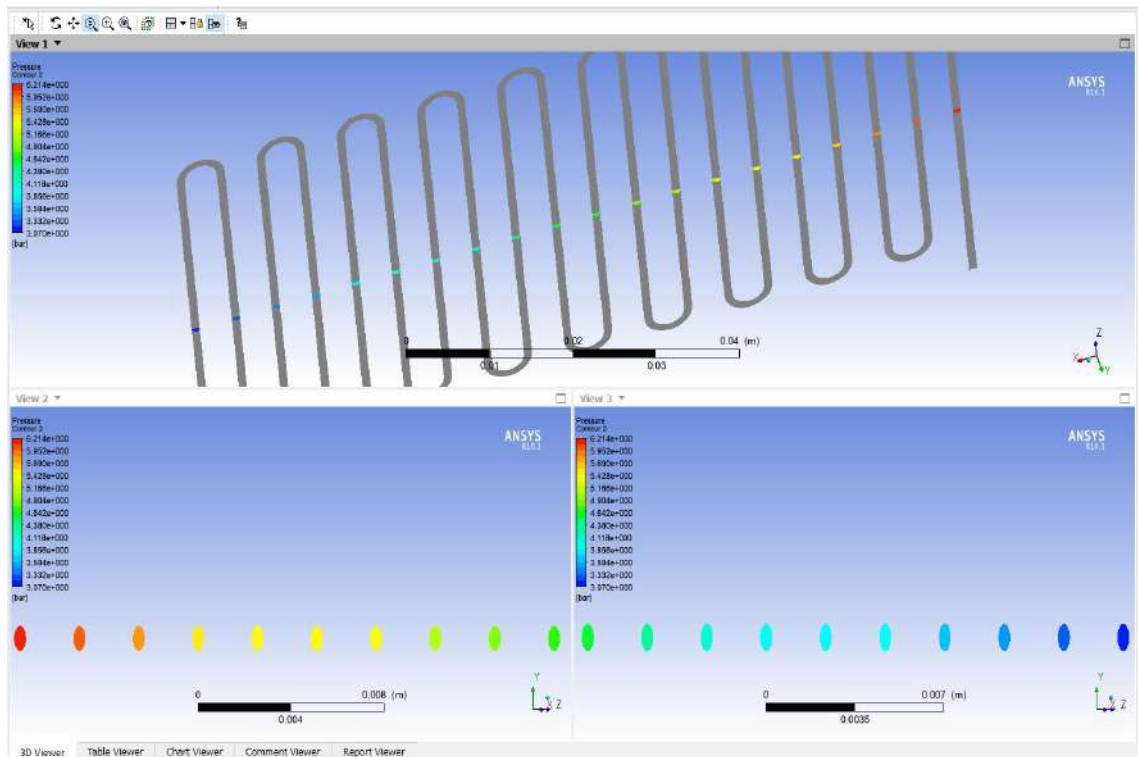


Figure (5.41b): Pressure contour of 0.01%Ag for the plane in cross section of the pipe.

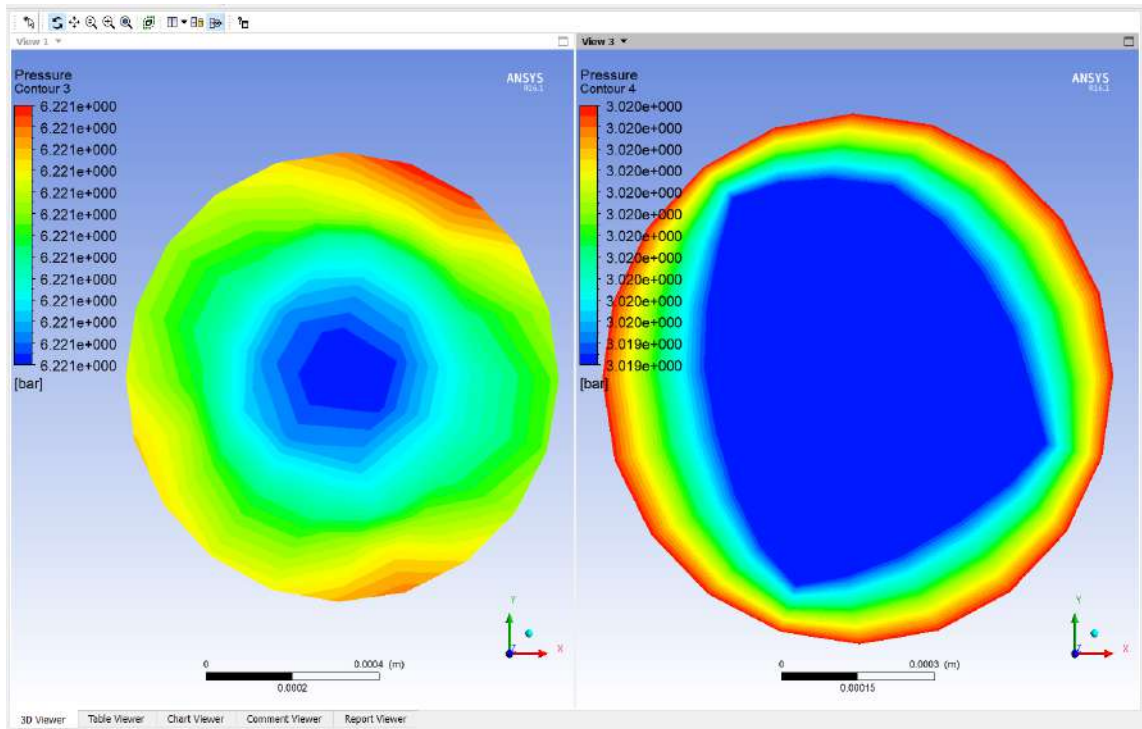


Figure (5.41c): Pressure contour of 0.01%Ag for inlet and outlet of the pipe.

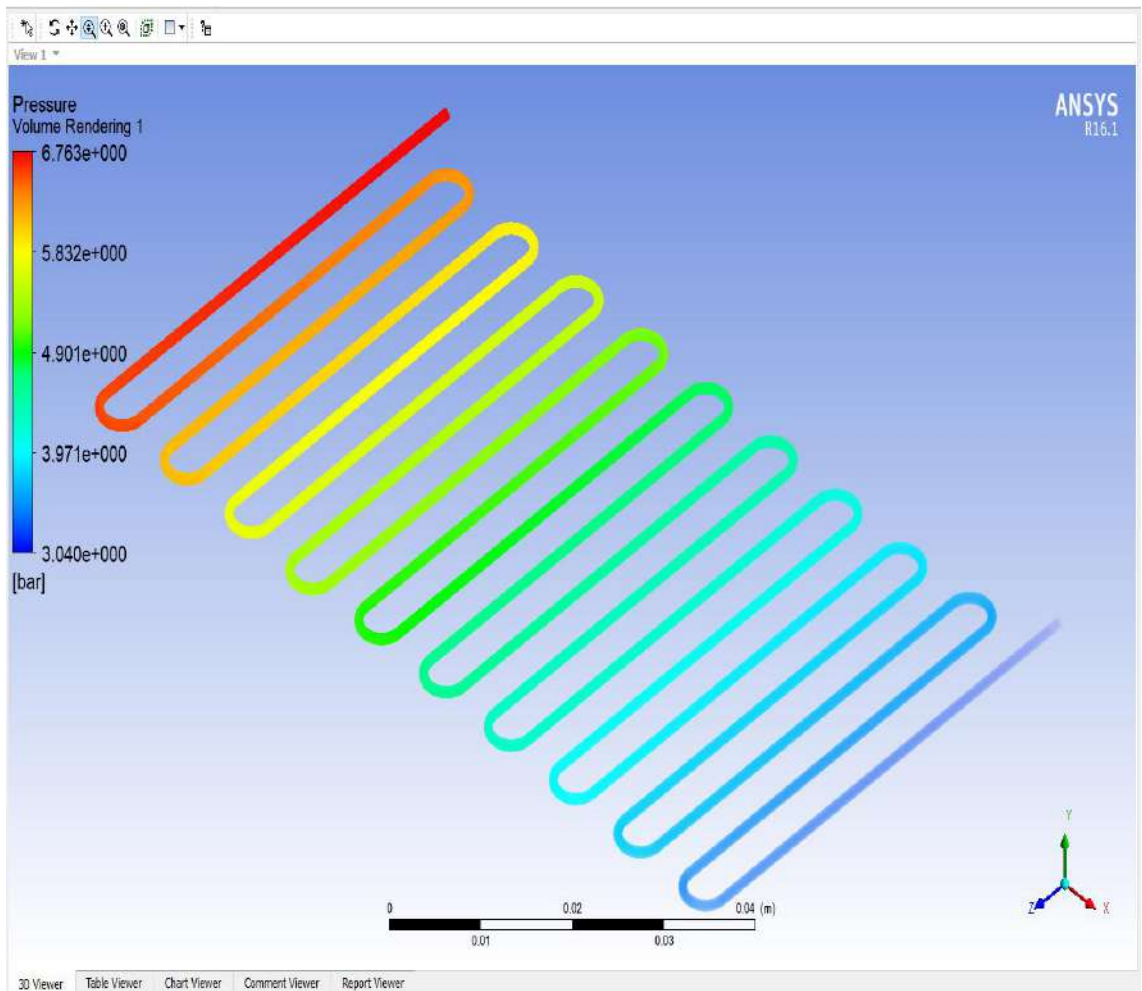


Figure (5.41d): Pressure contour of 0.01%Ag for the pipe.

Figure (5.42) indicates the contour of 0.05%Ag of the temperature for the mid plane in pipe and the plane in cross section of each pipe as well as the inlet and outlet sections. The enhancement in temperature is investigated when using nanofluid and this result were nearly the same the experimental work.

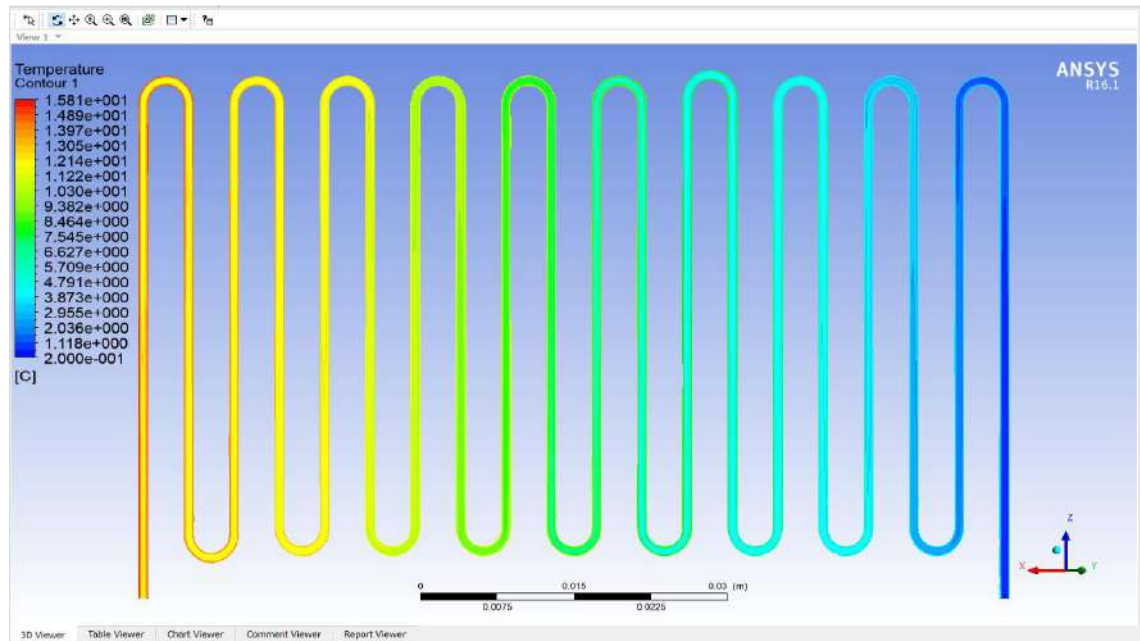


Figure (5.42a): Temperature contour of 0.05%Ag for mid plane in the pipe.

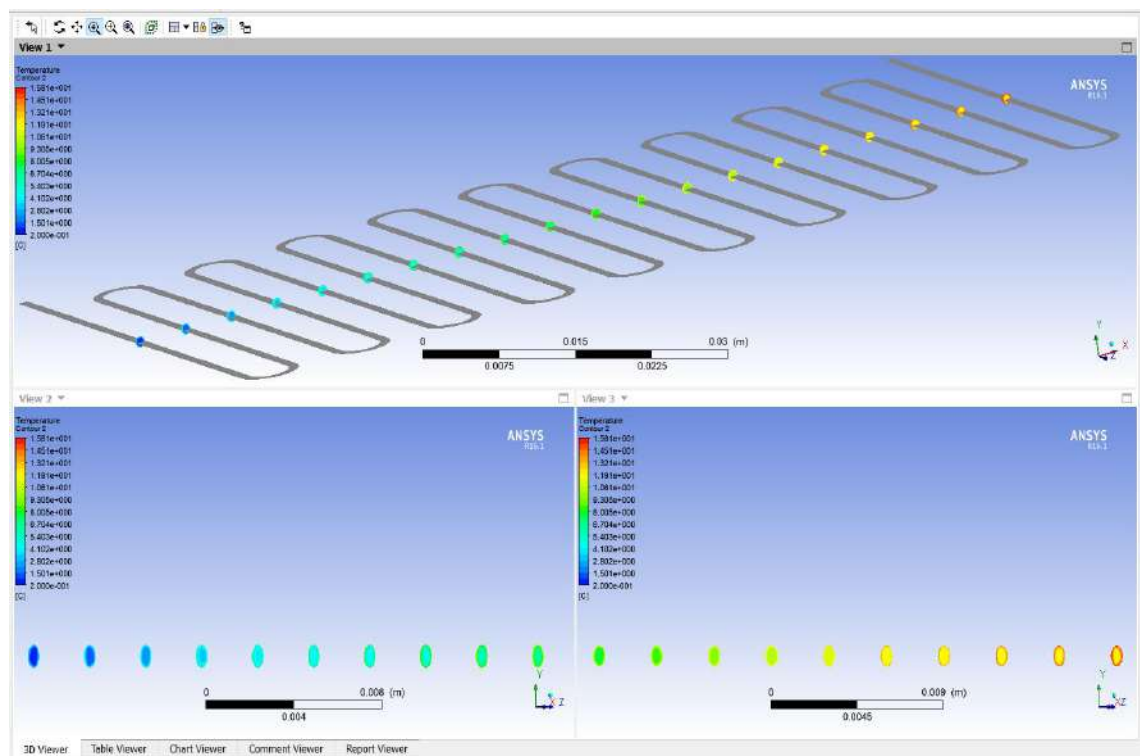


Figure (5.42b): Temperature contour of 0.05%Ag for the plane in cross section of the pipe.

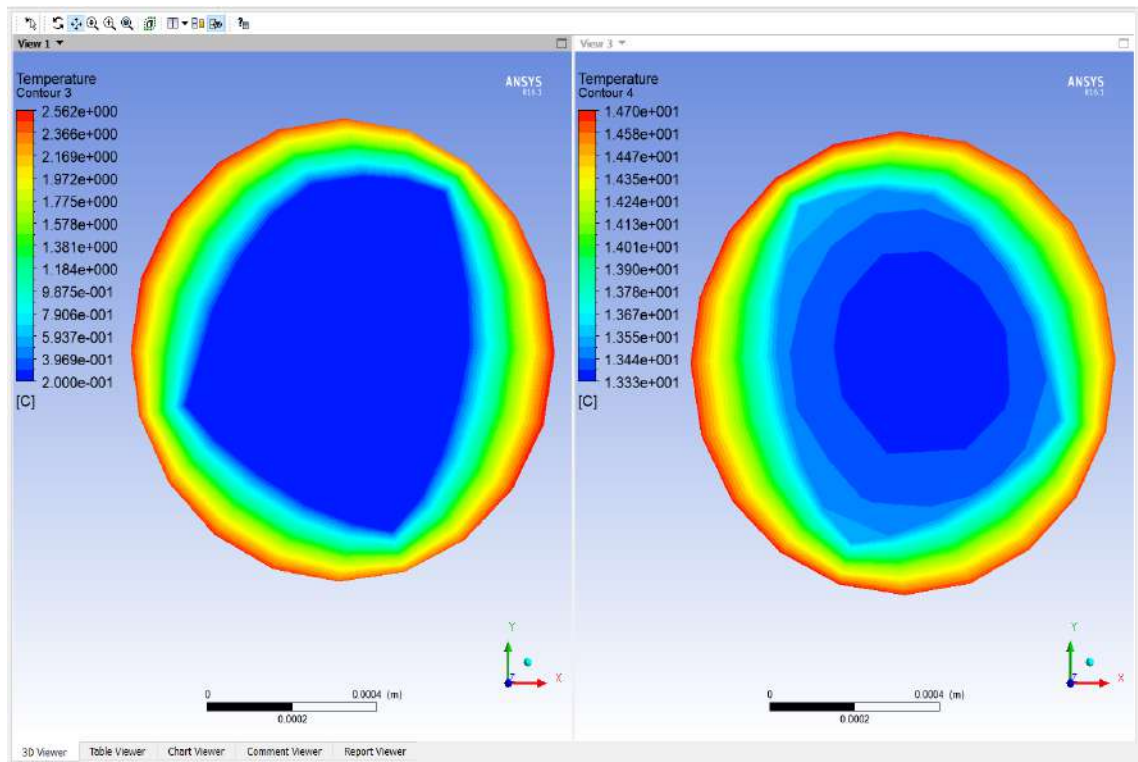


Figure (5.42c): Temperature contour of 0.05% Ag for inlet and outlet of the pipe.

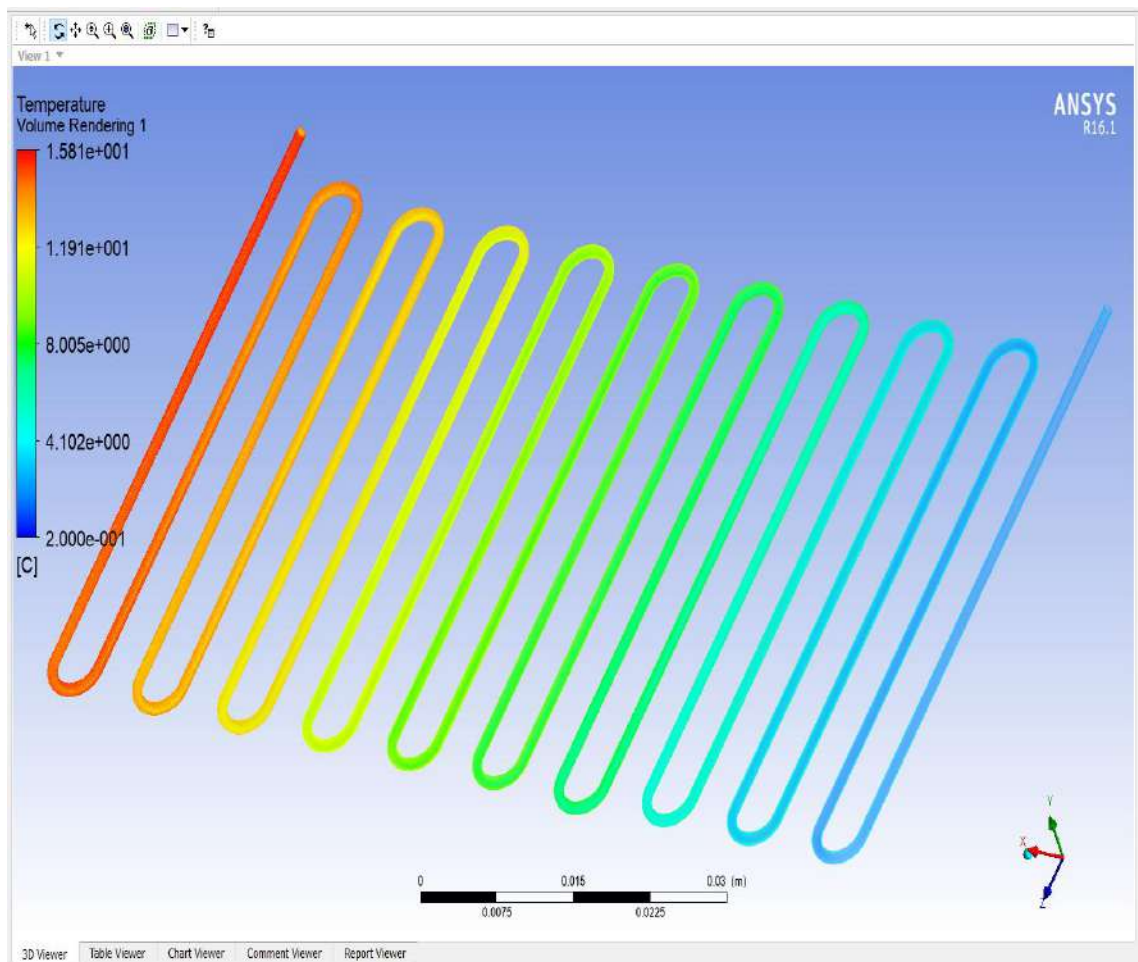


Figure (5.42d): Temperature contour of 0.05% Ag for the pipe.

Figure (5.43) shows the contour of 0.05%Ag of pressure for the mid plane in pipe and the plane in cross section of each pipe as well as the inlet and outlet sections. The pressure decreased as a little with the length of the evaporator pipe.

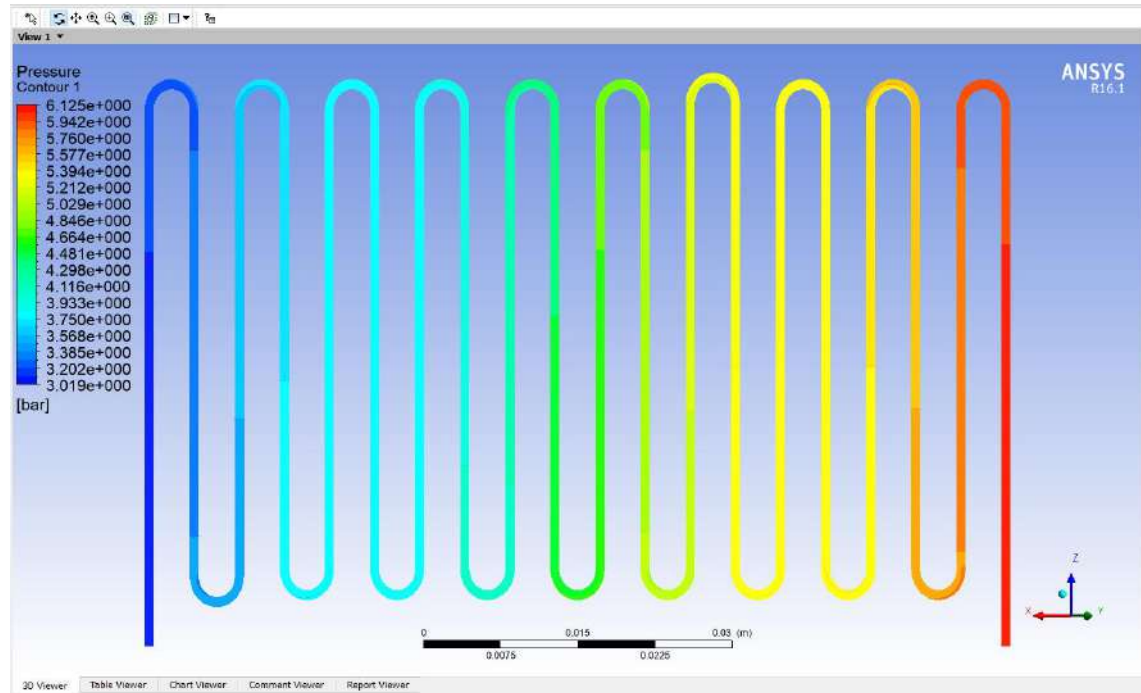


Figure (5.43a): Pressure contour of 0.05%Ag for mid plane in the pipe.

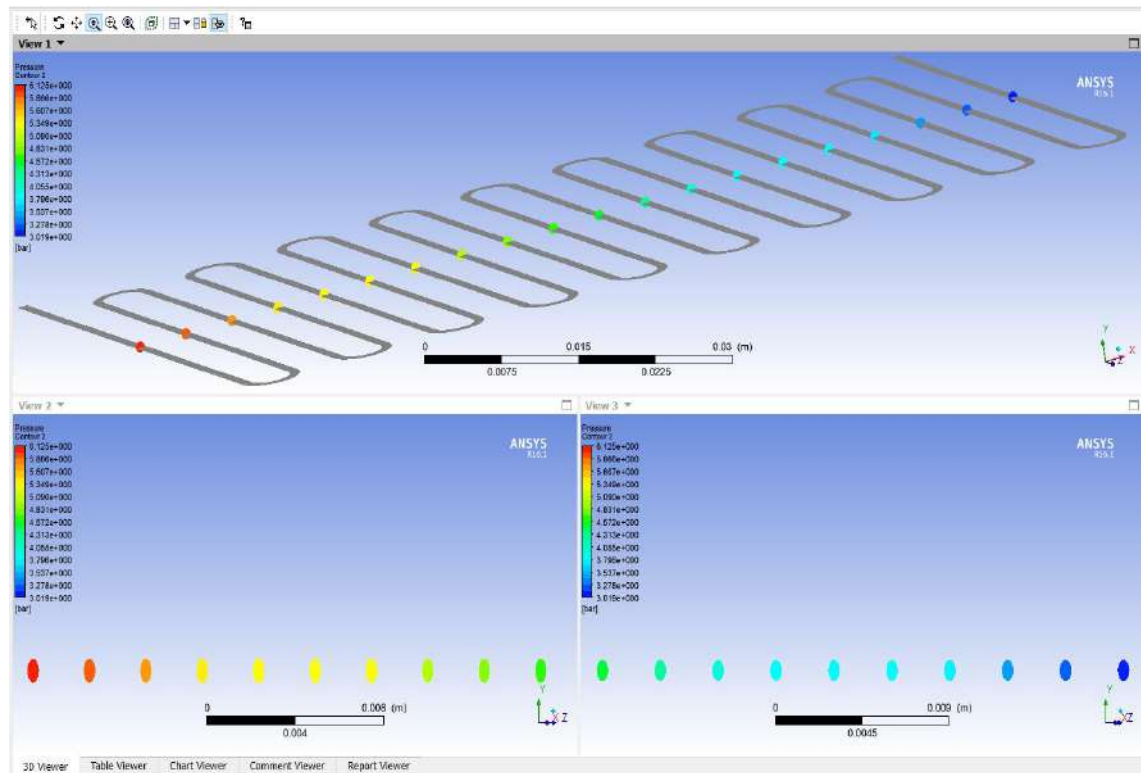


Figure (5.43b): Pressure contour of 0.05%Ag for the plane in cross section of the pipe.

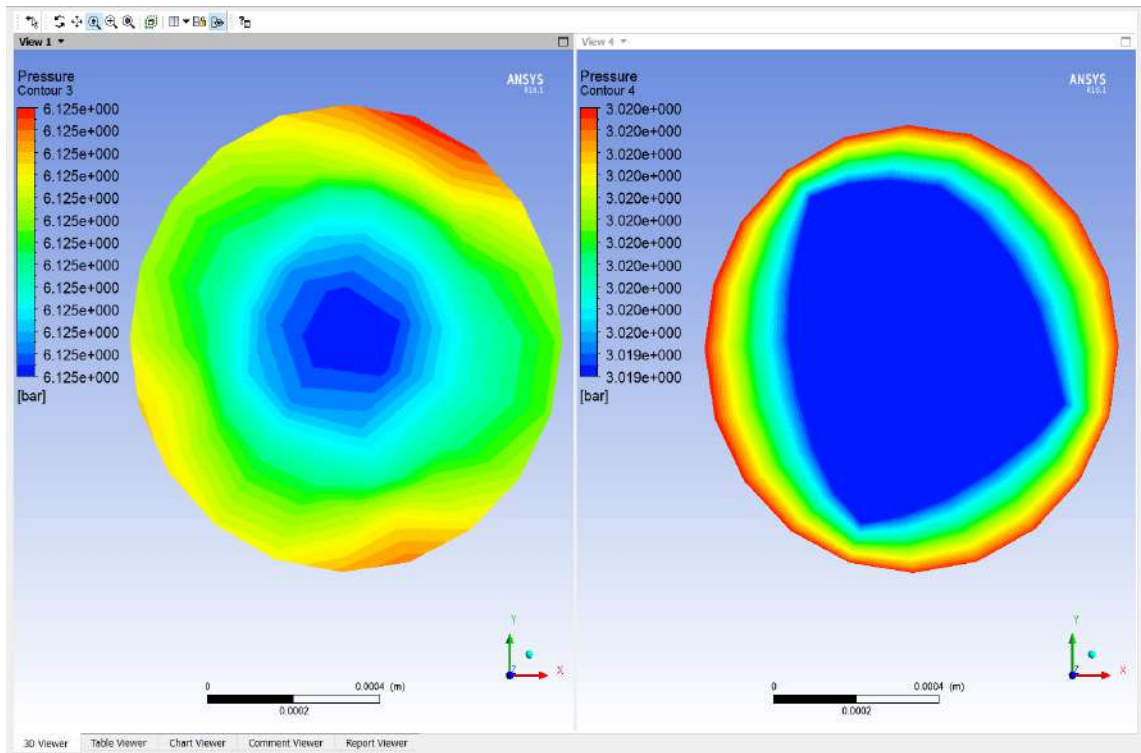


Figure (5.43c): Pressure contour for inlet and outlet of the pipe.

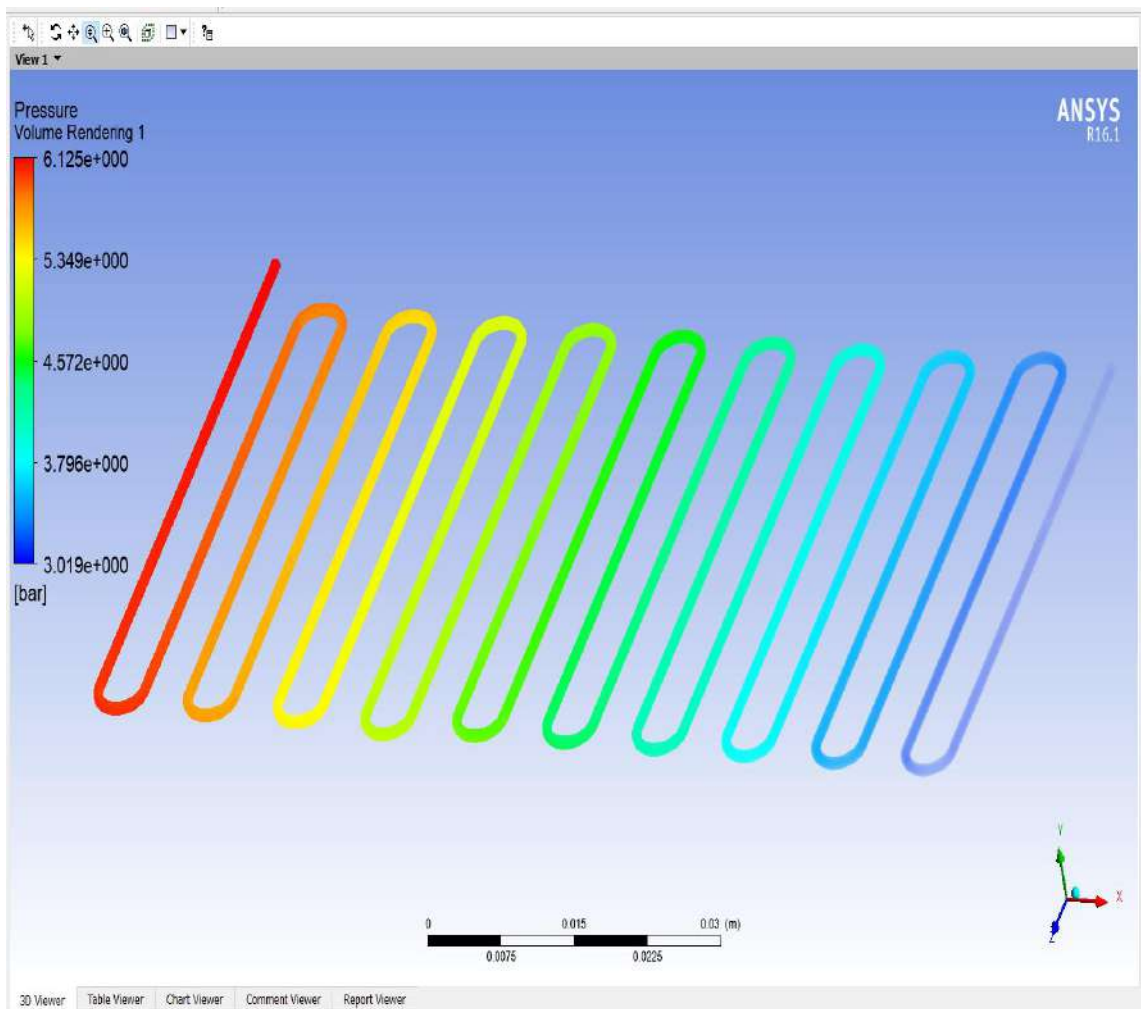


Figure (5.43d): Pressure contour for the pipe.

Figure (5.44) indicates the contour of 0.1%Ag of the temperature for the mid plane in pipe and the plane in cross section of each pipe as well as the inlet and outlet sections. The enhancement in temperature was investigated when using nanofluid and this result was nearly the same as the experimental work.

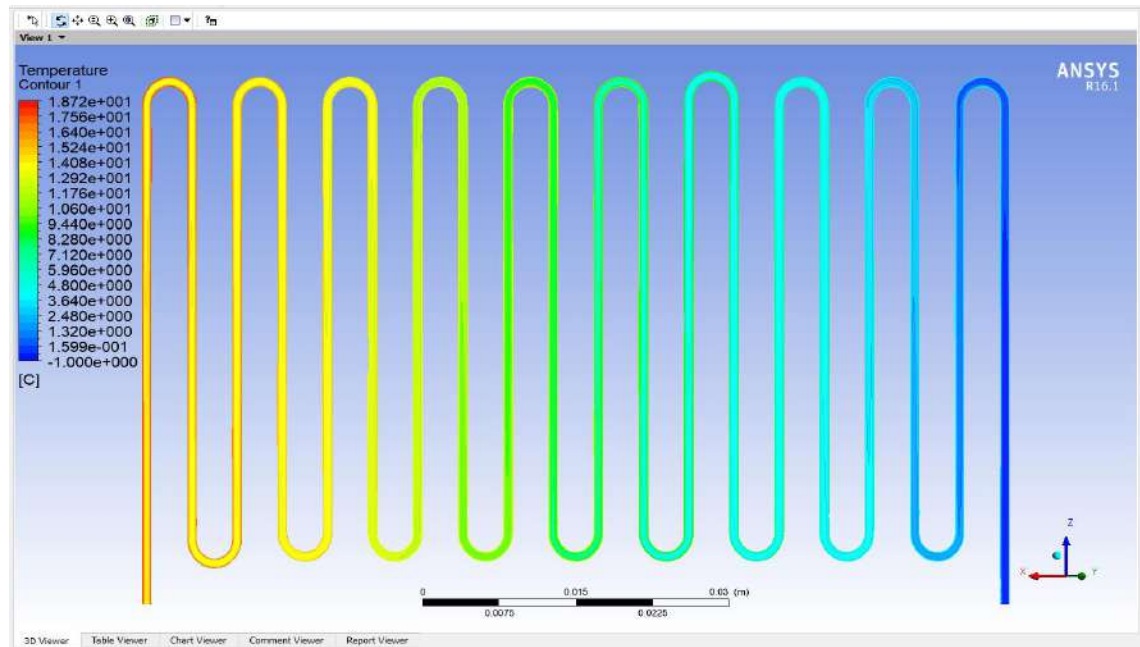


Figure (5.44a): Temperature contour of 0.1%Ag for mid plane in the pipe.

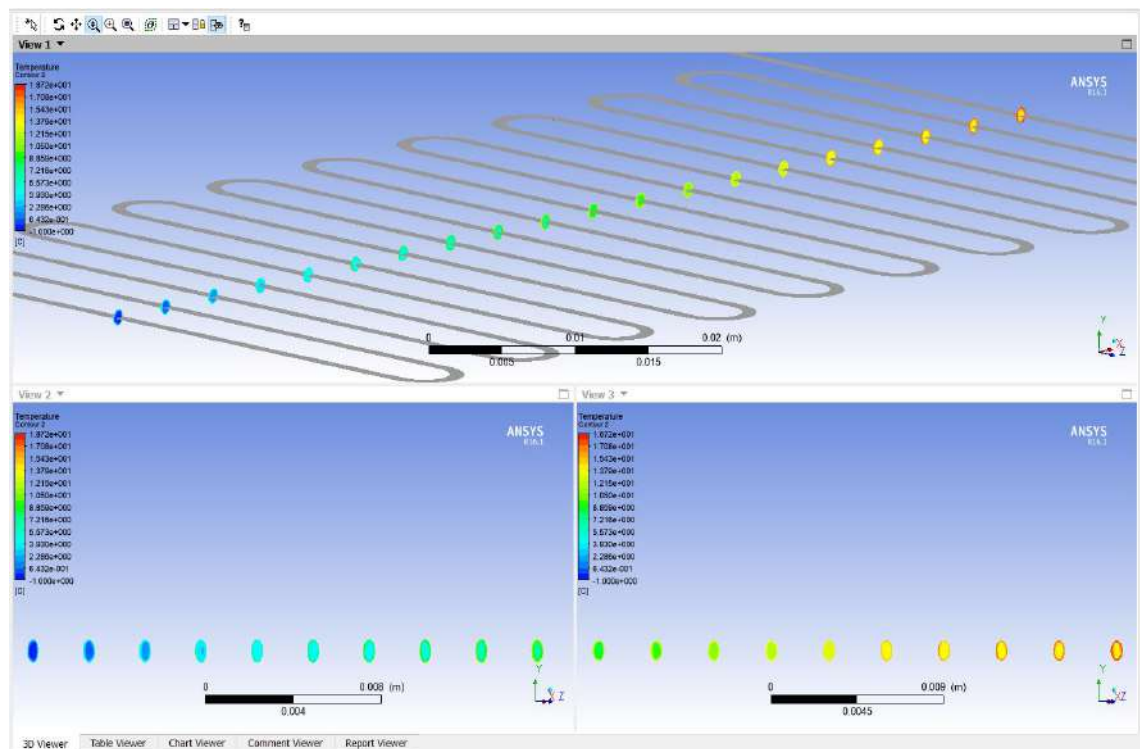


Figure (5.44b): Temperature contour of 0.1%Ag for the plane in cross section of the pipe.

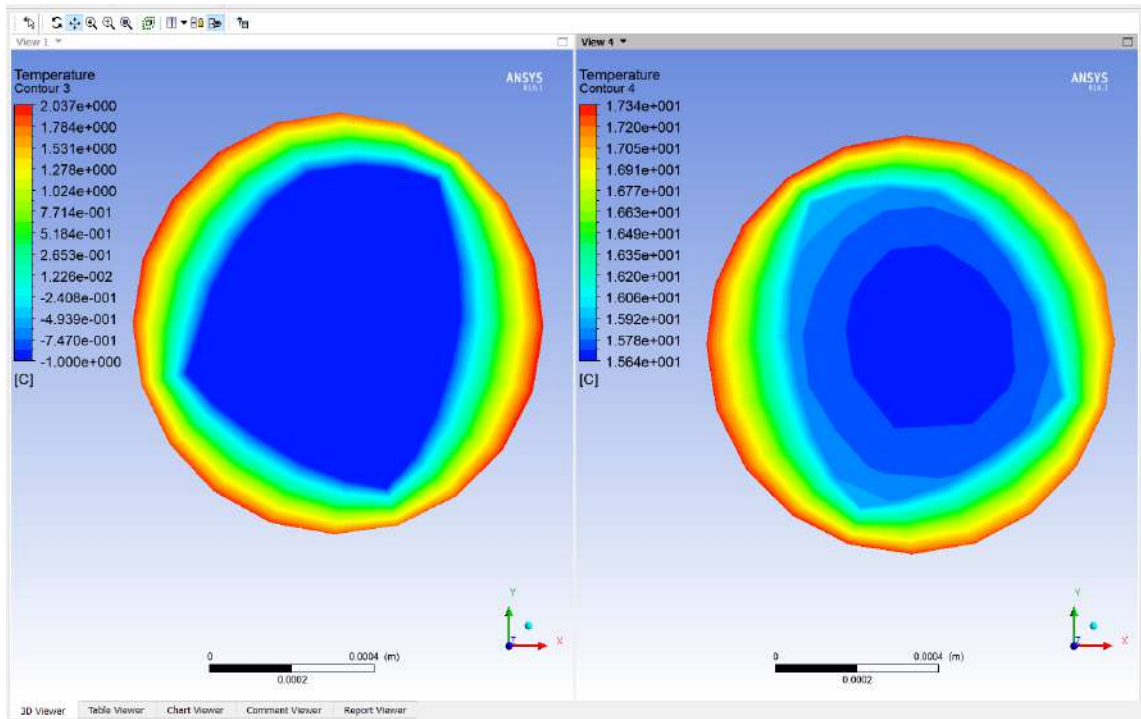


Figure (5.44c): Temperature contour of 0.1%Ag for inlet and outlet of the pipe.

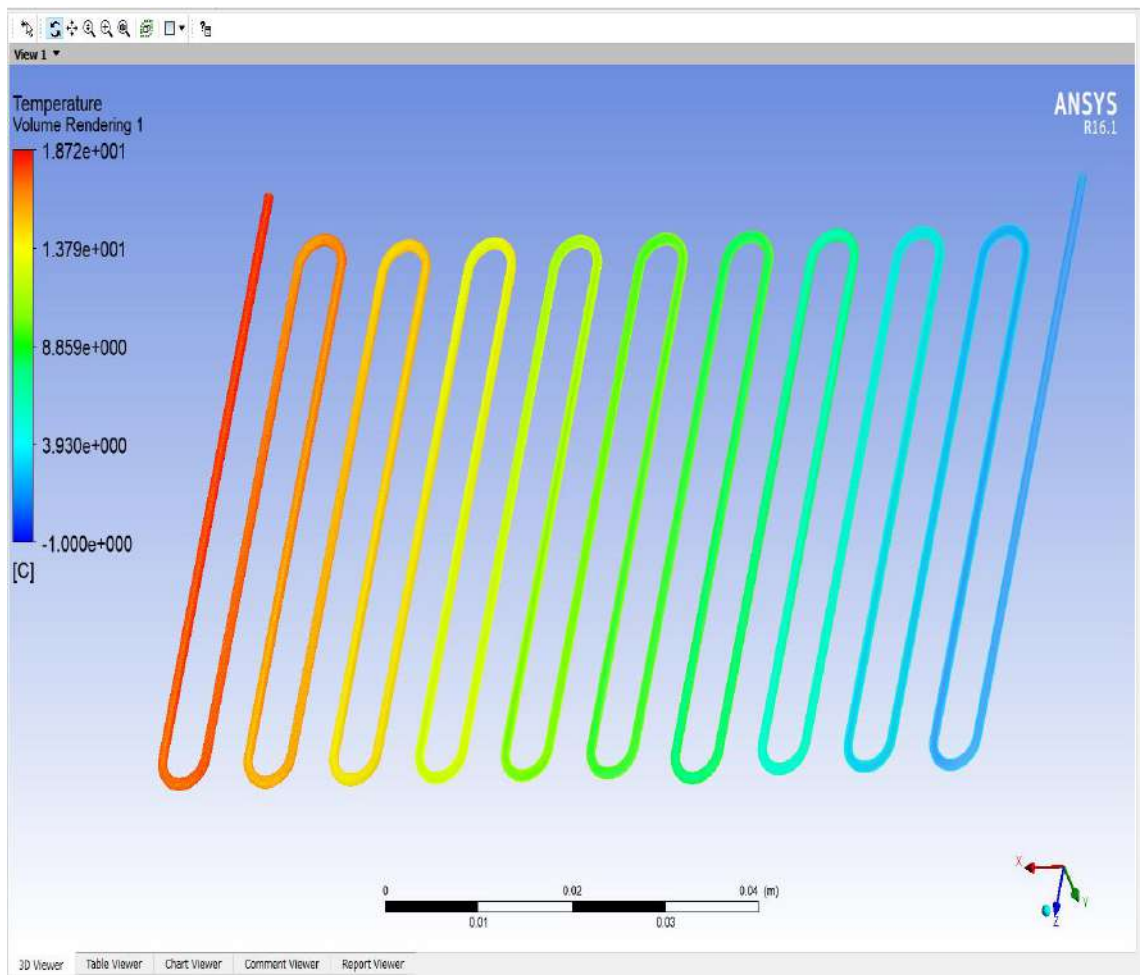


Figure (5.44d): Temperature contour of 0.1%Ag for the pipe.

Figure (5.45) shows the contour of 0.1%Ag of pressure for the mid plane in pipe and the plane in cross section of each pipe as well as the inlet and outlet sections. The pressure decreased as a little with the length of the evaporator pipe.

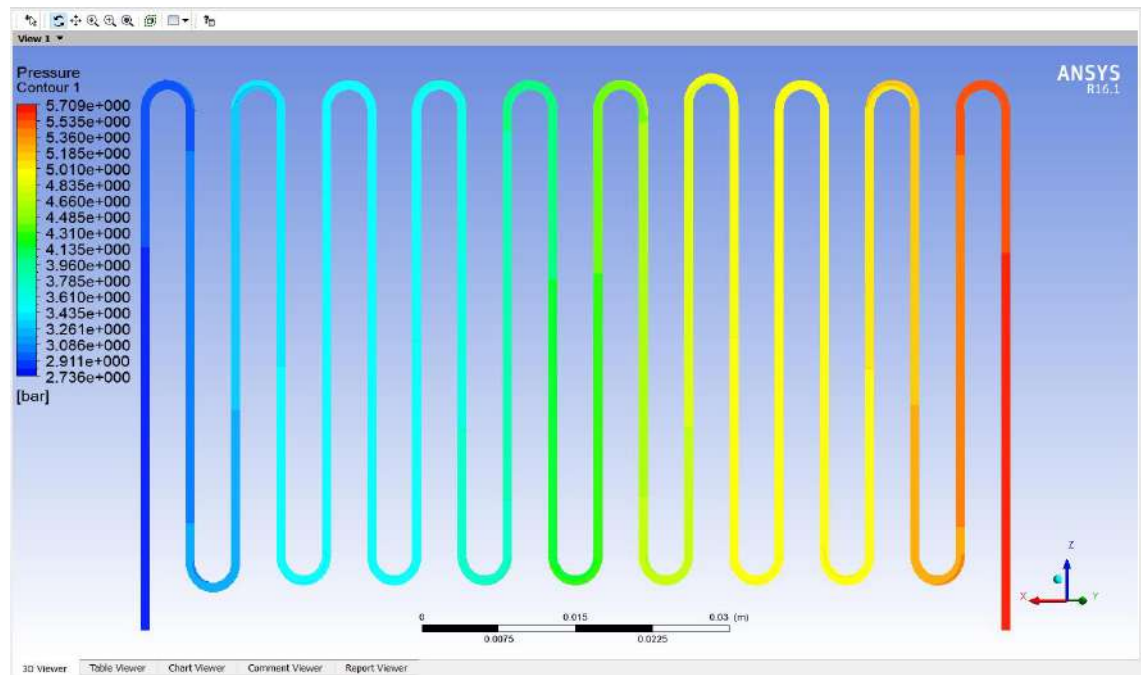


Figure (5.45a): Pressure contour of 0.1%Ag for mid plane in the pipe.

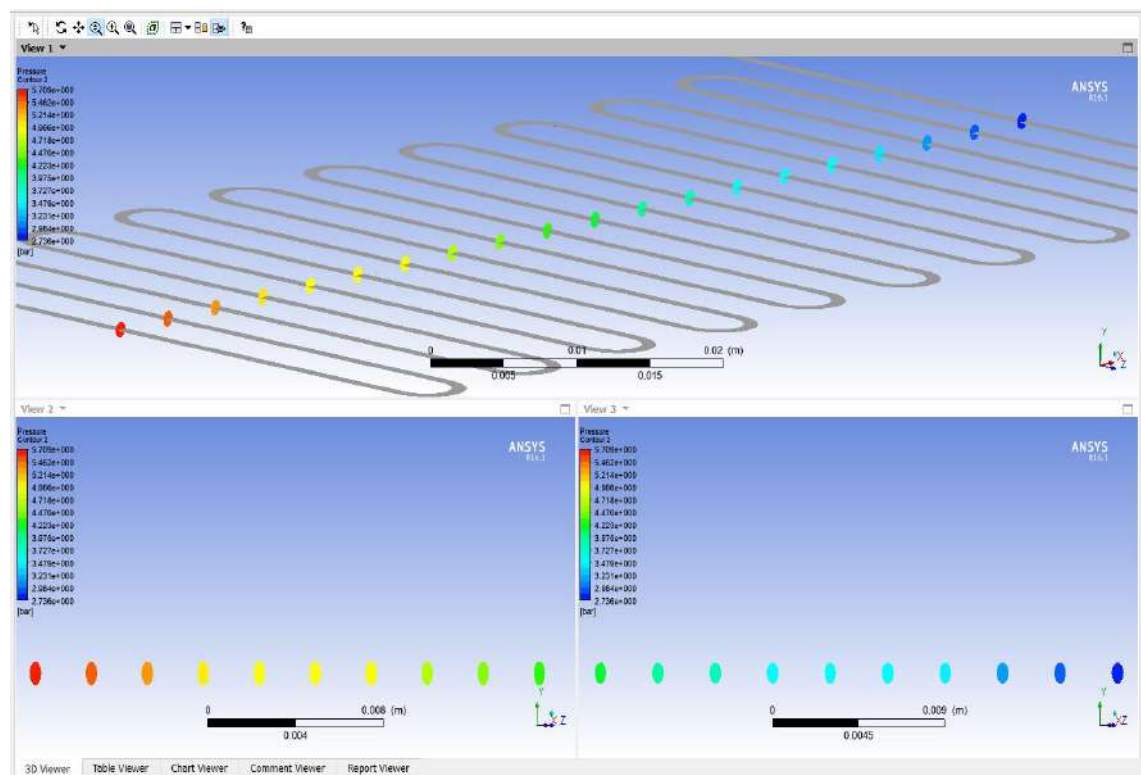


Figure (5.45b): Pressure contour of 0.1%Ag for the plane in cross section of the pipe.

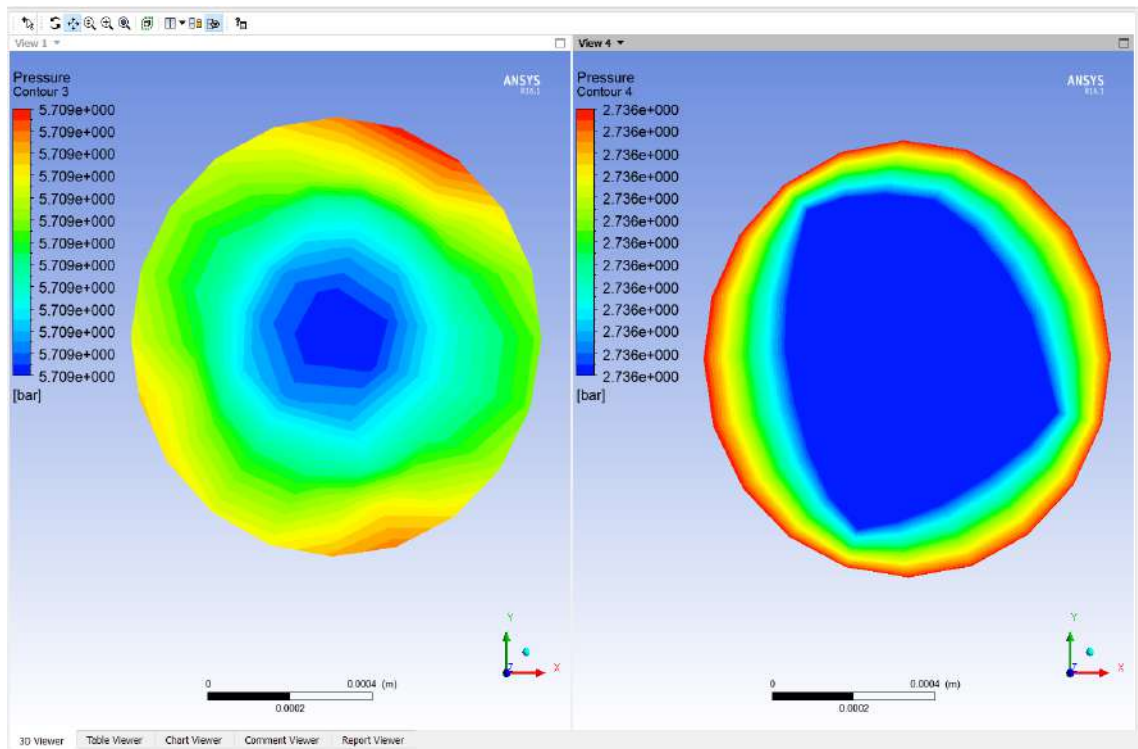


Figure (5.45c): Pressure contour of 0.1% Ag for inlet and outlet of the pipe.

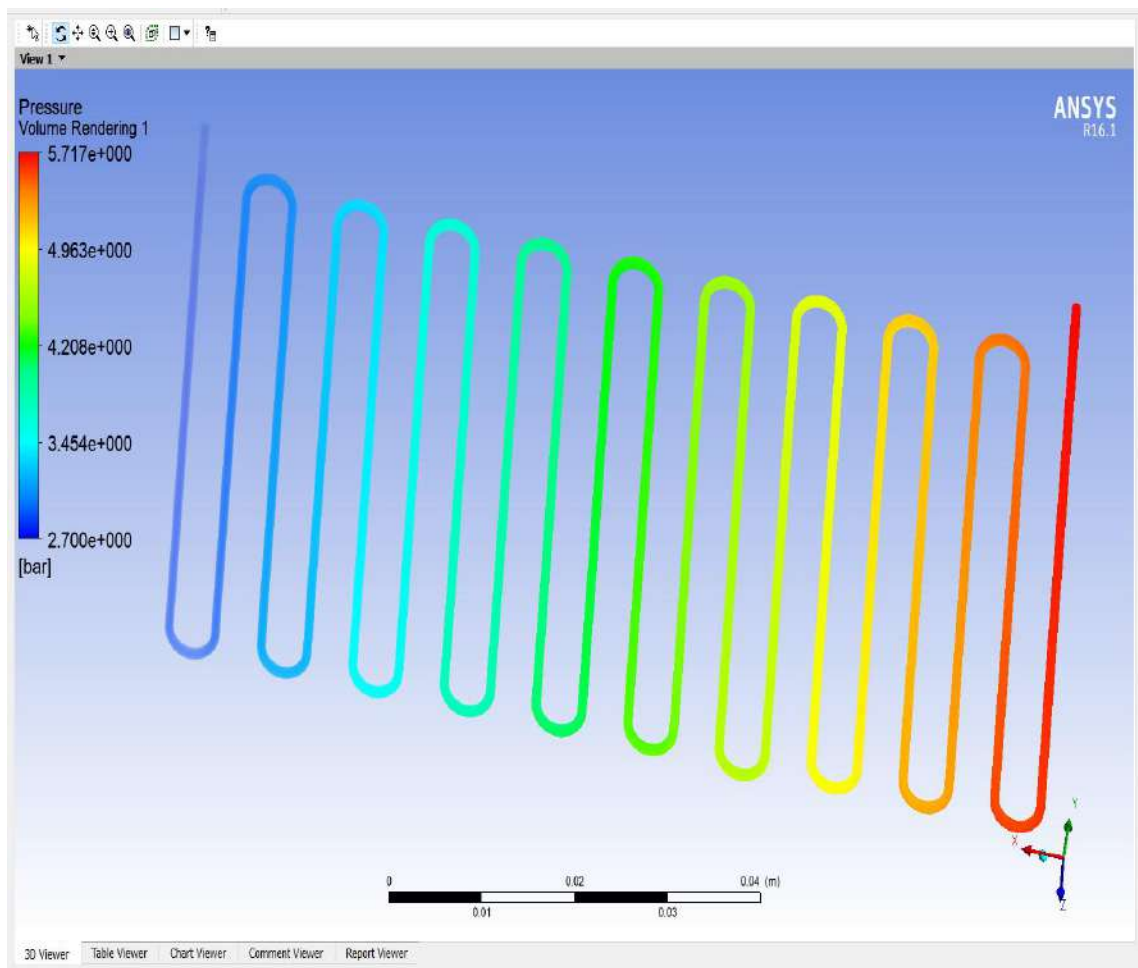


Figure (5.45d): Pressure contour of 0.1% Ag for the pipe.

Figure (5.46) indicates the contour of 0.15%Ag of the temperature for the mid plane in pipe and the plane in cross section of each pipe as well as the inlet and outlet sections. The enhancement in temperature was investigated when using nanofluid and this result was nearly the same as the experimental work.

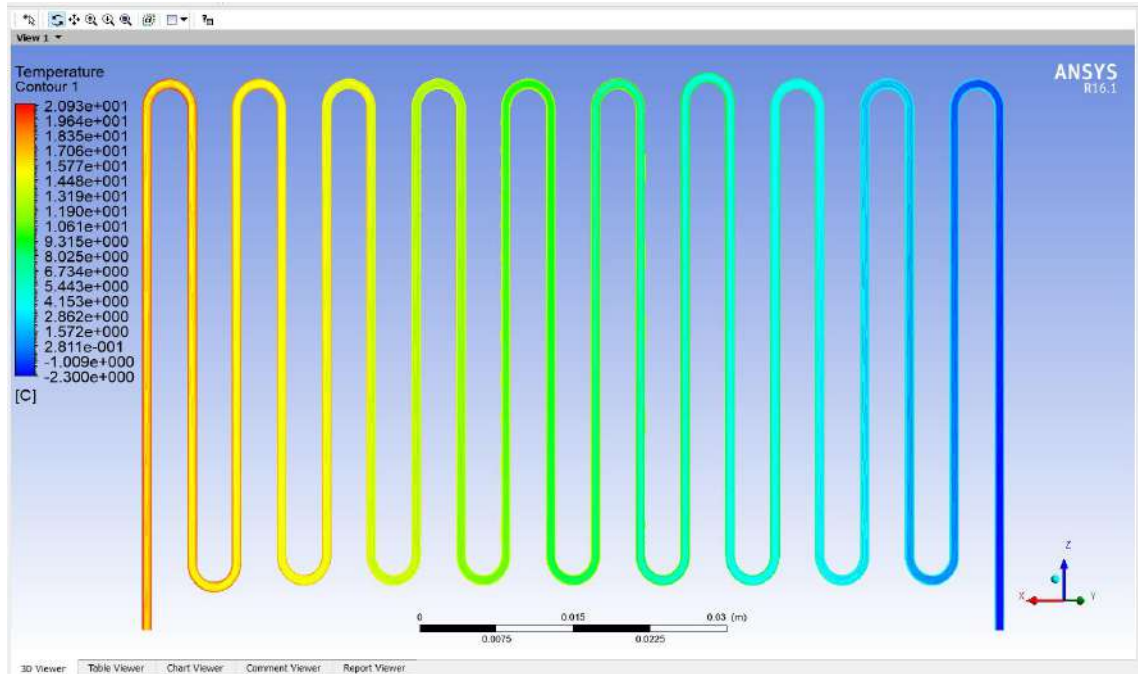


Figure (5.46a): Temperature contour of 0.15%Ag for mid plane in the pipe.

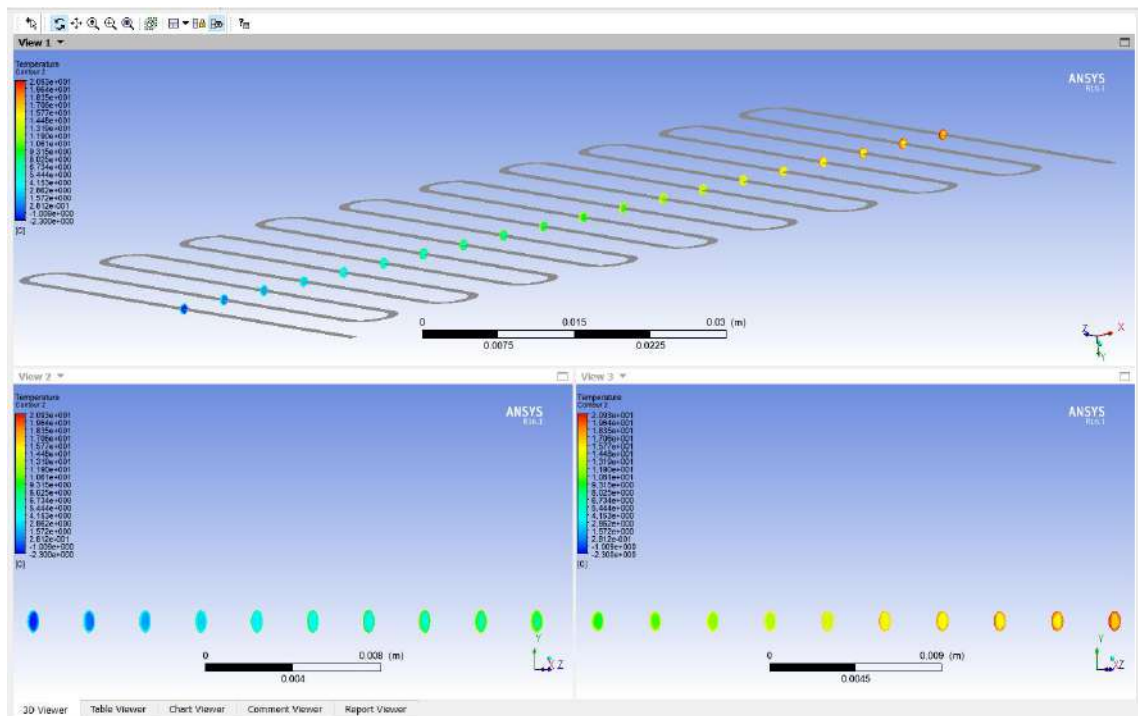


Figure (5.46b): Temperature contour of 0.15%Ag for the plane in cross section of the pipe.

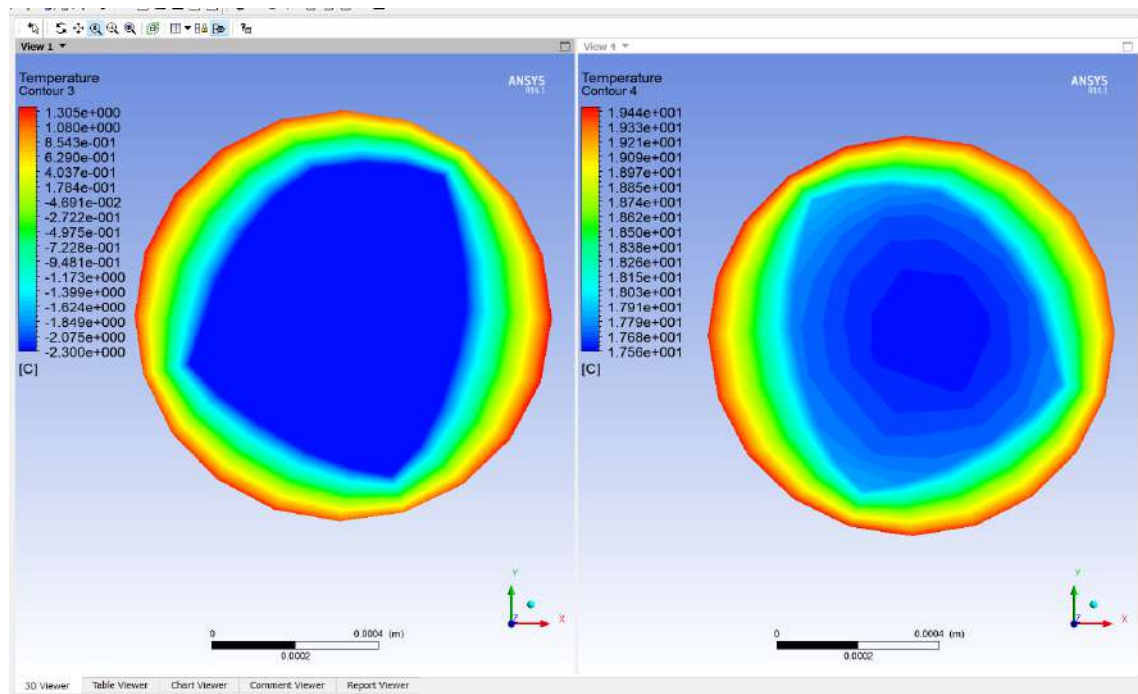


Figure (5.46c): Temperature contour of 0.15%Ag for inlet and outlet of the pipe.

Figure (5.47) shows the contour of 0.15%Ag of pressure for the mid plane in pipe and the plane in cross section of each pipe as well as the inlet and outlet sections. The pressure decreased as a little with the length of the evaporator pipe.

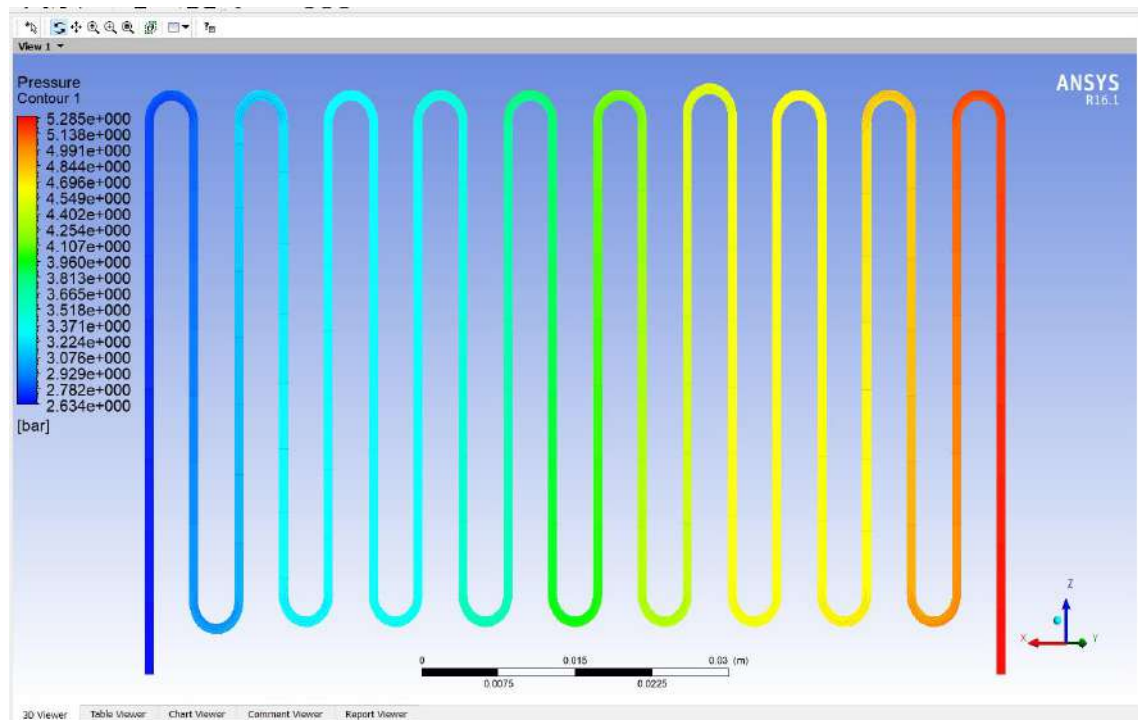


Figure (5.47a): Pressure contour of 0.15%Ag for mid plane in the pipe.

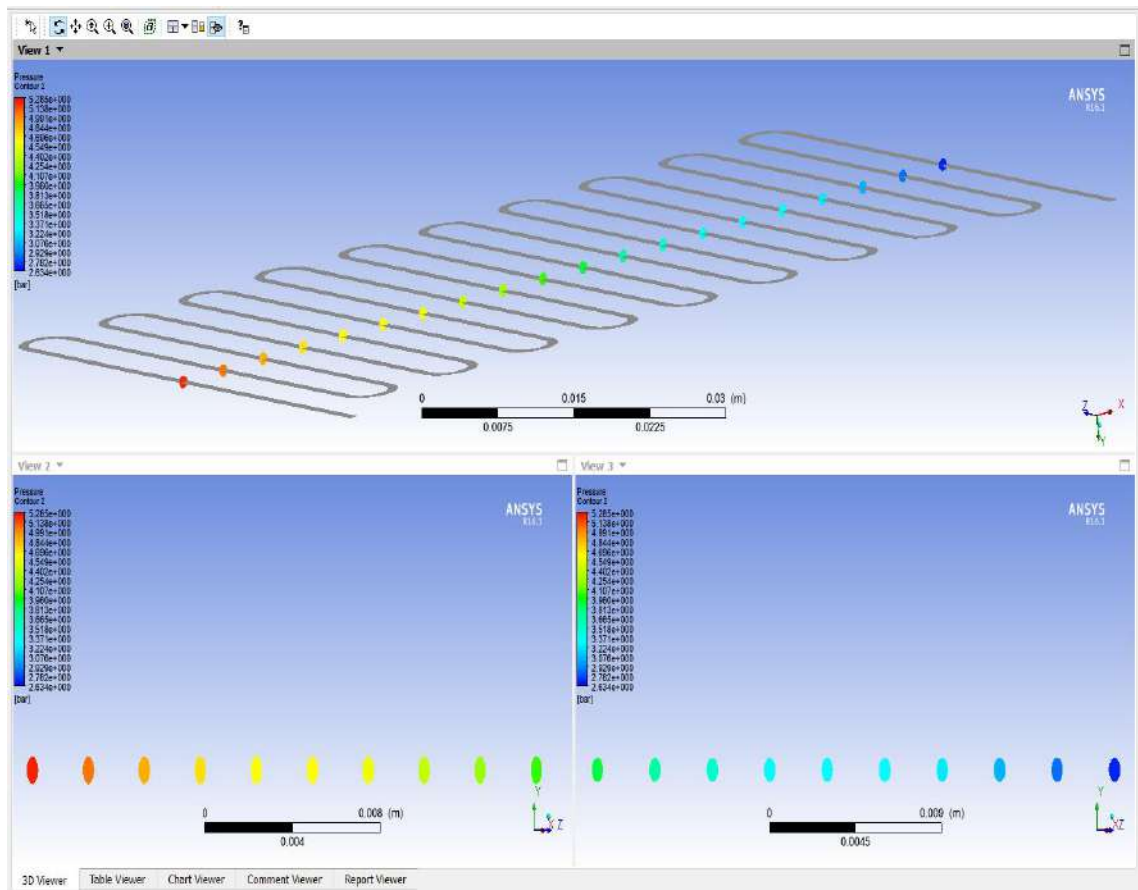


Figure (5.47b): Pressure contour of 0.15% Ag for the plane in cross section of the pipe.

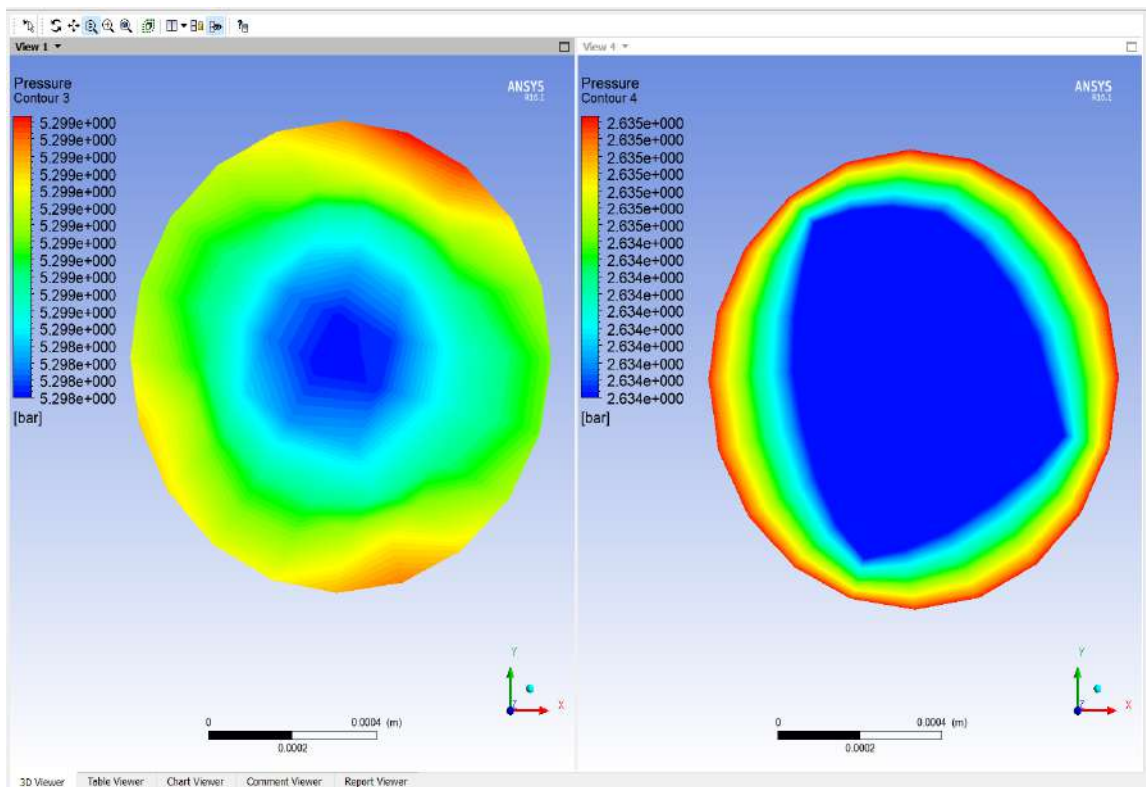


Figure (5.47c): Pressure contour of 0.15% Ag for inlet and outlet of the pipe.

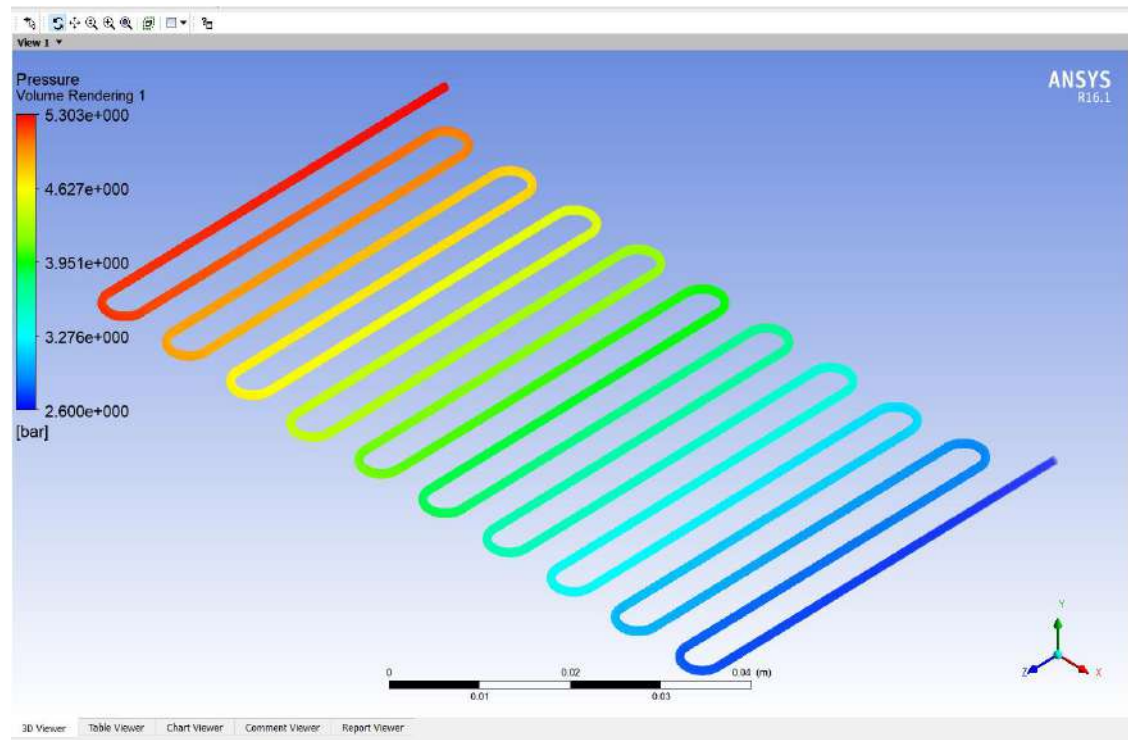


Figure (5.47d): Pressure contour of 0.15%Ag for the pipe.

Figure (5.48) indicates the contour of 0.2%Ag of the temperature for the mid plane in pipe and the plane in cross section of each pipe as well as the inlet and outlet sections. The enhancement in temperature was investigated when using nanofluid and this result was nearly the same as the experimental work.

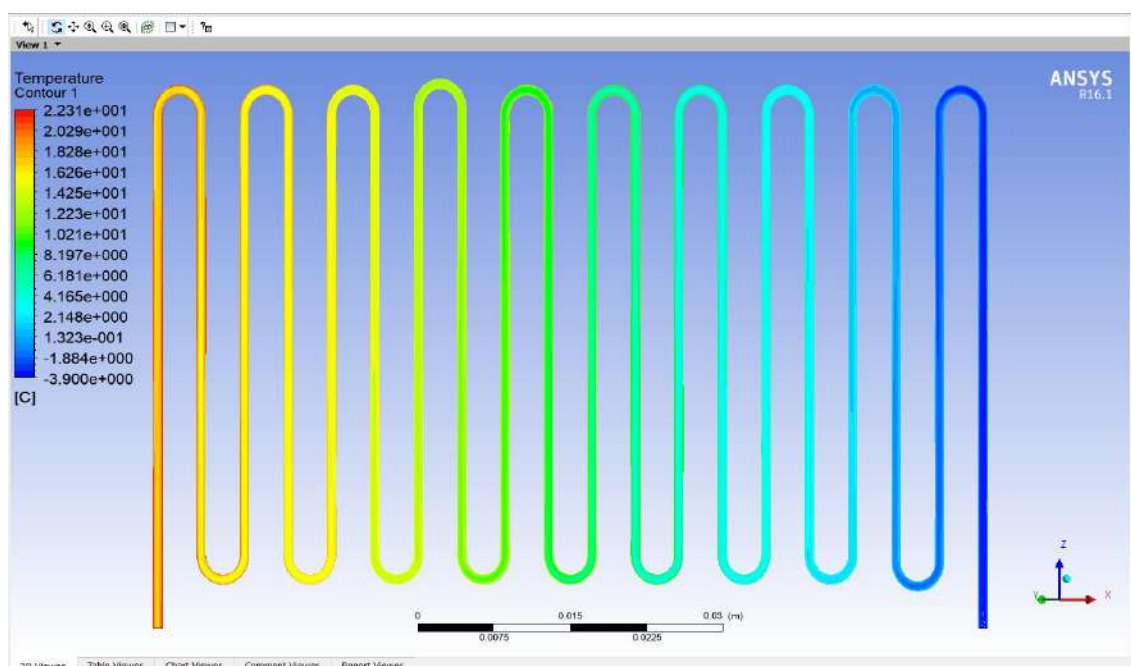


Figure (5.48a): Temperature contour of 0.2%Ag for mid plane in the pipe.

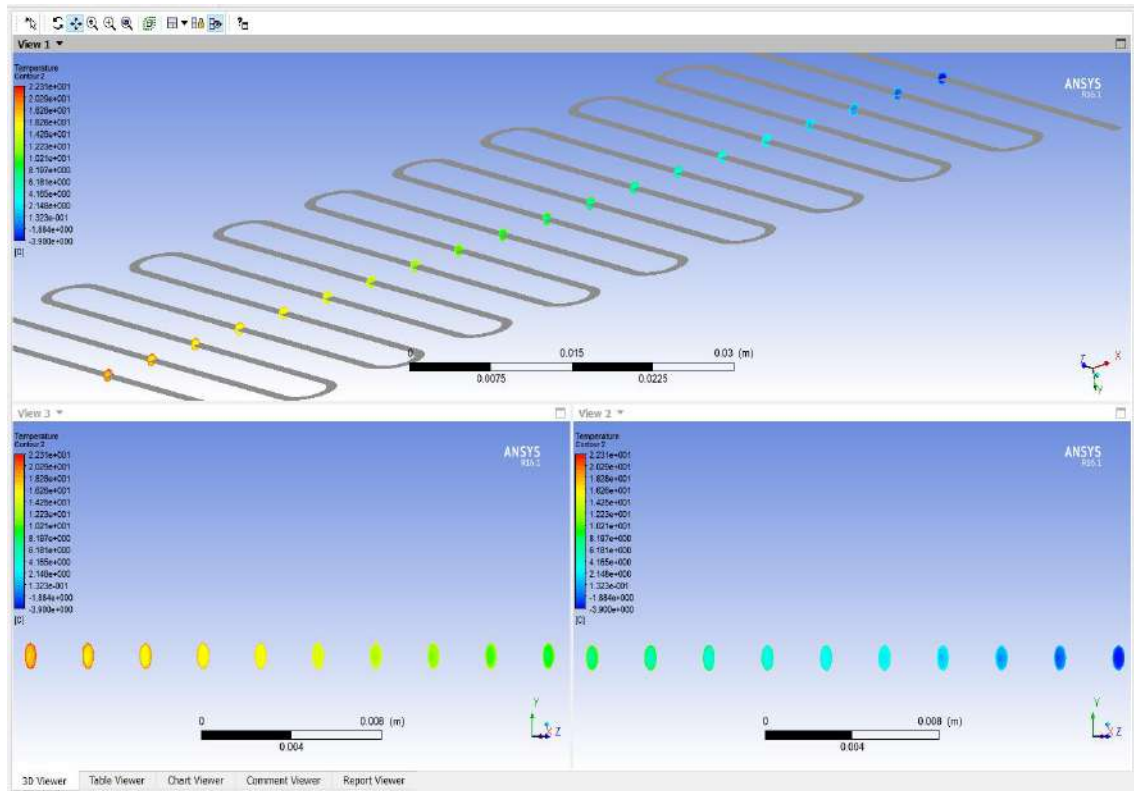


Figure (5.48b): Temperature contour of 0.2% Ag for the plane in cross section of the pipe.

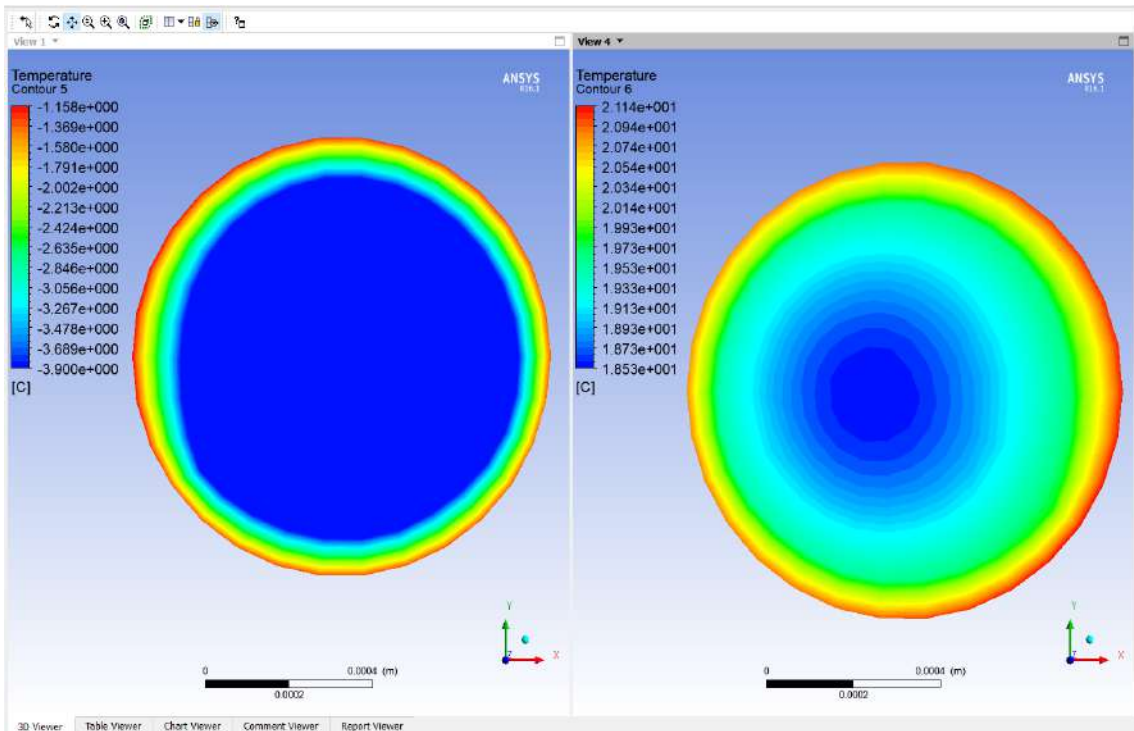


Figure (5.48c): Temperature contour of 0.2% Ag for inlet and outlet of the pipe.

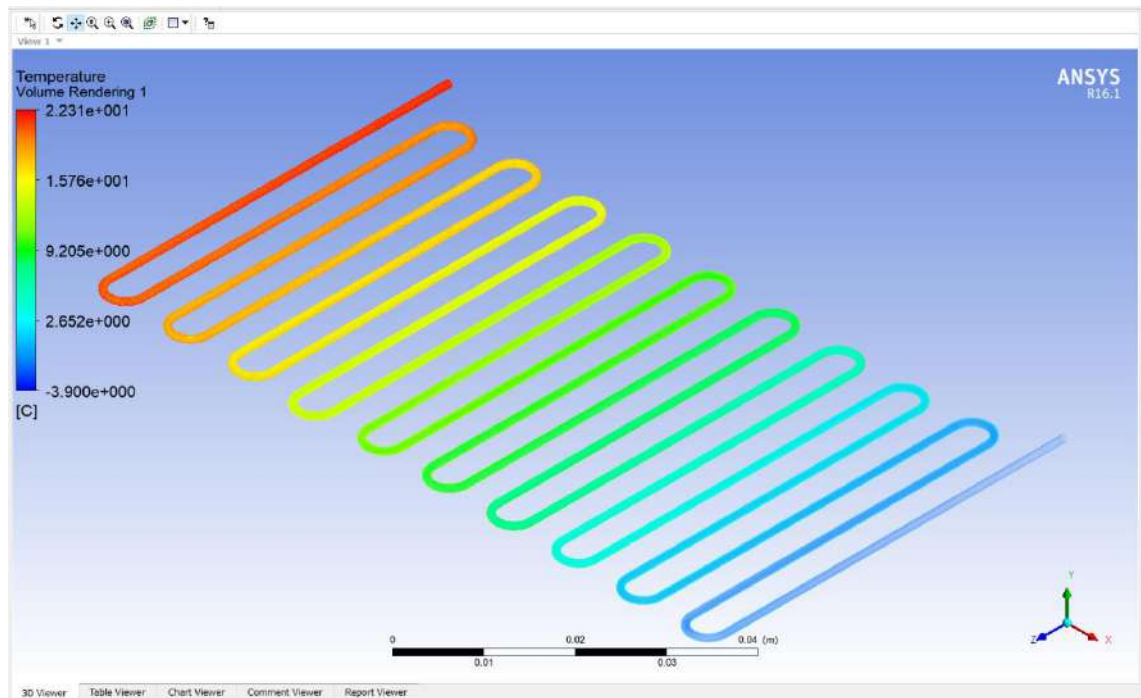


Figure (5.48d): Temperature contour of 0.2% Ag for the pipe.

Figure (5.49) shows the contour of 0.2% Ag of pressure for the mid plane in pipe and the plane in cross section of each pipe as well as the inlet and outlet sections. The pressure decreased as a little with length of the evaporator pipe.

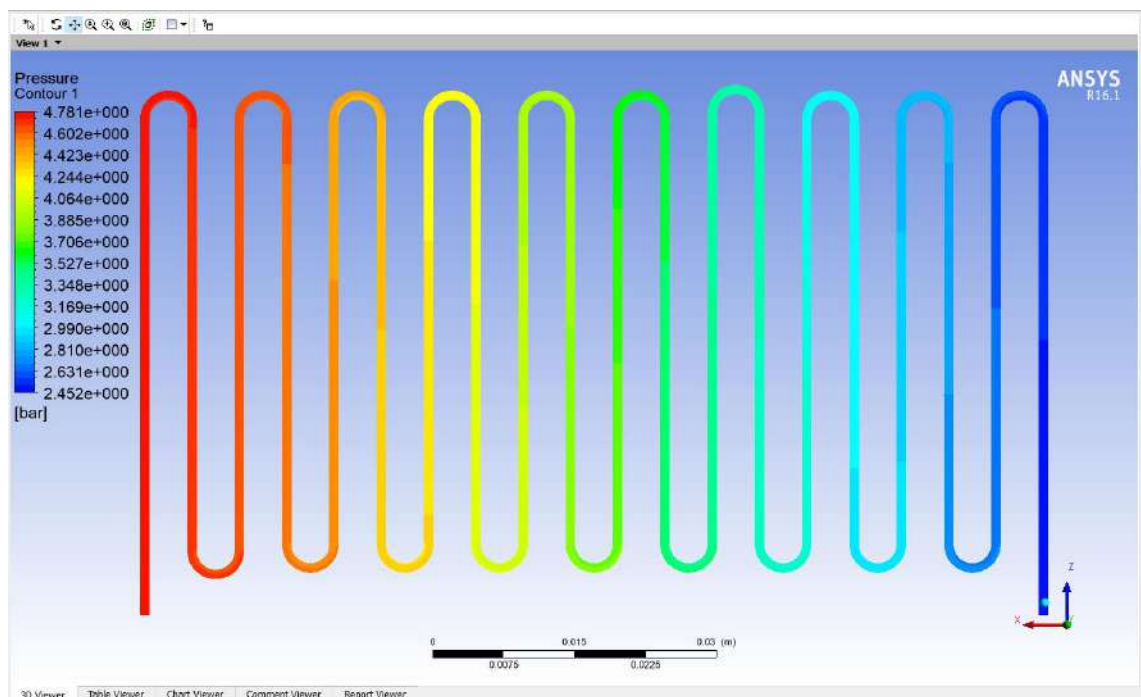


Figure (5.49a): Pressure contour of 0.2% Ag for mid plane in the pipe.

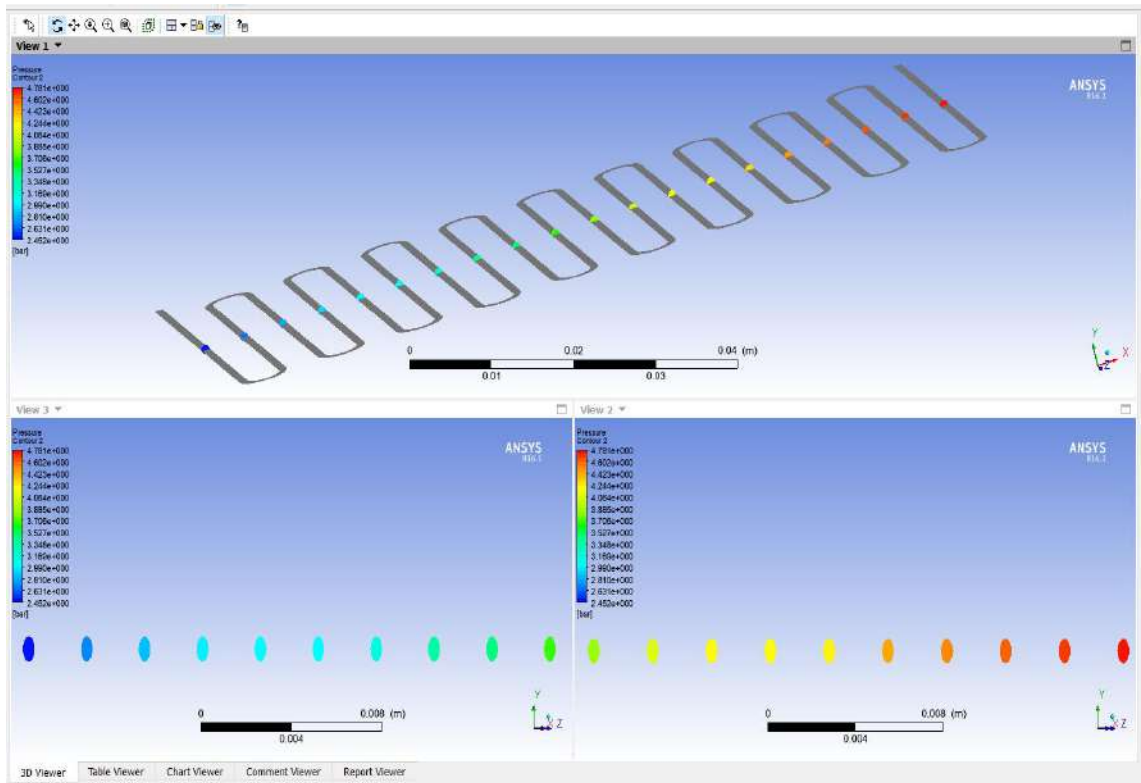


Figure (5.49b): Pressure contour of 0.2%Ag for the plane in cross section of the pipe.

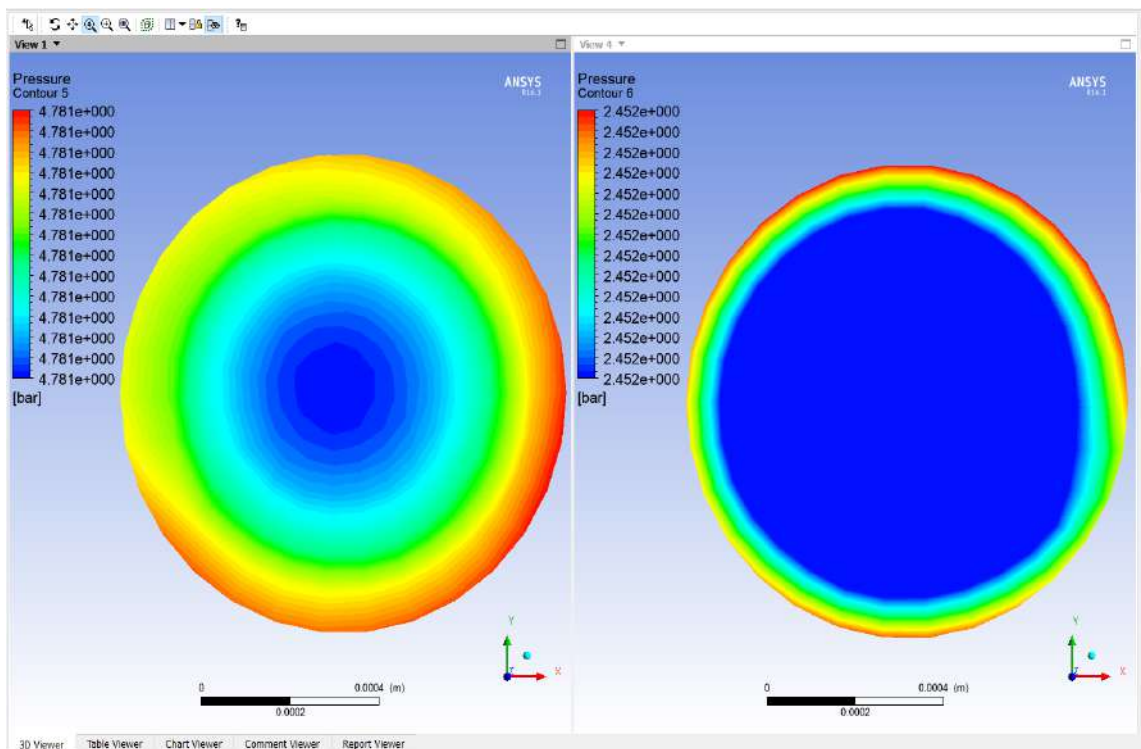


Figure (5.49c): Pressure contour of 0.2%Ag for inlet and outlet of the pipe.

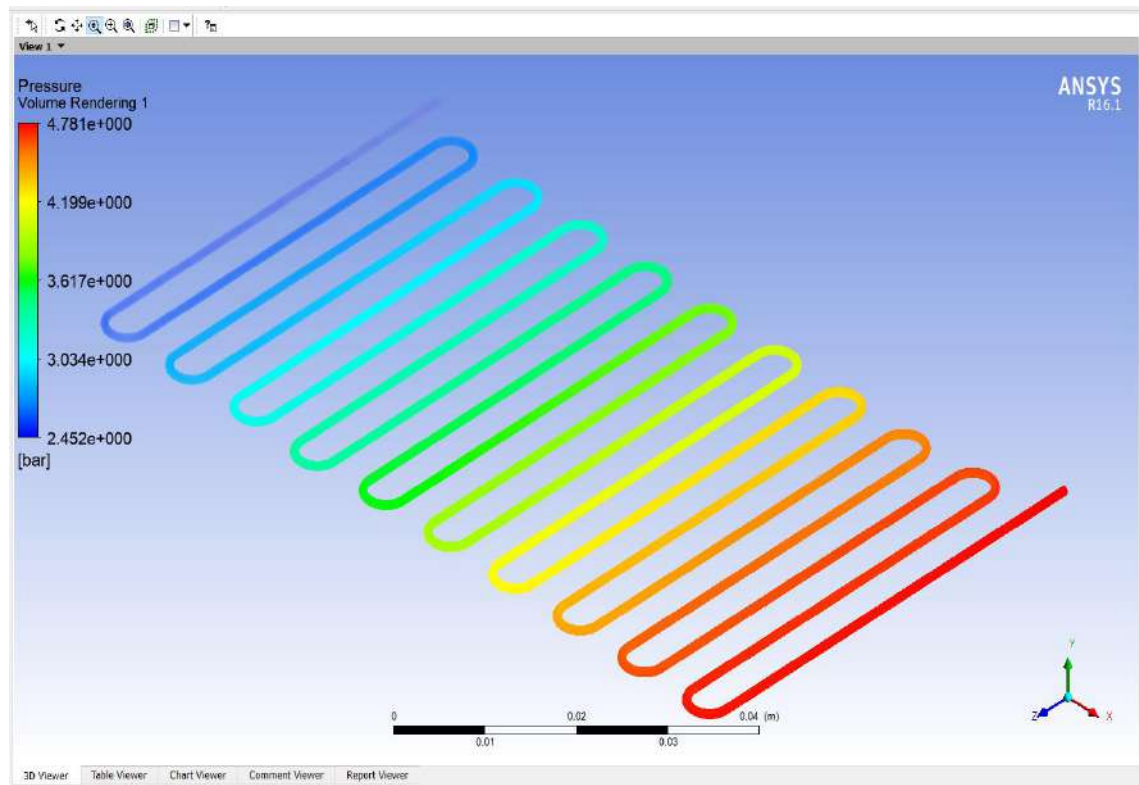


Figure (5.49d): Pressure contour of 0.2% Ag for the pipe.

5.3.4 Summary of the Results Analysis

The temperature can be extracted from the simulation Figures that showed previously in order to obtain the theoretical results, so it became easy to compare with experimental results. Figures (5.50), (5.51) and (5.52) showed the distribution of the temperature for along pipe for each pure refrigerant, Al₂O₃-R22 and Ag-R22 for all concentration. It has explained that the temperature increased when the temperature grew for along pipe of the evaporator with incrementing the concentration. Therefore, the different temperatures between the evaporator inlet and outlet were increased with concentration for each R22-Al₂O₃ and R22-Ag nanorefrigerant as shown in figure (5.53). This occurred where the outlet temperature increased as the rate of heat transfer through evaporator increased and the rate of heat transfer depended on the thermal properties of the working fluid which it was improved when adding nanoparticles to it. While the inlet temperature

of evaporator decreased with the concentration where this relative to other parts of the system.



Figure (5.50): The temperature of R22-Al₂O₃ with along evaporator.

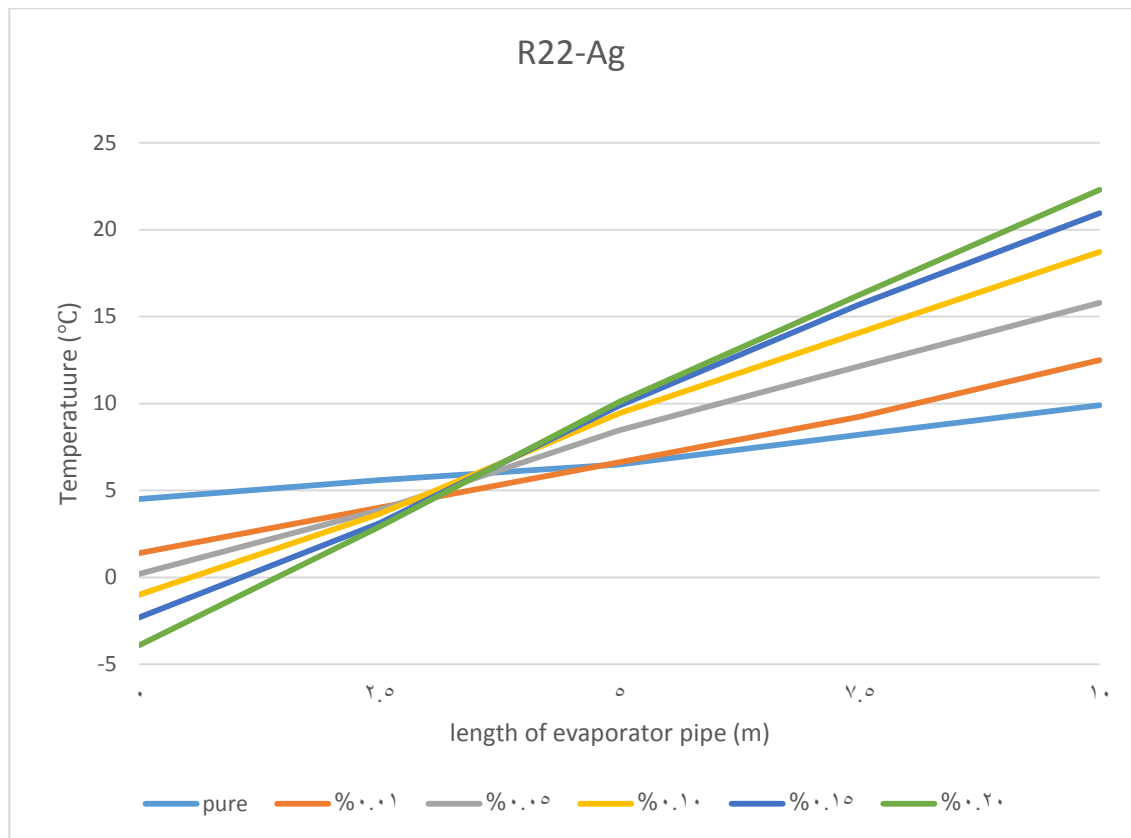


Figure (5.51): The temperature of R22-Ag with along evaporator.

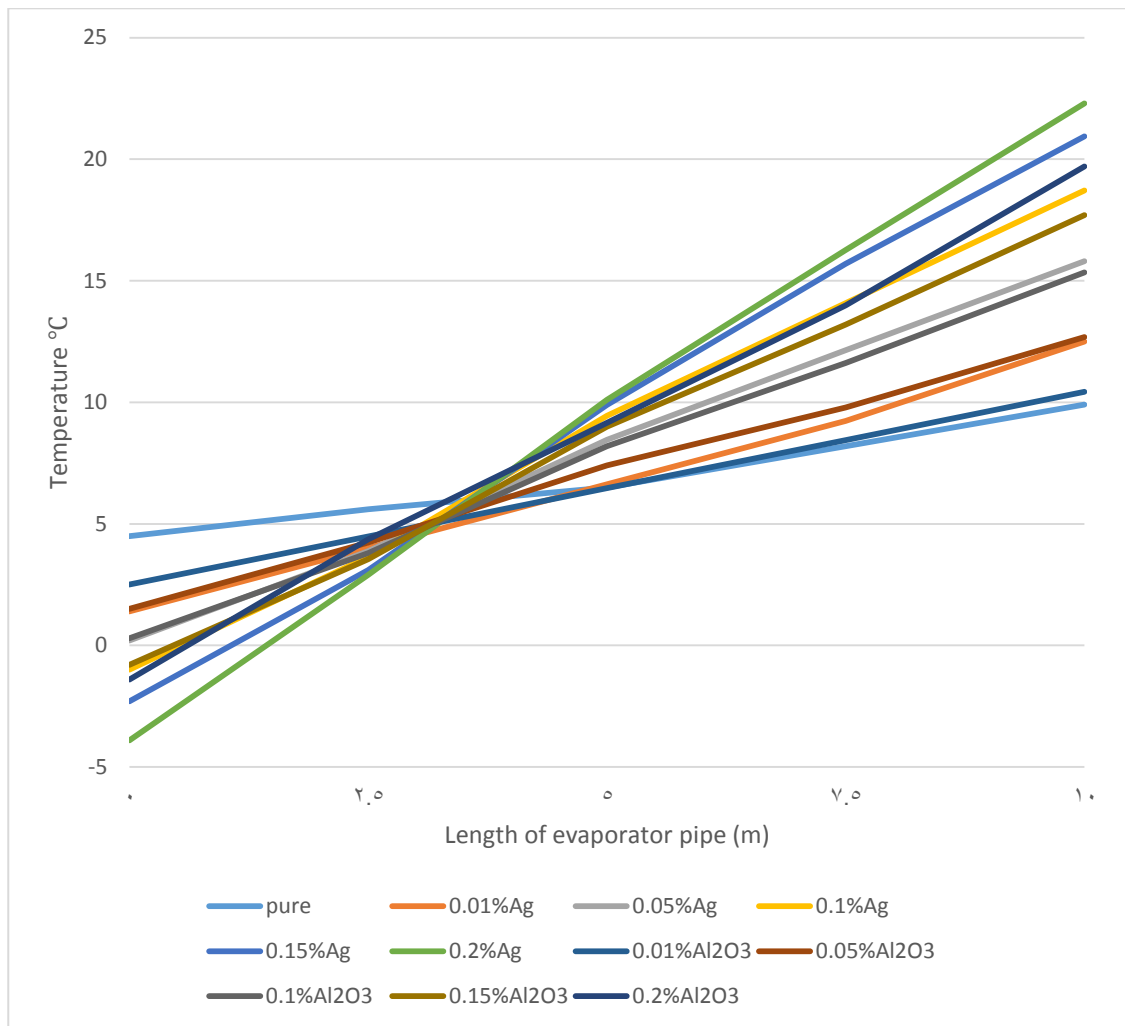


Figure (5.52): The temperature for R22, R22-Al₂O₃ and R22-Ag with along evaporator.

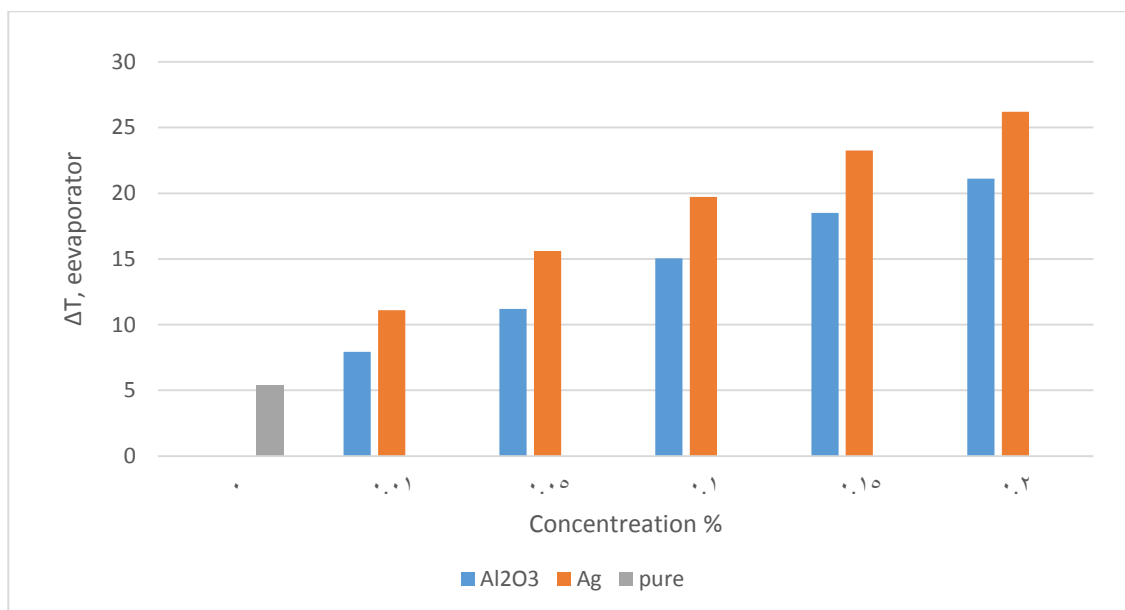


Figure (5.53): The different temperature of evaporator with a concentration.

5.4 Comparison between the Experimental and Theoretical Results

After extracted the experimental and theoretical results, the comparison between them has been done in this section. The theoretical temperature was simulated so the comparison would be for the temperature of the evaporator only. Figures (5.54), (5.55) and (5.56) Show the comparison in the temperature between the theoretical and experimental results at the evaporator outlet for pure refrigerant R22, nanorefrigerants R22-Al₂O₃, and R22-Ag respectively. The maximum difference value between the theoretical and experimental was 0.1.

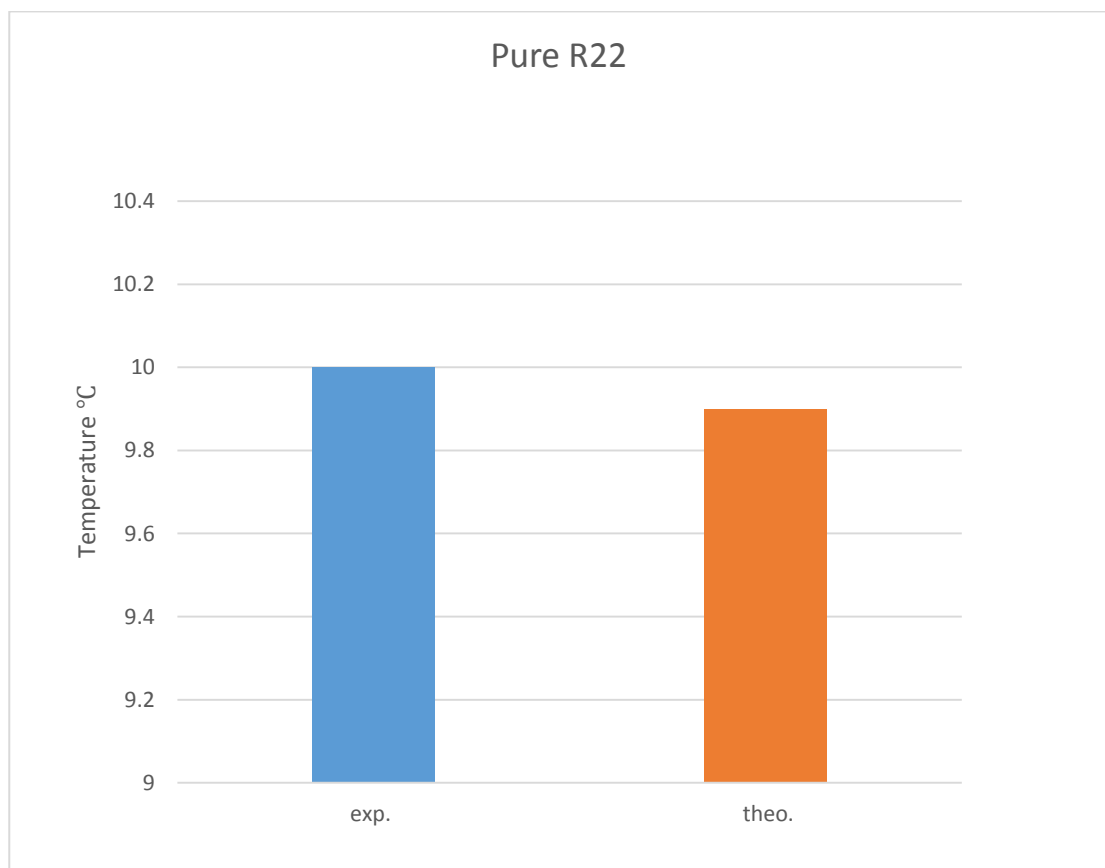


Figure (5.54): The experimental and theoretical temperature at the evaporator outlet for the pure R22.

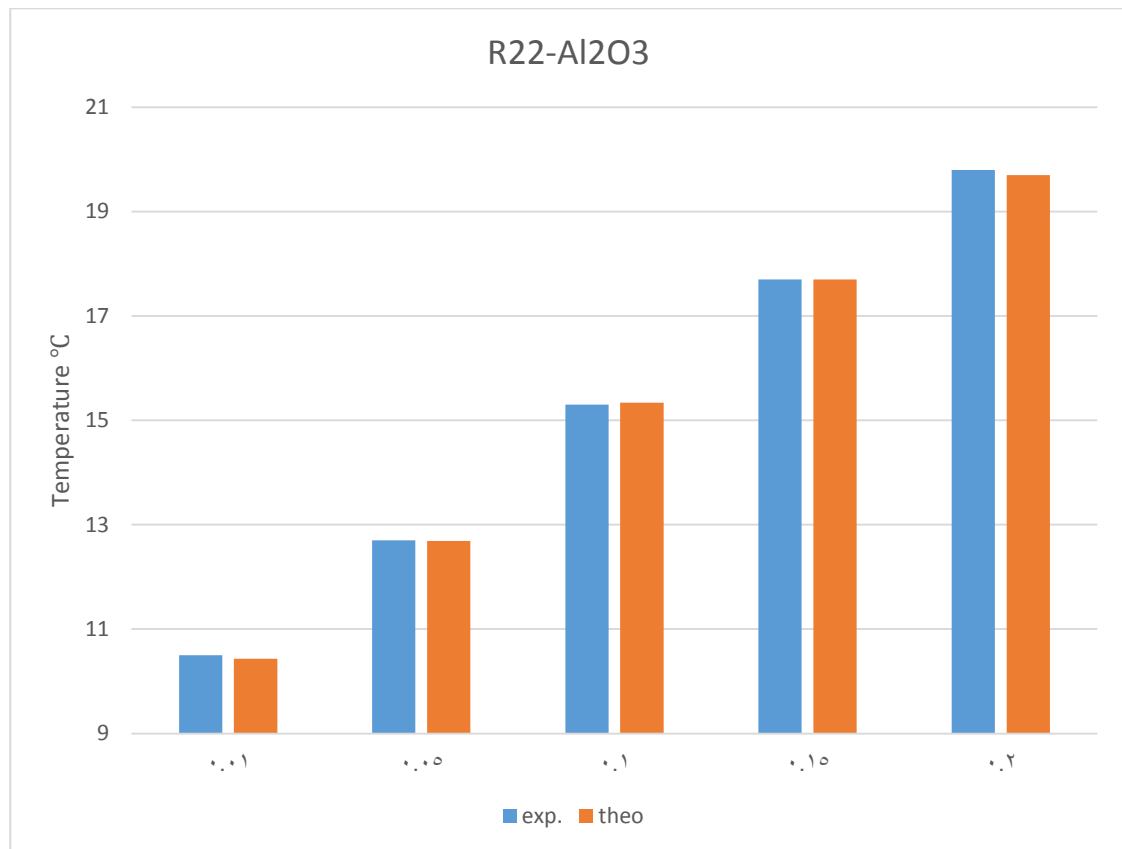


Figure (5.55): The experimental and theoretical temperature at the evaporator outlet for the R22-Al₂O₃.

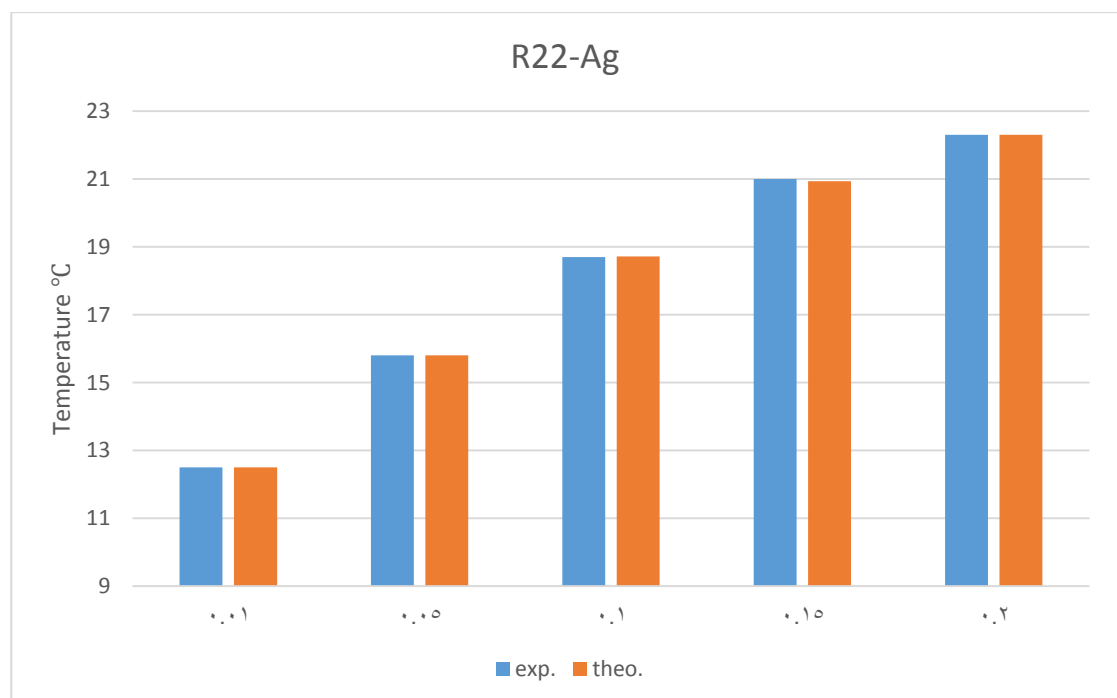


Figure (5.56): The experimental and theoretical temperature at the evaporator outlet for the pure R22.

Chapter Six

Conclusions and Recommendations

This chapter explains the conclusions related to the results of the experimental work.

6.1 Conclusions

1. The temperature of the working fluid at the compressor inlet and the evaporator outlet increase by increasing the mass fraction of the nanoparticles.
2. The temperature of the working fluid at the compressor outlet and the evaporator inlet decrease by increasing the mass fraction of the nanoparticles.
3. The temperature of the room air at the outlet decrease by increasing the mass fraction of the nanoparticles.
4. The pressure of working fluid decrease by increasing the mass fraction of the nanoparticles at all location.
5. The pressure ratio increase by increasing the mass fraction of the nanoparticles at all location.
6. The work consumption in the compressor decrease by increasing the mass fraction until reaches a critical point then increase.
7. The critical point of the consumption workplace between 0.1% and 0.15% mass fraction for each Al₂O₃ and Ag nanoparticles.
8. The maximum enhancement in the consumption work of the critical points was 56.14% for Ag and 36.84% for Al₂O₃.
9. The refrigeration effect of the evaporator increase by increasing the mass fraction of the nanoparticles.
10. The maximum enhancement of the refrigeration effect was 5.61% for the Al₂O₃ and 8.73% for Ag.

11. The Coefficient of performance increase by increasing the mass fraction until reaches a critical point then decrease.
12. The critical point of the coefficient of performance was equal to 9.064 and 6.188 at 0.15% mass fraction for Ag and Al₂O₃ nanoparticles respectively.
13. The maximum enhancement in the coefficient of performance of the critical points was 144.71% for Ag and 67.06% for Al₂O₃.

6.2 Recommendations

The recommendations for future works are listed below:

1. Investigating the effect of changing the mass charging of the refrigerant with the metallic nanoparticles.
2. Take more low concentration to find the exact critical point.
3. Investigating the other metallic nanoparticles to find out the influence on the air conditioning.
4. Study the properties of the working fluid for the Nano metallic.
5. Investigating adding the nano metallic to the refrigerant directly.
6. Investigating the other refrigerant with nano metallic.
7. Study the more nano oxides with refrigerant R22.
8. Investigating the change of heat flux by adding nanoparticles to working fluid in the air conditioning.

References

1. Bi, S.-s., L. Shi, and L.-l. Zhang, Application of nanoparticles in domestic refrigerators. *Applied Thermal Engineering*, 2008. 28(14): p. 1834-1843.
2. H. Peng, G. Ding, W. Jiang, H. Hu, and Y. Gao, 2009, *International Journal of Refrigeration*, vol. 32, no. 7, (Measurement and correlation of frictional pressure drop of refrigerant based nano fluid flow boiling inside a horizontal smooth tube,) p. 1756– 1764.
3. M. A. Kedzierski, 2011, *International Journal of Refrigeration*, vol.34, no. 2, (Effect of Al₂O₃ nanolubricant on R134a pool boiling heat transfer,) p. 498–508.
4. H. Peng, G. Ding, H. Hu, and W. Jiang, 2010 *International Journal of Thermal Sciences*, vol. 49, no. 12, (Influence of carbon nanotubes on nucleate pool boiling heat transfer characteristics of refrigerant-oil mixture,) p. 2428–2438.
5. Bi, S., et al., Performance of a domestic refrigerator using TiO₂-R600a nano-refrigerant as working fluid. *Energy Conversion and Management*, 2011. 52(1): p. 733-737.
6. Subramani, N. and M. Prakash, Experimental studies on a vapour compression system using nanorefrigerants. *International Journal of Engineering, Science and Technology*, 2011. vol. 3, no. 9, p. 95-102.
7. E.A. Abdel-Hadi, S. H. Taher, A. H. M. Torki, and S. S.Hamad, 2011, in *Proceedings of the International Conference on Advanced Materials Engineering IPCSIT*, vol. 15, (Heat transfer analysis of vapor compression system using nano CuO-R134a,) p. 80–84.
8. Kumar, D.S. and R. Elansezhian, Experimental study on Al₂O₃-R134a nano refrigerant in refrigeration system. *International Journal of Modern Engineering Research*, 2012. 2(5): p. 3927-3929.

9. Kedzierski, M.A., 2012. Viscosity and density of CuO nanolubricant, *Int. J. Refrig.* 35(7), 1997-2002.
10. Kedzierski, M.A., 2013. Viscosity and density of aluminum oxide nanolubricant, *Int. J. Refrig.* 36(4), 1333-1340.
11. Mahbubul, I.M., Saidur, R., Amalina, M.A., 2013. Influence of particle concentration and temperature on thermal conductivity and viscosity of Al₂O₃/R141b nanorefrigerant, *Int. Com. Heat Mass Trans.* 43, 100-104.
12. KT, S., et al., PERFORMANCE ANALYSIS OF NANOFLUID BASED LUBRICANT. *International Journal of Innovative Research in Science, Engineering and Technology*, 2013. 2(1).
13. Abbas, M., et al. Efficient Air—Condition Unit By Using Nano—Refrigerant. in 1 st Engineering undergraduate research catalyst conference. 2013.
14. B. Sun and D. Yang, 2013, *International Journal of Heat and Mass Transfer*, vol. 64, (Experimental study on the heat transfer characteristics of nanorefrigerants in an internal thread copper tube,) p. 559–566.
15. Mahbubul, I., R. Saidur, and M. Amalina, Heat transfer and pressure drop characteristics of Al₂O₃-R141b nanorefrigerant in horizontal smooth circular tube. *Procedia Engineering*, 2013. 56: p. 323-329.
16. Mahbubul, I., et al., Thermophysical properties and heat transfer performance of Al₂O₃/R-134a nanorefrigerants. *International Journal of Heat and Mass Transfer*, 2013. 57(1): p. 100-108. Coumaressin, T. and K. Palaniradja, Performance analysis of a refrigeration system using nano fluid. *International Journal of Advanced Mechanical Engineering*, 2014. 4(4): p. 459-470.
17. Fadhilah, S., R. Marhamah, and A. Izzat, Copper oxide nanoparticles

- for advanced refrigerant thermophysical properties: mathematical modeling. *Journal of Nanoparticles*, 2014. 2014.
18. Haider ali hussen, Experimental Investigation for TiO₂ nanoparticles as a Lubricant-Additive for a Compressor of Window Type Air-Conditioner System, *Journal of Engineering* 2014, NO2 V20.
 19. Aktas, M., et al., A theoretical comparative study on nanorefrigerant performance in a single-stage vapor-compression refrigeration cycle. *Advances in Mechanical Engineering*, 2015. 7(1): p. 138725.
 20. Alawi, O.A., N.A.C. Sidik, and A.S. Kherbeet, Measurements and correlations of frictional pressure drop of TiO₂/R123 flow boiling inside a horizontal smooth tube. *International Communications in Heat and Mass Transfer*, 2015. 61: p. 42-48.
 21. Bandgar, M., K. Kolhe, and S. Ragit, An experimental investigation of VCRS using R134a/POE oil/mineral oil/nano-SiO₂ as working fluid. 2016.
 22. Kamaraj, N., Experimental analysis of Vapour Compression Refrigeration System using the refrigerant with Nano particles. 2016.
 23. Hernández, D.C., C. Nieto-Londoño, and Z. Zapata-Benabithé, Analysis of working nanofluids for a refrigeration system. *Dyna*, 2016. 83(196): p. 176-183.
 24. Zhelezny, V., et al., A complex investigation of the nanofluids R600a-mineral oil-AL₂O₃ and R600a-mineral oil-TiO₂. Thermophysical properties. *International Journal of Refrigeration*, 2017. 74: p. 486-502.
 25. M.Z. Sharif, W.H. Azmi, A.A.M. Redhwan, R. Mamat, T.M. Yusof, Performance analysis of SiO₂/PAG nanolubricant in automotive air


conditioning system, International Journal of Refrigeration 2017. S0140-7007(17)30006-3

26. M. Anish, G. Senthil kumar, N. Beemkumar, B. Kanimozhi & T. Arunkumar, Performance Study of a domestic refrigerator using CuO/AL₂O₃-R22 a nano- refrigerant as working fluid, 2018, International Journal of Ambient Energy, 0143-0750 (Print) 2162-8246.
27. M. S. Bandgar, Dr. K. P. Kolhe and Dr. S. S. Ragit, experimental investigation of VCRS using R134a/ POE oil /mineral oil/nano-SiO₂ as working fluid) 2016 (An, Journal of Emerging Technologies and Innovative Research (JETIR) , vol. 3.
28. M. Aktas Melih Aktas, A. Selim Dalkilic, A. Celen, A. Cebi, O. Mahian, and S. Wongwises, 2016, Advances in Mechanical Engineering, vol. 138725, (A Theoretical Comparative Study on Nanorefrigerant Performance in a Single-Stage Vapor-Compression Refrigeration Cycle).
29. R J Bhatt, H J Patel and O G Vashi, 2014, (Nano Fluids: A New Generation Coolants)International Journal of Research in Mechanical Engineering & Technology, IJRMET Vol. 4, Issue 2, ISSN: 2249-5762 (Online) | ISSN : 2249-5770 (Print).
30. Coumaressin, T. and K. Palaniradja, *Performance analysis of a refrigeration system using nano fluid*. International Journal of Advanced Mechanical Engineering, 2014. **4**(4): p. 459-470.

Appendix A

A.1 The Calibration of Instruments used in Thesis


A.1.1 The temperature meter and thermocouple




Calibration Certificate
 Central Organization for Standardization and Quality
 Control (COSQC)
 Metrology Department

P.O. Box 13032 Algeria street, Baghdad, Tel: 7765180 E-Mail : cosqc@yahoo.com
 Certificate No.: PH 406 / 2016
 Date of issue : 09/05/2016

Customer			
Name:	وزارة التعليم العالي والبحث العلمي / جامعة كربلاء / كلية الهندسة		
Address:	العراق		
Item under calibration			
Description:	TEMPERATURE RECORDER + TC (K)		
Manufacturer:	---	---	---
Model:	---	---	---
Serial number:	2	---	---
Other identification:	(0 ----- 100) °C	---	---
Date of reception:	28/04/2016	---	---
Condition of reception:	GOOD	---	---
Standard(s) used in the calibration			
Description:	Thermometer readout	PT100	Water bath
Manufacturer:	Fluke / USA	Fluke / USA	Hetogfrig / Danmark
Model:	1529	5615	---
Serial number:	B2C801	10860	---
Other identification:	---	---	---
Calibration information			
Date of calibration:	09/05/2016		
Place of calibration:	Temperature measurement lab		
Method(s) of calibration:	Calibration method using Working Thermometer - Calibration Procedure 2008		
Calibrated quantity:	Temperature / Celcius / °C		
Results of calibration:	Attached a complete result in Annex 1 of this certificate		
Measurement uncertainty:	There ported expanded uncertainty is based on GUM Standard and the standard Uncertainty multiplied by coverage factor k=2 to give confidence level of 95%		
Metrological traceability:	The traceability of measurement results to the SI units is assured by the National standard maintained at at :- Central Organization for standardization and Quality Control through calibration - COSQC/ Electrical lab (Cert. 028/2016/E) - Temp. measurement lab (Cert. PH - 01-124-00) - NVLAB (REPORT NO. B3114057)		
Environmental conditions of calibration:	Temp. (25 °C):	±1°C	R. H.(50%) ±5%
Observations, opinions or recommendations:			

Performed by: 
MUSTAFA + NEDAL
 10/05/2016



Lumya I.M.Saad Ayoub
 10/05/2016

1 of 1

This certificate is issued in accordance with the laboratory accreditation requirements. It provides traceability of measurement to recognized national standards and to the units of measurement realized at the COSQC or other recognized national standards laboratories. This certificate may not be reproduced other than in full by photographic process. This certificate refers only to the particular item submitted for calibration.

Calibration Certificate

Central Organization for Standardization and Quality
Control (COSQC)
Metrology Department

P.O. Box 13032 Algerin street, Baghdad, Tel:7765180

E-Mail : cosqc@yahoo.com

Certificate No.: PF

406 / 2016

Date of issue :

09/05/2016

Results

Set Value C°	Reference Value C°	Indicate Value C°	Correction C°	ERROR C°	Uncertainty
25	25.6142	26.6	-0.9858	0.9858	0.610482103
50	50.6868	51.2	-0.5132	0.5132	0.613647664
80	81.0452	80.4	0.6452	-0.6452	0.625897796

Performed by:
MUSTAFA NEDAL

Revised by:
JAMAL

Approved by:
Lamiya Saad Ayoub

2 of 1

This certificate is issued in accordance with the laboratory accreditation requirements (traceability of measurement to recognized national standards, and to the units of measurement realized at the COSQC or other recognized national standards laboratories. This certificate may not be reproduced other than in full by photographic process. This certificate refers only to the particular item submitted for calibration



Calibration Certificate

Central Organization for Standardization and Quality
Control (COSQC)
Metrology Department

P.O. Box13032 Algeria street, Baghdad .Tel:7765180

E-Mail : cosqc@yahoo.com

Certificate No.: PF

404 / 2016

Date of issue :

09/05/2016

Results

Set Value C°	Reference Value C°	Indicate Value C°	Correction C°	ERROR C°	Uncertainty
25	25.6142	27	-1.3858	1.3858	0.610482103
50	50.6868	51.8	-1.1132	1.1132	0.613647664
80	81.0452	81.7	-0.6548	0.6548	0.625897796


Performed by:
MUSTAFA + NEDAL


Revised by:
JAMAL


Approved by:
Lamya I.M.Saad Ayoub

2 of 1

This certificate is issued in accordance with the laboratory accreditation requirements. It provides traceability of measurement to recognized national standards, and to the units of measurement realized at the COSQC or other recognized national standards laboratories. This certificate may not be reproduced other than in full by photographic process. This certificate refers only to the particular item submitted for calibration.



Figure (A.1): The calibration of temperature meter and thermocouples.

A.1.2 The Gage pressure



Calibration Certificate

Central Organization for Standardization and Quality Control (COSQC)/(FOR-TC-012)

Metrology Department Mass and Pressure/Pressure Lab

P.O. Box 13032 Algeria street, Baghdad, Tel: 7765180

E-Mail: cosqc@cosqc.gov.iq

Certificate No: PRE/ 391 /2017

Date of issue: 14/ 8 /2017

Customer			
Name:	جامعة كربلاء / كلية الهندسة		
Address:	العراق - كربلاء		
Item under calibration			
Description:	Pressure gauge dial		
Manufacturer:	WIKA		
Model:	Bourdon Tube		
Serial number:	1 4571		
Other identification:	Rang = 100 bar	d = 2 bar	
Date of reception:	3 / 8 /2017	Order No.	120
Condition of reception:	Good		
Standard(s) used in the calibration			
Description:	Pressure Controller		
Manufacturer:	Mensor-Calibration Line		
Model:	CPC6000/Barometer		
Serial number:	41000E54/41000D1S		
Other identification:	Rang = 100 bar	d = 0.0001 bar	
Calibration information			
Date of calibration:	13 / 8 /2017		
Place of calibration:	Pressure Lab		
Method(s) of calibration:	Calibration method are based on DKD-6-1		
Calibrated quantity:	Pressure		
Results of calibration:	Attached a complete result in Annex 1 of this certificate		
Measurement uncertainty:	The reported expanded uncertainty is based on JCGM104:2009 (GUM) Standard and the standard Uncertainty multiplied by coverage factor k=2 to give confidence level of 95% .		
Metrological traceability:	The traceability of measurement to the SI units issued by the National Standard maintained at central organization for standardization and quality control through calibration certificat issued from (WIKA)		
Environmental conditions of calibration:	Temp. (22°C):	±2°C	R. H.(42%) ±10%
Observations, opinions or Recommendations:	The results are within the tolerance according to DKD-6		

Approved by:

khulood khalid shukri

Head of Mass & Pressure Section

page 1 of 2

14/8/2017

This certificate is issued in accordance with the laboratory accreditation requirements. It provides traciability of measurement to recognized national standards, and to the units of measurement realized at the COSQC or other recognized national standards laboratories. This certificate may not be reproduced other than in full by photographic process. This certificate refers only to the particular item submitted for calibration



Calibration Certificate

Central Organization for Standardization and Quality Control (COSQC)/(FOR-TC-012)

Metrology Department Mass and Pressure/Pressure Lab

P.O. Box13032 Algeria street, Baghdad ,Tel:7765180

E-Mail : cosqc@cosqc.gov.iq

Certificate No: PRE/ 391 /2017

Date of issue : 14/ 8 /2017

Annex 1/ Results

Applied Pressure	Reference Reading		Mean Reading	Deviation	Error	Expanded Uncertainty
	Upward	Downword				
bar	bar	bar	bar	bar	% of F.S	bar
0.0	0.00	0.00	0.00	0.00	0.00	0.11548
10.0	10.00	10.00	10.00	0.00	0.00	0.11548
20.0	20.00	20.00	20.00	0.00	0.00	0.11549
40.0	40.00	40.00	40.00	0.00	0.00	0.11549
60.0	60.00	60.00	60.00	0.00	0.00	0.11551
90.0	90.00	90.00	90.00	0.00	0.00	0.11552

Calibrated by:
Nabeel Lateef

Revised by :
Ahmed Salman

Approved by:
khulood khalid shukri
Head of Maas & Pressure Section

page 2of 2

This certificate is issued in accordance with the laboratory accreditation requirements It provides tracibility of measurement to recognized national standards, and to the units of measurement realized at the COSQC or other recognized national standards laboratories. This certificate may not be reproduced other than in full by photographic process. This certificate refers only to the particular item submitted for calibration

Figure (A.2): The calibration of gage pressure.

A.2 The Tests of the Nanoparticles and Properties

A.2.1 Al₂O₃ Nanoparticles Tests and Properties

Aluminum Oxide Nanoparticle (Al₂O₃)
US Research Nanomaterials, Inc.

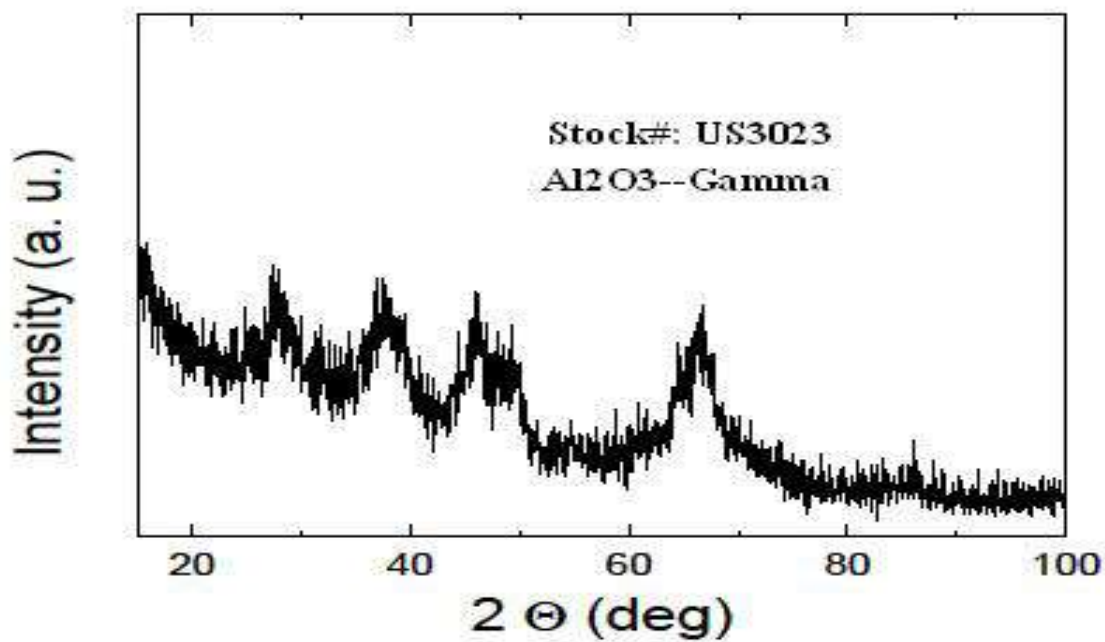


Figure (A.3): X-Ray of Al₂O₃-gamma Nanoparticles.

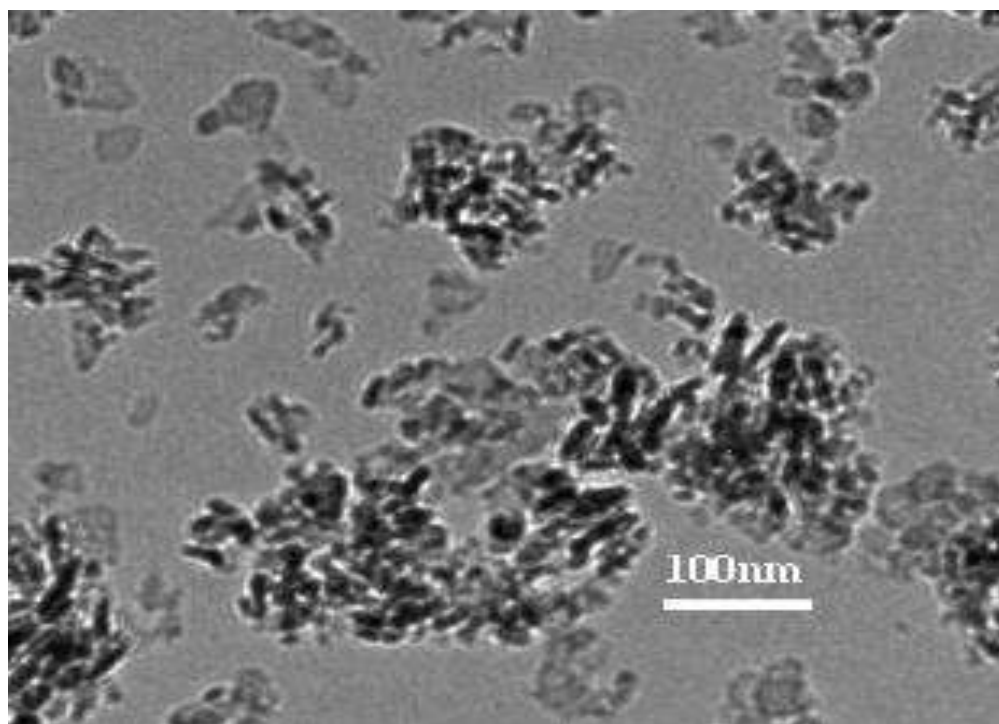


Figure (A.4): The SEM of Al₂O₃ Nanoparticles.

Aluminum Oxide Nanopowder (gamma)--Hydrophilic
 Nanoparticles Al₂O₃ Purity: 99+%
 Nanoparticles Al₂O₃ APS: 20 nm
 Nanoparticles Al₂O₃ Making Method: High-Temperature Combustion Method
 Nanoparticles Al₂O₃ SSA: >138 m²/g
 Nanoparticles Al₂O₃ Morphology: nearly spherical
 Nanoparticles Al₂O₃ Color: white
 Specific heat capacity: 880 J/(Kg-K)
 Density: 3890 Kg/m³

Aluminum Oxide Nanoparticles (Al ₂ O ₃ , Gamma) Certificate of Analysis						
Al ₂ O ₃	Ca	Fe	Cr	Na	Mn	Co
≥99%	≤25ppm	≤80ppm	≤4ppm	≤70ppm	≤3ppm	≤2ppm

Aluminum Oxide Nanoparticles Al₂O₃ Product Features:

US3023 g-phase nano-Al₂O₃ with small size, high activity and low melting temperature, it can be used for producing synthetic sapphire with the method of thermal melting techniques; the g-phase nano-Al₂O₃ with large surface area and high catalytic activity, it can be made into microporous spherical structure or honeycomb structure of catalytic materials. These kinds of structures can be excellent catalyst carriers. If used as industrial catalysts, they will be the main materials for petroleum refining, petrochemical and automotive exhaust purification. In addition, the g-phase nano-Al₂O₃ can be used as analytical reagent.

Aluminum Oxide Nanoparticles Al₂O₃ Applications:

1. transparent ceramics: high-pressure sodium lamps, EP-ROM window; 2. cosmetic filler; 3. single crystal, ruby, sapphire, sapphire, yttrium aluminum garnet; 4. high-strength aluminum oxide ceramic, C substrate, packaging materials, cutting tools, high purity crucible, winding axle, bombarding the target, furnace tubes; 5. polishing materials, glass products, metal products, semiconductor materials, plastic, tape, grinding belt; 6. paint, rubber, plastic wear-resistant reinforcement, advanced waterproof material; 7. vapor deposition materials, fluorescent materials, special glass, composite materials and resins; 8. catalyst, catalyst carrier, analytical reagent; 9. aerospace aircraft wing leading edge.

Aluminum Oxide Nanoparticles Al₂O₃ Dosage:

Recommended dosage is usually 1 to 5%, users should be based on different systems to test, and then determine the best dosage for the best use.

Figure (A.5): The properties Al₂O₃ nanoparticles.

A.2.1 Ag Nanoparticles Tests and Properties

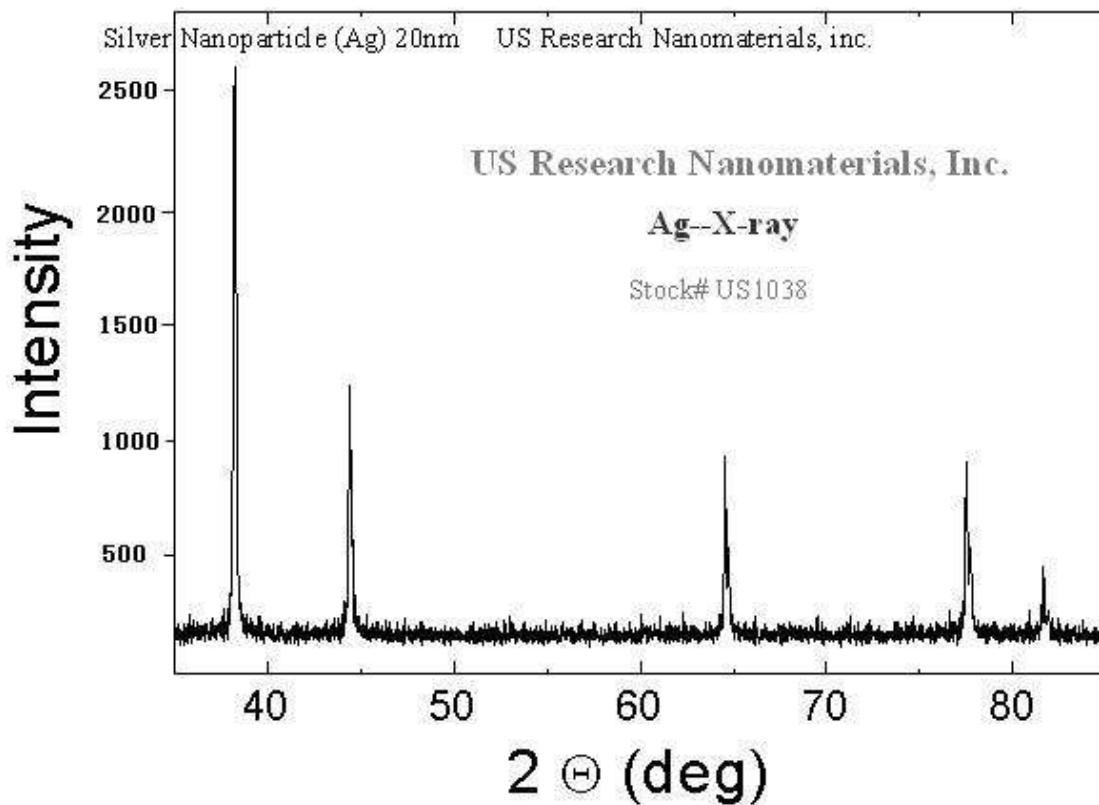


Figure (A.6): X-Ray of Ag-Metal Basis Nanoparticles.

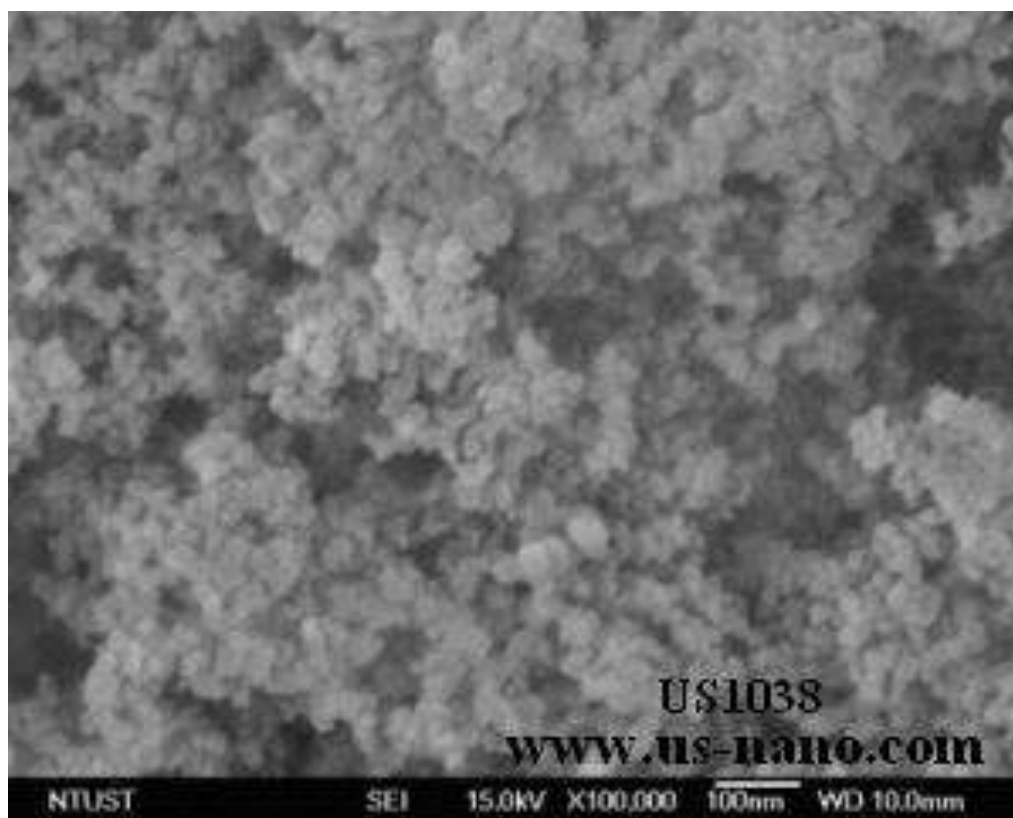


Figure (A.7): The SEM of Ag Nanoparticles.

Silver Nanopowder / Nanoparticles (Ag, metal basis)

Silver nanoparticles true density: 10.5 g/cm³

Silver nanoparticles purity: 99.99%

Silver nanoparticles APS: 20 nm

Silver nanoparticles SSA: ~18-22 m²/g

Silver nanoparticles color: black

Silver nanoparticles morphology: spherical

Silver Nanopowder / Nanoparticles Certificate of Analysis --PPM					
Cu	Bi	Fe	Pb	Sb	Ag
10	2	3	2	2	99.99%

Silver Nanopowder / Nanoparticles Application:

Ag Nanoparticles can be used as pharmaceutical antibacterial, disinfectant; some of countries use Ag Nanoparticles for anti-AIDS drugs, mixed with zinc oxide powder for disinfection; Ag Nanoparticles used as chemical catalyst. Also, Ag Nanoparticles used as Antivirus antibacterial material: adding 0.1% silver nanoparticles, the inorganic antibacterial powder, can play an important role in the suppression and killing of dozens of pathogenic micro-organisms such as Escherichia coli, Staphylococcus aureus. Silver nanoparticles as a new anti-infective product which has broad-spectrum, non-resistance, free from the pH effects, antibacterial, durable, non-oxidized black and many other properties, Ag Nanoparticles can be widely used in medical, household fabrics and health care supplies. Adding Nano Ag powder as antibacterial, anti-corrosion coating paint materials can also be used successfully in the construction and the preservation of relics. Manufacturers produce household items that utilize the antibacterial properties of silver nanoparticles. These products include nano-silver lined refrigerators, air conditioners and washing machines. Ag Nanoparticles for Other current applications: Toys, Baby pacifiers, Clothing, Food storage containers, Face masks, HEPA filters, Laundry detergent. Conductive slurry: Ag Nanoparticles are Widely used for wiring, encapsulation and connection in microelectronic industry, silver nanoparticles play an important role in the minimization of electronic devices and circuits. Efficacious catalyst: silver nanoparticles can Greatly enhance the chemical reaction speed and efficiency, such as Ethylene oxidation. Biological pharmacy: The silver nanopowder can be used in the cell dyeing and the gene diagnosis.

Figure (A.8): The properties Ag nanoparticles.

الملخص

الهدف من هذا البحث هو دراسة تأثير استخدام المواد النانوية اوكسيد الالمنيوم- فريون والفضة- فريون كعوامل محسنة للنقل الحراري في منظومة تكييف الهواء.

التحقيق في هذه الدراسة تم إجراءه مختبريا بواسطة استخدام جهاز اختبار وتحليل عددي من خلال تصميم نماذج ثلاثية الأبعاد بواسطة استخدام برنامج ديناميكيات الموائع الحسابية (CFD)

الاختبارات التجريبية تكون من مكيف الهواء وزيت التشحيم والمائع التشغيلي (R22) وأجهزة متحسس حراري للهواء والمقاييس مثل مقياس الضغط ، جهاز قياس درجة الحرارة و متحسسات الحرارة. حيث تم قياس درجة الحرارة والضغط في مواقع مختلفة.

في التحليل العددي ، تم تحديد السلوك السكوني للموائع في جزء المبخر من مكيف الهواء، تم تنفيذ الشروط الحدودية المناسبة والمعادلات الحاكمة والتحليل من خلال (CFD) الثلاثي الأبعاد و (ANSYS workbench version 16.1) تم الحصول على درجة حرارة والضغط عند الدخول والخروج من ANSYS FLUENT بعد استخدام النتائج التجريبية ثم مقارنتها مع النتائج التجريبية.

أثبتت كل من النتائج العددية والتجريبية أن الضغط المائع التشغيلي في مدخل ومخرج المبخر انخفض قليلا مع استخدام المائع النانوي الملائم. في حين ارتفعت درجة الحرارة مع المائع النانوي.

تظهر النتيجة التجريبية أن الحد الأقصى لفرق درجات الحرارة تم الحصول عليه عند (0.15% كتلية) من المائع النانوي لـ Ag-R22 .

وأقصى تحسين في COP مع إضافة الجسيمات النانوية (Ag) إلى المبرد R22 مع 0.15% كتلي وازداد التحسين بنسبة (144.71)



جمهورية العراق
وزارة التعليم العالي والبحث العلمي
جامعة كربلاء - كلية الهندسة
قسم الهندسة الميكانيكية

تحقيق تجريبي وعددي لتحسين تبريد مكيف الهواء باستخدام مواد نانوية

رسالة مقدمة الى قسم الهندسة الميكانيكية في كلية الهندسة بجامعة كربلاء كجزء من متطلبات
نيل درجة ماجستير
علوم في الهندسة الميكانيكية - ميكانيك موائع وحراريات

من قبل

هديل صلاح هادي

بكالوريوس هندسة ميكانيكية (2015)

بأشراف

أ.م.د. عباس ساهي شريف

م.د. حيدر ناظم عزيز